# ROBUST INFERENTIAL CONTROL: A METHODOLOGY FOR CONTROL STRUCTURE SELECTION AND INFERENTIAL CONTROL SYSTEM DESIGN IN THE PRESENCE OF MODEL/PLANT MISMATCH

Dissertation by

Jay H. Lee

In Partial Fulfillment of the Requirements

for the Degree of

Doctor of Philosophy

California Institute of Technology

Division of Chemistry & Chemical Engineering

Pasadena, California

1991

(Submitted December 12, 1990)

To my parents, with love.

# Acknowledgements

It is with my deepest appreciation that I acknowledge my advisor, Manfred Morari, for his contribution to this thesis work. I am grateful for his intellectual guidance and financial support during the past four and a half years. Over the years, he earned my respect with his serious attitude toward research and insight to provide his students with the "big" picture. I know that I will succeed in whatever I do if I can match half of his intensity and dedication. I also thank him for standing by me during my "difficult" initial period.

I would like to acknowledge the rest of the committee: Profs. J. Doyle, A. Sideris, and J. Seinfeld. I thank Prof. Doyle for his work on the Structured Singular Value theory, Prof. Sideris for a number of helpful control courses, and Prof. Seinfeld for his willingness to serve as a committee member.

I had the privilege of working with a number of knowledgeable researchers: Dr. Carlos Garcia, Prof. Andy Packard, Marc Gelormino, Petter Lundström, and Morten Hovd. Without their contributions, the quality of this thesis would not have been the same. I look forward to many more fruitful interactions with them.

On the contrary to my expectation when I first arrived at Caltech, I am leaving the place with many fond memories. Many friends came along during the past four and a half years and their love and friendship abound in memories. Even though my heart is overwhelmed with sadness for having to leave so much love and friendship behind, I am a better person for having known them.

Many of the fond memories belong to the past and present members of the Morari research group: H. Andersen, N. Bekiaris, R. Braatz, H. Budman, P. Campo, R. Colberg, F. Doyle, T. Holcomb, L. Laroche, D. Laughlin, D. Lewin, D. Raven, D. Rivera, C. Scali, A. Skjellum, S. Skogestad, C. Webb, and E. Zafiriou (did I leave anybody

out?). I respect and admire their intelligence, persistence, and willingness to help, which made my stay at Caltech both stimulating and enjoyable. Special thanks are due to my officemates, Lionel and Tony. Lionel was somehow sentenced to being both my roommate and officemate and he withstood this difficult test wonderfully. Tony helped me in many occasions with computer programming and English composition. He set a very high standard for how a senior group member should guide a junior member. Thank you all for the good times.

The "Korean Maffia" on campus meant both excitement and troubles. They made my years at Caltech less lonely, but more tiring (only physically, though). I especially thank Mr. & Mrs. Yong Kim for countless gourmet-dinner invitations, Dr. Cheol-Hoon Park for many helpful conversations, and Geun-Chang Chung for just being around.

I wish to thank the people at the Holy Trinity Church for providing me with experiences and lessons that Caltech was not able to. I thank Father Peter Bae for his many helpful sermons, classes, and discussions. Special thanks are also due to my godparents, Fabian and Scholastica, for being more-than-wonderful godparents.

I thank my sister, Eun-Young, and my cousins, Seung-Koo and Hye-Joo, for many conversations during my difficult and frustrating moments. I thank Uncle & Aunt Kim and my cousins, Soo-Young, Tae-Young, Soo-Kyung and Hyeon-Geun, for their special love and care expressed through many letters and telephone conversations. And last, but certainly not the least, I give special thanks to my parents. Without their love and support, I cannot imagine being here.

# Robust Inferential Control: A Methodology for Control Structure Selection and Inferential Control System Design in the Presence of Model/Plant Mismatch

Jay H. Lee

## Abstract

Two major tasks that are required to obtain a control system utilizing secondary measurements are measurement selection and inferential control system design. The first involves choosing an appropriate subset of the available measurements and the second involves designing a feedback controller based on the chosen measurements. The important issues to be addressed are not only the theoretical performance of the closed-loop system, but also the effects arising from the factors prevalent in practical environments such as model/plant mismatch, constraints, and failures of actuators and sensors.

General measurement selection methodology is developed accounting for all the factors that can affect the measurement selection in signifcant ways. These factors include model uncertainty, signal-to-noise ratios, and measurement dynamics. The underlying philosophy is to reduce the number of candidates to a sufficiently low level before going onto detailed analysis by eliminating those candidates for which there does not exist a linear time-invariant controller meeting the required level of robust performance. Based on this philosophy and using the Structured Singular Value theory as a vehicle, a number of numerically efficient screening tools are developed. Conditions are derived under which some of the new criteria reduce to previously published measurement selection criteria. The proposed tools are applied to the

*measurement selection* problems in a multi-component distillation column and a high-purity distillation column.

Two different approaches are considered for inferential control system design: an *output estimation based design approach* and a *state estimation* based design approach. The former approach involves independent design of an output estimator and a feedback controller while the latter involves direct one step design although the design can be actually separated into those of a *state estimator* and of a *feedback* regulator using the separation principle argument.

For the former approach, design of the output estimator was examined for two different cases: the case where a full dynamic model is available and the case where only the time records of the primary and secondary measurements are available either from simulations or from process measurements. For the former case, multi-rate Kalman filter design and $\mu$-Synthesis design are discussed. For the latter case, the estimator design problem is formulated as a regression problem and various regression techniques are evaluated in terms of their suitability to the output estimator design problem. For design of the feedback controller, traditional techniques such as LQG, IMC, and MPC were combined into a control technique that has nice algorithmic properties as well as many operational merits such as straightforward constraint handling and simple, intuitive on-line tuning. A heavy-oil fractionator was used as an example application.

For the latter approach, general state estimation techniques (*e.g.*, multi-rate Kalman filtering) used in LQG and finite receding horizon control used in traditional MPC were integrated into a control technique that can incorporate general disturbances and multi-rate sampled measurements and has desirable operational characteristics. The concept of classical IMC was extended to equip the control system with on-line tuning parameters that have direct connections with the speed of the closed-loop responses. Application to a high purity distillation column demon-

strates the effectiveness of the control technique in terms of closed-loop performance and operational flexibility.

# Contents

# List of Figures

# List of Tables

# Chapter 1

# Introduction

The objective of this thesis is to develop a rigorous, yet practical methodology for secondary measurement selection and control system design for processes the controlled variable measurements of which are either unavailable or unsuitable for feedback control because of technical and/or economic reasons. By "rigorous, yet practical," we mean that the methodology must have a solid theoretical foundation and at the same time must be useful in solving "real world" control problems. In order for the theory to be practical, it must not rest on assumptions that are unrealistic for real world processes and should also address *all* issues that can affect the final control system performance in significant ways. The key practical issues we address in this thesis are model/plant mismatch, process constraints, and actuator/sensor failure tolerance.

## 1.1 Motivation

Real world control problems are often complicated by "difficult" controlled variable measurements. Control difficulties may stem from one or more of the following measurement characteristics:

- *Slow Sampling Rate*

  The "primary measurements" (that is, the measurements of the controlled variables) may not be available at a sufficiently fast sampling rate required for the desired closed-loop bandwidth.

- *Large Sampling Delay*

  The primary measurements may necessarily accompany delays that are too long for the desired closed-loop bandwidth.

- *Poor Signal-To-Noise Ratio*

  The signal-to-noise ratios for the primary measurements may be too low for effective feedback control.

- *Operational Unreliability*

  The measurement devices may be operationally unreliable (that is, they may experience frequent failures or need frequent services and readjustments) leading to frequent shut-down of the control system.

These factors are represented schematically in Figure 1.1. When one or more of the above factors make the design of an effective feedback control system based on the primary measurements alone infeasible, "secondary measurements" (that is, measurements of other process variables) must be utilized. In this thesis, we define "inferential control" in its broadest possible sense:

> Inferential control refers to control techniques that use measurements other than those of controlled variables.

The above definition of inferential control naturally includes feedforward control.

A successful feedback control using secondary measurements depends on two important tasks: the selection of secondary measurements and inferential control system design. In practice, it is often the case that the number of secondary process variables that are available for measurements far exceeds the number of secondary measurements that are ultimately used by the control system. It could be argued that using more measurements should not degrade the final closed-loop performance in any way and hence using all the available measurements effectively removes the problem of measurement selection. While this is true in principle, it is often impractical from

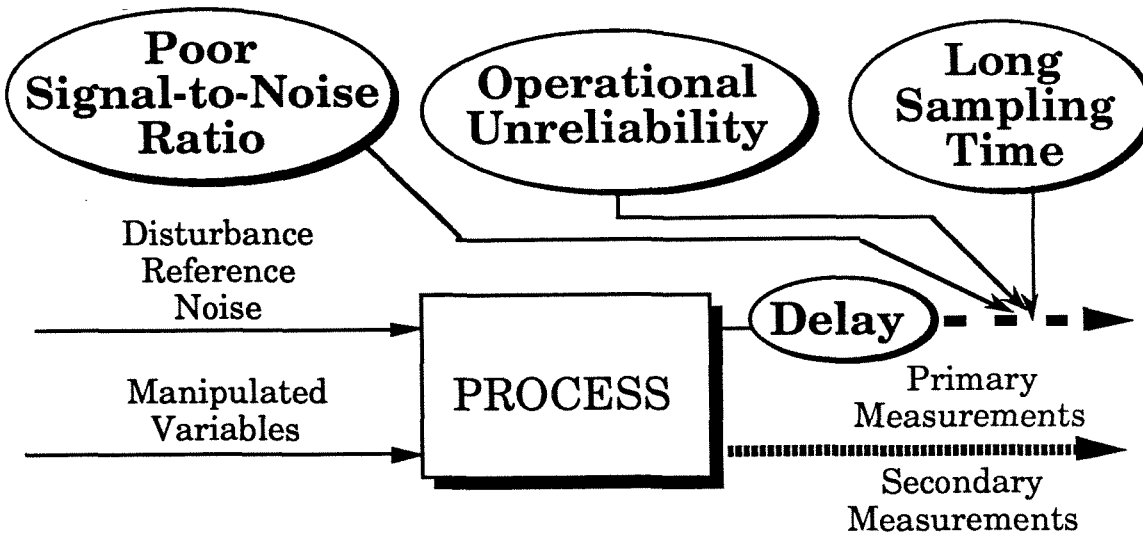


Figure 1.1. Motivations for Using Secondary Measurements

both technical and economic standpoints to build a control system that uses all the available measurements. Not only would such a control system be highly complex and therefore difficult to design and maintain, but it would also be prohibitively expensive. These considerations necessitate the selection of an appropriate subset of available measurements. There are strong practical and theoretical evidences pointing toward the importance of measurement selection for the success of feedback control. A wrong choice of measurements can put a fundamental limitation on the system's closed-loop performance that cannot be overcome by "smart" controller design.

A correct measurement selection must be followed by "good" inferential control system design. The control system design for systems with secondary measurements is more difficult and complex than that for systems for which the controlled variables coincide with the measured variables since good control of the secondary variables do not necessarily imply good control of the primary variables. In many cases, the primary measurements are available, though at a slow sampling rate and with low reliability, for improved feedback control. This naturally gives rise to a multi-rate sampled-data system, to which most control design methods are not applicable straightforwardly.

## 1.2 Issues of Practical Importance

As will be elucidated in the next section, there are a number of industrial processes that can benefit significantly from improved inferential control. However, even after several decades of numerous theoretical advances, the impact of modern control theory to these processes has been negligible. This unfortunate trend can probably be attributed to most modern control theories' difficiency in addressing practically relevant issues in a realistic, unified manner. Hence, it is important right from the start to examine carefully all the issues that can affect the measurement selection decision and final control system performance in signifcant ways.

For measurement selection, the essential question may be stated as "what makes one measurement set superior to another?" The factors that should be accounted for in measurement selection are as follows:

- *Model/Plant Mismatch*

  A mathematical model never represents the true physical system exactly. This is true even for very detailed first principles models or experimentally identified models. For low-order, linear models that are often used for the control system design, this "model/plant mismatch," or "model uncertainty," can be quite significant. In addition, various process parameters may change over the course of time giving rise to additional mismatch. A control system showing an excellent closed-loop performance for the model may suffer significant performance deterioration when implemented to the real system because of the mismatch. This deterioration may be arbitrarily large meaning the closed-loop system can even be unstable.

  For analysis, it is essential to express the model/plant mismatch in well-defined mathematical terms. The model/plant mismatch is often described mathematically as a set of norm-bounded perturations to the model. These perturbations

supposedly capture either partially or entirely the possible discrepancies between the model and the real process. It is conceivable that a measurement set is intrinsically more sensitive to these perturbations than another measurement set. Since a control system, when implemented to the real system, will be potentially subjected to these perturbations, a measurement set with low sensitivity to the perturbations is preferred over a set with high sensitivity.

- *Delays, Inverse Responses*

  Measurements which show significant delayed or inverse responses to various process disturbances may be undesirable because they may not be able to provide "efficient" enough estimates of the controlled variables. For example, if a secondary variable does not respond to a process disturbance for 10 minutes while the disturbance affects the controlled variables immediately, the secondary variable cannot predict the excursion of the controlled variables from their setpoints caused by the disturbance for at least 10 minutes. A similar argument can be made for measurements showing inverse reponses. A measurement set with delays and/or inverse responses that are insiginficant with respect to the desired closed-loop bandwidth must be chosen.

- *Signal-To-Noise Ratios*

  Measurements that are insensitive to process disturbances may be adversely affected by measurement noise. For example, if a secondary variable changes by an order of 1 to typical disturbances while the measurment noise associated with the variable is of an order of 10, the disturbance effects on the measurements will be masked entirely by the measurement noise. A measurement set with adequate signal-to-noise ratios must be chosen.

For control system design, most research efforts have been directed toward development of pure algorithms. However, various operational aspects of a control system

is as important to its success in a practical environment as its algorithmic merits. The following issues must be addressed in designing and analyzing an inferential control system:

- *Model/Plant Mismatch*

  The degree of performance deterioration of a control system caused by model/plant mismatch depends largely on the characteristics of the control system. A control system is said to be "robust" if its performance deteriorates insignificantly when implemented to processes the behavior of which is significantly different from what the model predicts. A control system must be designed to meet the required performance specifications for all systems that the perturbations used to describe potential model/plant mismatches render.

- *Constraints*

  Constraints are often of great relevance to process control since the economically optimal operating regions for most processes lie at the intersection of constraints [2]. On the other hand, most advanced control algorithms are developed under the assumption of infinite input/output domain. Controllers designed using such algorithms must be fixed subsequently to incorporate various constraint-handling capabilities. Some of popular *ad hoc* fixes are anti-reset windup mechanisms, selectors, overrides, *etc.* Such *ad hoc* fixes not only can cause undesirable performance degradation, but also require significant engineering efforts because their designs tend to be case-specific. In view of ever increasing complexity and sophistication of today's control algorithms, it is extremely important from both economic and safety standpoints that these constraints are taken into account at the design stage and do not have to be dealt with afterwards in some *ad hoc* fashion.

- *Actuator/Sensor Failure*

It is common in industrial processes that some of the actuators and sensors fail. One of the main motivations for inferential control was potential operational unreliability of the primary measurements. The primary measurement devices may need to be shut down frequently because they require servicing or the readings from these devices become unacceptably inaccurate for various reasons. In addition, some of the actuators may simply "get stuck" and become not manipulable. It is desirable that the required changes in the control system in the event of actuator/sensor failures can be made by the operating personnel in a straightforward manner without expert's intervention.

- *Ease and Flexibility of Design and Implementation*

  Given sufficient time and money, engineers can usually come up with adequate solutions to most control problems assuming such solutions exist. However, the investment of significant engineering efforts in the control system design can only be justified when its cost is outweighed by the promise of increased profitability of the control system. In practice, it is possible that the real process may behave entirely differently from what the engineer expected initially. This may necessitate several painstaking trial and error designs before obtaining an adequate control system. In addition, a control system that is applicable to a wide range of processes with minor modifications (for example, PID controllers) can save significant engineering efforts and expenses. From these considerations, the control systems equipped with flexible on-line tuning parameters are more desirable than those without. In addition, it is better if the control algorithm is intuitive and simple enough to be understood and accepted readily by plant operators.

## 1.3 Industrial Applications

The research is well motivated by the abundance of industrial processes for which the product quality measurements are hampered by long sampling delays and frequent shutdowns of the measurement devices. In order to further motivate the topic of this thesis, some of the potential applications are discussed in this section, paying particular attention to the process characteristics in concern with the issues outlined in the previous section.

### 1.3.1 Distillation Columns

One important application of the methodology developed in this thesis is distillation column control. Tight control of product compositions enables distillation columns to be operated at a point closer to the economically optimal operating point leading to significant energy savings and higher product yields. However, the product composition measurements through various composition analyzers such as gas chromatographs often require large sampling time and are prone to failures as the analyzers need frequent servicing and recalibration. In practice, the secondary process variables such as tray temperatures and the column pressure are often measured and used instead for feedback control of the product compositions. A large number of trays in most industrial distillation columns leads to a large number of potential secondary measurements and necessitates measurement selection. Industrial experience reports that the choice of temperature sensor location is of paramount importance to successful product composition control.

Despite a long history of intense efforts devoted to developing an accurate first principles model for distillation columns, the complexity of the process proved to be too high to render an accurate quantitative model for the process. Simple linear models that are often used for the control system design invariably lead to substantial model/plant mismatches for these processes. In addition, further mismatches

between the model and the real process are introduced by the inaccuracy of actuator valve positionings and sensor readings. Most columns are also subject to a number of constraints arising from plant-wide optimizations, actuator hardware limits, and various safety considerations (*e.g.*, column pressure). Control systems for distillation columns are subject to frequent actuator/sensor failures as columns are often switched to manual operation. These nontrivial model uncertainty and operational complexity probably explain why most industrial columns today are still controlled through single-loop PID controllers and measurement selection decisions are made on the basis of intuition and heuristics rather than through systematic methods. Potential benefits of a new measument selection and inferential control system design methodolgy for distillation columns are high if they correctly address all the issues outlined in the previous section.

### 1.3.2 Packed-Bed Reactors and Other Chemical Processes

Most chemical processes that require control of product or substrate concentrations share the same measurement difficulties. A packed-bed reactor for which the outlet concentration must be controlled as well as the maximum bed temperature serves as another good example. Essentially any number of temperature sensors can be placed along the packed-bed for the purpose of inferring the outlet product composition and the maximum bed temperature. Industrial experience reports that the location of temperature sensors has a strong influence on the final control system performance.

Because the process is a distributed parameter system described through a set of highly nonlinear partial differential equations, linear time-invariant (LTI) models used for control system design are only a coarse approximation of the real process. Again, model/plant mismatch is a key factor for the sensor placement and control system design. Hot spot temperature must be maintained below a certain critical level giving rise to an output constraint in addition to the input saturation constraints. The new

methodology may be able to solve control problems arising in these processes that traditional methods failed to.

### 1.3.3 Pulp Digesters

In paper manufacturing, it is important that the quality of the pulp is maintained at a constant, desired level. The quality of the pulp is measured through what is known as the "Kappa Number," which expresses the degree of delignification. Heterogeneous nature of feed woodchips introduce unmeasurable disturbances to the process and proper control of the Kappa Number is imperative to an efficient, economic production of superior, constant quality paper. The devices used for the Kappa Number measurements share many similar characteristics as those used for the composition measurements. The Kappa Number measurements require large sampling time (sometimes of an order of hours) and the measurements may disappear without warning for a sustained period of time. For reliable, efficient Kappa Number control, secondary process variables such as the PH number, conductivity and temperatures of the digester liquor can be utilized for the real-time estimation of the Kappa Number.

The control problems for pulp digesters share many characteristics of those for the process industry. First, the process is poorly understood. Despite intense activities in the field, quantitatively accurate models for the delignification process are yet to be available. It is unclear what measurements must be used for the best on-line estimation of the Kappa Number. There are a number of potential constraints arising from the optimization layer since various units of pulp and paper mills are often interactive with extensive recycling. Improved inferential control methodology can bring potentially significant savings to the industry.

The potential benefits of the new methodology that we are intent on developing as the end goal of this thesis are well exemplified by the above-discussed applications. Other potential application areas include fermentation reactors, coating processes,

and navigation.

## 1.4 Previous Work

In this section, we examine some of the major research results on the topics of measurement selection and inferential control system design that were available prior to the time when this thesis work began. It will be made apparent that there has been a lack of systematic methodology that addresses all of the practically relevant issues outlined in the previous section. The intent of this section is not to provide a complete, extensive literature survey on the topics; this survey inevitably left out some of the relevant work on the topics. Instead, the purpose of this section is to elucidate the need for more systematic measurement selection and inferential control system design methods.

### 1.4.1 Previous Work on Measurement Selection

During the 60s and 70s, a popular approach in the control research community was to model the system in a stochastic framework. When this modelling approach was combined with a time-domain quadratic performance index, the "optimal" (in probablistic sense) controller known as the "Linear Quadratic Gaussian (LQG)" controller could be found analytically. The celebrated "separation principle" showed that the LQG controller could be decomposed into the optimal state observer (Kalman filter) and the optimal LQ state feedback regulator that can be designed independently of each other [62]. An implication of the separation principle for measurement selection is that the choice of measurement set can be optimized by minimizing an appropriate scalar measure of the state estimation error covariance matrix, that can be calculated straightforwardly. Based on this idea, a number of researchers proposed measurement selection criteria in the context of sensor location problem for packed-bed reactors [35,34] as well as in more general contexts [29].

A serious deficiency of the LQG framework as a ground for developing practial measurement selection criteria is its inability to address the model/plant mismatch explicitly. The idea of model/plant mismatch has to be incorporated in an *ad hoc* fashion, such as through arbitrarily chosen state excitation noise. Not only is the choice of this noise that gives rise to a physically plausible model unclear, but the effects of state excitation noise on the closed-loop systems is also qualitatively different from those of model/plant mismatch. For example, the latter can introduce instability to an otherwise stable system while the former can't. Hence, the practical applicability of the criteria developed using the LQG control theory must be seriously questioned.

In the late 70s, Brosilow and coworkers attempted to address the issue of model/plant mismatch more rigorously to the problem of measurement selection [61,32,7,31]. They studied the effect of a perturbation (an error on the gain matrix relating disturbances to measured variables) on the accuracy of the steady-state disturbance estimates when a "least-square" type estimator is used. They proposed what is known as the "Condition Number Criterion" by showing that an upperbound of its effect can be minimized by choosing the measurement set with the lowest condition number of the gain matrix. They also indicated that the Condition Number Criterion often conflicts with minization of the nominal (that is, in the absence of the perturbation) estimation error and left the compromise to engineering judgments.

The work by Brosilow and coworkers can be regarded as the first attempt toward the right direction for developing practically useful measurement selection criteria. However, these studies were conducted at a time when robust control theory was not developed to its full maturity, and naturally, there are serious problems associated with the proposed criteria. First, model/plant mismatch for practical systems is neither adequately nor parsimoniously captured by the unstructured perturbation that led to the Condition Number Criterion. In practice, model/plant mismatches

are often best described as a highly structured set of perturbations. Consequently, the perturbation that the Condition Number Criterion subsumes can not only exclude some of realistic model/plant mismatches, but also include many gain matrices that are physically inplausible. It is conceivable that measurement selection criteria which are based on an overly conservative model uncertainty description may lead to a wrong choice of measurements. In addition, the "least-square" type estimator that is inherent in their criteria is generally not the best choice in the presence of model/plant mismatch. Finally, the steady-state analysis alone may not provide a sufficient amount of information needed for measurement selection since dynamic merits of measurement candidate sets cannot be neglected (as explained in the previous section).

The decade of 80s was a brand-new era for control research. The research community recognized model/plant mismatch as a key issue for most practical control problems and such an awareness led to the development of a number of new measurement selection criteria. Moore and coworkers suggested a set of empirical rules for measurement selection based on the singular value decomposition (SVD) of the steady-state gain matrix relating manipuated variables to measured variables [47]. In one of the proposed criteria, they defined what is called "intersivity index" and suggested that the index be minimized in selecting the measurements. Two factors determine the intersivity index: the sensitivity of measurements to manipulated variables and the condition number of the gain matrix. Intuitively, it is clear that neither factors should have significant effects on the closed-loop performance since the ultimate role of the secondary measurements is to provide estimates for the effect of *disturbances* on various system states and controlled outputs. Even though the criteria may have provided correct results to the particular application that they studied, they should be dismissed as general measurement selection criteria.

Bequette and Edgar suggested a slightly different approach to measurement selec-

tion [5]. They proposed to minimize the maximum singular value of the "inferential error" matrix, which is a measure of the "worst-possible" steady-state errors in the controlled variables when the secondary variables are controlled perfectly through a controller with integral action. They also suggest that minimization of the inferential error should be balanced against the sensitivity of measurements to manipulated variables and leave the final trade-off to engineering judgments. Their criteria have two major problems. First, the sensitivity of measurements to the manipulated variables is not a relevant issue for measurement selection as pointed out previously. Second, it is generally not the best (although often done in practice) to use controllers with integral action for inferential control as the perfect control of the secondary variables can lead to arbitrarily large errors in the primary variables.

To summarize, there is a clear need for better measurement selection criteria that address the "real-world-relevant" issues in a general, correct manner. Fortunately, the time is ripe for directing efforts to such a need as there has been a major development in robust control. Doyle introduced a powerful new theory called the "Structured Singular Value (SSV)" that enables analysis of frequency-domain performance of a closed-loop system in the presence of general "structured" perturbations describing model uncertainty [22]. As demonstrated in this thesis, the SSV theory provides a convenient framework to develop measurement selection criteria addressing the issue of model/plant mismatch generally and explicitly.

### 1.4.2 Previous Work in Inferential Control System Design

Inferential control system design methods can be classified into two major categories: a state estimation based approach and an output estimation based approach. In the state estimation based approach, a mathematical model relating various system inputs to the outputs is used to build implicitly or explicitly an estimator for the system states and/or controlled outputs. Then this state estimator is combined with

a control law which calculates the control inputs on the basis of these estimates. In the output estimation based approach, an explicit relationship (either static or dynamic) between the secondary measurements and the primary variables is derived using a mathematical model or plant data and is combined with a control system that is designed under the assumption that the primary measurements are reliably available at the sampling rate of secondary measurements.

Before the era of optimal control (and even today to a wide extent), inferential control was mostly accomplished through PID controllers with *ad hoc* fixes. This approach was based on the premise that secondary measurements with similar behavior in responding to disturbances and manipulated inputs as the primary variables could be chosen. When this premise was not satisfied, the resulting steady-state offsets in the primary variables were quite substantial. To resolve this serious problem, auxiliary PID controllers using the "slow" primary measurements were cascaded to the main inferential controllers to provide setpoints for them [44]. These so called "parallel cascade controllers" were heuristically designed for most cases and dynamic performance was at times quite poor [53].

In the 60s and 70s, many control research efforts were directed toward the time-domain stochastic optimal control. The Linear Quadratic Gaussian optimal control theory, or the $H_2$-optimal control theory, provided a unified design method for general multivariable linear systems, based on the objective of minimizing the variance of the chosen (possibly frequency weighted) controlled variables under certain stochastic assumptions on the system disturbances and measurement noise [36,3]. A nice property of the LQG controller is that its design can be decomposed into those of the optimal state estimator (Kalman filter) and of the optimal state feedback regulator. This separation naturally fit to the interpretation of an inferential control system as a composite of an estimator and a regulator.

Various modified forms of the standard Kalman filter design appeared. One no-

table version is that proposed by Morari and Stephanopoulos who showed how the problem of indetectability caused by the presence of nonstationary noise could be overcome in an optimal way [49]. Brosilow and coworkers suggested a slightly different approach in which a "least-square" type static estimator is combined with *ad hoc* chosen lead-lag dynamic elements [32,31,7]. The approach is clearly related to the Kalman filter design as the "least-square" type static estimator correponds to the steady-state Kalman filter gain when all the disturbances are modelled as nonstationary noises.

After decades of much excitement and intense research efforts, it became apparent that the LQG design method suffered some serious drawbacks as a general methodology to solve practical control system design problems, especially those for the process industry. The failure of the LQG design in terms of general practical applicability can be attributed to its two major deficiencies: its inability to incorportate the model uncertainty explicitly and its inability to deal with constraints. As Doyle [21] showed, there is no inherent robustness margin for LQG controllers. However, there are clearly enough degrees of freedom in LQG controllers to achieve desirable robustness characteristics for most problems. The main problem is that robustness has to be achieved through various indirect design parameters such as input penalty weights and noise covariance matrices. At the time when a rigorous robustness analysis method such as the SSV theory was not available, it must have been very frustrating, if not impossible, for engineers to determine these indirect parameters such that a closed-loop system with desirable performance and robustness characteristics is obtained. In addition, a lack of general theory for designing anti-windup, bumpless transfer schemes that are commonly employed in industry to deal with various problems arising from process constraints was another major impediment to successful application of the LQG design method.

Two notable developments during the 80s have partially alleviated these deficien-

cies of the LQG design method. First, with the SSV analysis method [22], engineers can at least readily check the robustness of the designed controller (although significant trial and error may be necessary before obtaining a satisfactory design). In addition, a general theory on the topic of anti-windup and bumpless transfer has been developed for multivariable controllers [10].

In the 80s, the failure of the LQG design in practical environments spurred two distinct approaches to control system design, opening a new era of feedback control: $H_\infty$-optimal control and Model Predictive Control (MPC). The $H_\infty$-optimal control was initiated by the work of Zames in which he suggested that performance specifications for most practical control problems may be better posed in terms of the $H_\infty$-norm rather than the $H_2$-norm (*i.e.*, the standard integral square norm used in the LQG theory) [65]. Since then, the $H_\infty$-optimal control has grown to become the topic of the 80s receiving much attention and substantial research efforts. Today a complete state-space solution to the general $H_\infty$-optimal design problem is available [18]. Much of the enthusiasm and attention devoted to the $H_\infty$-optimal control comes from the fact that the $H_\infty$-optimal synthesis can be combined with Doyle's SSV analysis into an iterative design algorithm called "$\mu$-Synthesis [17]." A distinct merit of this algorithm is that it directly exploits the given description of model uncertainty. Today the $\mu$-Synthesis stands alone in the list of design methods that can incorporate the available information on model/plant mismatch directly.

Although the $H_\infty$-optimal design method can be regarded as a theoretically complete design method and $\mu$-Synthesis holds high promises as a design method for the future, it will probably take some time before they can have a strong impact on practical applications. In order for them to be useful for the inferential control problem posed in this thesis, the issue of multi-rate sampling and sensor failure tolerance must be addressed. In addition, the theory does not extend to systems described through nonlinear operators, and consequently, the constraint issues cannot be ad-

dressed directly in the designs, even though the aforementioned developments in the anti-windup, bumpless transfer significantly widened the scope of application for these design methods.

In parallel to the developments in the $H_\infty$-optimal control which came mostly from researchers in applied mathematics and electrical engineering, process industry developed a technique called Model Predictive Control that can address various operational issues in a general, systematic way. This development was motivated by increasing cost and engineering efforts required to design and debug various constraint handling schemes for increasingly sophisticated control configurations used by the industry. Today's enthusiasm for MPC probably originated from the work of Cutler, in which he suggested a technique called "Dynamic Matrix Control (DMC) [15]." Even though the intial version of MPC was rather intuitively based and heuristic in derivation, a number of researchers, notably Garcia and Morari [24], have since discovered that there is a connetion between the MPC and various modern design methods. Much of the attraction for MPC comes from the fact that various constraints are handled directly in the formulation through the use of on-line optimization. In addition, the technique was originally developed for nonparametric (finite impulse response or step response) models and therefore were more accessible to process engineers who lack traditional control backgrounds.

Since the introduction of DMC, a number of different versions of MPC have appeared in both academic community and industry, some of them using parametric models [42,57,12,13]. However, there has been a lack of a unifying framework which connects all the MPC techniques and also various LTI design techniques such as the LQG method. A consequence of this lack of a unifying framework is that MPC cannot stand as a truly general design methodology. The scope of application for various MPC techniques are limited to the problems where the primary measurements are available (or their estimates are provided through an independently designed output

estimator). Their extensions to inferential control problems have not been available.

An MPC controller in its unconstrained form amounts to nothing more than a linear time invariant controller. In the presence of active constraints, however, the controller is inherently nonlinear and its stability and robustness analysis becomes very difficult, if not impossible. Various strange behaviors of MPC controllers in the presence of active constraints have been observed and documented [64]. Another deficiency is a lack of intuitive robustness tuning parameters. There are clearly enough on-line tuning parameters to make MPC controllers robust. However, none of them have a very direct interpretation to system robustness such as an explicit relationship with closed-loop bandwidth. The overabundance of tuning parameters simply confuses engineers and makes tuning more difficult. In order for MPC to continue its success in a practical environment, it is important that a new version of MPC equipped with tuning parameters having specific, well-understood effects on the system robustness become available in the near future.

An additional issue for the output estimation based approach is how to design an estimator based on the available plant data. Standard regression techniques such as the Least Square (LS) regression would be directly applicable if the regressor inputs (the secondary measurement data) could be freely chosen by engineers as in open-loop identification experiments. However, such is not the case and the regression matrix often tends to be ill-conditioned, leading to an estimator with high sensitivity to measurement noise. More sophisticated techniques such as the Partial Least Square (PLS) regression has been suggested as an alternative to overcome this difficulty [45].

The above-discussed developments and unresolved issues are outlined schematically in Figure 1.2. In summary, there is a number of research issues that must be resolved before these advanced control techniques can be applied successfully (in a general sense of the word) to "real world" inferential control problems. Some of more pressing issues include

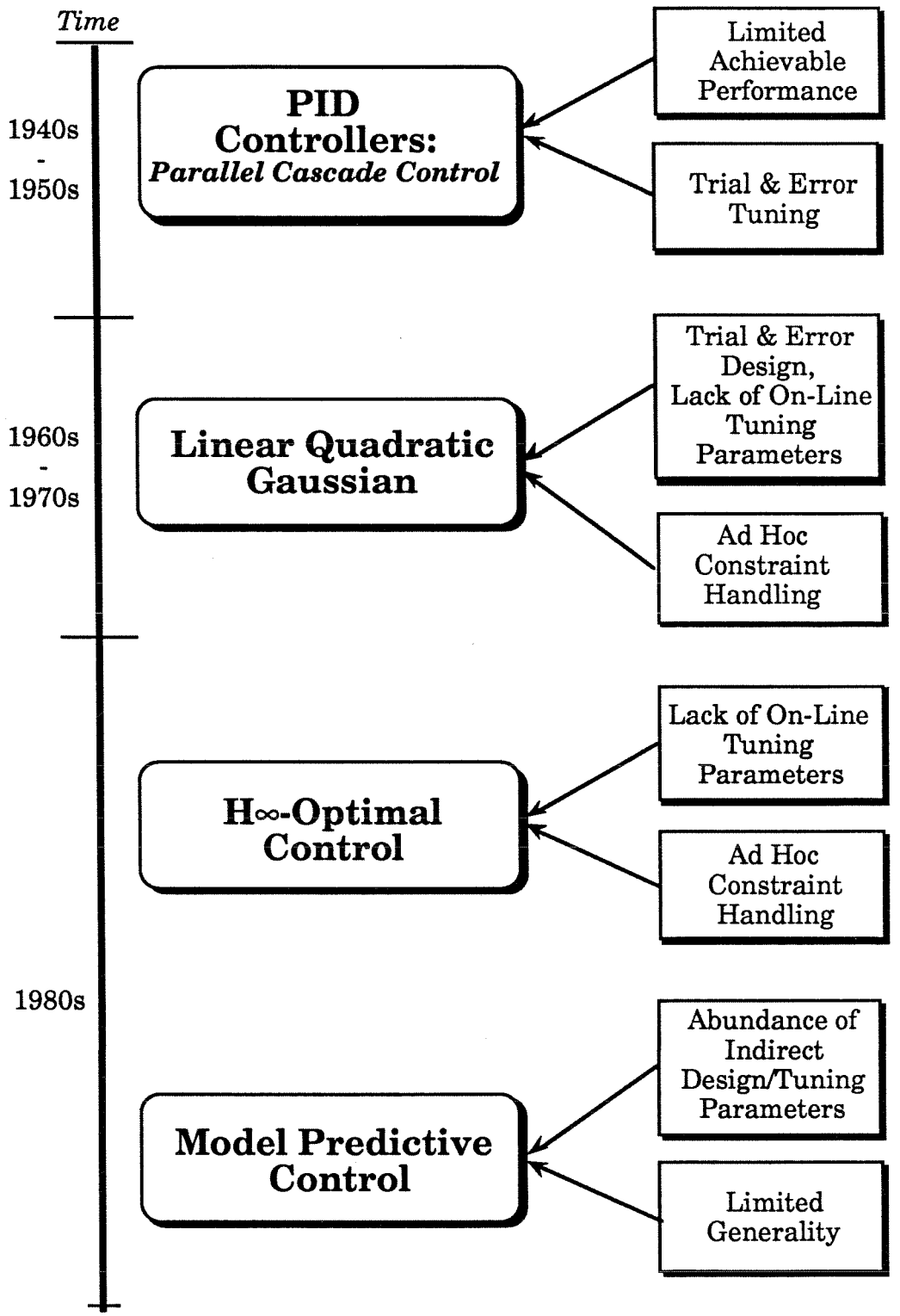


Figure 1.2. Schematic Representation of Issues for Inferential Control System Design and Past Developments

1. Establishment of a unifying framework for MPC in which a clear connection is drawn between various MPC controllers and LTI controllers and subsequent extension of traditional MPC techniques to general inferential control problems.

2. Providing MPC and LQG controllers with tuning/design parameters that have specific, well-understood effects on the system robustness.

3. Devising constraint handling strategies and failure tolerance schemes for LQG, MPC, and $\mu$-Synthesis controllers.

This thesis will provide answers (some complete and others only partial) to these issues.

## 1.5 Thesis Overview

Chapter 2 provides a necessary mathematical background for the further developments in the thesis. Some definitions and terminologies used in robust control are given and the inferential control problem studied in this thesis is formally introduced. The section also provides a brief summary of major results for the Structured Singular Value theory, which is the main theoretical basis for the work in this thesis.

The rest of the thesis is roughly divided into two parts: Chapter 3 which is devoted to the topic of measurement selection and Chapters 4-5 that are devoted to inferential control system design.

In Chapter 3, an approach to the problem of measurement selection is outlined. The approach taken is to eliminate systematically undesirable candidates for which a controller satisfying a given performance specification cannot be designed. Within this framework, the SSV theory is used as a main vehicle to develop a number of measurement screening tools that address the issue of model/plant mismatch as well as other aforementioned issues in a rigorous and general way. Some proposed tools are independent of the design methods while others are tied to specific design methods.

Various previously proposed criteria are discussed in perspective of the new method. Even though we develop the chapter in the context of measurement selection, the presented method is applicable to the general problem of control structure selection (which involves selection of actuators as well as measurements) without modification. Two example applications of the new tools are discussed: applications to a binary high-purity distillation column and multi-component distillation column.

Chapter 4 is devoted to the output estimation based approach to inferential control systems design. This approach involves two independent design steps: design of an output estimator which calculates the estimates for the primary variables from the available measurements and that of a controller which computes the manipulated input moves on the basis of the estimates. The strategic positioning of the output estimation based approach before the state estimation based approach (which is the major contribution of this thesis) in this thesis is due to the fact that the control system design for the former approach is a special case of the state estimation based design presented in Chapter 5 and is therefore much simpler. By presenting the simper methods first, we hope that readers will acquire background knowledge and familiarity with our notation before moving onto more complex and general cases.

The output estimator design is discussed in two different contexts: the case where a full dynamic model relating manipulated inputs and disturbances to primary and secondary variables is available and the case where only plant data for primary and secondary variables are available. For the former case, two major design approaches, Kalman filter design and $\mu$-Synthesis design, are outlined and their relative merits are compared. For the latter case, various regression techniques in the literature and their suitability for the estimator design are discussed.

For control system design, traditional techniques such as LQG and IMC are discussed and extended. We also present a novel MPC technique which combines the general state estimation of LQG and operational merits of the tranditional MPC

techniques. It is also shown that LQG and MPC controllers can be equipped with a set of intuitive, simple on-line tuning parameters without introducing additional complexity to the controllers. Their connections to the traditional techniques such as IMC and DMC are clearly drawn and some of the limitations of these traditional techniques are pointed out.

In order to make the discussion complete, we also discuss $\mu$-Synthesis, which can directly exploit the given uncertainty model. It is presented as more of a forward-looking research topic and a number of open theoretical/practical issues are pointed out. The chapter concludes with an application of the techniques to a heavy oil fractionator ("Shell Control Problem") [54].

Chapter 5 is devoted to the development of a general inferential control system design method via state estimation. In contrast to the output estimation based approach of Chapter 4, the approach taken in this chapter is to design directly a full inferential controller that computes the input moves from available measurements. We address the stability/performance issues in the presence of model/plant mismatch as well as various operational issues such as constraint handling and actuator/sensor failure tolerance. First, the traditional LQG design method is presented for a modified state space model to which most process control problems fit in more a natural way. Constraint-handling strategies and actuator/sensor failure handling schemes for the LQG controllers are discussed. Finally, an augmented form of the LQG controller which eliminates nonintuitive, redundant design parameters and provides for intuitive on-line tuning is introduced. The main purpose of the discussion on the LQG design is not in itself, but to lead into the subsequent development of a Model Predictive Control technique.

One of the main contributions of this thesis is a novel Model Predicitve Control technique that is applicable to the general inferential control problem. State estimation techniques for the LQG design method is combined with finite receding horizon

control used by the tranditional MPC techniques and the end result is an inferential control system design method that is capable of dealing with the issue of model uncertainty as well as various operational issues. A drawback of the method is that it does not exploit the given information on model uncertainty in a direct way as $\mu$-Synthesis does for example. Design/tuning parameters are rather to be selected on the basis of qualitative understandings, and the quantitative performance of the designed control system in the presence of possible mismatches have to be tested through the SSV analysis. Chapter 5 concludes with an application of discussed design methods to a binary high-purity distillation column.

In Chapter 6, the contributions of the thesis are summarized and put in perspective. In addition, suggestions for future research work on the topic of measurement seletion and inferential control system design are given.

Appendix A presents an MPC technique that is analogous to the state-space MPC technique presented in Chapter 4 and uses step response models. Main contributions of this work is that it extends the applicability of the step response model based MPC techniques to integrating systems and to systems with "slow" disturbances and that it provides for intuitive tuning parameters that has direct relationships with closed-loop response time.

Appendix B presents a case study of a high-purity distillation column in which some of the techniques developed in the thesis are brought together and applied to a practical control problem.

# Chapter 2

# Preliminaries

## 2.1 Definitions, Nomenclature

In this section, we present a few mathematical definitions that are necessary for further development of the paper.

### 2.1.1 Function Norms

#### $\mathcal{L}_2$-Norm of Continuous-Time Signals

A continuous-time-domain signal $x(t)$ $(\mathcal{R} \rightarrow \mathcal{R}^n)$ belongs to the function space $\mathcal{L}_2[0,\infty)$ if

1. $x(t) = 0 \quad \forall t < 0$
2. $\|x(t)\|_{\mathcal{L}_2} < \infty$

where the $\mathcal{L}_2$-norm of $x(t)$ is defined as follows:

$$\|x(t)\|_{\mathcal{L}_2} = \left(\int_0^\infty x^T(t)x(t)dt\right)^{1/2} \tag{2.1}$$

From Parseval's relation,

$$\|x(t)\|_{\mathcal{L}_2} = \left(\frac{1}{2\pi}\int_{-\infty}^{\infty} \hat{x}^*\hat{x}|_{s=j\omega}d\omega\right)^{1/2} \tag{2.2}$$

where $\hat{x}$ represents the Laplace-transform of signal $x(t)$ and $(\cdot)^*$ denotes the complex conjugate.

### $H_2$-Norm of Continuous-Time, Causal Convolution Operators

Let $M$ be a convolution operator mapping $\mathcal{L}_2[0,\infty)$ to $\mathcal{L}_2[0,\infty)$. Then, $H_2$-norm of $M$ is defined as follows:

$$\|M\|_2 = \left(\frac{1}{2\pi}\int_{-\infty}^{\infty} \text{trace}\left(\hat{M}^*\hat{M}|_{s=j\omega}\right) d\omega\right)^{1/2} \tag{2.3}$$

where $\hat{M}$ is the Laplace transform of the impulse response matrix of $M$.

### $H_\infty$-Norm (Induced $\mathcal{L}_2$-Norm) of Continuous-Time, Causal Convolution Operators

Let $M$ be a convolution operator mapping $\mathcal{L}_2[0,\infty)$ to $\mathcal{L}_2[0,\infty)$. $H_\infty$-norm of $M$ is defined as the induced-norm of $M$ in the space of $\mathcal{L}_2[0,\infty)$ that can be expressed as follows:

$$\|M\|_\infty = \sup_{x\in\mathcal{L}_2[0,\infty)} \frac{\|Mx\|_{\mathcal{L}_2}}{\|x\|_{\mathcal{L}_2}} = \sup_\omega \bar{\sigma}(\hat{M}|_{s=j\omega}) \tag{2.4}$$

where $\hat{M}$ is again the Laplace transform of the impulse response matrix of $M$ and $\bar{\sigma}(\cdot)$ denotes the maximum singular value.

An analogous set of definitions are available for discrete-time signals and covolution operators as well.

### $\ell_2$-Norm of Discrete-Time Signals

A discrete-time-domain signal $x(k)$ $(\mathcal{I} \to \mathcal{R}^n)$ belongs to the function space $\ell_2[0,\infty)$ if

1. $x(k) = 0 \quad \forall k < 0$
2. $\|x(k)\|_{\ell_2} < \infty$

where the $\ell_2$-norm of $x(k)$ is defined as follows:

$$\|x(k)\|_{\ell_2} = \left(\sum_{k=0}^{\infty} x^T(k)x(k)\right)^{1/2} \tag{2.5}$$

Again, from Parseval's relation,

$$\|x(k)\|_{\ell_2} = \left(\frac{T}{2\pi}\int_{-\frac{\pi}{T}}^{\frac{\pi}{T}} \hat{x}^*\hat{x}|_{z=e^{j\omega T}} d\omega\right)^{1/2} \tag{2.6}$$

where $\hat{x}(z) = \mathcal{Z}(x(k))$. $\mathcal{Z}\{x(k)\}$ is defined as

$$\mathcal{Z}\{x(k)\} = \sum_{k=0}^{\infty} x(k)\frac{1}{z^k} \tag{2.7}$$

$T$ is the time interval that each discrete time unit represents. The reason for specifying $T$ in the formula instead of letting $T = 1$ as many text books do is because we want to give the frequency $\omega$ the same meaning as in the continuous-time case.

## $H_2$-Norm of Discrete-Time, Causal Convolution Operators

Let $M$ be a convolution operator mapping $\ell_2[0,\infty)$ to $\ell_2[0,\infty)$. Then, $H_2$-norm of $M$ is defined as follows:

$$\|M\|_2 = \left(\frac{T}{2\pi}\int_{-\frac{\pi}{T}}^{\frac{\pi}{T}} \text{trace}\left(\hat{M}^*\hat{M}|_{z=e^{j\omega T}}\right) d\omega\right)^{1/2} \tag{2.8}$$

where $\hat{M}(z)$ is defined as

$$\hat{M}(z) = \mathcal{Z}\{M\delta(k)\}; \quad \delta(k) = \begin{cases} 1 \text{ for } k = 0 \\ 0 \text{ for } k \neq 0 \end{cases} \tag{2.9}$$

### $H_\infty$-Norm (Induced $\ell_2$-Norm) of Discrete-Time, Causal Convolution Operators

Let $M$ be a convolution operator mapping $\ell_2[0,\infty)$ to $\ell_2[0,\infty)$. The induced-norm of $M$ in the space of $\ell_2[0,\infty)$ ("$H_\infty$-norm") is expressed as

$$\|M\|_\infty = \sup_{x\in\ell_2[0,\infty)} \frac{\|Mx\|_{\ell_2}}{\|x\|_{\ell_2}} = \sup_{0\le\omega\le\frac{\pi}{T}} \bar{\sigma}(\hat{M}|_{z=e^{j\omega T}}) \tag{2.10}$$

## 2.1.2 Linear Fractional Transformation

We will use the following notations for linear fractional transformations (LFT):

$$\mathcal{F}_u(X,Y) = X_{22} + X_{21}Y(I - X_{11}Y)^{-1}X_{12} \tag{2.11}$$

$$\mathcal{F}_\ell(X,Y) = X_{11} + X_{12}Y(I - X_{22}Y)^{-1}X_{21} \tag{2.12}$$

where $X$ is partitioned in such a way that $X_{11}$ has the same dimension as $Y^T$ for the upper LFT ($\mathcal{F}_u$) and $X_{22}$ has the same dimension as $Y^T$ for the lower LFT ($\mathcal{F}_\ell$). These definitions are illustrated in terms of block diagram in Figure 2.1. $X$ and $Y$ can be either transfer functions or complex matrices.

## 2.1.3 Strucutured Singular Value

The Structured Singular Value ($\mu : \mathcal{C}^{n\times n} \times \Delta \to \mathcal{R}_{0+}$) is defined as follows:

**Definition 2.1 Structured Singular Value ($\mu$)**

*Let $M \in \mathcal{C}^{n\times n}$ and define the set $\mathbf{\Delta}$ as follows:*

$$\mathbf{\Delta} = \left\{ \text{diag}\,[\Delta_1 \cdots, \Delta_\ell, \delta_1 I_{r_1}, \cdots, \delta_m I_{r_m}]\,; \Delta_i \in \mathcal{C}^{p_i\times p_i}, \delta_j \in \mathcal{C}; \sum_{i=1}^{\ell} p_i + \sum_{j=1}^{m} r_j = n \right\} \tag{2.13}$$

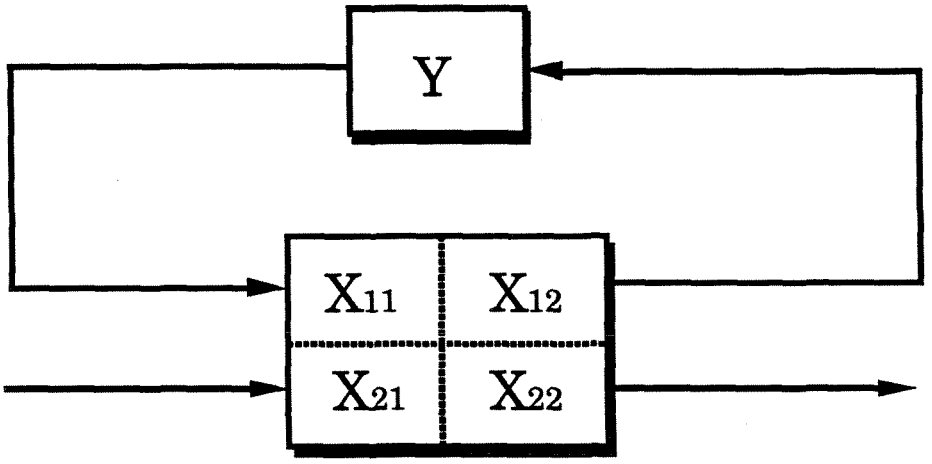


(a) Upper Linear Fractional Transformation

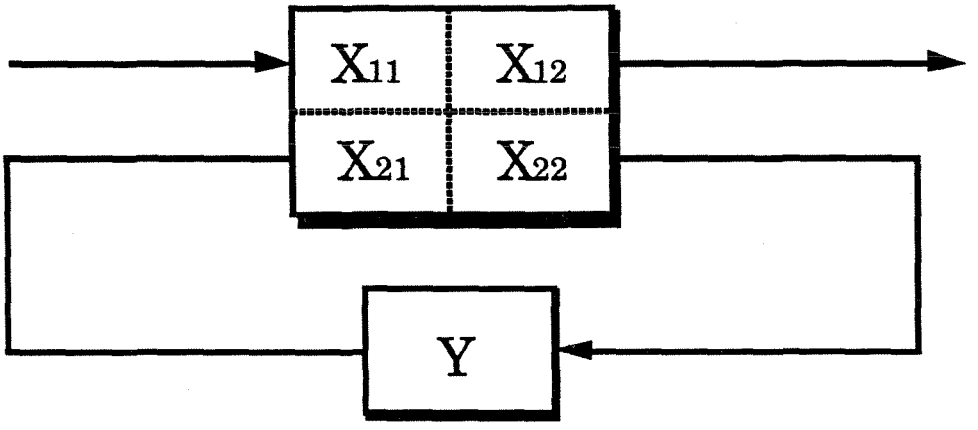


(b) Lower Linear Fractional Transformation

Figure 2.1. Upper and Lower Linear Fractional Transformations

*Then $\mu_{\mathbf{\Delta}}(M)$ ($\mu$ of $M$ with respect to the uncertainty structure $\mathbf{\Delta}$) is defined as*

$$\mu_{\mathbf{\Delta}}(M) = \begin{cases} [\min_{\Delta} \{\bar{\sigma}(\Delta) : \det(I + M\Delta) = 0,\ \Delta \in \mathbf{\Delta}\}]^{-1} \\ \\ 0 \text{ if } \exists \text{ no } \Delta \in \mathbf{\Delta} \text{ such that } \det(I + M\Delta) = 0 \end{cases} \tag{2.14}$$

The structured singular value has the following lower and upper bounds:

$$\max_{Q \in \mathcal{Q}} \rho(QM) = \mu_{\mathbf{\Delta}}(M) \leq (\approx) \inf_{D \in \mathcal{D}} \bar{\sigma}(DMD^{-1}) \tag{2.15}$$

where

$$\mathcal{Q} = \{Q \in \mathbf{\Delta} : Q^*Q = I_n\} \tag{2.16}$$

$$\mathcal{D} = \{\text{diag}\,[d_1 I_{p_1}, \cdots, d_\ell I_{p_\ell}, D_1, \cdots, D_m] : d_j \in \mathcal{R}_+, D_i \in \mathcal{C}^{r_i \times r_i}, D_i = D_i^* > 0\} \tag{2.17}$$

and $\rho(\cdot)$ denotes the spectral radius. The maximum of the lower bound is always equal to $\mu$, but the maximization is a nonconvex optimization [52]. The minimization of the upper bound in general does not achieve $\mu$ except for a few special cases (*e.g.*, cases where $\Delta$ has the block structure of three or less blocks). However, the infimum is very close (essentially equal within the accuracy of engineering significance) to $\mu$ even for general cases. The minimization can be formulated into a convex optimization and, for that reason, the infimum has been used extensively in various tests involving the numerical calculation of $\mu$.

## 2.2 Modelling of Systems

Most real systems are modelled more naturally in continuous time. However, discrete time models are often used in digital control system design and analysis for mathe-

matical convenience. In this section, we present general system descriptions, both for the continuous- and discrete-time domains, that are used for the inferential control problem treated in this thesis.

Because our problem involves multiple sampling rates, it is convenient to introduce the following time units and express the time in terms of these units:

**Definition 2.2 Shortest Time Unit (STU)**

*Let the sampling times of measurements be* $n_1\tau, n_2\tau, \cdots, n_m\tau$. *Then* $\tau_S$ *(denoting STU) is defined as follows:*

$$\tau_S = \{g.c.d.(n_1, n_2, \cdots, n_m)\}\tau \tag{2.18}$$

*where* $g.c.d.\{\cdot\}$ *represents the greatest common divisor.*

**Definition 2.3 Basic Time Unit (BTU)**

*Let the sampling times of measurements be* $n_1\tau, n_2\tau, \cdots, n_m\tau$. *Then,* $\tau_B$ *(denoting BTU) is defined as follows:*

$$\tau_B = \{\ell.c.m.(n_1, n_2, \cdots, n_m)\}\tau \tag{2.19}$$

*where* $\ell.c.m.\{\cdot\}$ *represents the least common multiple.*

The time $t$ will be sometimes represented by the pair $(k, j)$ denoting $t = (kN + j)\tau_S$ where $k \in \mathcal{I}^{0+}, j = 1, \cdots, N-1$ and $N = \tau_B/\tau_S$. For convenience of exposition, we will occasionally write $t = (k, mN + j)$ to mean $t = (k + m, j)$.

### 2.2.1 Continuous Time

#### Nominal Model

The nominal process model we use is the following state-space differential equation:

**Process:**

$$\dot{x}(t) = A^c x(t) + B_u^c u(t) + B_d^c d(t) \tag{2.20}$$

$$y_c(t) = C_c^c x(t) \tag{2.21}$$

$$y_s(t) = C_s^c x(t) \tag{2.22}$$

$$\tag{2.23}$$

**Measurements:**

$$\begin{bmatrix} \hat{y}_{c_{\theta_c}}(k,j) \\ \hat{y}_{s_{\theta_s}}(k,j) \end{bmatrix} = \begin{bmatrix} C_c(j)x(k,j-\theta_c) \\ C_s(j)x(k,j-\theta_s) \end{bmatrix} + \begin{bmatrix} v_c(k,j) \\ v_s(k,j) \end{bmatrix} \tag{2.24}$$

$x$ : state vector

$d$ : disturbance vector

$r$ : primary variable reference input vector

$v_c$: primary measurement noise vector

$v_s$: secondary measurement noise vector

$u$ : manipulated input vector

$y_c$: primary variable vector

$y_e$: primary variable error $(y_c - r)$ vector

$y_s$: secondary variable vector

$\hat{y}_c$: noise-corrupt primary measurement vector

$\hat{y}_s$: noise-corrupt secondary measurement vector

$w$: external input vector $(w = [d^T\ r^T\ v_c^T\ v_s^T]^T)$

$e$ : controlled variable vector $(e = [y_e^T\ u^T]^T)$

The superscript $\{\cdot\}^c$ is used to distinguish the model parameters from those of the discrete-time model that is introduced subsequently. $C_c^c(j)$ and $C_s^c(j)$ are $C_c^c$ and $C_s^c$

with the elements of all rows corresponding to the measurements unavailable at $j^{\text{th}}$ sampling instant set to zeros. It is assumed that $(A^c, B_u^c)$ is a stabilizable pair and $\left(\begin{bmatrix} C_c^c \\ C_s^c \end{bmatrix}, A^c\right)$ is a detectable pair. $\theta_c$ and $\theta_s$ are the measurement delays (in terms of STU) of the primary and secondary measurements respectively.

Figure 2.2 is a block diagram representation of the inferential control problem for the system described through (2.20)-(2.24). The relationships between the input-output representation and the state space model are as follows:

$$G_{y_c d}(s) = C_c^c (sI - A^c)^{-1} B_d^c \tag{2.25}$$

$$G_{y_s d}(s) = C_s^c (sI - A^c)^{-1} B_d^c \tag{2.26}$$

$$G_{y_c u}(s) = C_c^c (sI - A^c)^{-1} B_u^c \tag{2.27}$$

$$G_{y_s u}(s) = C_s^c (sI - A^c)^{-1} B_u^c \tag{2.28}$$

The above model assumes that the effect of the disturbances ($d$) and manipulated inputs ($u$) on the system outputs ($y_c$ and $y_s$) are described by *strictly proper* transfer functions and the measurement noise ($v_c$ and $v_s$) and the system disturbances ($d$) are uncorrelated. These assumptions are satisfied for almost all practical problems. Otherwise, the formulation is general enough to treat any conceivable control problem.

## Uncertain Model

An inexactly known continuous-time system can be represented as an LFT of $G(s)$ and $\Delta_u$ (see Figure 2.3). $G(s)$ is the transfer function model relating the input vector $\left[v_o^T \; w^T \; u^T\right]^T$ to the output vector $\left[v_i^T \; e^T \; \hat{y}_c^T \; \hat{y}_s^T \; r^T\right]^T$. $\begin{bmatrix} G_{22} & G_{23} \\ G_{32} & G_{33} \end{bmatrix}$ ($\triangleq P_{\text{nom}}$) is the *nominal* model of the sytem. $\Delta_u$ is a set of complex perturbations to the frequency response matrix of the nominal model. More specifically, the "true" system can be any system $P_\Delta(s)$ satisfying the following two conditions:

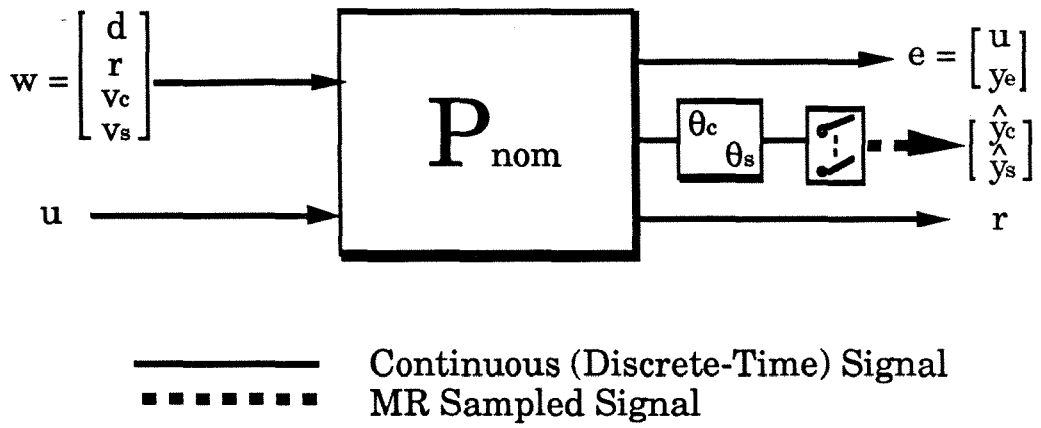


$$P_{\text{nom}} = \left[\begin{array}{cccc|c} G_{y_c d} & -I & 0 & 0 & G_{y_c u} \\ 0 & 0 & 0 & 0 & I \\ G_{y_c d} & 0 & I & 0 & G_{y_c u} \\ G_{y_s d} & 0 & 0 & I & G_{y_s u} \\ 0 & I & 0 & 0 & 0 \end{array}\right] \tag{2.29}$$

Figure 2.2. General Block Diagram Representation of a Multi-Rate Sampled-Data System

1. The frequency response matrix of the system $P_\Delta|_{s=j\omega}$ for each frequency belongs to the set $\mathbf{P_u}(\omega)$ where

$$\begin{aligned} \mathbf{P_u}(\omega) &= \left\{ (\mathcal{F}_u(G, \Delta_u)|_{s=j\omega} : \Delta_u \in \mathbf{B\Delta_u} \right\} \\ \mathbf{B\Delta_u} &= \{\Delta \in \mathbf{\Delta_u} : \bar{\sigma}(\Delta) \leq 1\} \\ \mathbf{\Delta_u} &= \Big\{ \text{diag}(\Delta_1, \cdots, \Delta_\ell, \delta_1 I_{r_1}, \cdots, \delta_m I_{r_m}) : \Delta_i \in \mathcal{C}^{p_i \times p_i}, \delta_j \in \mathcal{C}, \\ &\qquad \sum_i p_i + \sum_j r_j = \dim\{v_o\} = \dim\{v_i\}, 1 \leq i \leq \ell, 1 \leq j \leq m \Big\} \end{aligned} \tag{2.30}$$

2. $P_\Delta(s)$ has the same number of unstable poles (poles in the closed RHP) as the nominal model $P_{\text{nom}}(s)$.

We will refer to the set of systems satisfying the above conditions as $\mathbf{P_\Pi}$. The above uncertainty type is called *structured* since $\Delta_u$ carries a specific block-structure as

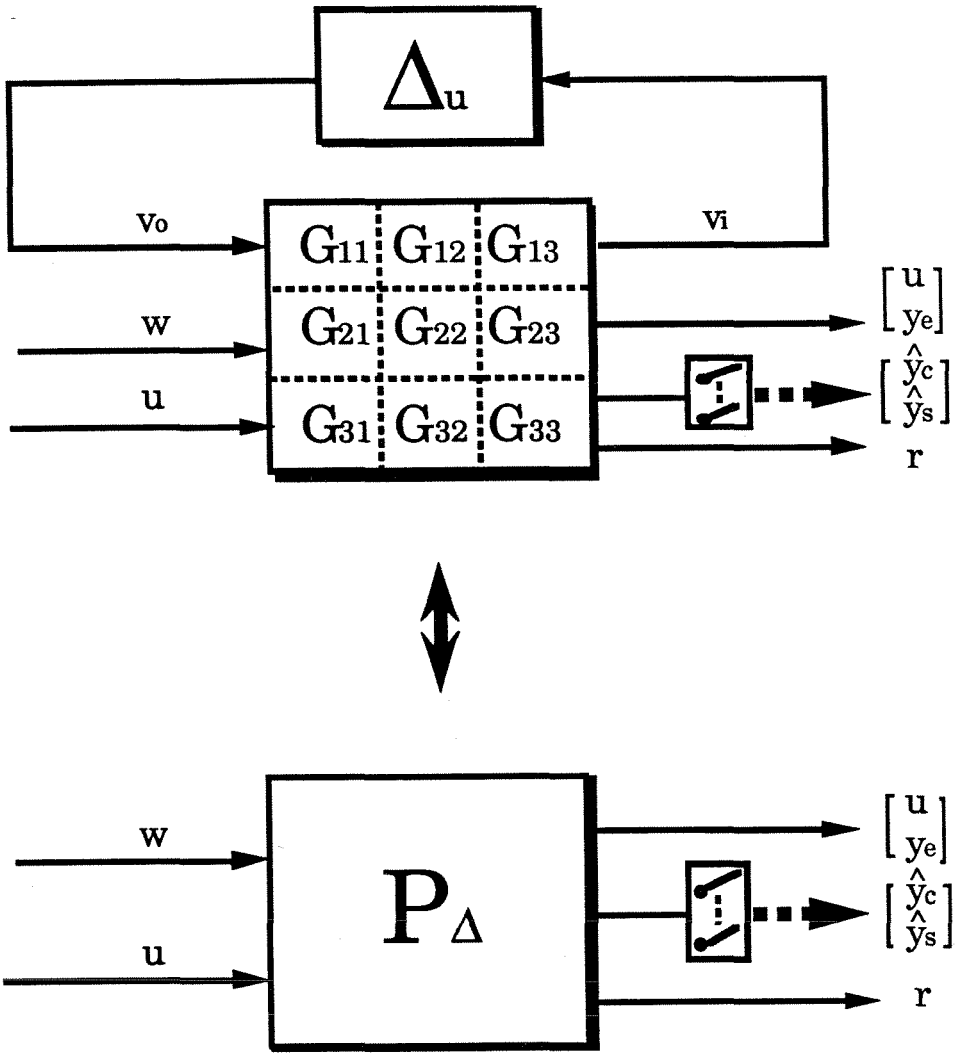


Figure 2.3. General Block Diagram Representation of a System with Norm-Bounded Perturbations Describing Model/Plant Mismatch

opposed to being a single full block. We assumed that each $\Delta_i$ is square. This is without loss of generality since we can always express a $m \times n$ or $n \times m$ $(m > n)$ nonsquare $\Delta_i$ as the product of a $m \times m$ square $\Delta_i$ and a weighting matrix:

$$\Delta_i^{m\times n} = \Delta_i^{m\times m} \begin{bmatrix} I_n \\ 0 \end{bmatrix} \tag{2.31}$$

$$\Delta_i^{n\times m} = \begin{bmatrix} I_n & 0 \end{bmatrix} \Delta_i^{m\times m} \tag{2.32}$$

### 2.2.2 Discrete Time

#### Nominal Model

The process may be sometimes described as a discrete-time system where each discrete time unit represents the time interval of $\tau_S$, the STU. The discrete-time model that corresponds to the continuous-time model described through (2.20)-(2.24) is given by the following state-space difference equation:

**Process:**

$$x(k,j) = Ax(k,j-1) + B_u u(k,j-1) + B_d d(k,j-1) \tag{2.33}$$

$$y_c(k,j) = C_c x(k,j) \tag{2.34}$$

$$y_s(k,j) = C_s x(k,j) \tag{2.35}$$

$$\tag{2.36}$$

**Measurements:**

$$\begin{bmatrix} \hat{y}_{c_{\theta_c}}(k,j) \\ \hat{y}_{s_{\theta_s}}(k,j) \end{bmatrix} = \begin{bmatrix} C_c(j)x(k,j-\theta_c) \\ C_s(j)x(k,j-\theta_s) \end{bmatrix} + \begin{bmatrix} v_c(k,j) \\ v_s(k,j) \end{bmatrix} \tag{2.37}$$

Again, it is assumed that $(A, B_u)$ is a stabilizable pair and $\left( \begin{bmatrix} C_c \\ C_s \end{bmatrix}, A \right)$ is a detectable pair.

The input/output representation for the system is given by the pulse transfer function

$$G_{y_c d}(z) = C_c(zI - A)^{-1}B_d \tag{2.38}$$

$$G_{y_s d}(z) = C_s(zI - A)^{-1}B_d \tag{2.39}$$

$$G_{y_c u}(z) = C_c(zI - A)^{-1}B_u \tag{2.40}$$

$$G_{y_s u}(z) = C_s(zI - A)^{-1}B_u \tag{2.41}$$

where $z$ represents a forward-shift operator. Again, the above model assumes that the effect of the disturbances ($d$) and manipulated inputs ($u$) on the system outputs ($y_c$ and $y_s$) are described by *strictly proper* pulse transfer functions (implying delay of at least one STU) and the measurement noise ($v_c$ and $v_s$) and the system disturbances ($d$) are uncorrelated.

## Uncertain Model

In an analogous manner to the continuous-time case, an inexactly known discrete-time system can be represented as an LFT of $G(z)$ and $\Delta_u$. $G(z)$ is again the pulse transfer function model relating the input vector $\left[v_o^T \; w^T \; u^T\right]^T$ to the output vector $\left[v_i^T \; e^T \; \hat{y}_c^T \; \hat{y}_s^T \; r^{T'}\right]^T$. The only minor difference is in the characterization of the perturbation $\Delta_u$. For a discrete-time system, the set of potential "true" systems is characterized by $P_\Delta(z)$ satisfying the following two conditions:

1. The frequency response matrix of the system $P_\Delta|_{z=e^{j\omega T}}$ for $0 \leq \omega$ belongs to the set $\mathbf{P_u}(\omega)$ where

$$\begin{aligned}
\mathbf{P_u}(\omega) &= \{(\mathcal{F}_u(G, \Delta_u)|_{z=e^{j\omega T}} : \Delta_u \in \mathbf{B\Delta_u}\} \\
\mathbf{B\Delta_u} &= \{\Delta \in \mathbf{\Delta_u} : \bar{\sigma}(\Delta) \leq 1\} \\
\mathbf{\Delta_u} &= \Big\{\mathrm{diag}(\Delta_1, \cdots, \Delta_\ell, \delta_1 I_{r_1}, \cdots, \delta_m I_{r_m}) : \Delta_i \in \mathcal{C}^{p_i \times p_i}, \delta_j \in \mathcal{C}, \\
&\qquad \sum_i p_i + \sum_j r_j = \dim\{v_o\} = \dim\{v_i\}, 1 \leq i \leq \ell, 1 \leq j \leq m\Big\}
\end{aligned} \tag{2.42}$$

   $T$ represents the time interval that each discrete time unit represents ($\tau_S$ in this case).

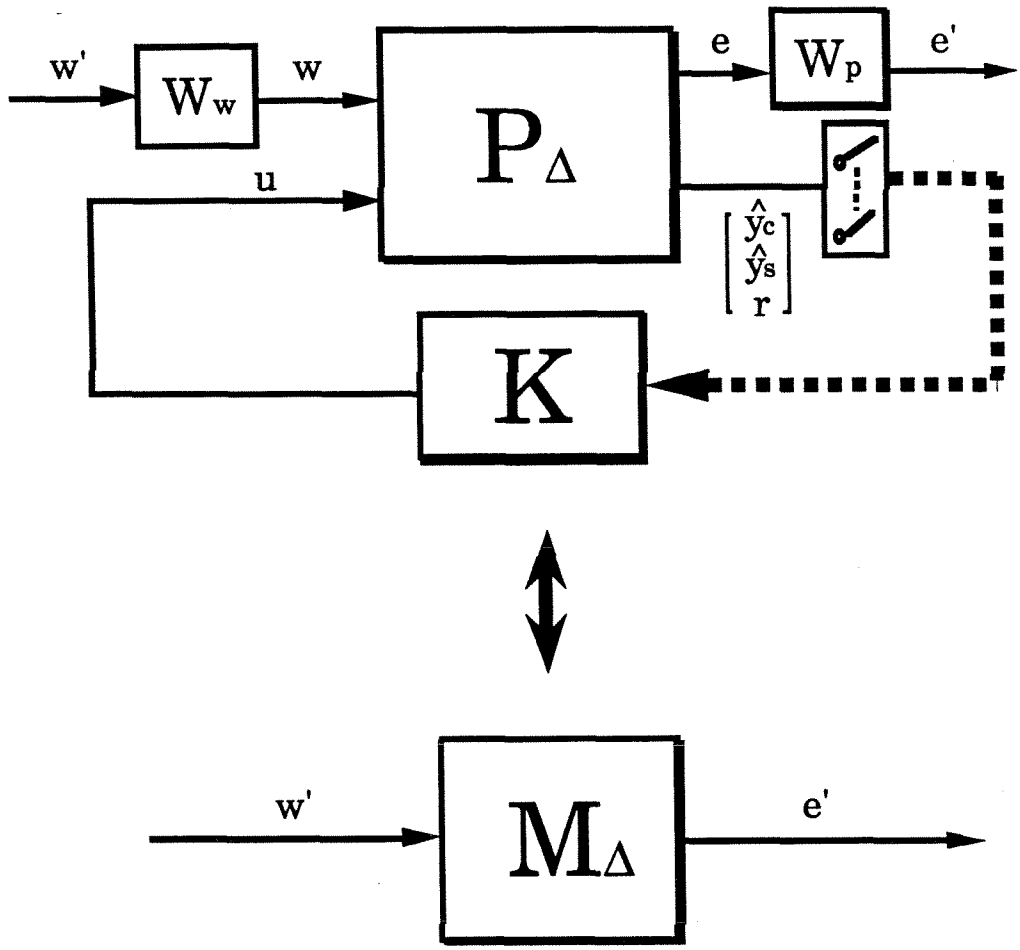


Figure 2.4. Closed-Loop Performance Specifications for a General System with Norm-Bounded Perturbations

2. $P_\Delta(z)$ has the same number of unstable poles (poles outside the open unit disk) as the nominal model $P_{\text{nom}}(z)$.

Again, we will refer to the set of systems satisfying the above conditions as $\mathbf{P}_\Pi$.

## 2.3 Performance Measures

Two popular performance measures are the $H_2$- and $H_\infty$-norm (as defined in Section 2.1.1) of the closed-loop operator $M_\Delta$ shown in Figure 2.4. $M_\Delta$ is the closed-loop operator relating the normalized inputs $w'$ to the weighted outputs $e'$ (through

frequency-dependent weights $W_w$ and $W_p$ respectively). Hence,

$$M_\Delta = W_p \mathcal{F}_\ell(P_\Delta, K) W_w \tag{2.43}$$

In the robust control terminology, a control system is said to achieve *nominal performance* when it satisfies the performance specification in the absence of any model/plant mismatch ($\Delta_u = 0 \ \ \forall\omega$). In addition, it is said to achieve *robust performance* when it satisfies the performance specification in the face of all prespecified model/plant mismatches (in other words, for every system belonging to $\mathbf{P}_\Pi$).

### 2.3.1 Continuous Time

A difficulty associated with assessing the closed-loop performance in the continuous time domain is that the presence of samplers cause the closed-loop system to be time-varying (although it is *periodically* time varying). Dailey [16] showed how the periodicity of time variance of samplers can be exploited to derive "conic sector" bounds which enable rigorous, though conservative, performance analysis. However, the conservativeness of the analysis method can be quite significant for some cases, limiting the method's universal applicability. When the sampling time is chosen to be small relative to the closed-loop bandwidth, a sampled-data system can be well approximated as an LTI system. In this section, we summarize first typical performance specifications and performance analysis methods for LTI systems. Then, we briefly discuss how sampled-data systems can be modified so that the introduced analysis methods can be applied to them.

#### $H_2$ Performance Measure for LTI Systems

Consider a hypothetical experiment where a unit impulse is injected to each input channel one by one. The $H_2$-norm of $M_\Delta$ measures the sum of the squared $\mathcal{L}_2$-norm

of the output vectors $e'(t)$. In other words,

$$\|M_\Delta\|_2 = \left( \sum_{i=1}^{\dim\{d'\}} \int_0^\infty (M_\Delta \delta_i(t))^T M_\Delta \delta_i(t) dt \right)^{1/2} \tag{2.44}$$

where $\delta_i$ is the unit impulse in the $i^{\text{th}}$ channel. By appropriate choices of normalizing weights $W_d$ and $W_p$, we can define the following two performance objectives:

1. The nominal performance is achieved if

$$\|M_{\text{nom}}\|_2 < 1 \tag{2.45}$$

$M_{\text{nom}}$ is $M_\Delta$ for $\Delta_u = 0$ and can be expressed as

$$M_{\text{nom}} = W_p(G_{22} + G_{23}K(I - G_{33}K)^{-1}G_{32})W_w \tag{2.46}$$

2. The robust performance is achieved if

$$\max_{P_\Delta \in \mathbf{P_\Pi}} \|M_\Delta\|_2 < 1 \tag{2.47}$$

Unfortunately, there is no method to test the condition (2.47) at current time.

## $H_\infty$ Performance Measure for LTI Systems

Consider all input signals $w'$ such that $\|w'\|_{L_2} < 1$. As a performance objective, we may want to minimize the "worst-possible" $\mathcal{L}_2$-norm of the output $e'(k)$. This "worst-possible" $\mathcal{L}_2$ norm of $e'(k)$ is the $H_\infty$-norm of $M_\Delta$. Again, by appropriately choosing the weighting functions $W_w$ and $W_p$, we can define the following two objectives:

1. The nominal performance is achieved if

$$\|M_{\text{nom}}\|_\infty < 1 \tag{2.48}$$

2. The robust performance is achieved if

$$\max_{P_\Delta \in \mathbf{P_\Pi}} \|M_\Delta\|_\infty < 1 \tag{2.49}$$

The condition (2.49) can be tested through a function called the Structured Singular Value (often denoted as "$\mu$") [17]:

$$\max_{P_\Delta \in \mathbf{P_\Pi}} \|M_\Delta\|_\infty < 1 \tag{2.50}$$

if and only if

1. *Nominal Stability*:

   $M_{\text{nom}}$ is stable

2. *Structured Singular Value Condition*:

$$\mu\left[\begin{array}{cc}\mathbf{\Delta_u} & \\ & \mathbf{\Delta_p}\end{array}\right]\left[\left\{\left\{\left[\begin{array}{cc}I & \\ & W_p\end{array}\right]\mathcal{F}_\ell(G,K)\left[\begin{array}{cc}I & \\ & W_w\end{array}\right]\right\}\Big|_{s=j\omega}\right]\right] < 1 \quad \forall\omega \in [0,\infty) \tag{2.51}$$

$$\mathbf{\Delta_p} = \left\{\Delta : \Delta \in \mathcal{C}^{\dim\{G_{22}\}}\right\} \tag{2.52}$$

## Frequency-Domain Performance Analysis for Single-Rate Sampled-Data Systems

A block diagram representing a typical sampled-data system is shown in Figure 2.5. The problem in performing frequency-domain analysis for sampled-data systems is that the samplers cannot be represented as transfer functions since they are time-varying. However, we may approximate them as LTI operators under certain as-

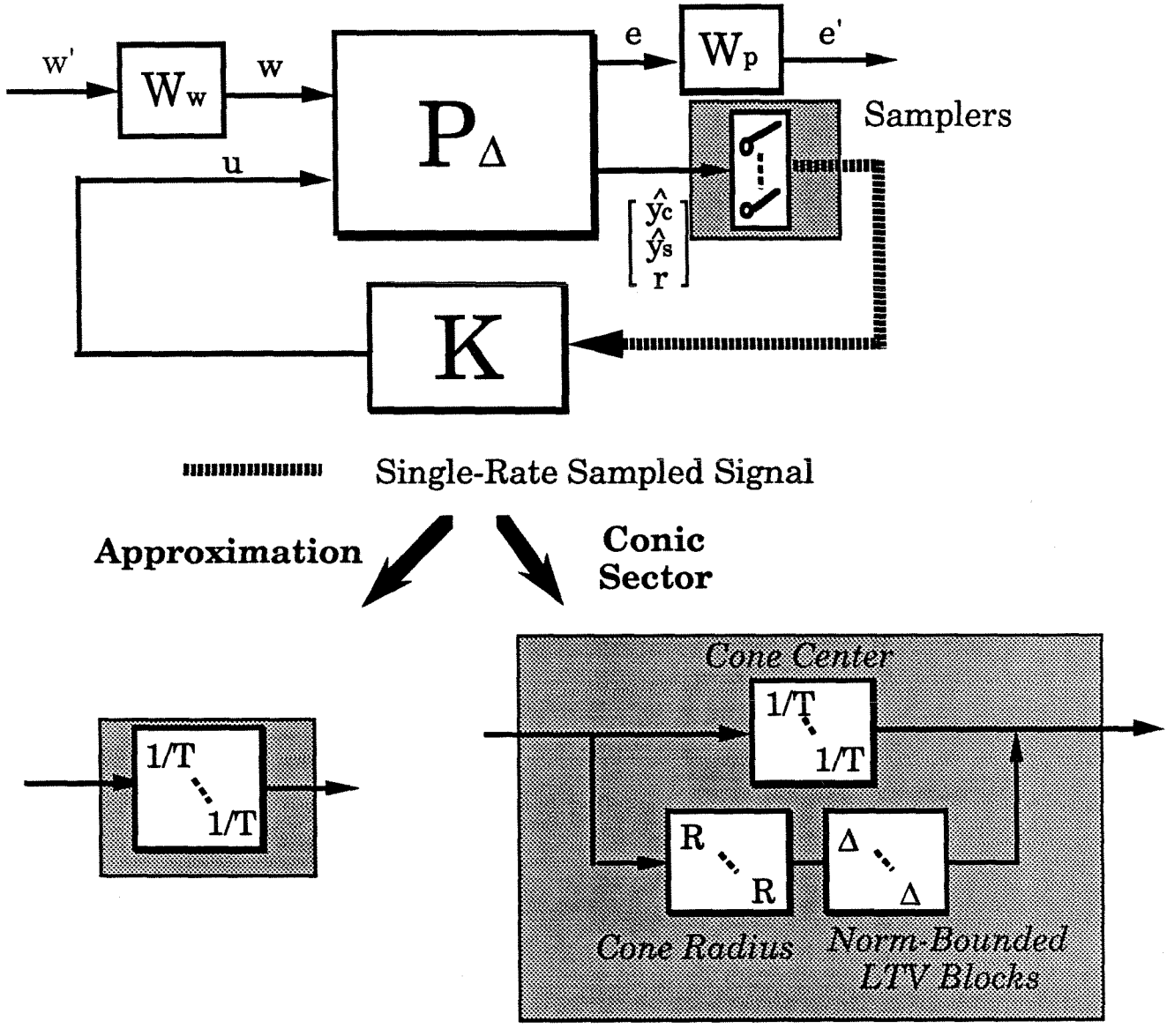


Figure 2.5. Block Diagram Representation of Typical Sampled-Data Systems Modifications for Frequency-Domain Analysis

sumptions.

The Fourier-transform of the sampled singal $\{y_m\}_T^*$ (expressed as impulse trains) is

$$\mathcal{L}\{(y_m)_T^*\}|_{s=j\omega} = \frac{1}{T}\sum_{k=-\infty}^{\infty} \mathcal{L}\{y_m\}|_{s=j\omega+k\frac{2\pi}{T}} \tag{2.53}$$

The notation $\mathcal{L}\{\cdot\}$ represents the Laplace transform. Now assume that frequency content of signal $y_m$ is limited to within the Nyquist band. That is, assume

$$|\mathcal{L}\{y_m\}|_{s=j\omega}| \approx 0 \text{ for } \frac{\pi}{T} \leq \omega < \infty \tag{2.54}$$

Then,

$$\mathcal{L}\{(y_m)_T^*\}|_{s=j\omega+k\frac{2\pi}{T}} = \frac{1}{T}\mathcal{L}\{y_m\}|_{s=j\omega} \text{ for } 0 \leq \omega \leq \frac{\pi}{T}, \forall k \tag{2.55}$$

Hence, within the Nyquist band ($0 \leq \omega \leq \frac{\pi}{T}$), the sampler is well approximated as $\frac{1}{T}$ assuming (2.54) is true. When the signals are properly anti-aliased, (2.54) is a good approximation. Note that he approximation of the samplers as $\frac{1}{T}$ does not hold outside the Nyquist band. However, the performance outside the Nyquist band is often of little interest since signals above the Nyquist frequency are attenuated through "holds" and "anti-aliasing filters." The Bode plot of a zero-order-hold is shown in Figure 2.6.

Another method that allows for a rigorous, conservative analysis is the "conic sector" method. In the conic sector method, the samplers are expressed conservatively as an LTI operator (called "cone center") plus an LTV block the norm-bound of which (called "cone radius") is expressed through another LTI operator – see Figure 2.5. It turns out that the optimal cone center for the sampler is exactly $\frac{1}{T}$. Most of the $\mu$-analysis results can be extended to treat the norm-bounded LTV blocks (together with the usual LTI blocks). Further details will not be discussed in this thesis; interested readers are referred to Dailey [16].

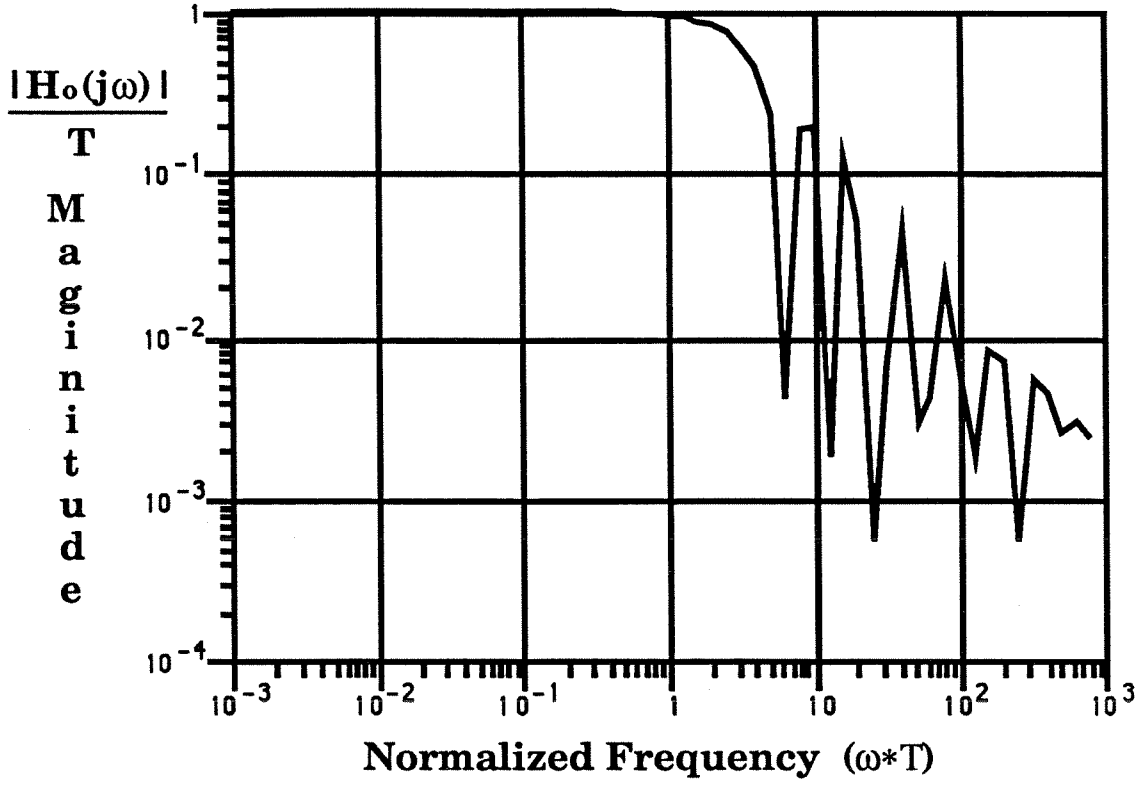


Figure 2.6. Bode Plot of Zero-Order-Hold

## Frequency-Domain Performance Analysis for Multi-Rate Sampled-Data System

The approximation method and the conic sector method that were discussed for single-rate sampled-data systems extend straightforwardly to multi-rate sampled-data systems. Namely, each sampler can be approximated (or its cone center can be chosen) as $\frac{1}{T_i}$ where $T_i$ is its respective sampling time. For multi-rate systems, however, the assumption of band-limitedness of signals may not hold for "slow-sampled" signals and a conservative approach such as the conic sector method may be necessary. In addition, another difficulty may arise from the fact that some of the sampled signals may go through parts of the controller that are shift-varying with respect to their sampling times. To elucidate this point, a typical control system for a double-rate sampled-data system is shown in Figure 2.7. The samplers within the controller

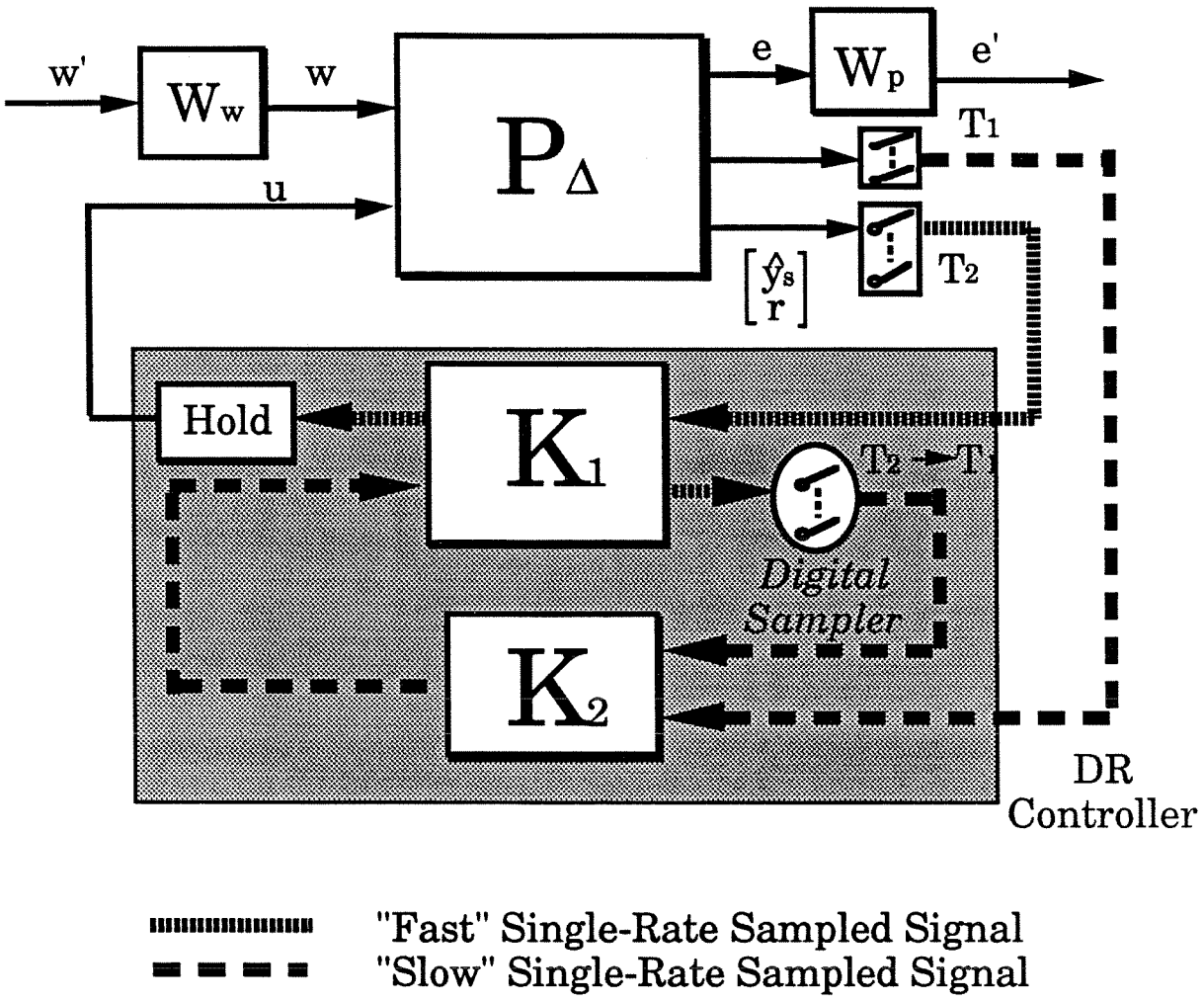


Figure 2.7. Block Diagram for Typical Double-Rate Sampled-Data Systems

(referred to as "digial sampler" in this thesis) must also be approximated or bounded with conic sectors (with shift-invariant cone center, radius and shift-varying $\Delta$ block). This will be discussed in the context of discrete-time systems in Section 2.3.2.

### 2.3.2 Discrete Time

In an analgous manner to the continuous-time case, one can specify performance requirements based on the $H_2$- and $H_\infty$-norm of the discrete-time closed-loop operator. Discrete-time performance analysis should be adequate for continuous-time systems if sampling time is chosen to be insignificant relative to the closed-loop bandwidth

and appropriate "anti-aliasing" of the measurements are performed [3,50].

## $H_2$ Performance Measure for SR Discrete-Time Systems

Suppose that $M_\Delta$ is a discrete-time closed-loop operator for a single-rate (SR) discrete-time system where all measurements are available at every time unit. Consider a hypothetical experiment where a unit impulse is injected to each input channel one by one. The $H_2$-norm of $M_\Delta$ measures the sum of the squared $\ell_2$-norm of the output vectors $e'(k)$. In other words,

$$\|M_\Delta\|_2 = \left( \sum_{i=1}^{\dim\{d'\}} \sum_{k=0}^{\infty} (M_\Delta \delta_i(k))^T M_\Delta \delta_i(k) \right)^{1/2} \tag{2.56}$$

where $\delta_i$ is the discrete-time unit pulse in the $i^{\text{th}}$ channel. Again, by appropriate normalization of $e'$, we can define the following two performance objectives:

1. The nominal performance is achieved if

$$\|M_{\text{nom}}\|_2 < 1 \tag{2.57}$$

where

$$M_{\text{nom}} = W_p(G_{22} + G_{23}K(I - G_{33}K)^{-1}G_{32})W_w \tag{2.58}$$

2. The robust performance is achieved if

$$\max_{P_\Delta \in \mathbf{P}_\Pi} \|M_\Delta\|_2 < 1 \tag{2.59}$$

As for the continuous-time case, there is no method to test the condition (2.59) at present.

## $H_2$ Performance Measure for MR Discrete-Time Systems

When the measurements are sampled at multiple rates, the resulting $M_\Delta$ is a periodically shift-varying (PSV) system with the period of $\tau_B$. Hence, $\delta_i$ entering the system at $t = (k, j)$ and $t = (m, n)$ lead to different outputs $M_\Delta \delta_i$ if $j \neq n$. However, the periodicity of the system ensures that the outputs are the same for $k \neq m$ as long as $j = n$. The natural way of extending the definition of $H_2$-norm to MR systems is as follows:

$$\|M_\Delta\|_2 = \left( \frac{1}{N} \sum_{\ell=0}^{N-1} \sum_{i=1}^{\dim\{w'\}} \sum_{t=(0,0)}^{\infty} (M_\Delta[\delta_i]_\ell(t))^T M_\Delta[\delta_i]_\ell(t) \right)^{1/2} \tag{2.60}$$

where $[\delta_i]_\ell$ denotes unit impulse entering at $i^{\text{th}}$ channel at $t = (0, \ell)$. Note that the above definition reduces to the standard $H_2$-norm definition if the system is shift-invariant. In addition, the resulting $H_2$-norm for a PTV system is independent of the choice of time zero. The nominal performance and robust performance can be defined in exactly the same way as for SR systems.

## $H_\infty$ Performance Measure for SR Discrete-Time Systems

Consider all input signals $d'$ such that $\|d'\|_{L_2} < 1$. As a performance objective, we may want to minimize the "worst-possible" $\ell_2$-norm of the output $e'(k)$. This "worst possible" $\ell_2$ norm of $e'(k)$ is the $H_\infty$-norm of $M_\Delta$. As before, we can define the following two objectives:

1. The nominal performance is achieved if

$$\|M_{\text{nom}}\|_\infty < 1 \tag{2.61}$$

2. The robust performance is achieved if

$$\max_{P_\Delta \in \mathbf{P_\Pi}} \|M_\Delta\|_\infty < 1 \tag{2.62}$$

The condition (2.62) can be tested through the following condition on the Structured Singular Value:

$$\max_{P_\Delta \in \mathbf{P_\Pi}} \|M_\Delta\|_\infty < 1 \tag{2.63}$$

if and only if

1. *Nominal Stability*:

   $M_{\text{nom}}$ is stable.

2. *Structured Singular Value Condition*:

$$\mu \left[ \begin{array}{cc} \mathbf{\Delta_u} & \\ & \mathbf{\Delta_p} \end{array} \right] \left[ \left\{ \left[ \begin{array}{cc} I & \\ & W_p \end{array} \right] \mathcal{F}_\ell(G,K) \left[ \begin{array}{cc} I & \\ & W_w \end{array} \right] \right\} \Big|_{z=e^{j\omega T}} \right] < 1 \quad 0 \le \omega \le \frac{\pi}{T} \tag{2.64}$$

$$\mathbf{\Delta_p} = \left\{ \Delta : \Delta \in \mathcal{C}^{\dim\{G_{22}\}} \right\} \tag{2.65}$$

## $H_\infty$ Performance Measure for MR Discrete-Time Systems

For systems where one or more measurements are available only at every integer-multiple $\tau_S$, the resulting $M_\Delta$ is a shift-varying operator. Let us define the $H_\infty$-norm for a PSV operator as its induced $\ell_2$-norm. Clearly, the induced norm does not depend on the choice of time zero even for PSV operators. The main difficulty with the $H_\infty$ performance analysis of a MR system, however, lies in that the system is shift-varying and the pulse transfer function representation of the closed-loop system does not exist (in terms of time unit $\tau_S$). Hence, the frequency-domain techniques just described cannot be applied to MR systems straightforwardly. As for the sampled-data systems in the continuous-time domain, the samplers can either be approximated as shift-invariant operators or be bounded using conic sectors.

## Frequency-Domain Performance Analysis for MR Discrete-Time Systems

Suppose the system is represented as a discrete-time system of $\tau_S$, which is a common divider of all sampling times. Consider a continuous-time signal $y_m^c$. The fourier transform of the signal sampled at every $\tau_S$ is

$$\mathcal{L}\{(y_m^c)^*_{\tau_S}\}\Big|_{s=j\omega} = \frac{1}{\tau_S}\sum_{k=-\infty}^{\infty}\mathcal{L}\{y_m^c\}|_{s=j\omega+k\frac{2\pi}{\tau_S}} \tag{2.66}$$

If the sampling time of $y_m^c$ is $N_1\tau_S$, then the fourier transform of the sampled-signal is

$$\mathcal{L}\{(y_m^c)^*_{N_1\tau_S}\}\Big|_{s=j\omega} = \frac{1}{N_1\tau_S}\sum_{k=-\infty}^{\infty}\mathcal{L}\{y_m^c\}|_{s=j\omega+k\frac{2\pi}{N_1\tau_S}} \tag{2.67}$$

Now let $y_m(k)$ be a general discrete-time signal where each time unit represents the time interval of $\tau_S$ and denote its sampled signal sampled at every N time unit as $(y_m(k))^*_{N_1}$. From the above discussion, it is apparent that the fourier transform of $(y_m(k))^*_{N_1}$ (expressed as impulse trains) can be expressed as

$$\mathcal{Z}\{(y_m(k))^*_{N_1}\}\Big|_{z=e^{j\omega\tau_S}} = \frac{1}{N_1}\sum_{k=0}^{N_1-1}\mathcal{Z}\{y_m(k)\}|_{z=e^{j\omega\tau_S}+k\frac{2\pi}{N_1\tau_S}} \tag{2.68}$$

where $\mathcal{Z}\{y_m(k)\}$ represents $\sum_{k=0}^{\infty} y_m(k)\frac{1}{z^k}$. Assuming that the inputs to the samplers are band-limited (*i.e.*, $\mathcal{Z}\{y_m(k)\}|_{z=e^{j\omega\tau_S}} \approx 0$ for $\frac{\pi}{N_1\tau_S} \leq \omega \leq \frac{\pi}{\tau_S}$),

$$\mathcal{Z}\{(y_m)^*_{N_1}\}\Big|_{z=e^{j\omega\tau_S}} = \frac{1}{N_1}\mathcal{Z}\{y_m(k)\}|_{z=e^{j\omega\tau_S}} \text{ for } 0 \leq \omega \leq \frac{\pi}{N_1\tau_S} \tag{2.69}$$

Typical discrete-time multi-rate sampled-data systems are represented schematically in Figure 2.8. Under the assumption of band-limitedness of the signals, the above discussion implies that each sampler may be replaced with $1/N_i$ where $N_i$ is its respective sampling time expressed in terms of the discrete time unit, $\tau_S$. Similar arguments can be made to the samplers within the controller as well. The samplers

within the controller may be replaced by $N_I/N_O$ where $N_I$ and $N_O$ are the sampling intervals (in terms of $\tau_S$) for the input and output signals of the sampler respectively (see Figure 2.8). A more conservative approach is to represent these samplers as LSI operator plus the norm-bounded LSV block as in the conic sector approach for the continuous time system. Details of this method will not be discussed in this thesis.

## 2.4 Description of Constraints

Typical linear constraints in process control can be described as follows:

$$u_{low}(k,j) \leq u(k,j) \leq u_{high}(k,j) \quad \forall k,j \tag{2.70}$$

$$|\Delta u(k,j)| \leq \Delta u_{max}(k,j) \quad \forall k,j \tag{2.71}$$

$$(y_c)_{low}(k,j) \leq y_c(k,j) \leq (y_c)_{high}(k,j) \quad \forall k,j \tag{2.72}$$

$u_{low}$ and $u_{high}$ are the upper and lower bounds on the control inputs, $\Delta u_{max}$ is the maximum allowed changes in the control inputs, and $(y_c)_{low}$ and $(y_c)_{high}$ are the upper and lower bounds on the control outputs. Note that we allow the constraints to vary with time.

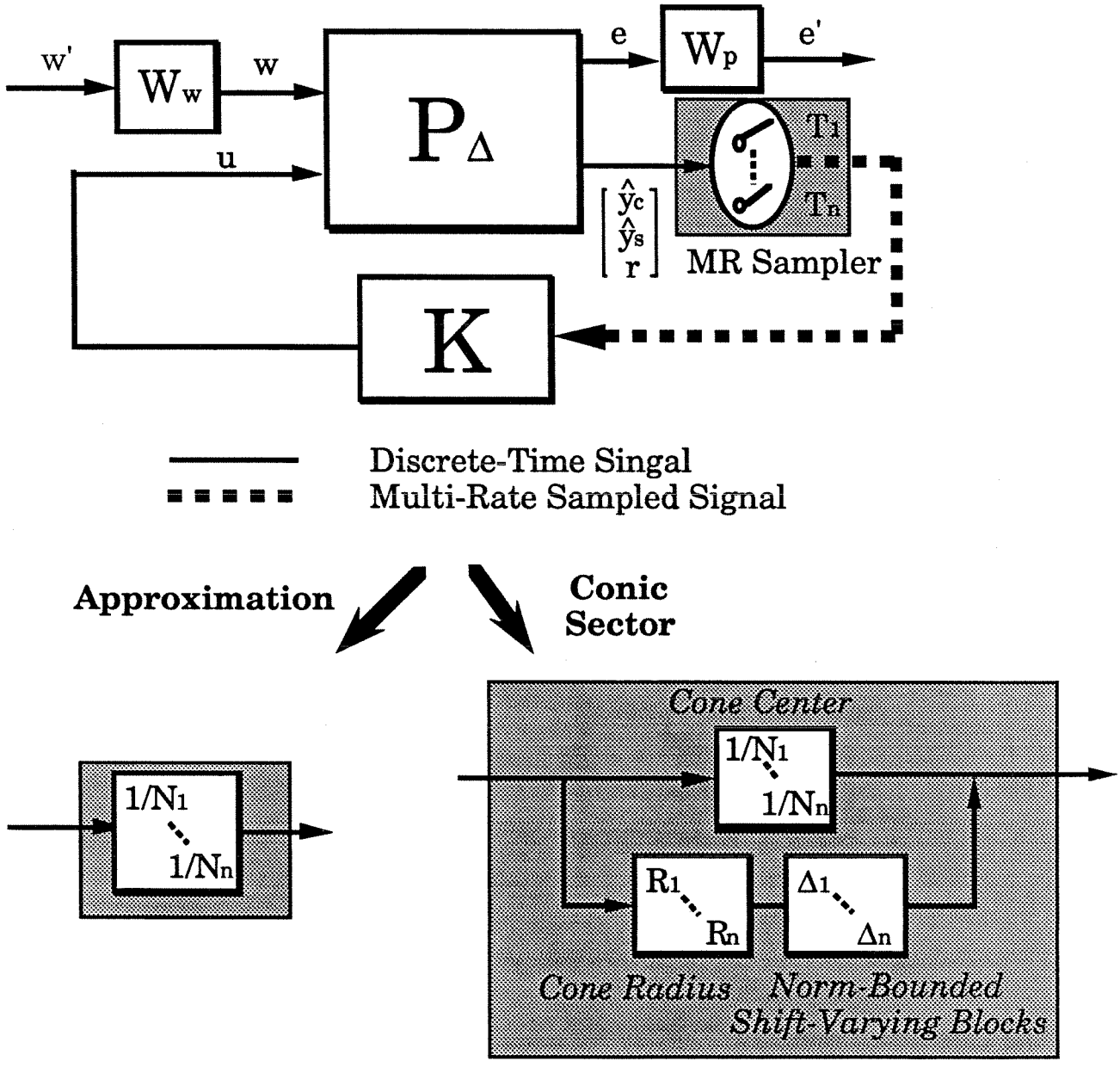


Figure 2.8. Block Diagram for Typical Multi-Rate Sampled-Data Systems and Modifications for Frequency Domain Analysis

# Chapter 3

# Robust Control Structure Selection – Secondary Measurement Selection in the Presence of Model/Plant Mismatch

The purpose of this chapter is to present a unified methodology for measurement selection in the presence of model/plant mismatch. First, we outline an underlying philosophy on which we base our efforts to develop measurement selection tools. The rest of the chapter presents various measurement selection tools that have been developed thus far within this philosophy. Some tools require only the system-intrinsic information (*i.e.*, information that is independent of the controller) while other tools are developed assuming certain properties of the controller and are therefore tied to specific controller design methods. Even though we develop this chapter in the context of measurement selection only, all the proposed methods are applicable to the more general problem of control structure selection (which involves selection of actuators as well as measurements) without modification.

## 3.1 General Approach/Philosophy

The conventional approach to the problem of measurement selection has been to develop a criterion or a set of criteria based on which the comparative merits of measurement candidates are evaluated and the best candidate is chosen [5,31,35,29]. However, we believe there must be another layer to the measurement selection pro-

cedure. For most practical problems, the number of *measurement candidates* (that consist of all the possible combinations of the available sensors) is extremely large. The criteria that accout for all the relevant characteristics of measurements with sufficient generality and precision are not only very difficult to develop, but also tend to be numerically complex. Reducing the number of candidates through simple criteria before applying detailed analysis should lessen the required efforts for measurement selection dramatically.

Hence, the approach we take to the problem of measurement selection is to eliminate first systematically those candidates for which a controller meeting a given performance specification cannot be designed (as illustrated in Figure 3.1). This added layer resolves one difficult problem for the conventional approach: In practical applications, a nonconservative, rigorous uncertainty model is often unavailable. It is generally not desirable to make the ultimate measurement selection based on the uncertainty information that is either incomplete or conservative. When the objective is to eliminate undesirable candidates, however, "parsimonious" uncertainty models (that is, models that encompass only those mismatches that are highly probable to arise in practice and have strong influences on the closed-loop stability and performance) can be used. In other words, the elimination process can be carried out even with incomplete knowledge of system uncertainty. Once the number of candidates has been reduced to a sufficiently low level, detailed analysis (such as actual control system design and simulations) can be carried out to make the final decision.

The screening of the candidates can be accomplished in two steps as illustrated in Figure 3.1. The first proposed step is to eliminate the candidates for which a controller achieving a desired level of robust performance does not exist regardless of what controller design method is used. The criteria that can be used to accomplish this design-independent screening will be referred to as "*general screening tools.*" This screening process leaves candidates for which a control system leading to satisfactory

performance may potentially exist. However, this alone may not reduce the number of candidates down to a sufficiently low level. In some cases, the control design methods available to the engineer may invariably lead to controllers with certain intrinsic properties. We may exploit these properties and carry out an additional screening in the context of a particular design method. That is, one may choose to further eliminate those candidates for which the particular design approach under consideration cannot yield a controller achieving a desired level of robust performance. The criteria that can be used under a particular design approach will be referred to as "*design-specific screening tools.*" If the second screening under a particular design approach does not leave any viable candidate, it is implied that a more complex, involved design approach is necessary. The screening process may be repeated in the context of another design approach.

In the subsequent parts of this chapter, we introduce a number of numerically efficient screening tools, both general and design-specific, that can be used to reduce the number of measurement candidates. The whole approach will be based on the Structured Singular Value theory, therefore, allowing a general norm-bounded uncertainty description.

## 3.2 Measurement Selection Problem Formulation

The general measurement selection problem we treat in this thesis is depicted in Figure 3.2. $y_m^j$ represents the $j^{\text{th}}$ set of measurements (including the primary, secondary measured variables) excluding those variables that cannot be measured reliably. The reason for excluding the operationally unreliable measurements is because it is desirable to choose a measurement set such that a required level of performance can be maintained even when some of the failure-prone measurements become unavailable. In many practical applications, the primary variables that are sampled at a slow rate are also operationally unreliable. In this case, $y_m$ consists only of the secondary

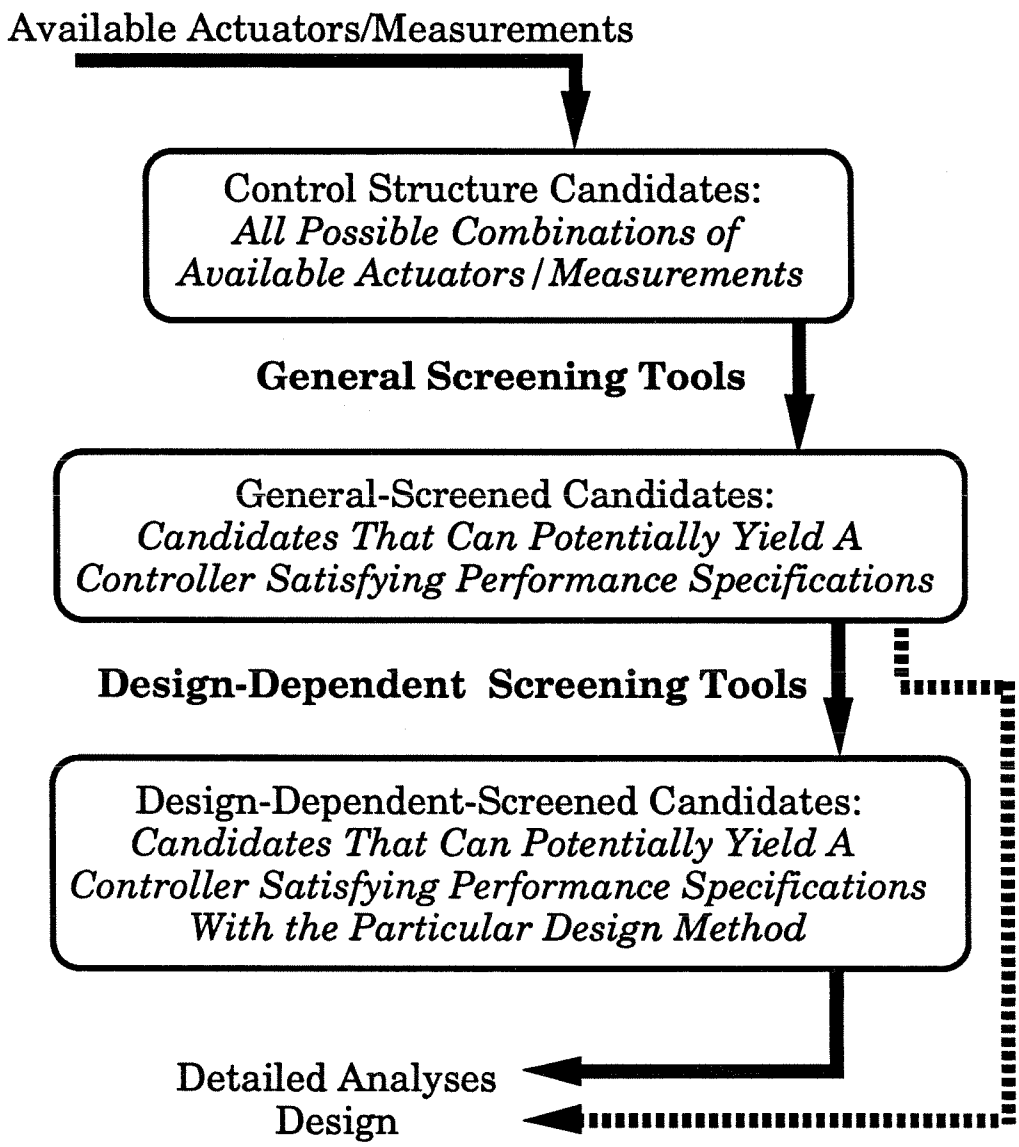


Figure 3.1. Schematic Representation of Proposed Measurement Selection Procedure

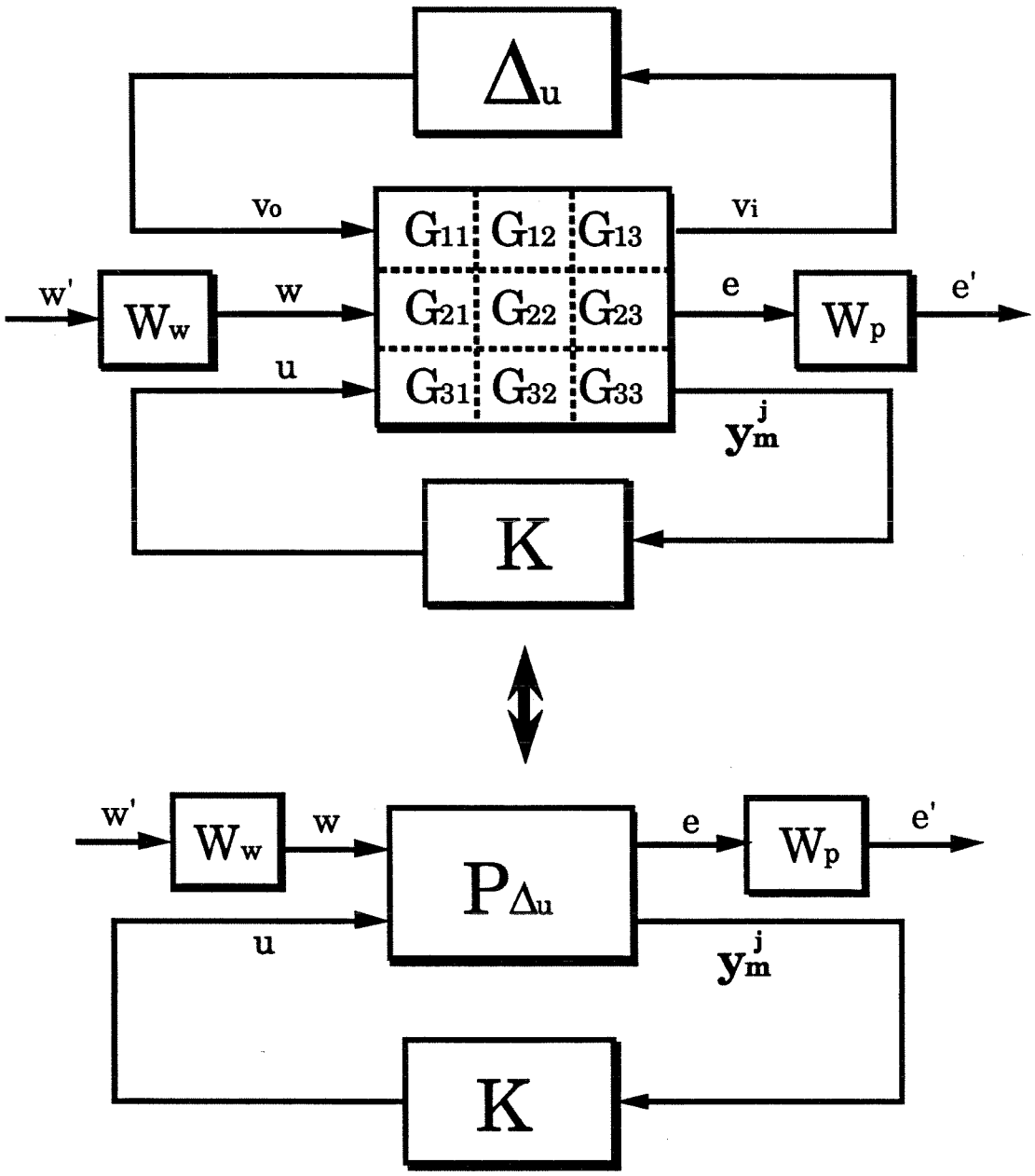


Figure 3.2. Formulation of Measurement Selection Problem

variables that are often sampled at a uniform sampling rate.

The ultimate objective of measurement selection in this thesis is to select a measurement set such that $K$ can be designed satisfying the $H_\infty$ robust performance requirement:

$$\max_{P_\Delta \in \mathbf{P_{II}}} \|W_p \mathcal{F}_\ell(P_\Delta, K) W_w\|_\infty < 1 \tag{3.1}$$

Our main theoretical basis for developing measurement selection tools will be the Structured Singular Value theory. Because the theory does not extend straightforwardly to sampled-data systems and multi-rate sampled-data systems for continuous- and discrete-time systems respectively, one of the following two approach must be taken:

1. Bound the time varying parts (for a continous-time system) or the shift-varying parts (for a discrete-time system) of the system with conic sectors.

2. Assume that the signals sampled are band-limited and approximate the samplers as time-invariant or shift-invariant operators (as explained in Chapter 2).

The first apporach, though rigorous, introduces significant conservativeness and is not suitable for developing measurement screening tools. The second approach relies on the assumption that the signals going into the samplers are band-limited. When signals are anti-aliased properly, the assumption is well justified. In addition, the operator obtained with the approximation is exactly the "cone center" for the conic sector used in the first approach. Hence, robust performance under the second approach is a necessary condition for robust performance under the first approach. From these considerations, we conclude that the second approach is more suitable for measurement selection.

In this thesis, we develop all our measurement selection tools in the continuous time domain, with the added assumption that all measurements are available continuously. Extensions to discrete-time systems follows trivially from the discussion in

Section 2.3 since most tools are based on frequency-domain conditions. The proposed tools can be applied to continuous-time systems with sampled measurements as well by using the above-discussed approximation.

## 3.3 General Screening Tools

In this section, we develop screening tools that can be used to eliminate measurement candidates for which a controller meeting the robust performance requirement does not exist. First, we derive a necessary and sufficient (but not testable) condition for the existence of a controller achieving robust performance. Based on the condition, we derive several necessary conditions that can be checked efficiently. For example, by relaxing the causality requirement of the controller, we can derive necessary conditions that can be formulated into convex optimization. The necessary conditions are proposed as screening tools.

We base further development of this section on the assumption that the infimum of the upper bound of $\mu$ is always equal to $\mu$ for all cases (not just for cases with block structures of three or less blocks). This assumption is well justified since there has been no example where the upperbound of $\mu$ differs from $\mu$ significantly enough for engineering interest).

**Approximation 3.1** *The infimum of the upper bound of $\mu$ is same as $\mu$.*

$$\mu_{\mathbf{\Delta}}(M) = \inf_{D \in \mathcal{D}} \bar{\sigma}(DMD^{-1}) \tag{3.2}$$

From Approximation 3.1, the structured singular value condition (2.51) is equivalent to

$$\inf_{D \in \mathcal{D}_{rp}} \bar{\sigma} \left( D \begin{bmatrix} I & \\ & W_p \end{bmatrix} \mathcal{F}_\ell(G,K) \begin{bmatrix} I & \\ & W_w \end{bmatrix} \Big|_{s=j\omega} D^{-1} \right) < 1 \quad \forall \omega \tag{3.3}$$

where

$$\mathcal{D}_{rp} = \{\text{diag}\left[d_1 I_{p_1}, \cdots, d_\ell I_{p_\ell}, D_1, \cdots, D_m, d_{\ell+1} I_{\dim\{e'\}}\right] : d_j \in \mathcal{R}_+,\ D_i \in C^{r_i \times r_i}, D_i = D_i^* > 0\} \tag{3.4}$$

### 3.3.1 Test Condition for Existence of a Causal Controller Achieving Robust Performance

Our goal is to test whether or not a controller meeting the robust performance requirement exists for a given set of measurements. Mathematically, we test if the following condition is satisfied:

$$\inf_{K \in \mathcal{K}_s} \sup_{\omega} \inf_{D(\omega) \in \mathcal{D}_{rp}} \bar{\sigma} \left( D(\omega) \left( \begin{bmatrix} I & \\ & W_p \end{bmatrix} \mathcal{F}_\ell(G^j, K) \begin{bmatrix} I & \\ & W_w \end{bmatrix} \right) \Bigg|_{s=j\omega} D^{-1}(\omega) \right) < 1 \tag{3.5}$$

where $G^j$ and $W_w^j$ denote the plant model $G$ and the disturbance weight $W_w$ for the $j^{\text{th}}$ set of measurements respectively. For simplicity of notation, we will drop the superscript $\{\cdot\}^j$ from this point on.

$\mathcal{K}_s$ represents the set of all stabilizing, "causal" controllers. The causality of the controller implies that the controller's current/future inputs cannot affect its past outputs. Hence, the causality is necessary for the controller to be physically realizable. Mathmatically, $\mathcal{K}_s$ is expressed as

$$\mathcal{K}_s = \left\{ K \in \mathcal{R}_s : \begin{bmatrix} (I - G_{33}K)^{-1} & G_{33}(I - KG_{33})^{-1} \\ K(I - G_{33}K)^{-1} & (I - KG_{33})^{-1} \end{bmatrix} \in \mathcal{RH}_\infty \right\} \tag{3.6}$$

where $\mathcal{R}_s$ represents the set of all proper rational transfer functions (of size $\dim\{u\} \times (\dim\{y_m\} + \dim\{r\})$) and $\mathcal{RH}_\infty$ represents the set of all proper rational transfer functions (of appropriate size) that are analytic in the closed RHP. Note that $K$ has nonlinear constraints and enters $\mathcal{F}_\ell(G^j, K)$ in a nonlinear fashion as well. The

following parametrization of $\mathcal{K}_s$ [63] yields an affine parametrization of the closed-loop operator without any nonlinear constraints:

$$\mathcal{K}_s = \left\{K : K = (Y - TQ)(X - SQ)^{-1}, Q \in \mathcal{RH}_\infty\right\} \tag{3.7}$$

$$= \left\{K : K = (\tilde{X} - Q\tilde{S})^{-1}(\tilde{Y} - Q\tilde{T}), Q \in \mathcal{RH}_\infty\right\} \tag{3.8}$$

where $(S, T)$ and $(\tilde{S}, \tilde{T})$ are right and left coprime factors of $G_{33}$ respectively (*i.e.*, $G_{33} = ST^{-1} = \tilde{T}^{-1}\tilde{S}$), and $(X, Y, \tilde{X}, \tilde{Y})$ is a solution to the following Bezout identity:

$$\begin{bmatrix} \tilde{X} & -\tilde{Y} \\ -\tilde{S} & \tilde{T} \end{bmatrix} \begin{bmatrix} T & Y \\ S & X \end{bmatrix} = I \tag{3.9}$$

Note that, for open-loop stable systems, we can choose $T = \tilde{T} = -I$, $S = \tilde{S} = G_{33}$, $X = \tilde{X} = -I$ and $Y = \tilde{Y} = 0$; the parametrization (3.7) simply becomes $\mathcal{K}_s = \{K : K = Q(I + G_{33}Q)^{-1}, Q \in \mathcal{RH}_\infty\}$. In this case, the parametrization can be also expressed in terms of a block diagram as shown in Figure 3.3. Using the parametrization (3.7)-(3.8), (3.5) becomes

$$\inf_{Q \in \mathcal{RH}_\infty} \sup_{\omega} \inf_{D(\omega) \in \mathcal{D}_{rp}} \bar{\sigma}\left[D(\omega)\left(N_{11} + N_{12}QN_{21}\right)|_{s=j\omega} D^{-1}(\omega)\right] < 1 \tag{3.10}$$

where

$$N_{11} = \begin{bmatrix} G_{11} & G_{12} \\ G_{21} & G_{22} \end{bmatrix} + \begin{bmatrix} G_{13} \\ G_{23} \end{bmatrix} T\tilde{Y} \begin{bmatrix} G_{31} & G_{32} \end{bmatrix} \tag{3.11}$$

$$N_{12} = \begin{bmatrix} G_{13} \\ G_{23} \end{bmatrix} T \tag{3.12}$$

$$N_{21} = \tilde{T} \begin{bmatrix} G_{31} & G_{32} \end{bmatrix} \tag{3.13}$$

Hence, the Youla parametrization gives us a test condition, which is affine with re-

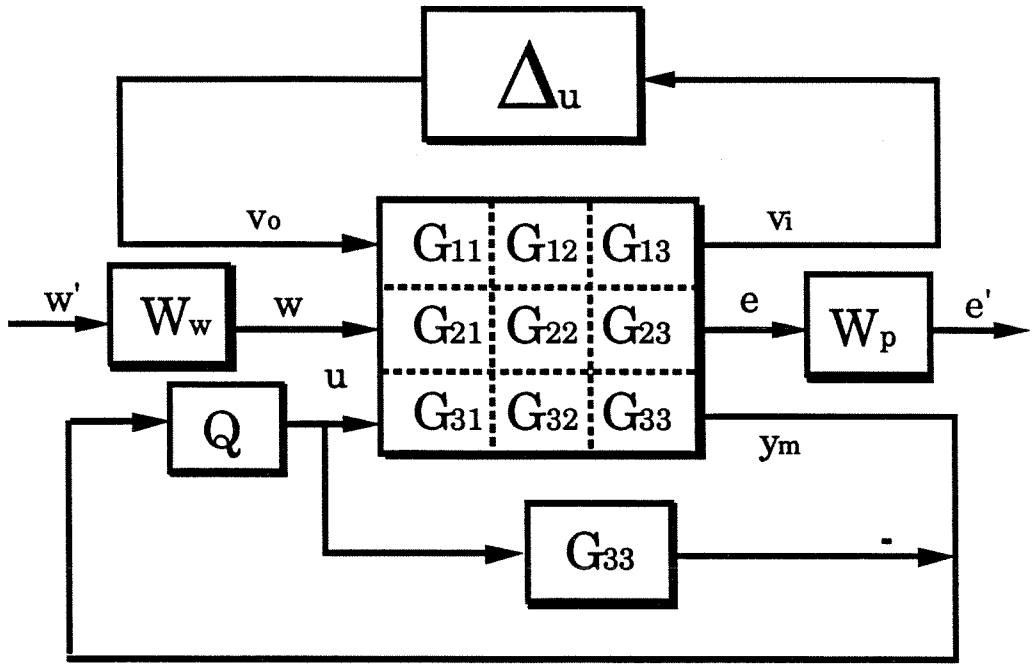


Figure 3.3. Block-Diagram Representation of Youla Parametrization of Nominally Stabilizing Controller for Open-Loop Stable Systems

spect to the parameter $Q$. The only restriction on $Q$ is that it should be analytic in the closed RHP. However, the coupling of the parameters $Q$ and $D$ makes the left-hand side of (3.10) a nonconvex optimization problem. There is currently no general method of checking it. $\mu$-Synthesis that combines the $H_\infty$-optimal design with the optimal $D$-scaling used in $\mu$-analysis in an iterative manner, is the only *ad hoc* solution. However, the procedure does not guarantee convergence to the true optimum and involves many numerically intensive steps and fragile approximations. Hence, (3.10) cannot be considered as a viable screening tool.

### 3.3.2 Test Condition for Existence of a Causal Controller Achieving Nominal Performance

One of necessary conditions for robust performance is nominal performance (*i.e.*, meeting the performance requirements when the real system matches the nominal model exactly). Hence, in order for (3.10) to be satisfied, the following condition

must be satisfied:

$$\inf_{Q\in\mathcal{RH}_\infty} \sup_{\omega} \bar{\sigma}\left[(\bar{N}_{11}+\bar{N}_{12}Q\bar{N}_{21})\Big|_{s=j\omega}\right] < 1 \tag{3.14}$$

where

$$\bar{N}_{11} = G_{22} + G_{23}T\tilde{Y}G_{32} \tag{3.15}$$

$$\bar{N}_{12} = G_{23}T \tag{3.16}$$

$$\bar{N}_{21} = \tilde{T}G_{32} \tag{3.17}$$

During the past decade, various methods have been developed that enables us to test the condition (3.14). According to the latest method by Doyle *et al.* [18], checking (3.14) essentially amounts to checking if positive semidefinite solutions to two Riccati equations exist and the spectral radius of the product of the two solutions is less than a certain constant (see [18] for detail).

**General Screening Tool #1** *Eliminate the measurement candidates for which*

$$\inf_{Q\in\mathcal{RH}_\infty} \sup_{\omega} \bar{\sigma}\left[(\bar{N}_{11}+\bar{N}_{12}Q\bar{N}_{21})\Big|_{s=j\omega}\right] \geq 1 \tag{3.18}$$

### 3.3.3 Test Condition for Existence of an Acausal Controller Achieving Robust Performance

Let us consider dropping the *causality* requirement on $Q$. Hence, we allow the controller parameter $Q$ to be "acausal" meaning the current/future inputs to the operator $Q$ may affect its past outputs. Mathematically, this is equivalent to replacing the requirement of $Q \in \mathcal{RH}_\infty$ with $Q \in \mathcal{R}_s$. The condition (3.10) with $Q \in \mathcal{R}_s$ is equivalent

to the following frequency-by-frequency condition:

$$\inf_{Q\in\mathcal{C}^K}\inf_{D\in\mathcal{D}_{rp}}\bar{\sigma}(D(N_{11}+N_{12}QN_{21})|_{s=j\omega}D^{-1})<1\quad\forall\omega \tag{3.19}$$

The superscript $\{\cdot\}^K$ in $\mathcal{C}^K$ implies that it is the set of complex matrices of size $\dim\{u\}\times(\dim\{y_m\}+\dim\{r\})$. The following lemma gives a necessary and sufficient condition for the existence of an *acausal* $Q$ satisfying (3.10) that does not require finding the double coprime factor or solving the Bezout identity.

**Lemma 3.1** *Let $N_{11}, N_{12}$ and $N_{21}$ be defined as in (3.11)-(3.13). Then*

$$\inf_{Q\in\mathcal{R}_s}\inf_{D\in\mathcal{D}_{rp}}\bar{\sigma}(D(N_{11}+N_{12}QN_{21})|_{s=j\omega}D^{-1})<1\quad\forall\omega \tag{3.20}$$

*if and only if*

$$\inf_{\tilde{Q}\in\mathcal{C}^K}\inf_{D\in\mathcal{D}_{rp}}\bar{\sigma}(D(\tilde{N}_{11}+\tilde{N}_{12}\tilde{Q}\tilde{N}_{21})|_{s=j\omega}D^{-1})<1\quad\forall\omega \tag{3.21}$$

*where*

$$\tilde{N}_{11}=\begin{bmatrix}G_{11}&G_{12}\\G_{21}&G_{22}\end{bmatrix}\quad\tilde{N}_{12}=\begin{bmatrix}G_{13}\\G_{23}\end{bmatrix}\quad\tilde{N}_{21}=\begin{bmatrix}G_{31}&G_{32}\end{bmatrix} \tag{3.22}$$

**Proof** Note that

$$N_{11}+N_{12}QN_{21}=\begin{bmatrix}G_{11}&G_{12}\\G_{21}&G_{22}\end{bmatrix}+\begin{bmatrix}G_{13}\\G_{23}\end{bmatrix}(TQ\tilde{T}+T\tilde{Y})\begin{bmatrix}G_{31}&G_{32}\end{bmatrix} \tag{3.23}$$

Define $\tilde{Q}=TQ\tilde{T}+T\tilde{Y}$. From the equivalence

$$\{\tilde{Q}:\tilde{Q}\in\mathcal{C}^K\}\equiv\{TQ\tilde{T}+T\tilde{Y}:Q\in\mathcal{C}^K\} \tag{3.24}$$

we arrive at (3.21). ■

**Comments on Lemma 3.1:**

1. There is no need for finding the double coprime factor of $G_{22}$ and solving the Bezout identity since the expression for $\tilde{N}$ involves only $G$.

2. For open-loop stable systems, (3.21) is a necessary and sufficient condition for existence of an *acausal* controller $K$ satisfying the robust performance requirement. In other words, dropping the causality requirement on $Q$ is equivalent to dropping the same requirement on $K$. When the causality requirement on $K$ is relaxed, the requirement of (3.6) on $K$ disappears leading to the condition

$$\inf_{K\in\mathcal{C}^K}\inf_{D(\omega)\in\mathcal{D}_{rp}}\bar{\sigma}\left(D(\omega)\left(\left[\begin{array}{cc} I & \\ & W_p \end{array}\right]\mathcal{F}_\ell(G^j,K)\left[\begin{array}{cc} I & \\ & W_w \end{array}\right]\right)\Bigg|_{s=j\omega} D^{-1}(\omega)\right) < 1 \quad \forall\omega \tag{3.25}$$

   Replacing $K \in \mathcal{C}^K$ with $K \in \{\tilde{Q}(I - G_{33}\tilde{Q})^{-1} : \tilde{Q} \in \mathcal{C}^K\}$ leads to the exact same result. However, it is more intuitive to think in terms of acausal $Q$ than acausal $K$. Since $Q$ is required to be stable for internal stability, we can write $Q = Q_1 + Q_2$ where $Q_1$ mapping $\mathcal{L}_2[0,\infty)$ to $\mathcal{L}_2[0,\infty)$ (Toeplitz operator) represents the *causal* part of the controller and $Q_2$ mapping $\mathcal{L}_2[0,\infty)$ to $\mathcal{L}_2[0,-\infty)$ (Hankel operator) represents the *acausal* part of the controller. Such a direct interpretation doesn't exist for $K$ since a stabilizing acausal $K$ is not necessarily a map from $\mathcal{L}_2[0,\infty) \to \mathcal{L}_2(-\infty,\infty)$ (it does not have to be stable for the closed-loop to be internally stable).

3. For open-loop unstable systems, (3.21) is only a necessary condition for the existence of an "acausal" controller $K$ achieving robust performance. This is because, when $Q$ is allowed to be acausal, the Youla parametrization (3.7) does not necessarily lead to a stabilizing controller $K$. For example, choosing $Q(j\omega) = T^{-1}Y(j\omega) \ \ \forall\omega$ leads to $K = 0$, which is not a stabilizing controller.

However, (3.21) is nevertheless a necessary condition for (3.10) since

$$\begin{aligned} & \sup_{\omega} \inf_{Q \in \mathcal{C}^K} \inf_{D \in \mathcal{D}_{rp}} \bar{\sigma}(D(N_{11} + N_{12}QN_{21})|_{s=j\omega} D^{-1}) \\ \leq & \inf_{Q \in \mathcal{RH}_\infty} \sup_{\omega} \inf_{D \in \mathcal{D}_{rp}} \bar{\sigma}(D(N_{11} + N_{12}QN_{21})|_{s=j\omega} D^{-1}) \end{aligned} \tag{3.26}$$

Hence, it can be used as a screening tool to eliminate candidates for open-loop unstable systems as well.

Thus far, we have shown that

$$\inf_{\tilde{Q} \in \mathcal{C}^K} \inf_{D \in \mathcal{D}_{rp}} \bar{\sigma}(D(\tilde{N}_{11} + \tilde{N}_{12}\tilde{Q}\tilde{N}_{21})|_{s=j\omega} D^{-1}) < 1 \quad \forall \omega \tag{3.27}$$

is a necessary condition for the existence of a controller achieving robust performance. It was interpreted as a necessary and sufficient condition for the existence of an *acausal* controller achieving robust performance for open-loop stable systems and a necessary condition for open-loop unstable systems. Next, we show that the condition (3.27) can be transformed into two separate conditions that can be formulated into convex optimization [39].

We first reparametrize $\tilde{Q}$ as follows:

$$\tilde{Q} \in \mathcal{C}^K \equiv \tilde{Q} \in \{(\tilde{N}_{12}^* \tilde{N}_{12})^{-1/2} \hat{Q} (\tilde{N}_{21} \tilde{N}_{21}^*)^{-1/2}|_{s=j\omega} : \hat{Q} \in \mathcal{C}^K\} \tag{3.28}$$

The notation $\{\cdot\}^*$ represents the adjoint operator for transfer functions (*i.e.*, $N^*(s) = N^T(-s)$ and the complex conjugate for constant matrices). Using the new parametrization, the condition (3.27) can now be transformed into

$$\inf_{\hat{Q} \in \mathcal{C}^K} \inf_{D \in \mathcal{D}_{rp}} \bar{\sigma}(D(\tilde{N}_{11} + \hat{N}_{12}\hat{Q}\hat{N}_{21})|_{s=j\omega} D^{-1}) < 1 \quad \forall \omega \tag{3.29}$$

where

$$\hat{N}_{12} = \tilde{N}_{12}(\tilde{N}_{12}^*\tilde{N}_{12})^{-1/2} \tag{3.30}$$

$$\hat{N}_{21} = (\tilde{N}_{21}\tilde{N}_{21}^*)^{-1/2}\tilde{N}_{21} \tag{3.31}$$

Note that $\hat{N}_{12}^*\hat{N}_{12}|_{s=j\omega} = I$ and $\hat{N}_{21}\hat{N}_{21}^*|_{s=j\omega} = I$ for all $\omega$. The following theorem shows that the condition (3.29) can be checked through two conditions each of which is a convex optimization problem.

**Theorem 3.1** *Let $R \in \mathcal{C}^{n\times n}, U \in \mathcal{C}^{n\times r}$ and $V \in \mathcal{C}^{t\times n}$. Suppose $U^*U = I_r, VV^* = I_t$ and $U_\perp \in \mathcal{C}^{n\times(n-r)}$ and $V_\perp \in \mathcal{C}^{(n-t)\times n}$ are chosen such that $\begin{bmatrix} U & U_\perp \end{bmatrix} \in \mathcal{C}^{n\times n}$ and $\begin{bmatrix} V \\ V_\perp \end{bmatrix} \in \mathcal{C}^{n\times n}$ are unitary. Then*

$$\inf_{Q\in\mathcal{C}^{r\times t}} \inf_{D\in\mathcal{D}_{rp}} \bar{\sigma}(D(R+UQV)D^{-1}) < \alpha \tag{3.32}$$

*if and only if $\exists X \in \mathcal{D}_{rp}$ such that*

$$\lambda_{\max}[V_\perp(R^*XR - \alpha^2 X)V_\perp^*] < 0 \tag{3.33}$$

*and*

$$\lambda_{\max}[U_\perp^*(RX^{-1}R^* - \alpha^2 X^{-1})U_\perp] < 0 \tag{3.34}$$

**Proof**

$$\inf_{Q\in\mathcal{C}^{r\times t}} \bar{\sigma}\left[D(R+UQV)D^{-1}\right] = \inf_{Q\in\mathcal{C}^{r\times t}} \bar{\sigma}\left[DRD^{-1} + (DU)Q(VD^{-1})\right] \tag{3.35}$$

We first replace $Q \in \mathcal{C}^{r\times t}$ with

$$Q \in \left\{[(DU)^*(DU)]^{-1/2}\tilde{Q}[(VD^{-1})(VD^{-1})^*]^{-1/2} : \tilde{Q} \in \mathcal{C}^{r\times t}\right\}$$

Then,

$$\inf_{Q\in\mathcal{C}^{r\times t}} \bar{\sigma}\left[D(R+UQV)D^{-1}\right] = \inf_{\tilde{Q}\in\mathcal{C}^{r\times t}} \bar{\sigma}\left(DRD^{-1}+\hat{U}\tilde{Q}\hat{V}\right) \tag{3.36}$$

where

$$\hat{U} = (DU)[(DU)^*(DU)]^{-1/2} \tag{3.37}$$

$$\hat{V} = [(VD^{-1})(VD^{-1})^*]^{-1/2}(VD^{-1}) \tag{3.38}$$

We want to find $\hat{U}_\perp$ and $\hat{V}_\perp$ such that $\begin{bmatrix} \hat{U} & \hat{U}_\perp \end{bmatrix}$ and $\begin{bmatrix} \hat{V} \\ \hat{V}_\perp \end{bmatrix}$ are both unitary. Simple calculation shows that

$$\hat{U}_\perp = (D^*)^{-1}U_\perp(U_\perp^*(D^*D)^{-1}U_\perp)^{-1/2} \tag{3.39}$$

$$\hat{V}_\perp = (V_\perp D^* D V_\perp^*)^{-1/2}V_\perp D^* \tag{3.40}$$

Now

$$\inf_{\tilde{Q}\in\mathcal{C}^{r\times t}} \bar{\sigma}\left(DRD^{-1}+\hat{U}\tilde{Q}\hat{V}\right) \tag{3.41}$$

$$= \inf_{\tilde{Q}\in\mathcal{C}^{r\times t}} \bar{\sigma}\left(DRD^{-1}+\begin{bmatrix} \hat{U} & \hat{U}_\perp \end{bmatrix}\begin{bmatrix} \tilde{Q} & 0 \\ 0 & 0 \end{bmatrix}\begin{bmatrix} \hat{V} \\ \hat{V}_\perp \end{bmatrix}\right) \tag{3.42}$$

$$= \inf_{\tilde{Q}\in\mathcal{C}^{r\times t}} \bar{\sigma}\left(\begin{bmatrix} \hat{U} & \hat{U}_\perp \end{bmatrix}^* DRD^{-1}\begin{bmatrix} \hat{V} \\ \hat{V}_\perp \end{bmatrix}^* + \begin{bmatrix} \tilde{Q} & 0 \\ 0 & 0 \end{bmatrix}\right) \tag{3.43}$$

$$= \inf_{\tilde{Q}\in\mathcal{C}^{r\times t}} \bar{\sigma}\left(\begin{bmatrix} \tilde{R}_{11}+\tilde{Q} & \tilde{R}_{12} \\ \tilde{R}_{21} & \tilde{R}_{22} \end{bmatrix}\right) \tag{3.44}$$

where

$$\tilde{R}_{11} = \hat{U}^* DRD^{-1}\hat{V}^* \tag{3.45}$$

$$\tilde{R}_{12} = \hat{U}^* DRD^{-1}\hat{V}_\perp^* \tag{3.46}$$

$$\tilde{R}_{21} = \hat{U}_\perp^* D R D^{-1} \hat{V}^* \tag{3.47}$$

$$\tilde{R}_{22} = \hat{U}_\perp^* D R D^{-1} \hat{V}_\perp^* \tag{3.48}$$

From Doyle (1984),

$$\inf_{\tilde{Q}\in\mathcal{C}^{r\times t}} \bar{\sigma}\left(\begin{bmatrix} \tilde{R}_{11}+\tilde{Q} & \tilde{R}_{12} \\ \tilde{R}_{21} & \tilde{R}_{22} \end{bmatrix}\right) = \max\left\{\bar{\sigma}\left(\begin{bmatrix} \tilde{R}_{21} & \tilde{R}_{22} \end{bmatrix}\right), \bar{\sigma}\left(\begin{bmatrix} \tilde{R}_{12} \\ \tilde{R}_{22} \end{bmatrix}\right)\right\} \tag{3.49}$$

Hence, the condition (3.32) is satisfied if and only if there exists $D \in \mathcal{D}_{rp}$ such that

$$\bar{\sigma}\left(\begin{bmatrix} \tilde{R}_{21} & \tilde{R}_{22} \end{bmatrix}\right) < \alpha \text{ and } \bar{\sigma}\left(\begin{bmatrix} \tilde{R}_{12} \\ \tilde{R}_{22} \end{bmatrix}\right) < \alpha \tag{3.50}$$

$$\bar{\sigma}\left(\begin{bmatrix} \tilde{R}_{21} & \tilde{R}_{22} \end{bmatrix}\right) \tag{3.51}$$

$$= \bar{\sigma}\left(\hat{U}_\perp^* D R D^{-1} \begin{bmatrix} \hat{V}^* & \hat{V}_\perp^* \end{bmatrix}\right) \tag{3.52}$$

$$= \bar{\sigma}\left(\hat{U}_\perp^* D R D^{-1}\right) \tag{3.53}$$

$$= \bar{\sigma}\left[\left((D^*)^{-1} U_\perp (U_\perp^* (D^* D)^{-1} U_\perp)^{-1/2}\right)^* D R D^{-1}\right] \tag{3.54}$$

$$= \bar{\sigma}\left[\left(U_\perp^* (D^* D)^{-1} U_\perp\right)^{-1/2} U_\perp^* R D^{-1}\right] \tag{3.55}$$

Similarly, one can show that

$$\bar{\sigma}\left(\begin{bmatrix} \tilde{R}_{12} \\ \tilde{R}_{22} \end{bmatrix}\right) = \bar{\sigma}\left[D R V_\perp^* (V_\perp D^* D V_\perp^*)^{-1/2}\right] \tag{3.56}$$

Now

$$\bar{\sigma}\left[\left(U_\perp^* (D^* D)^{-1} U_\perp\right)^{-1/2} U_\perp R D^{-1}\right] < \alpha \tag{3.57}$$

$$\leftrightarrow \lambda_{\max}\left[\left(U_\perp^* (D^* D)^{-1} U_\perp\right)^{-1/2} U_\perp^* R (D^* D)^{-1} R^* U_\perp \left(U_\perp^* (D^* D)^{-1} U_\perp\right)^{-1/2} - \alpha^2 I\right] < 0$$

$$\leftrightarrow \quad \lambda_{\max}[U_\perp^* R(D^*D)^{-1}R^*U_\perp - \alpha^2 U_\perp^*(D^*D)^{-1}U_\perp] < 0 \tag{3.58}$$

$$\leftrightarrow \quad \lambda_{\max}[U_\perp^* \left(R(D^*D)^{-1}R^* - \alpha^2(D^*D)^{-1}\right) U_\perp] < 0 \tag{3.59}$$

Likewise,

$$\begin{aligned} & \bar{\sigma}\left[DRV_\perp^*(V_\perp D^*DV_\perp^*)^{-1/2}\right] < \alpha \\ \leftrightarrow \quad & \lambda_{\max}[V_\perp \left(R^*(D^*D)^{-1}R - \alpha^2(D^*D)^{-1}\right) V_\perp^*] < 0 \end{aligned} \tag{3.60}$$

Defining $X = D^*D$ completes the proof. ■

**Comments on Theorem 3.1:**

1. (3.33) and (3.34) are convex with respect to $X$ and $X^{-1}$ respectively. Each of the two conditions is a necessary condition for the existence of a causal controller achieving robust performance and can be checked through standard algorithms such as "cutting-plane" method [6].

2. Checking the conditions (3.33)-(3.34) together is more difficult and is not resolved at the moment except for the following special cases:

   - **Full Control Case:**

     If $U$ has a full column rank, the condition (3.34) drops out and (3.33) is necessary and sufficient for (3.32).

   - **Full Information Case:**

     If $V$ has a full row rank, the condition (3.33) drops out and (3.34) is necessary and sufficient for (3.32).

- **2 Full-Block Case:**

  For the cases of 2 full-block $\Delta$, (3.32) is

$$\inf_{Q\in\mathcal{C}^{r\times t}}\inf_{d_1,d_2\in\mathcal{R}_+}\bar{\sigma}\left(\begin{bmatrix} d_1 I & \\ & d_2 I \end{bmatrix}(R+UQV)\begin{bmatrix} \frac{1}{d_1}I & \\ & \frac{1}{d_2}I \end{bmatrix}\right)<\alpha \qquad (3.61)$$

  By multiplying and then dividing the expression by $d_2$, (3.61) becomes

$$\inf_{Q\in\mathcal{C}^{r\times t}}\inf_{d\in\mathcal{R}_+}\bar{\sigma}\left(\begin{bmatrix} dI & \\ & I \end{bmatrix}(R+UQV)\begin{bmatrix} \frac{1}{d}I & \\ & I \end{bmatrix}\right)<\alpha \qquad (3.62)$$

  where $d=\frac{d_1}{d_2}$. Hence, for 2 full-block cases, the condition (3.33)-(3.34) can be expressed as follows:

$$g(d) \equiv \lambda_{\max}\left[V_\perp\left(R^*\begin{bmatrix} dI & \\ & I \end{bmatrix}R-\alpha^2\begin{bmatrix} dI & \\ & I \end{bmatrix}\right)V_\perp^*\right]<0 \qquad (3.63)$$

$$h(\frac{1}{d}) \equiv \lambda_{\max}\left[U_\perp^*\left(R\begin{bmatrix} \frac{1}{d}I & \\ & I \end{bmatrix}R^*-\alpha^2\begin{bmatrix} \frac{1}{d}I & \\ & I \end{bmatrix}\right)U_\perp\right]<0 \qquad (3.64)$$

  $\mathcal{T}_{FC}=\{s\in\mathcal{R}_+ : g(s)<0\}$ and $\mathcal{T}_{FI}=\{t\in\mathcal{R}_+ : h(t)<0\}$ are open intervals (since $g(s)$ and $h(t)$ are convex with respect to $s$ and $t$) and can be easily checked if they intersect.

Using the results from Theorem 3.1, we now propose the following screening tools:

**General Screening Tool #2** *Eliminate the measurement candidates for which*

$$\inf_{X\in\mathcal{D}_{rp}}\lambda_{\max}\left[(\hat{N}_{21})_\perp(\tilde{N}_{11}^*X\tilde{N}_{11}-X)(\hat{N}_{21})_\perp^*|_{s=j\omega}\right]\geq 0 \quad \text{for some } \omega \qquad (3.65)$$

**General Screening Tool #3** *Eliminate the measurement candidates for which*

$$\inf_{X \in \mathcal{D}_{rp}} \lambda_{\max} \left[ (\hat{N}_{12})_{\perp}^{*} (\tilde{N}_{11} X \tilde{N}_{11}^{*} - X)(\hat{N}_{12})_{\perp} |_{s=j\omega} \right] \geq 0 \quad \text{for some } \omega \tag{3.66}$$

**General Screening Tool #4** *Eliminate the measurement candidates for which*

$$\mathcal{T}_{FC}^{ij}(\omega) \bigcap \mathcal{T}_{FI}^{ij}(\omega) = \emptyset \qquad \begin{array}{l} \textit{for some } \omega \textit{ and} \\ \textit{for some } (i,j) \in \{(\tilde{i},\tilde{j}) : \tilde{i} \neq \tilde{j}; 1 \leq \tilde{i}, \tilde{j} \leq \ell + 1\} \end{array} \tag{3.67}$$

*where*

$$\begin{aligned}
\mathcal{T}_{FC}^{ij}(\omega) &= \left\{ s \in \mathcal{R}_{+} : \lambda_{\max} \left[ (\hat{N}_{21}^{ij})_{\perp} \left( (\tilde{N}_{11}^{ij})^{*} \begin{bmatrix} sI & \\ & I \end{bmatrix} \tilde{N}_{11}^{ij} \right.\right.\right. \\
&\qquad \left.\left.\left. - \begin{bmatrix} sI & \\ & I \end{bmatrix} \right) (\hat{N}_{21}^{ij})_{\perp}^{*} \Big|_{s=j\omega} \right] < 0 \right\} \qquad (3.68) \\
\mathcal{T}_{FI}^{ij}(\omega) &= \left\{ t \in \mathcal{R}_{+} : \lambda_{\max} \left[ (\hat{N}_{12}^{ij})_{\perp}^{*} \left( \tilde{N}_{11}^{ij} \begin{bmatrix} \frac{1}{t} I & \\ & I \end{bmatrix} (\tilde{N}_{11}^{ij})^{*} \right.\right.\right. \\
&\qquad \left.\left.\left. - \begin{bmatrix} \frac{1}{t} I & \\ & I \end{bmatrix} \right) (\hat{N}_{12})_{\perp}^{ij} \Big|_{s=j\omega} \right] < 0 \right\} \qquad (3.69) \\
\tilde{N}_{11}^{ij} &= \mathcal{X}^{ij} \tilde{N}_{11} (\mathcal{X}^{ij})^{T} \qquad (3.70) \\
\hat{N}_{21}^{ij} &= \hat{N}_{21} (\mathcal{X}^{ij})^{T} \qquad (3.71) \\
\hat{N}_{12}^{ij} &= \mathcal{X}^{ij} \hat{N}_{12} \qquad (3.72) \\
\mathcal{X}^{ij} &= \begin{bmatrix} 0 & \cdots & I_{\dim\{\Delta_i\}} & \cdots & \cdots & 0 \\ 0 & \cdots & \cdots & I_{\dim\{\Delta_j\}} & \cdots & 0 \end{bmatrix} \qquad (3.73)
\end{aligned}$$

The last screening tool exploits the fact that the robust performance condition must be satisfied for any combination of two blocks among the present $\Delta$ blocks.

## 3.4 Design-Specific Screening Tools

In this section, we develop screening tools that are tied to specific design methods. We first introduce a parametrization of the controller gain matrix that leads to an affine closed-loop gain expression with respect to the parameter. Then, we show that certain controller design approaches (LQG, MPC designs for example) invariably lead to a specific form of the gain matrix. Based on this property, we propose some screening tools and put them in perspective with other criteria that have been suggested by various authors.

### 3.4.1 Steady-State Screening Tools

#### Affine Parametrization of the Closed-Loop Gain Operator

The steady-state gain $K_{dc}$ for the controller $K$ can be parametrized as

$$K_{dc} \in \left\{ Q_{dc}(I - G_{33}Q_{dc})^{-1} : Q_{dc} \in \mathcal{R}^{\dim\{K\}} \right\} \tag{3.74}$$

Figure 3.4 shows a block-diagram representation of the parametrization. Using the parametrization, the nominal closed-loop expression from $w$ to $y_e$ can be shown to be as follows:

$$\left[ \begin{array}{cc} I_{\dim\{y_e\}} & 0 \end{array} \right] (G_{22} + G_{23}QG_{32}) \tag{3.75}$$

For convenience, we will adopt the following notation:

$$\left[ \begin{array}{cc} \bar{G}_{22} & \bar{G}_{23} \\ \bar{G}_{32} & \bar{G}_{33} \end{array} \right] = \left[ \begin{array}{c|c} \left[ \begin{array}{cc} I_{\dim\{y_e\}} & 0 \\ 0 & \end{array} \right] & \begin{array}{c} 0 \\ I \end{array} \end{array} \right] \left[ \begin{array}{cc} G_{22} & G_{23} \\ G_{32} & G_{33} \end{array} \right] \left[ \begin{array}{cc} H_w & 0 \\ 0 & I \end{array} \right] \tag{3.76}$$

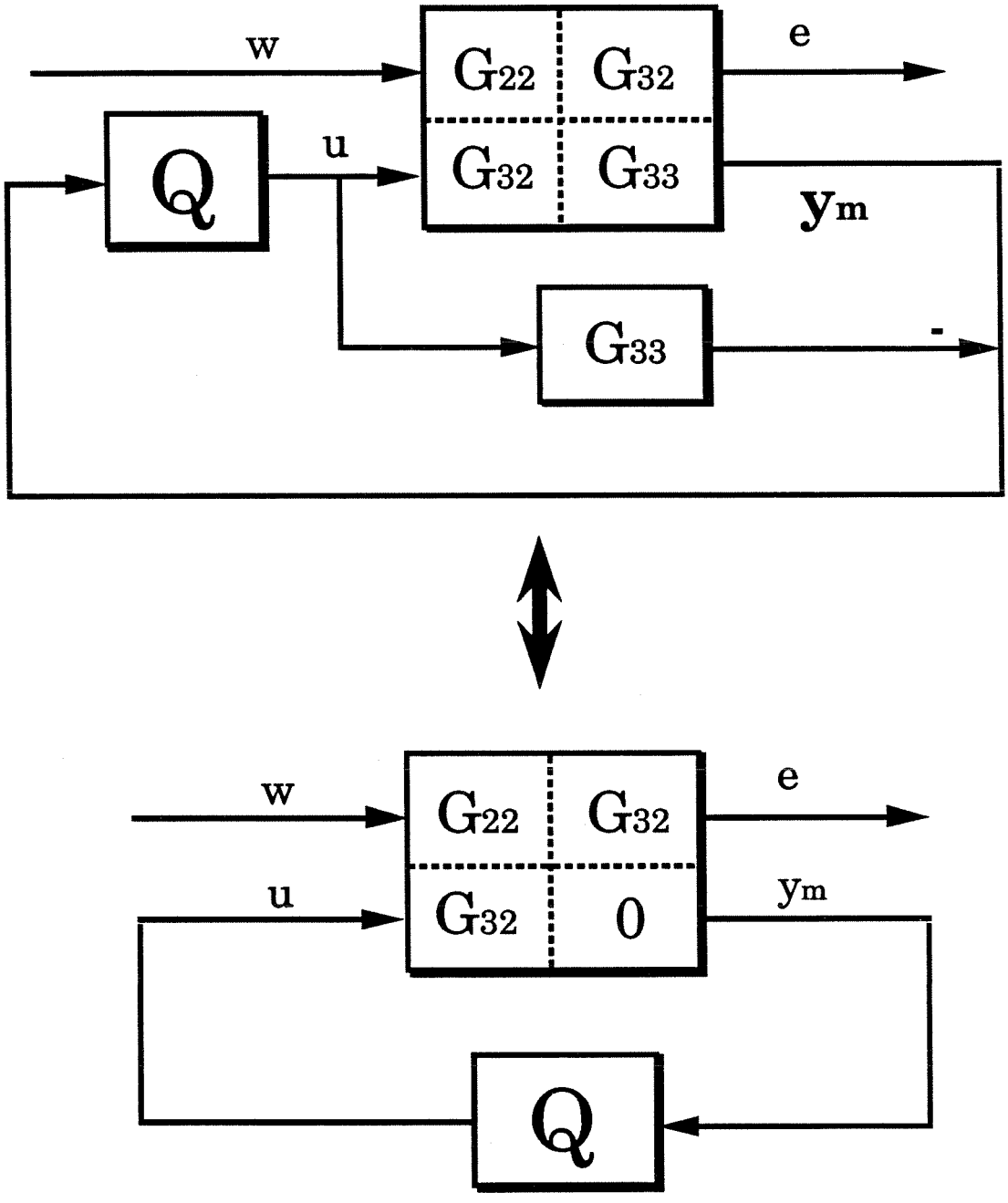


Figure 3.4. Affine Parametrization of the Closed-Loop Gain Operator

where $H_w$ is a diagonal matrix which expresses relative magnitudes of external inputs at steady state. For example, the elements corresponding to "nonpersistent" (or stationary in stochastic sense) inputs are set to zero.

## Controllers Minimizing Projection Error (LQG/MPC)

The LQG ("$H_2$-optimal") design method and the MPC design method that are introduced in Chapter 5 minimize the variance of $y_e$ at steady state. More specifically, these design methods invariably lead to $Q_{dc}$ that minimizes the quantity

$$\|\bar{G}_{22} + \bar{G}_{23}Q_{dc}\bar{G}_{32}\|_{\mathcal{F}} = \text{trace}\{(\bar{G}_{22} + \bar{G}_{23}Q_{dc}\bar{G}_{32})^T(\bar{G}_{22} + \bar{G}_{23}Q_{dc}\bar{G}_{32})\} \tag{3.77}$$

$\|\cdot\|_{\mathcal{F}}$ denotes the Frobenious norm which is the square root of the sum of the squares of all elements (which is equivalent to the right-hand-side expression). The following theorem gives an explicit expression for $Q_{dc}$ minimizing the quantity (3.77).

**Theorem 3.2** *Suppose $\bar{G}_{22}$, $\bar{G}_{32}$ and $\bar{G}_{23}$ are real matrices and $\bar{G}_{32}$ and $\bar{G}_{23}$ have full row and column rank respectively. Then,*

$$\inf_{Q_{dc}\in\mathcal{R}^{\dim\{K\}}} \|\bar{G}_{22} + \bar{G}_{23}Q_{dc}\bar{G}_{32}\|_{\mathcal{F}} \tag{3.78}$$

*is achieved by*

$$Q_{dc} = Q_{dc}^{\text{proj}} \equiv -(\bar{G}_{23}^T\bar{G}_{23})^{-1}\bar{G}_{23}^T\bar{G}_{22}\bar{G}_{32}^T(\bar{G}_{32}\bar{G}_{32}^T)^{-1} \tag{3.79}$$

**Proof** Define

$$\tilde{Q}_{dc} = (\bar{G}_{23}^T\bar{G}_{23})^{1/2}Q_{dc}(\bar{G}_{32}\bar{G}_{32}^T)^{1/2} \tag{3.80}$$

It follows straightforwardly that

$$\begin{aligned} & \inf_{Q_{dc}\in\mathcal{R}^{\dim\{K\}}} \|\bar{G}_{22}+\bar{G}_{23}Q_{dc}\bar{G}_{32}\|_{\mathcal{F}} \\ = & \inf_{\tilde{Q}_{dc}\in\mathcal{R}^{\dim\{K\}}} \|\bar{G}_{22}+\bar{G}_{23}(\bar{G}_{23}^T\bar{G}_{23})^{-1/2}\tilde{Q}_{dc}(\bar{G}_{32}\bar{G}_{32}^T)^{-1/2}\bar{G}_{32}\|_{\mathcal{F}} \end{aligned} \tag{3.81}$$

Denote the matrices $\bar{G}_{23}(\bar{G}_{23}^T\bar{G}_{23})^{-1/2}$ and $(\bar{G}_{32}\bar{G}_{32}^T)^{-1/2}\bar{G}_{32}$ as $U$ and $V$ respectively. Then, we can always find $U_\perp$ and $V_\perp$ such that $\begin{bmatrix} U & U_\perp \end{bmatrix}$ and $\begin{bmatrix} V \\ V_\perp \end{bmatrix}$ are unitary matrices. Now

$$\left\|\bar{G}_{22}+U\tilde{Q}_{dc}V\right\|_{\mathcal{F}} \tag{3.82}$$

$$= \left\|\bar{G}_{22}+\begin{bmatrix} U & U_\perp \end{bmatrix}\begin{bmatrix} \tilde{Q}_{dc} & 0 \\ 0 & 0 \end{bmatrix}\begin{bmatrix} V \\ V_\perp \end{bmatrix}\right\|_{\mathcal{F}} \tag{3.83}$$

$$= \left\|\begin{bmatrix} U & U_\perp \end{bmatrix}^T\bar{G}_{22}\begin{bmatrix} V \\ V_\perp \end{bmatrix}^T+\begin{bmatrix} \tilde{Q}_{dc} & 0 \\ 0 & 0 \end{bmatrix}\right\|_{\mathcal{F}} \tag{3.84}$$

$$= \left\|\begin{bmatrix} U^T\bar{G}_{22}V^T+\tilde{Q}_{dc} & U^T\bar{G}_{22}V_\perp^T \\ U_\perp^T\bar{G}_{22}V^T & U_\perp^T\bar{G}_{22}V_\perp^T \end{bmatrix}\right\|_{\mathcal{F}} \tag{3.85}$$

The choice for $\tilde{Q}_{dc}$ that minimizes the quantity (3.85) is $-U^T\bar{G}_{22}V^T$ which, in terms of original notation, can be written as

$$-(\bar{G}_{23}^T\bar{G}_{23})^{-1/2}\bar{G}_{23}^T\bar{G}_{22}\bar{G}_{32}^T(\bar{G}_{32}\bar{G}_{32}^T)^{-1/2} \tag{3.86}$$

Hence,

$$Q_{dc}^{\text{proj}} = -(\bar{G}_{23}^T\bar{G}_{23})^{-1}\bar{G}_{23}^T\bar{G}_{22}\bar{G}_{32}^T(\bar{G}_{32}\bar{G}_{32}^T)^{-1} \tag{3.87}$$

■

From Theorem 3.2, a necessary condition for robust performance for the LQG or MPC controllers regardless of their tuning is

$$\mu\left[\begin{array}{cc}\boldsymbol{\Delta}_{\mathbf{u}} & \\ & \boldsymbol{\Delta}_{\mathbf{p}}\end{array}\right](M^{\text{proj}}) < 1 \tag{3.88}$$

where $M^{\text{proj}} = \mathcal{F}_\ell\left(G, Q_{dc}^{\text{proj}}(I + G_{33}Q_{dc}^{\text{proj}})^{-1}\right)$ and can be written as

$$M^{\text{proj}} = \left[\begin{array}{cc} G_{11} + G_{13}Q_{dc}^{\text{proj}}G_{31} & (G_{12} + G_{13}Q_{dc}^{\text{proj}}G_{32})W_d \\ W_p(G_{21} + G_{23}Q_{dc}^{\text{proj}}G_{31}) & W_p(G_{22} + G_{23}Q_{dc}^{\text{proj}}G_{32})W_d \end{array}\right]\Bigg|_{s=0}$$

The following screening tools is proposed.

**Design-Specific Screening Tool for LQG/MPC #1** *Eliminate the candidates for which*

$$\mu\left[\begin{array}{cc}\Delta_u & \\ & \Delta_p\end{array}\right](M^{\text{proj}}) \geq 1 \tag{3.89}$$

## Controllers with Integral Action

It is common in practice to use controllers with integral action so that all measured variables have zero steady-state offsets in the face of asymptotically constant disturbances. For example, most industrial distillation columns are controlled by putting PID loops on the chosen tray temperatures. For controllers with integral action, the expression for $Q_{dc}$ can be written as

$$Q_{dc} = Q_{dc}^{\text{intg}} \equiv \left[\begin{array}{c|c} -(G_{y_m u})_r^{-1} & 0 \end{array}\right] \tag{3.90}$$

We naturally assumed that there are at least as many manipulated variables as the measured variables by assuming that $(G_{y_m u})_r^{-1}$, a right inverse of $G_{y_m u}$ exists (other-

wise, integral action on all measured variables is not possible). In addition, because the primary variables are not estimated directly in this approach, setpoint changes must be done by providing appropriate new setpoints for the measured variables. In the above formula for $Q_{dc}^{\text{intg}}$, we assumed that no reference inputs are to be given in order to keep the discussion simple. Given the expression for $Q_{dc}$, the following screening tool can be easily derived.

**Design-Specific Screening Tool for Controllers with Integral Action #1**

*Eliminate the candidates for which*

$$\mu \left[ \begin{array}{cc} \boldsymbol{\Delta}_{\mathbf{u}} & \\ & \boldsymbol{\Delta}_{\mathbf{p}} \end{array} \right] (M^{\text{intg}}) \geq 1 \tag{3.91}$$

$M^{\text{intg}}$ is defined as

$$M^{\text{intg}} = \left[ \begin{array}{cc} G_{11} + G_{13}Q_{dc}^{\text{intg}}G_{31} & (G_{12} + G_{13}Q_{dc}^{\text{intg}}G_{32})W_d \\ W_p(G_{21} + G_{23}Q_{dc}^{\text{intg}}G_{31}) & W_p(G_{22} + G_{23}Q_{dc}^{\text{intg}}G_{32})W_d \end{array} \right]\Bigg|_{s=0}$$

## 3.4.2 Relationships with Previous Criteria

The steady-state screening tools presented in Section 3.4.1 test whether the given performance specification is satisfied in the presence of the "worst-case" uncertainty. We can extend these ideas a bit further to obtain a method for calculating the actual "worst-case" closed-loop error at steady state. In this section, we present a method to compute the "worst-case" closed-loop error in the presence of general norm-bounded perturbations. Using this method, it is shown that some of the previously proposed criteria arise naturally under specific uncertainty structures and some restrictive assumptions on the performance/disturbance weights.

## Methodology for Calculating the "Worst-Case" Closed-Loop Error

The following lemma enables the explicit calculation of the "worst-case" closed-loop error at steady state [40].

**Lemma 3.2** *Let* $M_{11} \in \mathcal{C}^{p\times p}$ , $M_{12} \in \mathcal{C}^{p\times n}$ , $M_{21} \in \mathcal{C}^{n\times p}$ *and* $M_{22} \in \mathcal{C}^{n\times n}$. *Define the set* $\mathbf{B\Delta_u}$ *as follows:*

$$\mathbf{B\Delta_u} = \{\Delta \in \mathbf{\Delta_u} : \bar{\sigma}(\Delta) \leq 1\} \tag{3.92}$$

$$\mathbf{\Delta_u} = \Big\{\mathrm{diag}(\Delta_1, \cdots, \Delta_\ell, \delta_1 I_{r_1}, \cdots, \delta_m I_{r_m}) : \Delta_i \in \mathcal{C}^{p_i\times p_i}, \delta_j \in \mathcal{C}; \sum_i p_i + \sum_j r_j = p, 1 \leq i \leq \ell, 1 \leq j \leq m\Big\} \tag{3.93}$$

*Also define*

$$\bar{f}(c_p) = \mu_{\begin{bmatrix}\mathbf{\Delta_u} & \\ & \mathbf{\Delta_p}\end{bmatrix}}\left(\begin{bmatrix} M_{11} & M_{12} \\ c_p M_{21} & c_p M_{22}\end{bmatrix}\right) \tag{3.94}$$

*where*

$$\mathbf{\Delta_p} = \{\Delta : \Delta \in \mathcal{C}^{n\times n}\} \tag{3.95}$$

*Assume that* $\mu_{\mathbf{\Delta_u}}(M_{11}) < 1$. *Then,*

$$\max_{\Delta_u \in \mathbf{B\Delta_u}} \bar{\sigma}[M_{22} + M_{21}\Delta_u(I - M_{11}\Delta_u)^{-1}M_{12}] = \frac{1}{\bar{c}_p^*} \tag{3.96}$$

*where* $\bar{c}_p^*$ *solves the equation* $\bar{f}(\bar{c}_p) = 1$.

**Proof** We must prove that

$$\mu_{\begin{bmatrix}\mathbf{\Delta_u} & \\ & \mathbf{\Delta_p}\end{bmatrix}}\begin{pmatrix} M_{11} & M_{12} \\ \bar{c}_p^* M_{21} & \bar{c}_p^* M_{22}\end{pmatrix} = 1$$

$$\rightarrow \quad \bar{\sigma}[\bar{c}_p^* M_{22} + \bar{c}_p^* M_{21}\Delta_u(I - M_{11}\Delta_u)^{-1}M_{12}] = 1 \quad \forall \Delta_u \in \mathbf{\Delta_u} \tag{3.97}$$

The proof is done by contradiction.

First, suppose that

$$\bar{\sigma}[\bar{c}_p^* M_{22} + \bar{c}_p^* M_{21}\Delta_u(I - M_{11}\Delta_u)^{-1}M_{12}] < 1 \quad \forall \Delta_u \in \mathbf{B}\boldsymbol{\Delta}_\mathbf{u} \tag{3.98}$$

Then

$$\rho(\Delta_p(\bar{c}_p^* M_{22} + \bar{c}_p^* M_{21}\Delta_u(I - M_{11}\Delta_u)^{-1}M_{12})) \tag{3.99}$$

$$\leq \bar{\sigma}(\Delta_p)\bar{\sigma}(\bar{c}_p^* M_{22} + \bar{c}_p^* M_{21}\Delta_u(I - M_{11}\Delta_u)^{-1}M_{12}) \tag{3.100}$$

$$< 1 \quad \forall \Delta_u \in \mathbf{B}\boldsymbol{\Delta}_\mathbf{u} \text{ and } \Delta_p \in \{\Delta : \bar{\sigma}(\Delta) \leq 1, \Delta \in \mathcal{C}^{n\times n}\} \tag{3.101}$$

This implies that

$$\mu\begin{bmatrix} \boldsymbol{\Delta}_\mathbf{u} & \\ & \boldsymbol{\Delta}_\mathbf{p} \end{bmatrix} \begin{pmatrix} M_{11} & M_{12} \\ \bar{c}_p^* M_{21} & \bar{c}_p^* M_{22} \end{pmatrix} < 1 \tag{3.102}$$

which contradicts the assumption.

Next, suppose that

$$\bar{\sigma}[\bar{c}_p^* M_{22} + \bar{c}_p^* M_{21}\Delta_u(I - M_{11}\Delta_u)^{-1}M_{12}] > 1 \quad \text{for certain } \Delta_u \in \mathbf{B}\boldsymbol{\Delta}_\mathbf{u} \tag{3.103}$$

Let

$$\bar{c}_p^* M_{22} + \bar{c}_p^* M_{21}\Delta_u(I - M_{11}\Delta_u)^{-1}M_{12} = U\Sigma V^T \tag{3.104}$$

where $U$ and $V$ are unitary matrices and $\Sigma$ is a real, positive semidefinite diagonal matrix. Then

$$\rho(\Delta_p(\bar{c}_p^* M_{22} + \bar{c}_p^* M_{21}\Delta_u(I - M_{11}\Delta_u)^{-1}M_{12})) > 1 \text{ for } \Delta_p = VU^T \tag{3.105}$$

This means that $\exists \Delta_p \in \mathcal{C}^{n\times n}$ such that

$$\bar{\sigma}(\Delta_p) < 1 \quad \text{and} \quad \det(I + \Delta_p(\bar{c}_p^* M_{22} + \bar{c}_p^* M_{21}\Delta_u(I - M_{11}\Delta_u)^{-1}M_{12})) = 0 \quad (3.106)$$

This implies that

$$\mu\left[\begin{array}{cc} \mathbf{\Delta_u} & \\ & \mathbf{\Delta_p} \end{array}\right] \left(\begin{array}{cc} M_{11} & M_{12} \\ \bar{c}_p^* M_{21} & \bar{c}_p^* M_{22} \end{array}\right) > 1 \quad (3.107)$$

which again contradicts the assumption. ■

Since $f(c_p)$ is a nondecreasing function of $c_p$, $\bar{c}_p^*$ can be easily computed through simple search procedures such as the bisection method. In the statement of the theorem, we assumed that the performance block $\Delta_p$ is square. This is without loss of generality since a nonsquare block can always be represented as product between a square block and a constant matrix (see Chapter 2).

It is often convenient to use the "tight" upper-bound of $\mu$ (Approximation 3.1); hence, we will restate Lemma 3.2 in terms of the upperbound.

**Corollary 3.1** *Let* $M_{11} \in \mathcal{C}^{p\times p}$ , $M_{12} \in \mathcal{C}^{p\times n}$ , $M_{21} \in \mathcal{C}^{n\times p}$ *and* $M_{22} \in \mathcal{C}^{n\times n}$. *Define the set* $\mathbf{B\Delta_u}$ *as follows:*

$$\mathbf{B\Delta_u} = \{\Delta \in \mathbf{\Delta_u} : \bar{\sigma}(\Delta) \leq 1\} \quad (3.108)$$

$$\mathbf{\Delta_u} = \Big\{\mathrm{diag}(\Delta_1, \cdots, \Delta_\ell, \delta_1 I_{r_1}, \cdots, \delta_m I_{r_m}) : \Delta_i \in \mathcal{C}^{p_i\times p_i}, \delta_j \in \mathcal{C}; \quad (3.109)$$
$$\sum_i p_i + \sum_j r_j = p, 1 \leq i \leq \ell, 1 \leq j \leq m\Big\}$$

*Also define*

$$f(c_p) = \inf_{D\in\mathcal{D}_{rp}} \left(D \left[\begin{array}{cc} M_{11} & M_{12} \\ c_p M_{21} & c_p M_{22} \end{array}\right] D^{-1}\right) \quad (3.110)$$

*where*

$$\mathcal{D}_{rp} = \{\text{diag}\,[d_1 I_{p_1}, \cdots, d_\ell I_{p_\ell}, D_1, \cdots, D_m, I_n] : d_j \in \mathcal{R}_+,\ D_i \in \mathcal{C}^{r_i \times r_i}, D_i = D_i^* > 0\} \tag{3.111}$$

*Assume that*

$$\inf_{D \in \mathcal{D}_{rs}} (\tilde{D} M_{11} \tilde{D}^{-1}) < 1 \tag{3.112}$$

*where*

$$\mathcal{D}_{rs} = \{\text{diag}\,[d_1 I_{p_1}, \cdots, d_\ell I_{p_\ell}, D_1, \cdots, D_m] : d_j \in \mathcal{R}_+,\ D_i \in \mathcal{C}^{r_i \times r_i}, D_i = D_i^* > 0\} \tag{3.113}$$

*Then,*

$$\max_{\Delta_u \in \mathbf{B}\boldsymbol{\Delta}_\mathbf{u}} \bar{\sigma}[M_{22} + M_{21}\Delta_u(I - M_{11}\Delta_u)^{-1}M_{12}] \begin{cases} = \frac{1}{c_p^*} \text{ for } \ell \leq 2, m = 0 \\ \leq (\approx) \frac{1}{c_p^*} \text{ otherwise} \end{cases} \tag{3.114}$$

*where $c_p^*$ solves $f(c_p^*) = 1$.*

For convenience of notation, let us define the operator $\mathcal{E}_{worst}$ as follows:

$$\mathcal{E}_{worst}\left(\begin{bmatrix} M_{11} & M_{12} \\ M_{21} & M_{22} \end{bmatrix}, \mathbf{B}\boldsymbol{\Delta}_\mathbf{u}\right) = \frac{1}{c_p^*} \tag{3.115}$$

When the matrix $M$ holds a special structure, a simpler formula can be derived as the following lemma shows.

**Lemma 3.3** *Let $M_{12}, M_{21}$ and $\mathcal{D}_{rp}, \mathcal{D}_{rs}$ be defined as in Corollary 3.1. Then,*

$$\inf_{D \in \mathcal{D}_{rp}} \bar{\sigma}\left(D \begin{bmatrix} 0 & M_{12} \\ c_p M_{21} & 0 \end{bmatrix} D^{-1}\right) = \inf_{\tilde{D} \in \mathcal{D}_{rs}} \sqrt{\bar{\sigma}(c_p M_{21} \tilde{D}^{-1}) \bar{\sigma}(\tilde{D} M_{12})} \tag{3.116}$$

**Proof**

$$\inf_{\tilde{D}\in\mathcal{D}_{rs}} \bar{\sigma}\left(\begin{bmatrix} \tilde{D} & \\ & I_n \end{bmatrix}\begin{bmatrix} 0 & M_{12} \\ c_pM_{21} & 0 \end{bmatrix}\begin{bmatrix} \tilde{D}^{-1} & \\ & I_n \end{bmatrix}\right) \tag{3.117}$$

$$= \inf_{\tilde{D}\in\mathcal{D}_{rs}} \bar{\sigma}\left(\begin{bmatrix} 0 & \tilde{D}M_{12} \\ c_pM_{21}\tilde{D}^{-1} & 0 \end{bmatrix}\right) \tag{3.118}$$

$$= \inf_{\tilde{D}\in\mathcal{D}_{rs}} \inf_{d\in\mathcal{R}+} \bar{\sigma}\left(\begin{bmatrix} 0 & \frac{1}{d}\tilde{D}M_{12} \\ dc_pM_{21}\tilde{D}^{-1} & 0 \end{bmatrix}\right) \tag{3.119}$$

$$= \inf_{\tilde{D}\in\mathcal{D}_{rs}} \inf_{d\in\mathcal{R}+} \max\left(\bar{\sigma}\left(dc_pM_{21}\tilde{D}^{-1}\right), \bar{\sigma}\left(\frac{1}{d}\tilde{D}M_{12}\right)\right) \tag{3.120}$$

$$= \inf_{\tilde{D}\in\mathcal{D}_{rs}} \sqrt{\bar{\sigma}\left(c_pM_{21}\tilde{D}^{-1}\right)\bar{\sigma}\left(\tilde{D}M_{12}\right)} \tag{3.121}$$

■

The lemma implies that

$$\mathcal{E}_{worst}\left(\begin{bmatrix} M_{11} & M_{12} \\ M_{21} & M_{22} \end{bmatrix}, \mathbf{B}\mathbf{\Delta}_\mathbf{u}\right) = \inf_{\tilde{D}\in\mathcal{D}_{rs}} \sqrt{\bar{\sigma}\left(M_{21}\tilde{D}^{-1}\right)\bar{\sigma}\left(\tilde{D}M_{12}\right)} \tag{3.122}$$

Finally, the following lemma will prove to be useful in the further development.

**Lemma 3.4** *Let $M_{12}, M_{21}, M_{22}$ and $\mathcal{D}_{rp}, \mathcal{D}_{rs}$ be defined as in Corollary 3.1. Then,*

$$\inf_{D\in\mathcal{D}_{rp}} \bar{\sigma}\left(D\begin{bmatrix} 0 & M_{12} \\ c_pM_{21} & 0 \end{bmatrix}D^{-1}\right) \leq \inf_{D\in\mathcal{D}_{rp}} \bar{\sigma}\left(D\begin{bmatrix} 0 & M_{12} \\ c_pM_{21} & c_pM_{22} \end{bmatrix}D^{-1}\right) \tag{3.123}$$

**Proof** Let $D^*$ be the $D$-scale achieving

$$\inf_{D\in\mathcal{D}_{rp}} \bar{\sigma}\left(D\begin{bmatrix} 0 & M_{12} \\ c_pM_{21} & c_pM_{22} \end{bmatrix}D^{-1}\right) \tag{3.124}$$

In addition, let $v$ be the input vector corresponding to the maximum singular value of the matrix

$$\left( D^* \begin{bmatrix} 0 & M_{12} \\ c_p M_{21} & 0 \end{bmatrix} (D^*)^{-1} \right) \tag{3.125}$$

For convenience of notation, partition $v$ and $D^*$ as follows:

$$v = \begin{bmatrix} v_u \\ v_\ell \end{bmatrix} \qquad D^* = \begin{bmatrix} D_1^* & \\ & D_2^* \end{bmatrix} \tag{3.126}$$

Then

$$\left( D^* \begin{bmatrix} 0 & M_{12} \\ c_p M_{21} & c_p M_{22} \end{bmatrix} (D^*)^{-1} \right) v = \begin{bmatrix} D_1^* M_{12} (D_2^*)^{-1} v_\ell \\ c_p D_2^* M_{21} (D_1^*)^{-1} v_u + c_p D_2^* M_{22} (D_2^*)^{-1} v_\ell \end{bmatrix} \tag{3.127}$$

Now, note that

$$\left\| \begin{bmatrix} D_1^* M_{12} (D_2^*)^{-1} v_\ell \\ c_p D_2^* M_{21} (D_1^*)^{-1} v_u + c_p D_2^* M_{22} (D_2^*)^{-1} v_\ell \end{bmatrix} \right\|_2 \geq \left\| \begin{bmatrix} D_1^* M_{12} (D_2^*)^{-1} v_\ell \\ c_p D_2^* M_{21} (D_1^*)^{-1} v_u \end{bmatrix} \right\|_2 \tag{3.128}$$

or

$$\left\| \begin{bmatrix} -D_1^* M_{12} (D_2^*)^{-1} v_\ell \\ c_p D_2^* M_{21} (D_1^*)^{-1} v_u - c_p D_2^* M_{22} (D_2^*)^{-1} v_\ell \end{bmatrix} \right\|_2 \geq \left\| \begin{bmatrix} D_1^* M_{12} (D_2^*)^{-1} v_\ell \\ c_p D_2^* M_{21} (D_1^*)^{-1} v_u \end{bmatrix} \right\|_2 \tag{3.129}$$

Hence, by choosing the sign of $v_\ell$ appropriately, one can show that there exists a unitary vector $v$ such that

$$\left\| \left( D^* \begin{bmatrix} 0 & M_{12} \\ c_p M_{21} & c_p M_{22} \end{bmatrix} (D^*)^{-1} \right) v \right\|_2 \geq \left\| \left( D^* \begin{bmatrix} 0 & M_{12} \\ c_p M_{21} & 0 \end{bmatrix} (D^*)^{-1} \right) v \right\|_2 \tag{3.130}$$

Hence,

$$\inf_{D\in\mathcal{D}_{rp}} \bar{\sigma}\left(D\begin{bmatrix} 0 & M_{12} \\ c_pM_{21} & c_pM_{22} \end{bmatrix}D^{-1}\right) \tag{3.131}$$

$$\geq \left\|\left(D^*\begin{bmatrix} 0 & M_{12} \\ c_pM_{21} & c_pM_{22} \end{bmatrix}(D^*)^{-1}\right)v\right\|_2 \tag{3.132}$$

$$\geq \left\|\left(D^*\begin{bmatrix} 0 & M_{12} \\ c_pM_{21} & 0 \end{bmatrix}(D^*)^{-1}\right)v\right\|_2 \tag{3.133}$$

$$= \bar{\sigma}\left(D^*\begin{bmatrix} 0 & M_{12} \\ c_pM_{21} & 0 \end{bmatrix}(D^*)^{-1}\right) \tag{3.134}$$

$$\geq \inf_{D\in\mathcal{D}_{rp}} \bar{\sigma}\left(D\begin{bmatrix} 0 & M_{12} \\ c_pM_{21} & 0 \end{bmatrix}D^{-1}\right) \tag{3.135}$$

■

These lemmas will be used to derive simple measurement selection rules for specific uncertainty structures. The derived rules are analogous to some of the previously available criteria.

## Multiplicative Uncertainty on the Disturbance Gain Matrix

Consider the following multiplicative perturbation on the gain matrix relating the disturbances and the measured variables:

$$G_{y_md} = (I + W_o\Delta_o)G_{y_md}, \quad \Delta_o \in \mathbf{\Delta_o} = \{\Delta : \bar{\sigma}(\Delta_o) \leq 1\} \tag{3.136}$$

The uncertainty is represented schematically in Figure 3.5. Let us make the following assumptions to simplify the discussion:

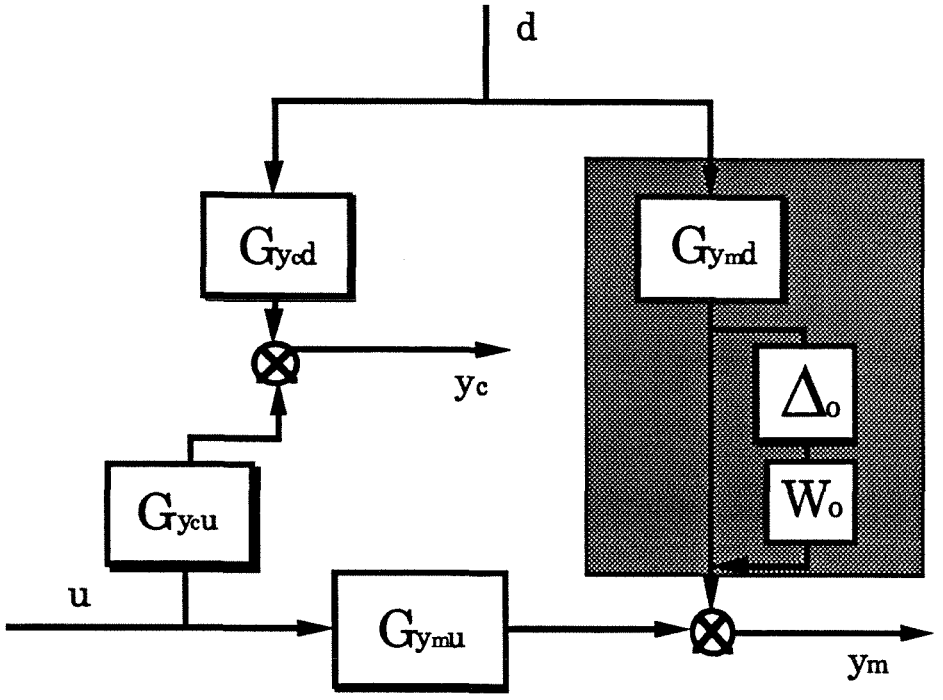


Figure 3.5. Multiplicative Uncertainty on the Disturbance Gain Matrix

1. $G_{y_c u}$ has full row rank. This means that there are at least as many manipulated variables as the controlled variables.

2. There is no noise corrupting the measurements at steady state.

3. No input weighting is used at steady state.

These assumptions amount to restricting the structures of the external input and performance weights to be

$$W_w = \begin{bmatrix} W_w^d & & & \\ & W_w^r & & \\ & & 0 & \\ & & & 0 \end{bmatrix} \tag{3.137}$$

$$W_p = \begin{bmatrix} W_p^{y_c} & \\ & 0 \end{bmatrix} \tag{3.138}$$

and

$$Q_{dc}^{\text{proj}} = G_{y_cu}^{-1}\left[\begin{array}{cc} -G_{y_cd}G_{y_md}^T(G_{y_md}G_{y_md}^T)^{-1} & I \end{array}\right] \tag{3.139}$$

With these assumptions,

$$M^{\text{proj}} = \left[\begin{array}{cc} M_{11} & M_{12} \\ M_{21} & M_{22} \end{array}\right] \tag{3.140}$$

where

$$M_{11}^{\text{proj}} = 0 \tag{3.141}$$

$$M_{12\text{proj}} = \left[\begin{array}{cccc} G_{y_md}W_w^d & 0 & 0 & 0 \end{array}\right] \tag{3.142}$$

$$M_{21}^{\text{proj}} = \left[\begin{array}{c} -W_p^{y_e}G_{y_cd}G_{y_md}^T(G_{y_md}G_{y_md}^T)^{-1}W_o \\ 0 \end{array}\right] \tag{3.143}$$

$$M_{22}^{\text{proj}} = \left[\begin{array}{cccc} W_pG_{y_cd}(I - G_{y_md}^T(G_{y_md}G_{y_md}^T)^{-1}G_{y_md})W_w^d & 0 & 0 & 0 \\ 0 & 0 & 0 & 0 \end{array}\right] \tag{3.144}$$

Since the rows and columns do not affect $\mu$, we can define $M^{\text{proj}}$ to be the following matrix instead:

$$M^{\text{proj}} = \left[\begin{array}{cc} 0 & G_{y_md}W_w^d \\ -W_p^{y_e}G_{y_cd}G_{y_md}^T(G_{y_md}G_{y_md}^T)^{-1}W_o & W_pG_{y_cd}(I - G_{y_md}^T(G_{y_md}G_{y_md}^T)^{-1}G_{y_md})W_w^d \end{array}\right] \tag{3.145}$$

From Lemma 3.4,

$$\mathcal{E}_{worst}(\hat{M}^{\text{proj}}, \mathbf{\Delta_o}) \leq \mathcal{E}_{worst}(M^{\text{proj}}, \mathbf{\Delta_o}) \tag{3.146}$$

where

$$\hat{M}^{\text{proj}} = \left[\begin{array}{cc} 0 & G_{y_md}W_w^d \\ -W_p^{y_e}G_{y_cd}G_{y_md}^T(G_{y_md}G_{y_md}^T)^{-1}W_o & 0 \end{array}\right] \tag{3.147}$$

Hence $\mathcal{E}_{worst}(\hat{M}^{\text{proj}}, \mathbf{\Delta_o})$ provides a lower bound for the "worst-case" closed-loop steady-state error. Note that $M_{22}^{\text{proj}}$ is the *nominal* (*i.e.*, in the absence of the pertur-

bation) closed-error matrix. When $G_{y_md}$ is a nonsingular, square matrix, $M_{22}^{\text{proj}} = 0$ and $\mathcal{E}_{worst}(\hat{M}^{\text{proj}}, \mathbf{\Delta_o}) = \mathcal{E}_{worst}(M^{\text{proj}}, \mathbf{\Delta_o})$.

**Special Case I: Unstructured $\Delta_o$ - Condition Number Criterion**

Suppose $\Delta_o$ has no particular structure within itself. Hence,

$$\Delta_o \in \mathbf{\Delta_o^{ust}} = \left\{\Delta : \bar{\sigma}(\Delta) \leq 1, \Delta \in \mathcal{C}^{\dim\{y_m\}\times\dim\{y_m\}}\right\} \tag{3.148}$$

Then, from Lemma 3.3

$$\mathcal{E}_{worst}(\hat{M}^{\text{proj}}, \mathbf{\Delta_o^{ust}}) = \inf_{d\in\mathcal{R}+} \bar{\sigma}(W_p^{y_e} G_{y_cd} G_{y_md}^T (G_{y_md} G_{y_md}^T)^{-1} W_o \frac{1}{d}) \bar{\sigma}(d G_{y_md} W_w^d) \tag{3.149}$$

Suppose $W_o = w_o I$, $W_p^{y_e} G_{y_cd} = w_p I$, and $W_w^d = w_d I$. The last two assumptions imply that the disturbances enter directly into the controlled variables (with same weights). Then (3.149) becomes

$$\bar{\sigma}(W_p^{y_e} G_{y_cd} G_{y_md}^T (G_{y_md} G_{y_md}^T)^{-1} W_o) \bar{\sigma}(G_{y_md} W_w^d) \tag{3.150}$$

$$= |w_p w_o w_d| \bar{\sigma}(G_{y_md}^T (G_{y_md} G_{y_md}^T)^{-1}) \bar{\sigma}(G_{y_md}) \tag{3.151}$$

$$= |w_p w_o w_d| \kappa(G_{y_md}) \tag{3.152}$$

where $\kappa$ denotes the condition number, the ratio between the maximum and minumum singular values. Hence, steady-state measurement selection criteria can be stated as

1. *Minimize the quantity* $\bar{\sigma}(W_p^{y_e} G_{y_cd} G_{y_md}^T (G_{y_md} G_{y_md}^T)^{-1} W_o) \bar{\sigma}(G_{y_md} W_w^d)$.

2. *If* $W_o = w_o I$, $W_p^{y_e} G_{y_cd} = w_p I$, *and* $W_w^d = w_d I$, *minimize the condition number of* $G_{y_md}$.

Thus we have shown that Brosilow's Condition Number Criterion [31] holds only under some very specific assumptions on model uncertainty and disturbance/performance weights.

**Special Case II: Diagonal $\Delta_o$ - Minimized Condition Number/ RGA Criterion**

Describing the gain uncertainty using the unstructured $\Delta_o$ is very conservative for most practical cases; usually model uncertainty occurs physically in a more structured manner [22,60]. For instance, a more physically meaningful $\Delta_o$ can be

$$\Delta_o \in \mathbf{\Delta_o^{st}} = \left\{ \begin{bmatrix} \delta_1 & & \\ & \ddots & \\ & & \delta_n \end{bmatrix} : |\delta_i| \le 1, \ \ \delta_i \in \mathcal{C}, \ \ 1 \le i \le n \right\} \tag{3.153}$$

With diagonal weighting matrix $W_o$, it represents the multiplicative uncertainty on each output of $G_{y_m d}$.

From Lemma 3.3,

$$\mathcal{E}_{worst}(\hat{M}^{\text{proj}}, \mathbf{\Delta_o^{st}}) = \inf_{\tilde{D} \in \mathcal{D}_{diag}} \bar{\sigma}(W_p^{y_e} G_{y_c d} G_{y_m d}^T (G_{y_m d} G_{y_m d}^T)^{-1} W_o \tilde{D}^{-1}) \bar{\sigma}(\tilde{D} G_{y_m d} W_w^d) \tag{3.154}$$

where

$$\mathcal{D}_{diag} = \left\{ \text{diag}(d_1, \cdots, d_{\dim\{y_m\}}) : d_i \in \mathcal{R}^+, 1 \le i \le \dim\{y_m\} \right\} \tag{3.155}$$

If we assume again $W_o = w_o I$, $W_p^{y_e} G_{y_c d} = w_p I$, and $W_w^d = w_d I$,

$$\begin{aligned} & \mathcal{E}_{worst}(\hat{M}^{\text{proj}}, \mathbf{\Delta_o^{st}}) \\ = \ & |w_p w_o w_d| \inf_{\tilde{D} \in \mathcal{D}_{diag}} \bar{\sigma}(G_{y_c d} G_{y_m d}^T (G_{y_m d} G_{y_m d}^T)^{-1} \tilde{D}^{-1}) \bar{\sigma}(\tilde{D} G_{y_m d}) \qquad (3.156) \\ \le \ & |w_p w_o w_d| \min_{\tilde{D} \in \mathcal{D}_{diag}} \kappa(\tilde{D} G_{y_m d}) \ (= \text{if } G_{y_m d} \text{ is a square matrix}) \qquad (3.157) \end{aligned}$$

Here we used the inequality (equality if $G_{y_m d}$ is a square matrix)

$$\bar{\sigma}(G_{y_m d}^T (G_{y_m d} G_{y_m d}^T)^{-1} \tilde{D}^{-1}) \le \{\underline{\sigma}(\tilde{D} G_{y_m d})\}^{-1}, \ \ \forall \tilde{D} \in \mathcal{D}_{diag} \tag{3.158}$$

Hence, for diagonal $\Delta_o$, the measurement selection criterion corresponding to Brosilow's Condition Number Criterion is to minimize the condition number of $G_{y_md}$ minimized with respect to output scaling matrices.

The following inequality (Nett and Manousiouthakis, [51]) shows that, for cases where $G_{y_md}$ is square, the RGA of $G_{y_md}$ can be used as a screening tool for measurement selection:

$$\begin{aligned} \|\Lambda\|_m - 1 &\leq \inf_{D_1, D_2 \in \mathcal{D}_{diag}} \kappa(D_1 G_{sd} D_2) && (3.159)\\ &\leq \inf_{\tilde{D} \in \mathcal{D}_{diag}} \kappa(\tilde{D} G_{sd}) && (3.160)\\ &= \frac{1}{|w_p w_s w_d|} \mathcal{E}_{worst}(\hat{M}^{\text{proj}}, \mathbf{\Delta_o^{st}}) && (3.161)\\ &\leq \frac{1}{|w_p w_s w_d|} \mathcal{E}_{worst}(M^{\text{proj}}, \mathbf{\Delta_o^{st}}) && (3.162) \end{aligned}$$

where

$$\begin{aligned} \Lambda &= G_{y_md} \otimes (G_{y_md}^{-1})^T && (3.163)\\ \|\Lambda\|_m &= 2\max\{\|\Lambda\|_{i1}, \|\Lambda\|_{i\infty}\} && (3.164) \end{aligned}$$

and $\otimes$, $\|\cdot\|_{i1}$ and $\|\cdot\|_{i\infty}$ denote the Schur product, induced 1-norm and $\infty$-norm respectively. (3.159) says that a large RGA of $G_{y_md}$ necessarily implies a large $\mathcal{E}_{worst}(M^{\text{proj}}, \mathbf{\Delta_o^{st}})$. Hence, the RGA of $G_{y_md}$ can be a useful screening tool to eliminate undesirable measurement sets for these cases. The measurement selection criteria can be summarized as

1. *Minimize the quantity*

$$\inf_{\tilde{D} \in \mathcal{D}_{diag}} \bar{\sigma}(W_p^{y_e} G_{y_cd} G_{y_md}^T (G_{y_md} G_{y_md}^T)^{-1} W_o \tilde{D}^{-1}) \bar{\sigma}(\tilde{D} G_{y_md} W_w^d)$$

2. *If* $W_o = w_o I$, $W_p^{y_e} G_{y_cd} = w_p I$, *and* $W_w^d = w_d I$,

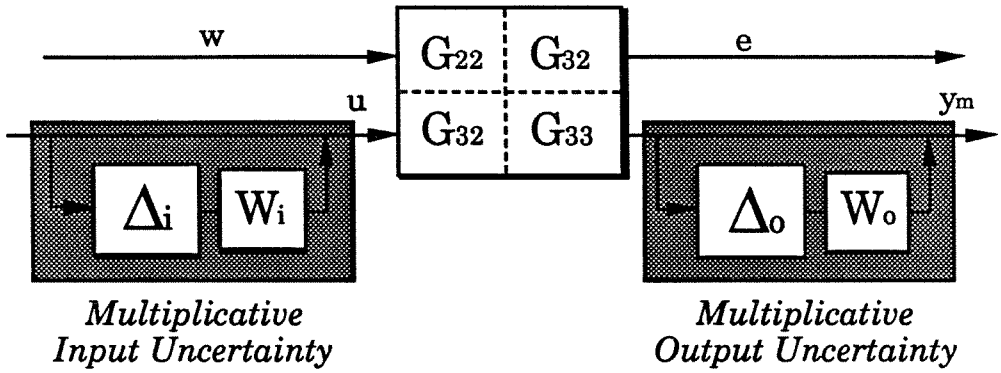


Figure 3.6. Multiplicative Uncertainty on Manipulated and Measured Signals

- *Eliminate the measurements with large RGA of the gain matrix* $G_{y_m d}$.
- *Minimize the condition number of* $G_{y_m d}$ *minimized with respect to output scaling matrices.*

## Uncertainty Present Within the Feedback Loop

When a controller with full integral action is used, the effect of all uncertainty present within the feedback loop disappears at steady state. For example, let us consider the following uncertainty descriptions:

$$u_{\text{real}} = (I + W_i\Delta_i)u; \quad \Delta_i \in \mathbf{\Delta_I} = \{\Delta : \bar{\sigma}(\Delta) \leq 1\} \tag{3.165}$$

$$(y_m)_{\text{real}} = (I + W_o\Delta_i)y_m; \quad \Delta_o \in \mathbf{\Delta_O} = \{\Delta : \bar{\sigma}(\Delta) \leq 1\} \tag{3.166}$$

The uncertainty is represented schematically in Figure 3.6. To keep the discussion as general as possible, we let $\mathbf{\Delta_I}$ and $\mathbf{\Delta_O}$ have specific structures within themselves. The perturbations $\mathbf{\Delta_I}$ and $\mathbf{\Delta_O}$ can be interpreted as multiplicative errors in the actuator and sensor signals respectively. Assuming no setpoint change is to be made

($w = \begin{bmatrix} d^T & v_m^T \end{bmatrix}$), the resulting $M^{\text{intg}}$ is as follows:

$$M^{\text{intg}} = \begin{bmatrix} \begin{bmatrix} -W_i & -G_{y_m u}^{-1} W_o \\ 0 & W_o \end{bmatrix} & \begin{bmatrix} G_{y_m u}^{-1} G_{y_m w} W_w \\ 0 \end{bmatrix} \\ \begin{bmatrix} 0 & W_p G_{eu} G_{y_m u}^{-1} W_o \end{bmatrix} & W_p (G_{ew} - G_{eu} G_{y_m u}^{-1} G_{y_m w}) W_w \end{bmatrix} \tag{3.167}$$

It is very easy to show that

$$\mathcal{E}_{worst}\left( M^{\text{intg}}, \begin{bmatrix} \mathbf{\Delta_I} & \\ & \mathbf{\Delta_O} \end{bmatrix} \right) = \bar{\sigma}\left( W_p (G_{ew} - G_{eu} G_{y_m u}^{-1} G_{y_m w}) W_w \right) \tag{3.168}$$

assuming

$$\mu_{\begin{bmatrix} \mathbf{\Delta_I} & \\ & \mathbf{\Delta_O} \end{bmatrix}} \left( \begin{bmatrix} -W_i & -G_{y_m u}^{-1} W_o \\ 0 & W_o \end{bmatrix} \right) < 1 \tag{3.169}$$

which is equivalent to

$$\mu_{\mathbf{\Delta_I}}(W_i) < 1 \text{ and } \mu_{\mathbf{\Delta_O}}(W_o) < 1 \tag{3.170}$$

The condition (3.169) is the condition for robust stability at $\omega = 0$. The expression for $\mathcal{E}_{worst}\left( M^{\text{intg}}, \begin{bmatrix} \mathbf{\Delta_I} & \\ & \mathbf{\Delta_O} \end{bmatrix} \right)$ is equivalent to the maximum singular value of the "inferential error" matrix that Bequette and Edgar [5] proposed to minimize in their measurement selection criteria.

## 3.5 Numerical Example 1: Multicomponent Distillation

We apply the screening tools to a multi-component distillation column that was studied by Weber & Brosilow [61]. We first apply a generalized version of Brosilow's criteria and show that they lead to a counter-intuitive result. Then, we apply the new

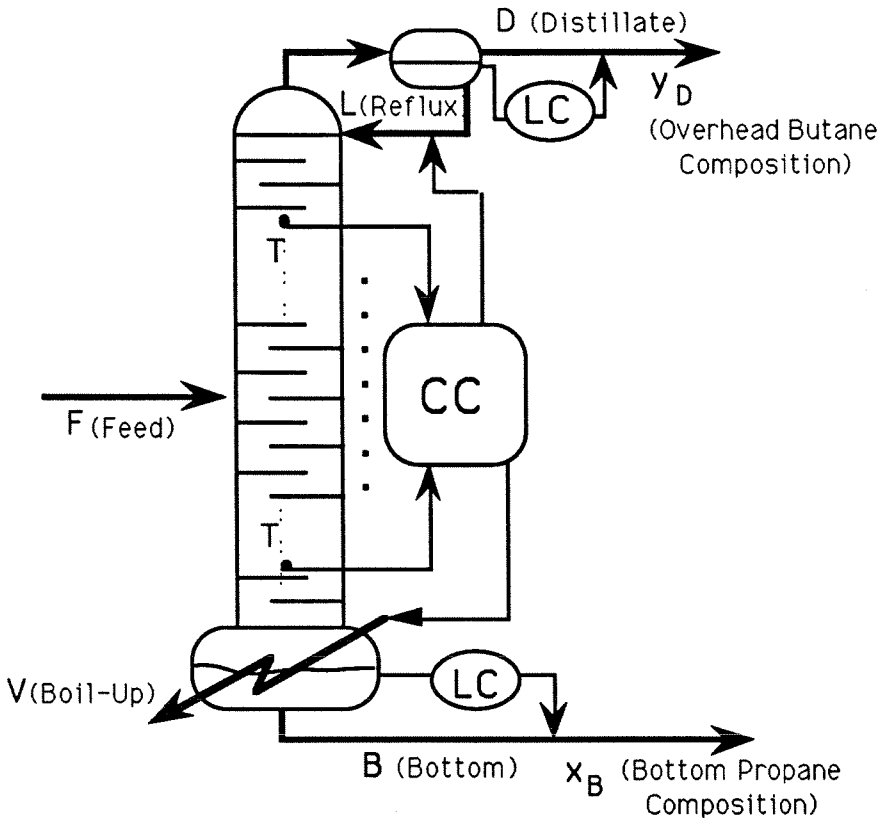


Figure 3.7. Schematic Diagram of a Multi-Component Distillation Column and its Control Structure

screening tools under various uncertainty assumptions. The example will demonstrate that the new screening tools provide an effective way of analyzing the sensitivity of candidate measurement sets to various uncertainty structures.

### 3.5.1 Problem Description

The schematic diagram of the column and proposed control configuration is shown in Figure 3.7. It is a 16 stage, 5 component distillation column with a total condenser and a total reboiler. The detailed information on the operating conditions and modelling assumptions of the column can be found in Tong & Brosilow [7]. The control objective is to maintain constant overhead and bottom product compositions ($y_D$ and $x_B$ respectively) in the presence of feed disturbances. The mainpulated variables

are the reflux ratio ($L$) and vapor boilup rate ($V$). The temperature measurements are available for the 1st, 3rd, 8th, 14th, and 16th trays ($T_1, T_3, T_8, T_{14}$ and $T_{16}$ respectively) of the column. The model for the input-output relationships between disturbances/manipuated variables and controlled/measured variables are as follows:

| | $d_1$ | $d_2$ | $d_3$ | $d_4$ | $d_5$ | $L$ | $V$ |
|---|---|---|---|---|---|---|---|
| $y_D$ | $\frac{-0.188}{72s+1}$ | $\frac{-0.163}{72s+1}$ | $\frac{0.0199}{70s+1}$ | $\frac{0.0043}{80s+1}$ | $\frac{0.002}{85s+1}$ | $\frac{-0.173}{70s+1}$ | $\frac{0.0305}{75s+1}$ |
| $x_B$ | $\frac{0.0174}{15s+1}$ | $\frac{0.0259}{13s+1}$ | $\frac{0.0045}{4s+1}$ | $\frac{-0.00029}{3s+1}$ | $\frac{-0.00099}{3s+1}$ | $\frac{0.015}{18s+1}$ | $\frac{-0.00768}{7s+1}$ |
| $T_1$ | $\frac{-7.99}{9s+1}$ | $\frac{-9.78}{9s+1}$ | $\frac{-5.28}{5s+1}$ | $\frac{3.59}{8s+1}$ | $\frac{6.09}{5s+1}$ | $\frac{7.47}{8s+1}$ | $\frac{2.70}{4s+1}$ |
| $T_3$ | $\frac{-11.29}{12s+1}$ | $\frac{-15.91}{12s+1}$ | $\frac{-4.23}{5s+1}$ | $\frac{3.63}{8s+1}$ | $\frac{4.75}{5s+1}$ | $\frac{9.80}{15s+1}$ | $\frac{3.79}{5s+1}$ |
| $T_8$ | $\frac{-18.28}{5s+1}$ | $\frac{-16.43}{10s+1}$ | $\frac{-0.47}{5s+1}$ | $\frac{3.96}{3s+1}$ | $\frac{4.60}{1.5s+1}$ | $\frac{8.20}{30s+1}$ | $\frac{2.30}{18s+1}$ |
| $T_{14}$ | $\frac{-42.02}{50s+1}$ | $\frac{-35.92}{70s+1}$ | $\frac{4.45}{65s+1}$ | $\frac{1.10}{70s+1}$ | $\frac{0.46}{75s+1}$ | $\frac{36.0}{65s+1}$ | $\frac{6.82}{70s+1}$ |
| $T_{16}$ | $\frac{-50.47}{25s+1}$ | $\frac{-25.26}{75s+1}$ | $\frac{3.15}{70s+1}$ | $\frac{0.68}{78s+1}$ | $\frac{0.32}{80s+1}$ | $\frac{30.0}{67s+1}$ | $\frac{3.46}{70s+1}$ |

To facilitate the exposition, we limit ourselves to the following combinations of temperature measurements:

**One Temperature Measurement:**

$$y_m^1 = T_1 \quad y_m^2 = T_3 \quad y_m^3 = T_8 \quad y_m^4 = T_{14} \quad y_m^5 = T_{16}$$

**Two Temperature Measurements:**

$$y_m^6 = \begin{pmatrix} T_1 \\ T_3 \end{pmatrix} \quad y_m^7 = \begin{pmatrix} T_1 \\ T_8 \end{pmatrix} \quad y_m^8 = \begin{pmatrix} T_1 \\ T_{14} \end{pmatrix} \quad y_m^9 = \begin{pmatrix} T_1 \\ T_{16} \end{pmatrix} \quad y_m^{10} = \begin{pmatrix} T_3 \\ T_8 \end{pmatrix}$$

$$y_m^{11} = \begin{pmatrix} T_3 \\ T_{14} \end{pmatrix} \quad y_m^{12} = \begin{pmatrix} T_3 \\ T_{16} \end{pmatrix} \quad y_m^{13} = \begin{pmatrix} T_8 \\ T_{14} \end{pmatrix} \quad y_m^{14} = \begin{pmatrix} T_8 \\ T_{16} \end{pmatrix} \quad y_m^{15} = \begin{pmatrix} T_{14} \\ T_{16} \end{pmatrix}$$

**Three Temperature Measurements:**

$$y_m^{16} = \begin{pmatrix} T_8 & T_{14} & T_{16} \end{pmatrix}^T$$

**Four Temperature Measurements:**

$$y_m^{17} = \begin{pmatrix} T_3 & T_8 & T_{14} & T_{16} \end{pmatrix}^T$$

**Five Temperature Measurements:**

$$y_m^{18} = \begin{pmatrix} T_1 & T_3 & T_8 & T_{14} & T_{16} \end{pmatrix}^T$$

### 3.5.2 Application of Brosilow's Criteria

#### Brosilow's Criteria

Brosilow and coworkers [61,31] suggested the following two *steady-state* criteria for measurement selection:

1. **Minimization of Projection Error (Nominal Estimation Error)**

   *Minimize the projection error* $\mathcal{E}$ *where*

$$\mathcal{E} = \bar{\sigma}\left[G_{y_c d} - G_{y_c d} G_{y_m d}^T (G_{y_m d}^T G_{y_m d})^{-1} G_{y_m d}\right] \tag{3.171}$$

2. **Minimization of Condition Number (Sensitivity to Modelling Error)**

   *Minimize the condition number* $\kappa$ *of* $G_{y_m d}$ *where*

$$\kappa(G_{y_m d}) = \frac{\bar{\sigma}(G_{y_m d})}{\underline{\sigma}(G_{y_m d})} \tag{3.172}$$

They indicate that the above two quantities conflict as the number of the measurements are varied, and leave the final trade-off to engineering judgement. We note

that the projection error $\mathcal{E}$ as was originally defined by Brosilow and coworkers is not that of (3.171), but

$$\mathcal{E} = \frac{\text{trace}\{R\}}{\text{trace}\{G_{y_cd}^T G_{y_cd}\}} \tag{3.173}$$

where

$$R = G_{y_cd}^T G_{y_cd} - G_{y_cd}^T G_{y_md}(G_{y_md} G_{y_md}^T)^{-1} G_{y_md}^T G_{y_cd} \tag{3.174}$$

The original definition of the projection error is appropriate when the disturbance vector is a random variable with zero mean and an identity covariance matrix (*i.e.*, $E\{d\} = 0, E\{dd^T\} = I$). In the "worst-case" error setting such as $H_\infty$ control, (3.171) is the appropriate generalization of (3.173), since it is the measure of the worst-possible 2-norm of $y_c$ for all $d$ such that $||d||_2 < 1$.

## Theoretical Justification of Brosilow's Criteria

Suppose that the model error on $G_{y_md}$ can be described as follows:

**Uncertainty A: Unstructured Multiplicative Ouput Uncertainty**

$$\{G_{y_md}\}_{\text{true}} = (I + w\Delta)G_{y_md}; \quad \Delta \in \mathbf{\Delta} \equiv \left\{\Delta \in \mathcal{R}^{\dim\{y_m\}\times\dim\{y_m\}} : \bar{\sigma}(\Delta) \le 1\right\} \tag{3.175}$$

$w$ is a real positive scalar indicating the size of the ball describing uncertainty. Furthermore, assume that the least-square type controller will be used. More precisely, $K$ is to be designed such that

$$K(0) = Q_{\text{ls}}(I + G_{y_mu}(0)Q_{\text{ls}})^{-1} \tag{3.176}$$

$$Q_{\text{ls}} = (G_{y_cu})_r^{-1} G_{y_cd} G_{y_md}^T (G_{y_md} G_{y_md}^T)^{-1} \tag{3.177}$$

Here, we assumed that $(G_{y_cu})_r^{-1}$, a right inverse of $G_{y_cu}$, exists. When $G_{y_cu}$ does not have a full column rank, $(G_{y_cu})_r^{-1}$ should be replaced by $(G_{y_cu}^T G_{y_cu})^{-1} G_{y_cu}^T$. However, we do not consider this case in order to simplify the derivation. The closed-loop

expression from $d$ to $y_c$ with the above choice of $K$ is as follows:

$$\mathcal{F}_{y_cd}(0) = \left[G_{y_cd} - G_{y_cd}G_{y_md}^T(G_{y_md}G_{y_md}^T)^{-1}G_{y_md}\right] + w\left[G_{y_cd}G_{y_md}^T(G_{y_md}G_{y_md}^T)^{-1}\Delta G_{y_md}\right] \tag{3.178}$$

Hence, the worst-possible 2-norm of the output $y_c$ for $\|d\|_2 < 1$ is expressed as

$$\begin{aligned}
& \max_{\Delta\in\mathbf{\Delta}} \bar{\sigma}(\mathcal{F}_{y_cd}(0)) \\
\leq\ & \bar{\sigma}\left[G_{y_cd} - G_{y_cd}G_{y_md}^T(G_{y_md}G_{y_md}^T)^{-1}G_{y_md}\right] + w\max_{\Delta\in\mathbf{\Delta}}\bar{\sigma}\left[G_{y_cd}G_{y_md}^T(G_{y_md}G_{y_md}^T)^{-1}\Delta G_{y_md}\right] \\
=\ & \bar{\sigma}\left[G_{y_cd} - G_{y_cd}G_{y_md}^T(G_{y_md}G_{y_md}^T)^{-1}G_{y_md}\right] + w\bar{\sigma}\left[G_{y_cd}G_{y_md}^T(G_{y_md}G_{y_md}^T)^{-1}\right]\bar{\sigma}\left[G_{y_md}\right] \\
=\ & \mathcal{E} + w'\kappa(G_{y_md}) \qquad \text{(with the assumption that } G_{y_cd} = kI\text{)}
\end{aligned} \tag{3.179}$$

Note that, in order to obtain the last step, we needed the assumption that $G_{y_cd}$ is a scalar-times-identity matrix ($w' = w * k$). Hence, the disturbances must be rescaled such that the assumption is satisfied before the criterion can be applied.

## Application to the Multi-Component Column

We just showed that minimizing $\mathcal{E} + w'\kappa(G_{y_md})$ minimizes only the upper-bound of the "worst-case" closed-loop output error. Actually, one can easily calculate the exact value of $\max_{\Delta\in\mathbf{\Delta}}\bar{\sigma}(\mathcal{F}_{y_cd}(0))$ by using Lemma 3.2. Figure 3.8 shows the worst-possible closed-loop error calculated through Lemma 3.2 (as well as the projection error and the condition number) for each measurement candidate when $w$ is set at 0.1. One notable result is that the closed-loop errors become worse as more measurements are added. This is counter-intuitive: Adding more measurements should not degrade the achievable performance since one can always set any measurement's effect to be zero through a control system. This counter-intuitive result can be attributed to the following two facts about Brosilow's criteria:

1. The uncertainty description (3.175) is "physically inconsistent." Note that, for example,

$$\left\{G_{y_m^1 d}(I + w\Delta) : \Delta \in \mathbf{\Delta}\right\} \neq \left\{\begin{bmatrix} 1 & 0 \\ 0 & 0 \end{bmatrix} G_{y_m^6 d}(I + w\Delta) : \Delta \in \mathbf{\Delta}\right\} \tag{3.180}$$

   From a physical standpoint, the two sets must be the same, since adding or taking out a measurement should not affect the uncertainty associated with the subsystem that does not involve the added/subtracted measurement.

2. The particular choice of $K$ (*i.e.*, $K(0) = Q_{\text{ls}}(I + G_{y_m u}(0)Q_{\text{ls}})^{-1}$) is in general not the best choice, since it does not consider the effect of uncertainty. The criterion depends explicitly on the assumption that such a controller is to be used.

### 3.5.3 Application of General Screening Tools

#### Physically Consistent Unstructured Ouput Uncertainty

First, we make the uncertainty description (3.175) physically consistent by modifying it as follows:

**Uncertainty B: Unstructured Additive Output Uncertainty**

$$\{G_{y_m d}\}_{\text{true}} = G_{y_m d} + w \begin{bmatrix} \delta_1 & 0 & 0 & 0 & 0 \\ 0 & \delta_3 & 0 & 0 & 0 \\ 0 & 0 & \delta_8 & 0 & 0 \\ 0 & 0 & 0 & \delta_{14} & 0 \\ 0 & 0 & 0 & 0 & \delta_{16} \end{bmatrix}^{\text{cond}} \Delta_{5\times 5} G_{y_m^{18} d} \tag{3.181}$$

where the $\delta_i = 1$ if $i^{\text{th}}$ tray temperature measurement is included in $y_m$ and 0 otherwise. The notation $[\cdot]^{\text{cond}}$ implies that the matrix is "condensated" meaning all

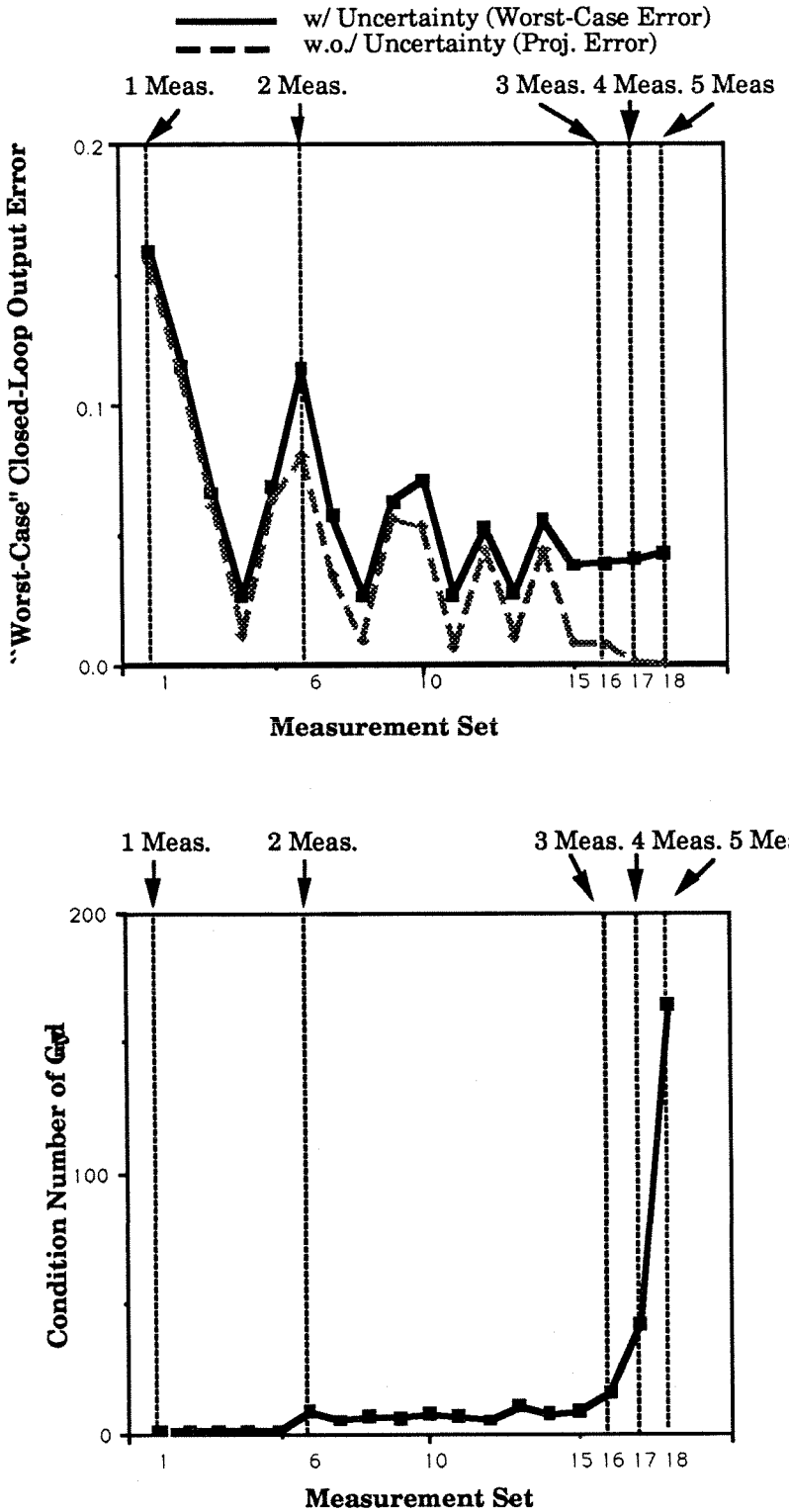


Figure 3.8. The 2-Norm of "Worst-Case" Steady-State Output Error, Projection Error and Condition Number of $G_{y_m d}$ for Various Measurement Sets Under Uncertainty A and "Least-Square" Controller

rows containg only zero elements are deleted. It is not our claim that the uncertainty description (3.181) is a physically meaningful one; we simply started from the uncertainty description that Brosilow & coworkers used in developing their criteria and modified it such that it became physically consistent.

Because the SSV test for robust performance involves 2-block $\Delta$ ($\Delta_{5\times 5}$ and $\Delta_p$), General Screening Tool #3 proposed in Section 3.3 is a necessary and sufficient condition for the existence of a constant matrix $K$ satisfying a given "worst-case" closed-loop error bound on the output. Instead of simply checking if a specific "worst-case" error bound can be satisfied for each measurement set, we calculated its achievable "worst-case" error, that is the "worst-case" error under the "$\mu$-optimal" controller expressed by

$$\min_{K} \max_{\Delta\in\mathbf{\Delta}} \bar{\sigma}(\mathcal{F}_{y_{cd}}(0)) \tag{3.182}$$

This can be easily done by multiplying a real positive scalar $c_p$ to $G_{y_{cd}}$ and $G_{y_{sd}}$ and increasing it just enough such that the condition corresponding to General Screening Tool #3 is no longer satisfied. The achievable "worst-case" error is the inverse of this particular value of $c_p$. The results are shown in Figure 3.9. Note that, although the achievable "worst-case" error decreases as more measurements are added (which is consistent with our physical intuition), the "worst-case" error for $y_m^{15}$ involving only two measurements is almost as low as that of $y_m^{18}$ involving five measurements. Hence, if the uncertainty description were indeed a physcially meaningful one, the use of more than two measurements is hardly justified in this case. Figure 3.10 shows the achievable "worst-case" closed-loop error for each measurement set when the "physically inconsistent" uncertainty description (3.175) is used. Figure 3.11 shows the "worst-case" closed-loop errors when the least-square controller (3.176) is used along with the uncertainty description (3.181). Note that, in both cases, the "worst-case" closed-loop errors increase as more measurements are added.

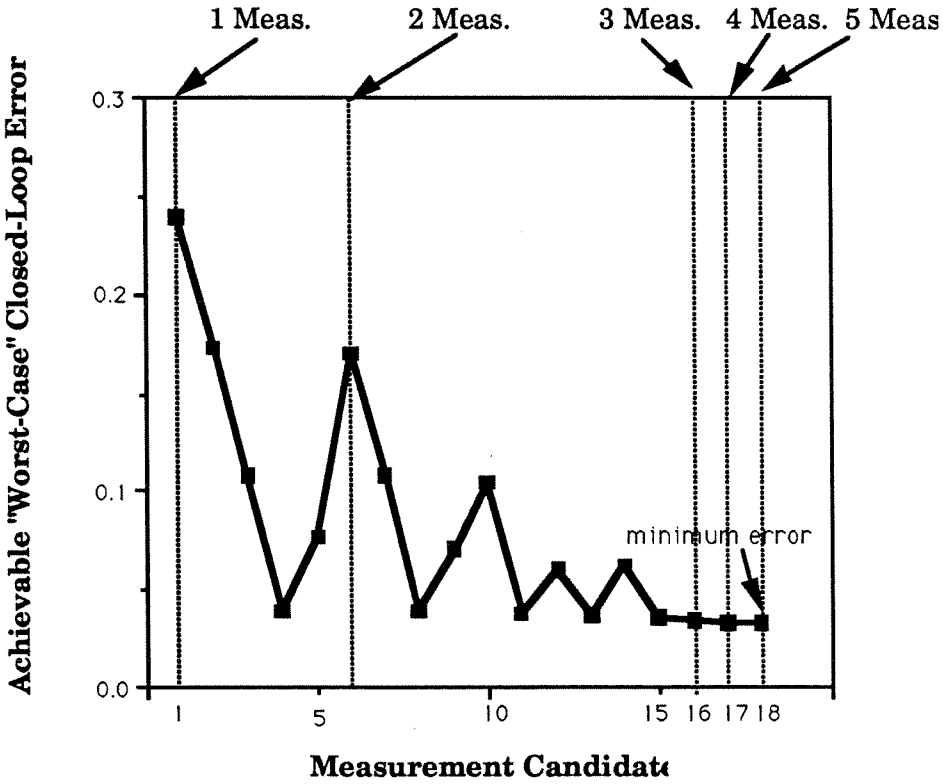


Figure 3.9. The 2-Norm of "Worst-Case" Steady-State Output Error for Various Measurement Sets Under Uncertainty B and "$\mu$-Optimal" Controller

## 3.6 Numerical Example 2: High-Purity Distillation Column

As an example application of proposed design-dependent screening tools, we study the high-purity distillation column shown in Figure 3.12. The column and the model are described in detail in Appendix A of Morari & Zafiriou [50]. The control problem of the column is presented in Figure 3.13.

### Problem Description

*Disturbances/Noise*

The most common disturbances are those in the feed; it often changes according to the conditions in another plant unit such as a reactor. Measurement error (noise) is often another important factor. We will study the effect of one physically moti-

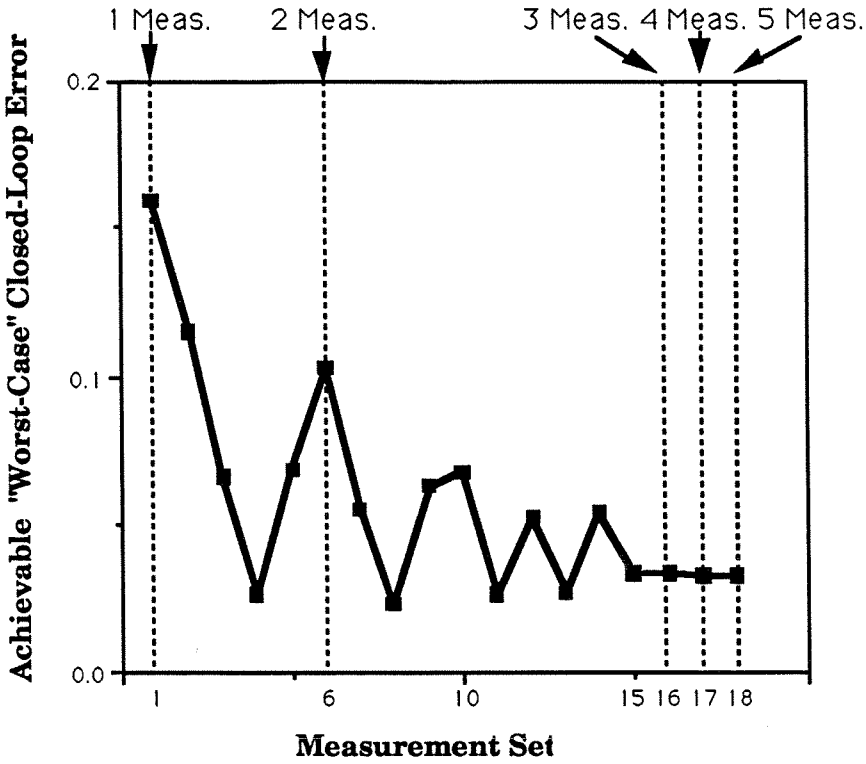


Figure 3.10. The 2-Norm of "Worst-Case" Steady-State Output Error for Various Measurement Sets Under Uncertainty A and "$\mu$-Optimal" Controller

vated measurement error: uncompensated pressure variation. The following set of disturbances/noise is considered:

Feed flowrate ($F$)

Feed composition ($z_F$)

Uncompensated pressure variation ($P$)

*Measured Variables*

Measurements are usually not limited to a specific number although it is common to use two tray temperatures for two-point composition control. In this example, for the sake of simplicity, we restrict ourselves to two tray temperatures ($T_a$ and $T_b$). In addition, for brevity of presentation, we consider only the placements symmetric with respect to the feedtray (such as tray #1/tray #41, tray #2/tray #40, and so on).

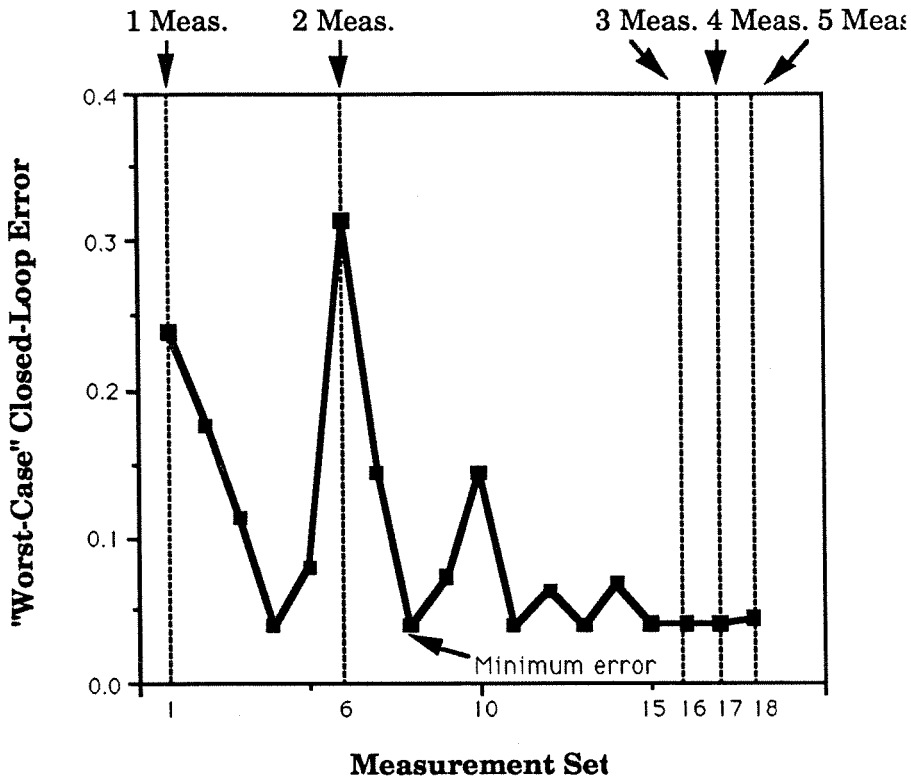


Figure 3.11. The 2-Norm of "Worst-Case" Steady-State Output Error for Various Measurement Sets Under Uncertainty B and "Least-Square" Controller

This is logical since the column is symmetric with respect to the feedtray.

*Uncertainty*

We limit ourselves to uncertainty in the manipulated variables. They have been shown to be the dominant uncertainty for high-purtity distillation columns [60]. We choose the same uncertainty weight $W_I$ that Skogestad & Morari [60] used in their study:

$$W_I = 0.2\frac{5s+1}{0.5s+1}I \tag{3.183}$$

*Performance and Disturbance Weight*

The performance weight $W_p$ and the disturbance weight $W_d$ are chosen as follows:

$$\begin{aligned} W_p &= 0.38\frac{100s+1}{10s+0.01}I \\ W_d &= [I \quad W_n] \end{aligned} \tag{3.184}$$

where

$$W_n = 0.04\frac{5s+1}{0.125s+1}\begin{bmatrix} \left(\frac{dT}{dP}\right)_{T=T_a} \\ \left(\frac{dT}{dP}\right)_{T=T_b} \end{bmatrix} \tag{3.185}$$

As usual, much tighter specifications are imposed in the low frequency region in order to ensure good steady-state response.

**Steady-State Performance**

We apply the Design-Dependent Screening Tool #1 for LQG/MPC of (3.89) to reduce the number of measurements to consider. The plot of the left-hand side of the inequality (3.89) vs. measurement sets is shown in Figure 3.14(a). It represents the measure of the "worst-possible" performance when the controller is designed yielding no steady-state offsets in compositions nominally (in the absence of uncertainty and measurement error). The measurement set of $T_7$ and $T_{35}$ shows the best steady-state performance. In fact, it is the only measurement set that satisfies the condition (3.89). This result can be interpreted physically. The temperatures measured close to the reboiler and the condenser have poor signal-to-noise ratio because the gains from disturbances to these measurements are "small." On the other hand, the measurements far away from the reboiler and the condenser are sensitive to model uncertainty since the relationships between the end-point compositions and the measurements become less direct. Hence, placement of the temperature sensors involves a compromise between these two factors. This is apparent from the plots shown in Figure 3.14(a) that represent the values for the left-hand side of the inequality (3.89) when measurement error (uncompensated pressure variation) / model uncertainty are neglected. The measurement set $T_7/T_{35}$ is apparently the best compromise between the signal-to-

noise ratio and the sensitivity to model uncertainty. Note that neglecting either the model uncertainty or the measurement error would have resulted in a wrong choice of measurements. Figure 3.14(b) represents the condition numbers of the steady-state gain matrices from the disturbances to the measurements ($G_{sd}(0)$). Note that the condition number (Brosilow's criterion) does not reflect the measurements' sensitivity to the uncertainty correctly in this particular problem.

**Output Estimation Based IMC Controller Design for Robust Performance**

To verify the result, we design controllers for the following three candidates: $T_1/T_{41}$, $T_7/T_{35}$ and $T_{17}/T_{25}$. For controllers, dynamic output estimators designed via Kalman filter design was combined with an IMC controller. IMC filters were designed separately for each candidate using the robust performance bounds derived for $\bar{\sigma}(F_{IMC}(j\omega))$ and $\bar{\sigma}(I - F_{IMC}(j\omega))$. The design method is explained in detail in Chapter 4. The robust performance bounds on $\bar{\sigma}(F_{IMC}(j\omega))$ and $\bar{\sigma}(I - F_{IMC}(j\omega))$ for the measurement set $T_7/T_{35}$ are shown in Figure 3.15(a). The bounds are "feasible" since the following transfer function meets at least one of the bounds at every frequency as we can see from Figure 3.15(a):

$$F_{IMC}(s) = g(s)I = \frac{107.5s + 1}{(100s + 1)(7.5s + 1)(2s + 1)}I \tag{3.186}$$

The bounds for the other two candidates were not "feasible" and the IMC filter was designed so that the bounds are satisfied for as wide a frequency range as possible. The $\mu$-plot for robust performance (Figure 3.15(b)) shows that robust performance is achieved for the measurement set $T_7/T_{35}$. Although not shown, the SSVs for the other two candidates exceeded 1 in some frequency regions, implying robust performance is not achieved. Figure 3.16 shows the simulated responses of $x_B$ and $y_D$ to unit step disturbances in $z_F$ and $F$ and a measurement noise in the form of a pseudo-random binary signal of unit magnitude filtered through $W_n$. The specific multiplicative

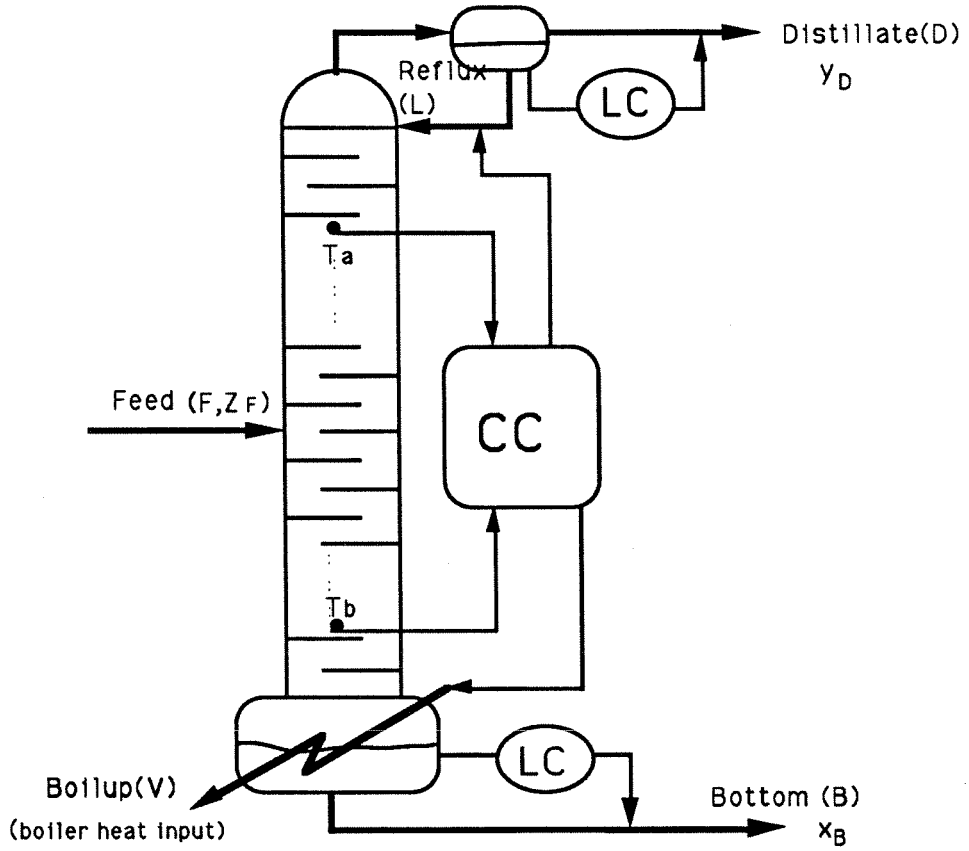


Figure 3.12. High-Purity Distillation Column

input uncertainty (*i.e.*, $W_I\Delta_I$) used for the simulation is $\begin{bmatrix} .2 & 0 \\ 0 & -.2 \end{bmatrix}$. The simulations confirm the physical interpretation given earlier.

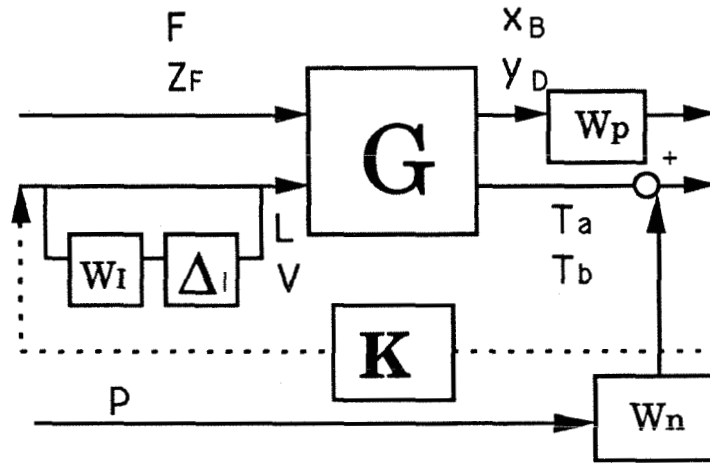


Figure 3.13. Control Problem In High-Purity Distillation Column

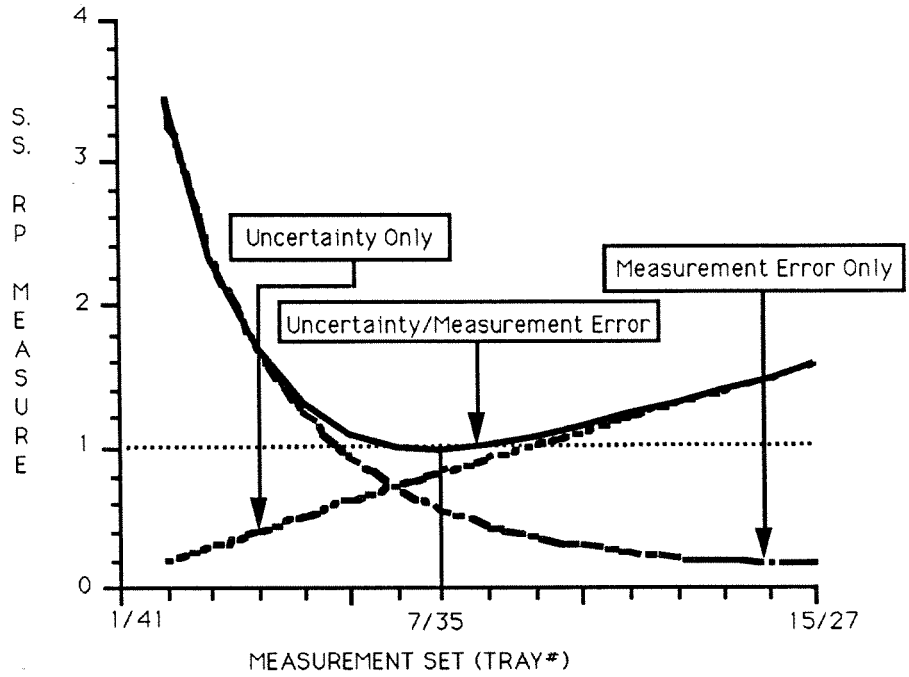


(a) Steady-State Robust Performance Measure

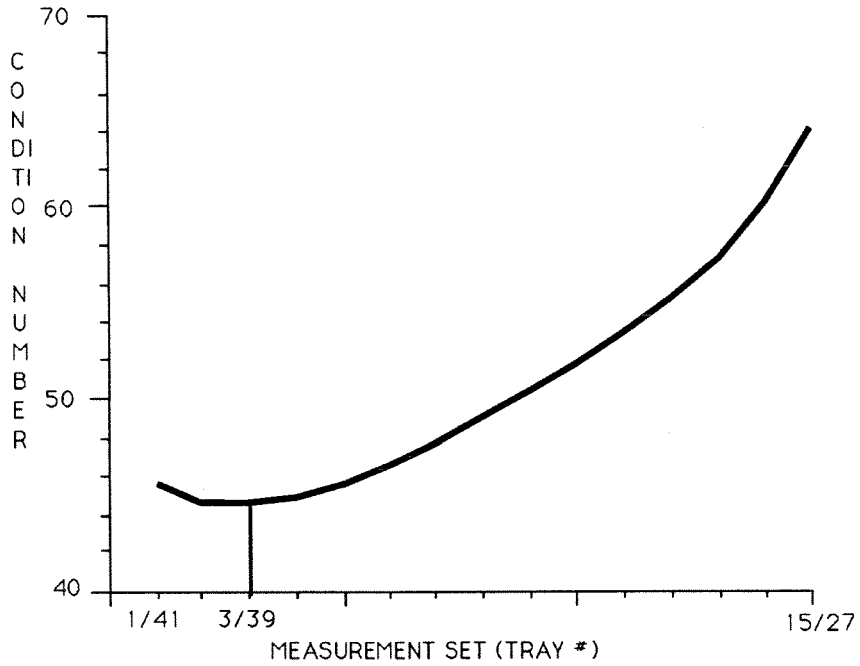


(b) Condition Number of $G_{ysd}$

Figure 3.14. Robust Performance Measure at Steady State

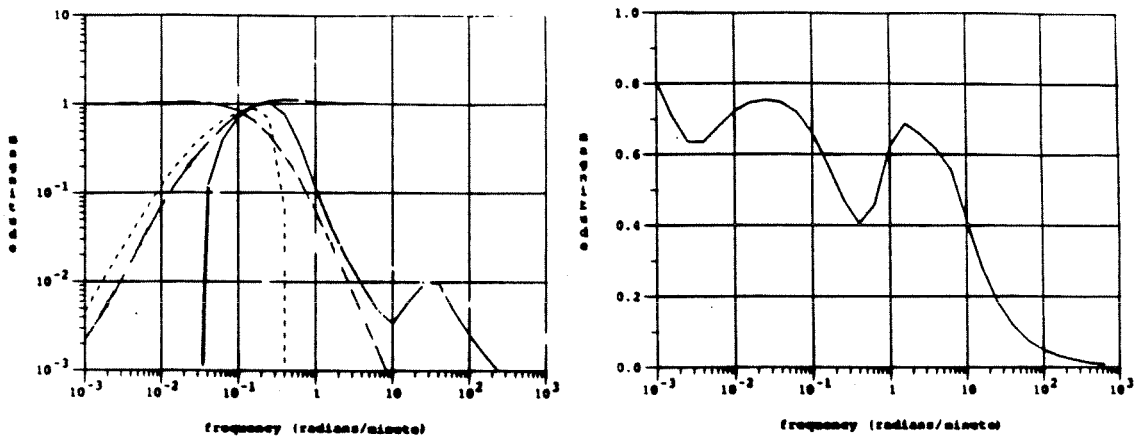


------- bound on $\bar{\sigma}(I - F_{IMC}(j\omega))$
— — — $|1 - g(j\omega)|$

(a) Meeting the Norm-Bounds

- - - - - bound on $\bar{\sigma}(F_{IMC}(j\omega))$
——— $|g(j\omega)|$

(b) SSV for Robust Performance

Figure 3.15. Meeting the Robust Performance Norm-bounds on $\bar{\sigma}(I - F_{IMC}(j\omega))$ and $\bar{\sigma}(\tilde{F_{IMC}}(j\omega))$ with $F_{IMC} = g(s)I$ for the Measurement Set $T_7/T_{35}$

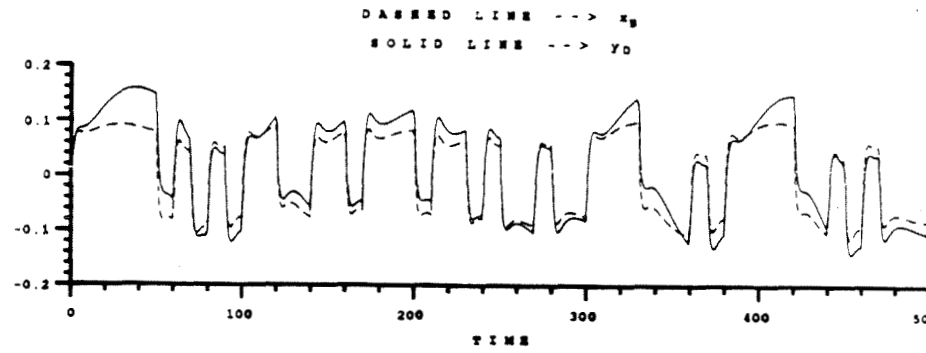


(a) Measurement Set Tray #1/Tray #41

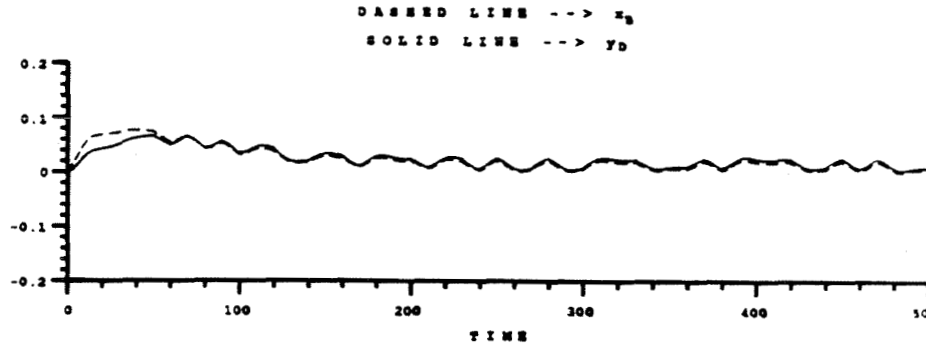


(b) Measurement Set Tray #7/Tray #35

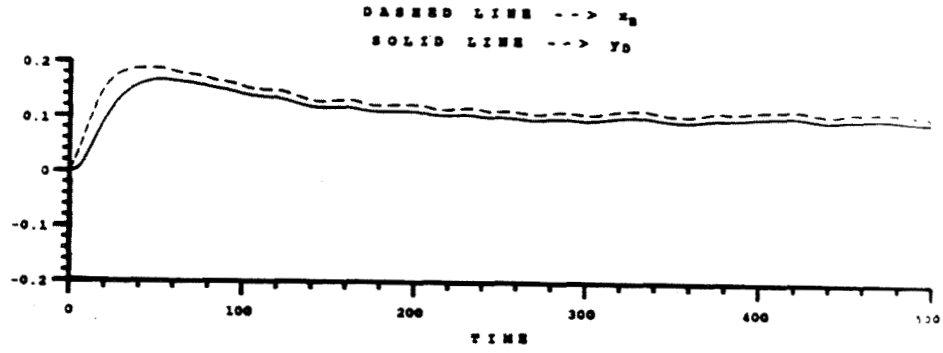


(c) Measurement Set Tray #17/Tray #25

Figure 3.16. Simulated Responses of $x_B$ and $y_D$ to the Unit Step Disturbances in $z_F$ and $F$ with 20 % Input Uncertainty and Pseudo-Random Binary Measurement Noise

# Chapter 4

# Output Estimation Based Inferential Control System Design

## 4.1 Overview

The topic of this chapter is inferential control system design based on *output estimation*. The output estimation based inferential control system design involves two independent design steps: design of an output estimator which constructs estimates

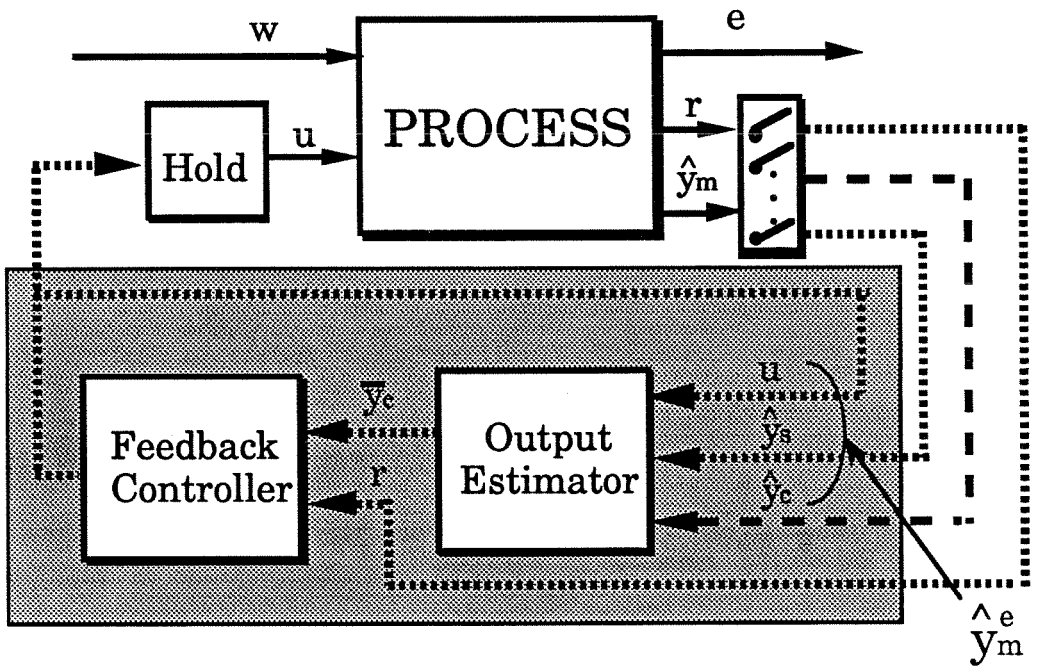


Figure 4.1. Output Estimation Based Inferential Control System

for the controlled outputs from the available measurements and that of a feedback controller that uses these estimates as feedback signals. The resulting inferential control system is represented schematically in Figure 4.1.

The advantages of this approach are that the design is divided into two simpler tasks and that it does not require a full dynamic model relating disturbances and primary/secondary variables. Plant data for primary and secondary variables may be used instead to construct an output estimator via regression techniques. A disadvantage is that, because secondary measurements are reduced to output estimates, some useful information on the future effects of disturbances may be lost. Hence, for systems with significant nonminimum-phase characteristics, the achievable performance can be lower when compared to the state estimation based approach discussed in Chapter 5.

The first topic of the chapter is output estimator design. Output estimator design is discussed in two different contexts: the case where a full dynamic model is to be used for the design and the case where only the plant data for primary and secondary variables are available. For the former case, design techniques such as Kalman filtering and $\mu$-Synthesis are discussed. For the latter case, standard linear regression techniques and their suitability for the estimator design are examined. In this case, the estimator design problem is formulated as a parametric identification problem. The standard Least Square (LS) regression method is discussed and potential problems that can arise from collinearity of the regression data are elucidated. Various modifications to the standard Least Square method available in the literature (in order to overcome the collinearity problem) are discussed and their merits for the estimator design are evaluated.

Since the estimator is designed to provide the control system with the *estimates* for the controlled variables at a desired rate with no delay, we next discuss feedback controller design for a limited class of systems for which the measurements of con-

trolled variables are provided in such a manner. We present four distinct, yet related design methods: LQG design in a form that is slightly different from the tranditional version in order to provide for integral action in the presence of nonstationary disturbances, IMC design which is a tailored version of LQG design with the advantage of simplified tuning, MPC design which is also an extension of LQG to handle various process constraints directly through on-line optimization, and finally $\mu$-Synthesis that exploits the given uncertainty model for robust design.

At a cursory glance, this chapter may seem like nothing more than a collection of well-known advanced design techniques. However, several important new ideas and interpretations for these modern techniques are given here. For example, for the first time, various $H_2$-optimal design methods such as LQG, IMC and MPC are interpreted in a unifying framework. This unification has some important practical implications:

1. MPC techniques based on state-space models have been around, but none of them had as transparent a connection with the tranditional techniques (DMC for example) as our version. Based on the new interpretation of MPC controllers as a state-observer-based compensator, the traditional techniques are shown to be special cases of the new technique under some restrictive assumptions about the system disturbances and measurement noise. The new version not only provides for wider applicability, but is also more readily extendable to other classes of control problems. One immediate extension of the new MPC technique is the inferential MPC technique discussed in Chapter 5.

2. Application of traditional MPC techniques was hampered by a lack of intuitive, simple on-line tuning parameters. The new version provides a set of simple, intuitive tuning parameters each of which has specific, well-understood effects on the closed-loop stability and performance.

3. The new state-space interpretation of IMC gives new insights and provides a basis for further extensions of the technique. For example, the interpretation of IMC as an observer-based-compensator renders naturally an anti-windup mechanism that is superior to the traditional IMC anti-windup scheme. In addition, the interpretation gives a basis upon which we can combine IMC with MPC to provide for simpler on/off-line tuning.

With the above-mentioned modifications, the potential for success of these modern methods in a practical environment is far enhanced.

All control techniques presented in this paper use the standard state-space model. For cases where use of step-response models is desired, Appendix A presents a MPC technique for step response models that is completely analogous to the technique presented in this chapter. An alternative is to convert the step-response model to a "low-order" state-space model by performing model reduction. Gu *et al.* [27] discusses a hankel model reduction technique that removes the difficulty of having to solve the Lyapunouv equation numerically.

The chapter concludes with an application of the IMC design method to a heavy oil fractionator. Example applications of the MPC method can be found in Appendix A and B.

## 4.2 Estimator Design

The topic of this section is design of the output estimator. The objective is to design either a static or a dynamic estimator that computes the estimates for the controlled outputs, $y_c$, based on the available measurements, $\hat{y}_m$, and the past input moves $u$. For convenience of notation, we will denote the input vector to the estimator, $\begin{bmatrix} u^T & \hat{y}_m^T \end{bmatrix}^T$, as $\hat{y}_m^e$ (see Figure 4.1). The output estimator design can be done in two ways: the first way is to use a first principles or identified model and the other way is through regression of the input/output records available from simulation or

actual process measurements. The use of the latter method is inevitable when it is impractical to develop a full dynamic model of the system and only the plant data of measurements and controlled outputs are available.

### 4.2.1 Model Based Design

We first discuss the design of the output estimator based on a dynamic (or static) model. There are many techniques available for output estimator design, but we limit our discussion to two most important and general methods: Kalman filter design and $\mu$-Synthesis.

#### Kalman Filter Design

The general multi-rate Kalman filter discussed in Chapter 5 provides the optimal estimates for the current controlled outputs (along with other state estimates) under certain stochastic assumptions on the external input signals. The estimator can accommodate measurements that are available at multiple sampling rates. Detailed design procedure can be found in Section 5.2 of Chapter 5.

In the case where some of the primary measurements are prone to failure, one can use the cascaded Kalman filter discussed in Section 5.2 of Chapter 5. The cascaded Kalman filter has the advantage that the estimator is guaranteed to maintain certain integrity in the events of failures of one or more primary measurements.

#### $\mu$-Synthesis Design

The objective of $\mu$-Synthesis is to find the estimator $E$ that minimizes the following quantity (see Figure 4.2):

$$\sup_{\omega} \inf_{D(\omega)\in\mathcal{D}_{rp}} \bar{\sigma}\left(D(\omega)\mathcal{F}_l\left(M^*, E\right)|_{s=j\omega}\left[D(\omega)\right]^{-1}\right) \tag{4.1}$$

$\mu$-Synthesis iterates between the follwing two steps (see Section 4.6 for detail):

- **Step A: $H_\infty$-Optimal Estimator Synthesis**

  Find $E$ that minimizes

$$\sup_{\omega} \bar{\sigma}\left(D(\omega)\mathcal{F}_\ell\left(M^*, E\right)|_{s=j\omega}\left(D(\omega)\right)^{-1}\right) \tag{4.2}$$

- **Step B: Optimal $D$-Scaling ($\mu$-Analysis)**

  For each $\omega$, find $D(\omega) \in \mathcal{D}_{rp}$ that minimizes

$$\bar{\sigma}\left(D(\omega)\mathcal{F}_\ell\left(M^*, E\right)|_{s=j\omega}\left(D(\omega)\right)^{-1}\right) \tag{4.3}$$

Because the minimization is nonconvex, the procedure does *not* guarantee convergence to the true optimum.

The main attraction for the design method is that it can incorporate the model uncertainty information explicitly. In order to put the use of $\mu$-Synthesis for estimator design in proper perspective, the following practical issues must be considered:

- $H_\infty$-optimal design problems for sampled-data systems and MR discrete-time systems have not been solved completely although progress is being made in the area [11,33]. Hence, at this point, we must approximate these systems as continuous-time systems and SR discrete-time systems respectively. Often in practice, secondary measurements can be sampled at a uniform rate. In this case, one can design the estimator based on the secondary measurements only and incorporate the primary measurements (that cannot be sampled at the same rate as the secondary measurements) through an auxiliary estimator. This is discussed in Section 4.2.3. Figure 4.2 depicts the estimator design for continuous systems with measurements available at a uniform sampling rate.

- $\mu$-analysis for sampled-data systems and MR discrete-time systems requires introducing either an approximation or conservativeness (see Section 2.3).

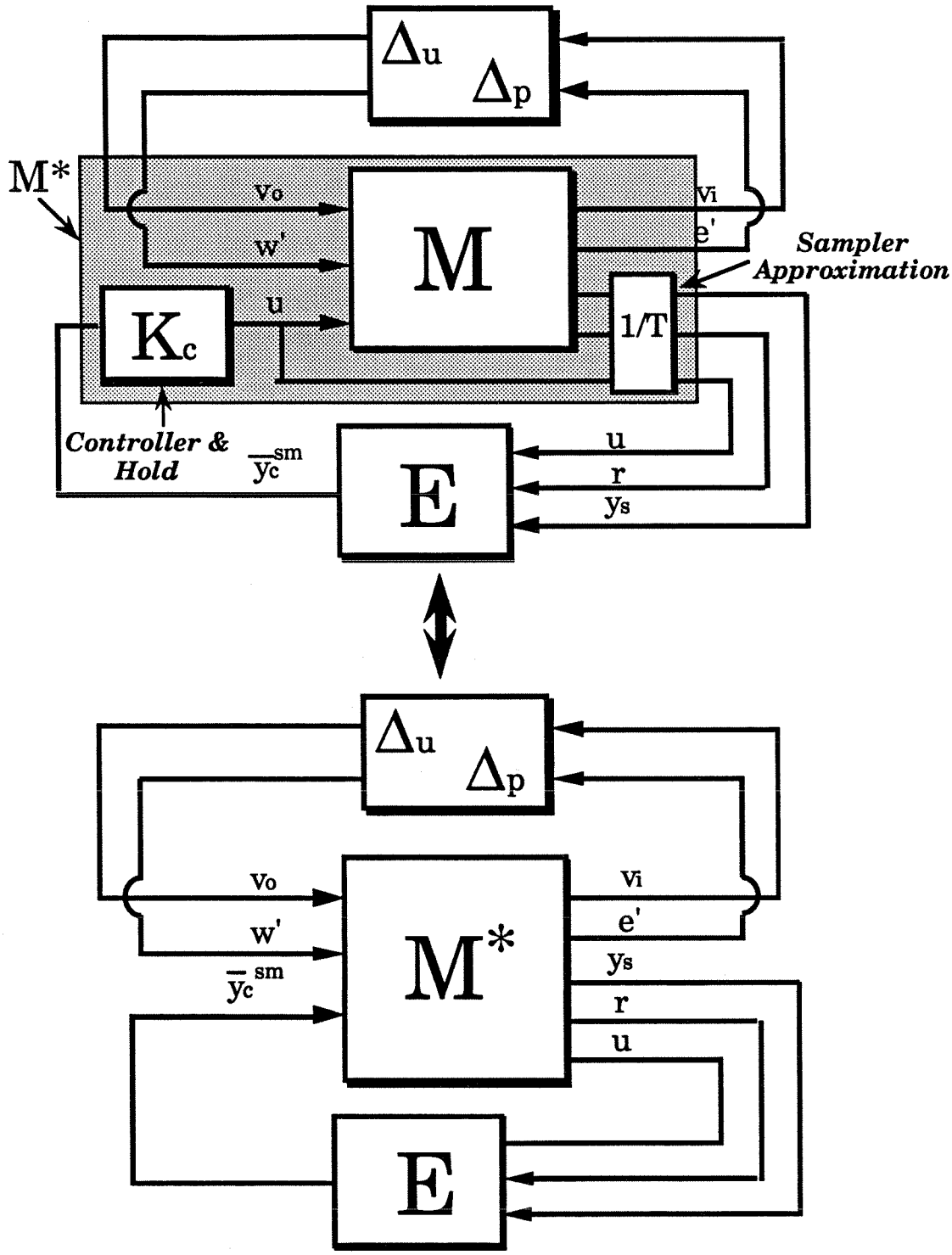


Figure 4.2. $\mu$-Synthesis for Output Estimator Design

- In order to ensure tolerance to failures of unreliable primary measurements, failure-prone primary measurements must be excluded from the estimator design even though they can be sampled at the same rate as the secondary measurements. These measurements can be used in improving the estimates through an auxiliary estimator (see Section 4.2.3 for details).

In addition to the lack of truly general theory, $\mu$-Synthesis requires an accurate, nonconservative uncertainty model which is often unavailble to engineers in practice. The method is to be looked at as more of a forward-looking research topic rather than as a practical estimator design method at this point.

### 4.2.2 Regression Based Design

In this section, we discuss the output estimator design based on the records of inputs and outputs for the estimator. These data may be obtained from simulation or from the actual process measurements. It is important that these data are obtained under a closed-loop environment similar to the one which the estimator will be subjected to. We first show that the estimator design problem can be formulated as a parameter identification problem and discuss various regression techniques.

Throughout this section, we assume that all the measured variables, the inputs to the estimator, can be made available to the estimator at a uniform rate. This is not very restrictive since, for most practical cases, the secondary measurements can be sampled at a uniform rate and the primary measurements that are often sampled at a much slower rate can be incorporated through an auxiliary estimator discussed in Section 4.2.3. The regression based estimator design for truly multi-rate systems has not been studied and is left as a future research topic.

## Formuation of Estimator Design Into A Parameter Identification Problem

For simplicity, let us first discuss design of a static estimator. Hence, we would like to find a constant matrix $E$ such that

$$y_c(k,j) \approx \bar{y}_c(k,j) \triangleq E\hat{y}^e_m(k,j) \tag{4.4}$$

where $\bar{y}_c(k,j)$ represents the estimate for $y_c(k,j)$ at time $(k,j)$. Suppose that we have $N$ data points available for the measured variable $\hat{y}^e_m$ and the controlled variable $y_c$. We assume that $N$ is greater than both the dimension of $y_c$ and that of $\hat{y}^e_m$. Ignoring measurement errors, we can write the estimator design problem as

$$Y = XE^T \tag{4.5}$$

where

$$X = [\hat{y}^e_m(1), \hat{y}^e_m(2), \cdots, \hat{y}^e_m(N)]^T \tag{4.6}$$

$$Y = [\hat{y}_c(1), \hat{y}_c(2), \cdots, \hat{y}_c(N)]^T \tag{4.7}$$

For dynamic estimator design, the same principle can be applied when an Auto Regressive Moving Average (ARMA) model is used to represent the relationship between each element of $\hat{y}^e_m$ and that of $y_c$ [43]. When the data for $\hat{y}_m$ and $y_c$ are available at different intervals, one must reformulate the model in terms of the basic time unit (BTU) beore regression techniques can be applied [28]. Design of a dynamic estimator will not be discussed in detail.

## Regression Techniques

The focus of discussion for the regression based estimator design is the choice of $E$ for the following problem:

$$Y = XE^T \tag{4.8}$$

If the matrix $X$ has full column rank, the choice that minimizes the least square error ($\|Y - XE^T\|_{\mathcal{F}}$ where $\|\cdot\|$ represents the Frobenious norm) is

$$E = E_{LS} \triangleq Y^T X(X^T X)^{-1} \tag{4.9}$$

In this case, one can show that the parameters converge to the true values exponentially as $N \rightarrow \infty$ in spite of white measurement noise in $Y$ (*i.e.*, $\hat{y}_c(k) = y_c(k) + v_c(k)$) [4]. When the dimension of $y_m^e$ is large, however, collinearity in the measurements often exists and $X$ tend to be singular or close to being singular (*i.e.*, singularity may be masked by measurement noise in the data $X$). This can be understood through a simple argument for a linear system. If there are $n$ inputs that affect $y_m^e$, $X$ can at most have the rank of $n$. When the number of measurements exceed $n$, the matrix $X$ will be singular.

Various modifications to the standard least square regression method have been suggested to overcome the collinearity problem. In this thesis, we look at the two most popular such techniques: Principle Component Analysis (PCA) and Partial Least Square (PLS). The basic idea for both methods is to use only those directions in the matrix $X$ that are excited by the inputs in finding the pseudo-inverse of $X$. Two methods differ in how these directions are chosen.

To understand the PCA method, let the singular value decomposition (SVD) of the matrix $X$ be as follows:

$$X = U\Sigma V^T \tag{4.10}$$

$$\triangleq \left[\begin{array}{c|c} U_1 & U_2 \end{array}\right] \left[\begin{array}{c|c} \Sigma_1 & \\ \hline & \Sigma_2 \end{array}\right] \left[\begin{array}{c} V_1^T \\ \hline V_2^T \end{array}\right] \tag{4.11}$$

We partition $U, \Sigma, V$ such that $\Sigma_2$ represents singular values that are zero or close to zero. Hence, $U_2$ and $V_2$ correspond to input and output directions of the matrix $X$ that are not excited by manipulated inputs and disturbances. The idea of PCA is to discard these directions in calculating the psedo-inverse of $X$. In other words, PCA finds $E$ according to the following formula:

$$E = E_{PCA} \triangleq Y^T U_1 \Sigma_1^{-1} V_1^T \tag{4.12}$$

A drawback of PCA is that, when the effect of manipulated inputs and disturbances on $y_m^e$ is small in certain directions, these directions can be discarded, while they (the manipulated inputs and disturbances in these particular directions) may affect the estimated variables $y_c$ in significant ways. PLS takes into account the directions in $Y$ as well as those in $X$ when finding the approximate pseudo-inverse of $X$. More specifically, PLS uses the dominant eigenvectors (*i.e.*, eigenvectors corresponding to nonnegligible eigenvalues) for the matrix $X^T Y Y^T X$ instead of those for the matrix $X^T X$ (*i.e.*, $V_1$). Let us express the matrix $X$ as follows:

$$X = \left[\begin{array}{c|c} T_1 & T_2 \end{array}\right] \left[\begin{array}{c} P_1^T \\ \hline P_2^T \end{array}\right] \tag{4.13}$$

where the columns of $P_1^T$ correspond to the dominant eigenvectors of the matrix $X^T Y Y^T X$. Then, the formula for $E$ is as follows:

$$E = E_{PLS} \triangleq Y^T T_1 \{T_1^T T_1\}^{-1} P_1^T \tag{4.14}$$

Note that, if we choose $P_1 = V_1$, then $T_1 = U_1 \Sigma_1$ and the formulas (4.12) and (4.14)

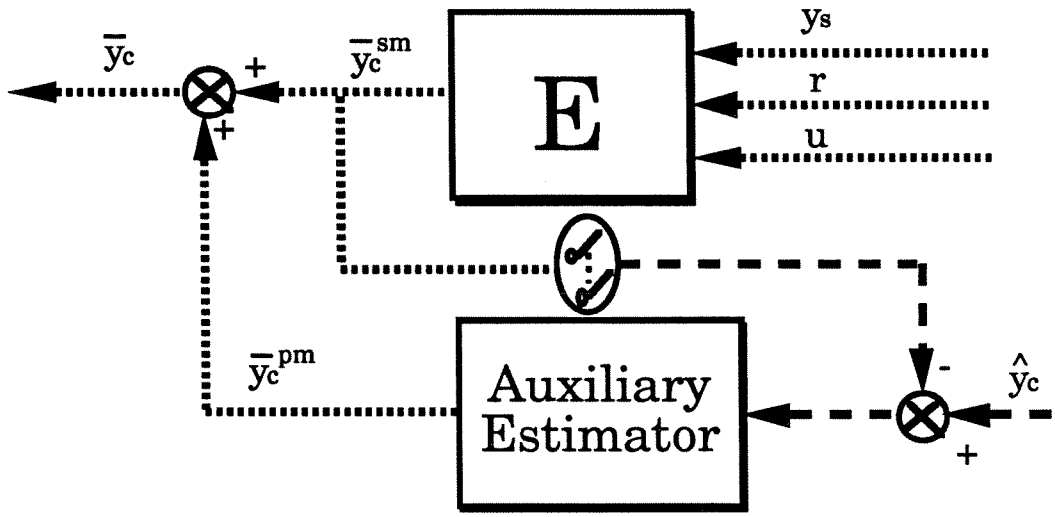


Figure 4.3. Use of "Slow" and "Unreliable" Primary Measurements for Output Estimation

become equivalent. An application of the PLS method to the static estimator design problem for a high-purity distillation column can be found in Mejdell [45].

### 4.2.3 Use of On-Line Primary Measurements

We mentioned that the primary measurements that are either available at a slow sampling rate or prone to failures should not be included as inputs to the output estimator (with the exception of the MR Kalman filter design that can incorporate general multi-rate sampled measurements). However, these primary measurements can be useful in improving the estimates when available. They can be incorporated as a part of the output estimator through an auxiliary estimator shown in Figure 4.3. The auxiliary estimator calculates the correction term for the estimates, $\bar{y}_c^{sm}$, on the basis of the difference between these estimates and the actual primary measurements. Details for the design of the auxiliary estimator can be found in Section 5.2 of Chapter 5. Because the auxiliary estimator is often designed to be diagonal, measurement failures can be dealt with through a simple switch box that sets the inputs to the estimator corresponding to the failed measurement to zero.

## 4.3 Linear Quadratic Gaussian (LQG)

### 4.3.1 Model

In the output-based approach, a general discrete-time model for control system design is given by the following state-space difference equation:

**Process:**

$$x(k) = Ax(k-1) + B_u u(k-1) + B_d d(k-1) \tag{4.15}$$

$$y_c(k) = C_c x(k) \tag{4.16}$$

**Controlled Variables:**

$$y_e(k) = C_c x(k) - r(k) \tag{4.17}$$

**Measurements:**

$$\hat{y}_c(k) = C_c x(k) + v_c(k) \tag{4.18}$$

$\hat{y}_c(k)$ represents the estimates of $y_c$ available from the output estimator. By performing some simple algebraic manipulation, we can put (4.15)-(4.18) into the following standard state-space form:

$$X(k) = \Phi' X(k-1) + \Gamma_u u(k-1) + \Gamma_d d(k-1) \tag{4.19}$$

$$\hat{y}_c(k) = \Xi X(k) + v_c(k) \tag{4.20}$$

where

$$X(k) = \begin{bmatrix} x(k) \\ y_c(k) \end{bmatrix} \tag{4.21}$$

$$\Phi' = \begin{bmatrix} A & 0 \\ C_c A & 0 \end{bmatrix} \quad \Gamma_u = \begin{bmatrix} B_u \\ C_c B_u \end{bmatrix} \quad \Gamma_d = \begin{bmatrix} B_d \\ C_c B_d \end{bmatrix} \tag{4.22}$$

$$\Xi = \begin{bmatrix} 0 & I_{\dim\{y_c\}} \end{bmatrix} \tag{4.23}$$

For LQG design method (or MPC design method introduced subsequently), it is convenient to express the model in terms of the changes in the inputs rather than the inputs themselves. For this purpose, we subtract the equation (4.19) at $t = k-1$ from that at $t = k$ to arrive at the following state-space representation of the system:

$$\Delta X(k) = \Phi \Delta X(k-1) + \Gamma_U \Delta U(k-1) + \Gamma_d \Delta d(k-1) \tag{4.24}$$

$$\hat{y}_c(k) = \Xi \Delta X(k) + v_c(k) \tag{4.25}$$

where

$$\Delta X(k) = \begin{bmatrix} \Delta x(k) \\ y_c(k) \end{bmatrix} \tag{4.26}$$

$$\Phi = \begin{bmatrix} A & 0 \\ C_c A & I \end{bmatrix} \tag{4.27}$$

$\Delta$ variable represents the change in the variable from the previous sampling time (*e.g.*, $\Delta x(k) = x(k) - x(k-1)$).

**Theorem 4.1** *The system described through (4.24)-(4.25) is*

1. *detectable if and only if* $(C_c, A)$ *is detectable.*
2. *stabilizable if and only if* $(A, B_u)$ *is stabilizable and* $\mathrm{Ker}\{(C_c(I-A)^{-1}B_u)^T\} = \emptyset$ *where* $\mathrm{Ker}\{\cdot\}$ *denotes the kernel space.*

**Proof** We first prove the detectability condition. From Hautus [30], $(\Xi, \Phi)$ is a

detectable pair if and only if

$$\text{rank}\left\{\left[\left[\begin{array}{cc} A^T & (C_cA)^T \\ 0 & I \end{array}\right] - \lambda I \middle| \left[\begin{array}{c} 0 \\ I \end{array}\right]\right]\right\} = \dim\{\Phi\} \quad \forall \lambda \in \mathcal{C}, |\lambda| \geq 1 \tag{4.28}$$

Clearly,

$$\text{rank}\left\{\left[\left[\begin{array}{cc} A^T & (C_cA)^T \\ 0 & I \end{array}\right] - \lambda I \middle| \left[\begin{array}{c} 0 \\ I \end{array}\right]\right]\right\} = \text{rank}\left\{\left[\begin{array}{cc} A^T & (C_cA)^T \end{array}\right] - \lambda I\right\} + \dim\{y_c\} \tag{4.29}$$

From Hautus [30],

$$\text{rank}\left\{\left[\begin{array}{cc} A^T & (C_cA)^T \end{array}\right] - \lambda I\right\} = \dim\{\Phi\} \quad \forall \lambda \in \mathcal{C}, |\lambda| \geq 1 \tag{4.30}$$

if and only if $(C_cA, A)$ is a detectable pair. In addition, $(C_cA, A)$ is a detectable pair if and only if $(C_c, A)$ is a detectable pair.

Next, we prove the stabilizability condition. Again, from Hautus [30], $(\Phi, \Gamma_u)$ is a detectable pair if and only if

$$\text{rank}\left\{\left[\left[\begin{array}{cc} A & 0 \\ C_cA & I \end{array}\right] - \lambda I \middle| \left[\begin{array}{c} B_u \\ C_cB_u \end{array}\right]\right]\right\} = \dim\{\Phi\} \quad \forall \lambda \in \mathcal{C}, |\lambda| \geq 1 \tag{4.31}$$

For all $\lambda \neq 1$, it is clear that the rank condition is satisfied if and only if

$$\text{rank}\left\{\left[\begin{array}{cc} A - \lambda I & B_u \end{array}\right]\right\} = \dim\{A\} \tag{4.32}$$

The above condition is equivalent to the stabilizablity of $(A, B_u)$. For $\lambda = 1$, the rank condition becomes

$$\text{rank}\left\{\left[\begin{array}{cc} A - I & B_u \\ C_cA & C_cB_u \end{array}\right]\right\} = \dim\{\Phi\} \tag{4.33}$$

Simple algebraic manipulation shows that

$$\text{rank}\left\{\begin{bmatrix} A-I & B_u \\ C_cA & C_cB_u \end{bmatrix}\right\} = \text{rank}\left\{\begin{bmatrix} A-I & B_u \\ C_c & 0 \end{bmatrix}\right\} \tag{4.34}$$

The condition

$$\text{rank}\left\{\begin{bmatrix} A-I & B_u \\ C_c & 0 \end{bmatrix}\right\} = \dim\{\Phi\} \tag{4.35}$$

is equivalent to

1. *Stabilizablity of* $(A, B_u)$

$$\text{rank}\left\{\begin{bmatrix} A-I & B_u \end{bmatrix}\right\} = \dim\{A\} \tag{4.36}$$

2. *Input/Output Controllability at Steady State*

$$\text{Ker}\{\left(C_c(I-A)^{-1}B_u\right)^T\} = \emptyset \tag{4.37}$$

■

Condition 2 implies that there must be at least as many manipulated variables as controlled variables.

The modified state-space model has the following advantages:

1. In the LQG design, the optimal state estimator design assumes that the inputs to model states and measurements are described as white noise of chosen covariances. On the other hand, most disturbances in process industry are non-stationary in nature. This necessitates augmenting system states to include integrators for the disturbances, which can cause indetectablity when the number of disturbances exceeds the number of measurements [49]. In the modified state-space model on the other hand, modelling $\Delta d$ as white noise implies that

the disturbances are integrated white noise (that is, sum of random steps amplitudes of which follow normal distribution and time of occurrence follows Poisson distribution), which are often very reasonable. If desired, these nonstationary inputs can be made to include more complex dynamics by further augmenting the system states.

2. The objective function for the LQG design has a term involving control inputs. When the function includes a finite weight on $u$, integral action on the controlled variables is not automatically provided. For the modified model, the objective function weights the changes in the control inputs ($\Delta u$) rather than the control inputs themselves ($u$). This automatically leads to a control system with integral action necessary to reject nonstationary disturbances or follow persistent reference inputs without offsets.

### 4.3.2 Minimization Objective

Let us consider the following inputs to the system:

$$\begin{bmatrix} \Delta d \\ \Delta r \\ v_c \end{bmatrix}_i = \begin{bmatrix} Q_d & & \\ & Q_r & \\ & & R_c \end{bmatrix} \delta_i \tag{4.38}$$

where $\delta_i$ is a unit impulse entering the $i^{\text{th}}$ channel at $t = 0$. The objective is to minimize the following function:

$$\sum_{i=1}^{q} \sum_{k=0}^{\infty} \left( y_e^T(k) \Lambda_{y_e} y_e(k) + \Delta u^T(k) \Lambda_{\Delta u} \Delta u(k) \right)_i \tag{4.39}$$

where $q = (\dim\{d\} + \dim\{r\} + \dim\{v_c\})$. The subscript $(\cdot)_i$ represents that $y_e(k)$ and $\Delta u(k)$ are those resulting from the input $\delta_i$. This problem can be formulated into the standard $H_2$-optimal control problem when the weights $W_w$ and $W_p$ in Chapter 2 are

chosen as follows:

$$W_w = \begin{bmatrix} \frac{z}{z-1}Q_d^{1/2} & & \\ & \frac{z}{z-1}Q_r^{1/2} & \\ & & R_c^{1/2} \end{bmatrix} \tag{4.40}$$

$$W_p = \begin{bmatrix} \frac{z-1}{z}\Lambda_{\Delta u}^{1/2} & \\ & \Lambda_{y_e}^{1/2} \end{bmatrix} \tag{4.41}$$

In the stochastic framework, the minimization objective is interpreted as minimizing the variance of $y_e$ and $\Delta u$ (weighted through $\Lambda_{y_e}^{1/2}$ and $\Lambda_{\Delta u}^{1/2}$ respectively) when $\Delta d$, $\Delta r$ and $v_c$ are independent white noises of covariance matrices $Q_d$, $Q_r$, and $R_c$ respectively. Often, the reason for including the 2-norm of $\Delta u$ in the minimization objective is to limit the controller moves in order to achieve better robustness. Hence, $\Lambda_{\Delta u}$ for most cases can be viewed as a robustness design parameter.

The above formulation assumes that reference vector is modelled as integrated white noise. In some cases, future reference trajectory may be known. In other cases, reference vector may be described better as other types of stochastic signals (such as double-integrated white noise). Extension of the subsequently developed technique to such cases is straightforward and will be discussed in detail.

### 4.3.3 Optimal Control Design

According to the separation principle, the $H_2$-optimal controller can be obtained by combining the optimal estimator with the optimal state feedback regulator.

**Optimal Estimator: Kalman Filter**

The optimal estimator for the given process and disturbances is the following Kalman filter:

$$\Delta\bar{X}(k|k) = \Phi\Delta\bar{X}(k-1|k-1) + \Gamma_u\Delta u(k-1)$$

$$+ \quad K_G[\hat{y}_c(k) - \Xi\{\Phi\Delta\bar{X}(k-1) + \Gamma_u\Delta u(k-1)\}] \tag{4.42}$$

where

$$K_G = \Sigma_s\Xi^T\{\Xi\Sigma_s\Xi^T + R_c\}^{-1} \tag{4.43}$$

$\Sigma_s$ represents the unique stabilizing solution (*i.e.*, the solution that leads to a stable $\Phi - K_G\Xi\Phi$) to the following Algebraic Riccati Equation (ARE):

$$\Sigma_s = \Phi\Sigma_s\Phi^T - \Phi\Sigma_s\Xi^T\{\Xi\Sigma_s\Xi^T + R_c\}^{-1}\Xi\Sigma_s\Phi^T + \Gamma_d Q_d\Gamma_d^T \tag{4.44}$$

The optimal estimator is probably expressed more intuitively and conveniently as the following two-step estimator:

$$\Delta\bar{X}(k|k-1) = \Phi\Delta\bar{X}(k-1|k-1) + \Gamma_u\Delta u(k-1) \tag{4.45}$$

$$\Delta\bar{X}(k|k) = \bar{X}(k|k-1) + K_G\{\hat{y}_c(k) - \Xi\bar{X}(k|k-1)\} \tag{4.46}$$

The notation $\{\bar{\cdot}\}(k|\ell)$ implies that it is the estimate at time $k$ using measurements up to time $\ell$. For simplicity of notation, we will denote $\Delta\bar{X}(k|k)$ as $\Delta\bar{X}(k)$ from this point on.

The unique stabilizing solution to ARE (4.44) ($\Sigma_s$) may be obtained by iterating on the following Riccati difference equation until a steady-state solution is reached:

$$\Sigma(k+1) = \Phi\Sigma(k)\Phi^T - \Phi\Sigma(k)\Xi^T(k)\{\Xi\Sigma(k)\Xi^T + R_c\}^{-1}\Xi\Sigma(k)\Phi^T + \Gamma_d Q\Gamma_d^T \tag{4.47}$$

To guarantee the exponential convergence of equation (4.47) to the unique, positive semidefinite solution, we need the following assumptions (besides the detectabilty of $(C_c, A)$):

1. $\Sigma(0) \geq 0$ and $R_c > 0$.

2. $(\Phi, \Gamma_d Q^{1/2})$ is a stabilizable pair.

The former condition states that the initial error covariance matrix has to be positive semi-definite and the measurement noise covariance matrix has to be positive definite. The latter condition states that all unstable dynamics of the system should be excited through the state excitation noise $\Delta d$.

**Optimal Compensator: LQ State Feedback**

The optimal state feedback compensator for the given objective (4.39) is as follows:

$$\Delta u(k) = -L_{LQ} \begin{bmatrix} \Delta x(k) \\ y_e(k) \end{bmatrix} \tag{4.48}$$

$$= -L_{LQ} \left\{ \begin{bmatrix} \Delta x(k) \\ y_c(k) \end{bmatrix} - \begin{bmatrix} 0 \\ r(k) \end{bmatrix} \right\} \tag{4.49}$$

where

$$L_{LQ} = \left[ \; (\Gamma_u^T \Psi_s \Gamma_u + \Lambda_{\Delta u})^{-1} \Gamma_u^T \Psi_s \Phi \;\middle|\; \mathcal{O}_{\dim\{y_s\}} \; \right] \tag{4.50}$$

$\Psi_s$ is the solution to the following algebraic Riccati equation (ARE):

$$\Psi = \Phi^T \Psi \Phi - \Phi^T \Psi \Gamma_u (\Gamma_u^T \Psi \Gamma_u + \Lambda_{\Delta u})^{-1} \Gamma_u^T \Psi \Phi + \mathrm{diag} \left[ \; 0_{\dim\{x\}} \quad \Lambda_{y_c} \; \right] \tag{4.51}$$

For the existence of a stablizing solution to the above equation, we need the stabilizability of the pair $(\Phi, \Gamma_u)$. Note that, in order for the rank condition on the matrix $C_c(I - A)^{-1}B_u$ of Theorem 4.1 to be satisfied, there must be at least as many linearly independent manipulated variables as the number of controlled variables (*i.e.*, $\dim\{u\} \geq \dim\{y_c\}$). Appendix 4.A discusses how the number of controlled variables can be reduced in an optimal way when the condition is not satisfied. In order for the Riccati difference equation correponding to (4.51) to converge exponentially to a stabilizing solution, we need the stabilizability of $(\Phi^T, \mathrm{diag}\{0_{\dim\{x\}}, \Lambda_{y_e}^{1/2}\})$ in addition

to the stabilizability of $(\Phi, \Gamma_u)$.

One notable point is that, in the above formulation, the reference input vector $r(k)$ is assumed to be a step (or integrated white noise in the stochastic framework). For more general types of reference inputs, the LQ controller must be calcualated for an augemented system. For example, suppose $\Delta r(k) = r(k) - r(k-1)$ is to be generated by the following equation:

$$x^r(k) = A^r x^r(k-1) + B^r \delta^r(k) \tag{4.52}$$

$$\Delta r(k) = C^r x^r(k) \tag{4.53}$$

where $\delta^r(k)$ is a random, but known impulse. In some cases, future information on reference trajectory may be available. For example, we may know the reference changes $p$ time steps ahead and describe the change in the reference at time $k+p$ to be the output of the above dynamical system driven by a known pulse:

$$x^r(k) = A^r x^r(k-1) + B^r \delta^r(k) \tag{4.54}$$

$$\Delta r(k+p) = C^r x^r(k) \tag{4.55}$$

The augmented system equation is

$$\begin{bmatrix} \Delta x(k) \\ x^r(k) \\ \Delta r(k+p) \\ \Delta r(k+p-1) \\ \vdots \\ \Delta r(k+1) \\ y_e(k) \end{bmatrix} = \left[\begin{array}{c|cccccc|c} A & 0 & 0 & 0 & 0 & 0 & 0 \\ 0 & A^r & 0 & 0 & 0 & 0 & 0 \\ 0 & C_r A r & 0 & 0 & \cdots & 0 & 0 \\ 0 & 0 & I & 0 & \cdots & 0 & 0 \\ 0 & 0 & 0 & I & \cdots & 0 & 0 \\ \vdots & \vdots & \ddots & \ddots & \ddots & \vdots & \vdots \\ 0 & 0 & 0 & \cdots & I & 0 & 0 \\ C_c A & 0 & -I & 0 & \cdots & 0 & I \end{array}\right] \begin{bmatrix} \Delta x(k-1) \\ x^r(k-1) \\ \Delta r(k+p-1) \\ \Delta r(k+p-2) \\ \vdots \\ \Delta r(k) \\ y_e(k-1) \end{bmatrix}$$

$$+ \begin{bmatrix} B_u \\ 0 \\ 0 \\ 0 \\ \vdots \\ 0 \\ C_c B_u \end{bmatrix} \Delta u(k-1) + \begin{bmatrix} 0 \\ B_r \\ C_r B_r \\ 0 \\ \vdots \\ 0 \\ 0 \end{bmatrix} \delta^r(k) \tag{4.56}$$

The corresponding LQ controller is

$$\Delta u(k) = -L_{LQ}^{aug} \begin{bmatrix} \Delta x(k) \\ x^r(k) \\ \Delta r(k+p) \\ \Delta r(k+p-1) \\ \vdots \\ \Delta r(k+1) \\ y_e(k) \end{bmatrix} \tag{4.57}$$

$$= -L_{LQ}^{aug} \left\{ \begin{bmatrix} \Delta x(k) \\ 0 \\ 0 \\ 0 \\ \vdots \\ 0 \\ y_c(k) \end{bmatrix} - \begin{bmatrix} 0 \\ x^r(k) \\ \Delta r(k+p) \\ \Delta r(k+p-1) \\ \vdots \\ \Delta r(k+1) \\ -r(k-1) - \Delta r(k) \end{bmatrix} \right\} \tag{4.58}$$

where $L_{LQ}^{aug}$ is the LQ optimal state feedback gain for the augmented system (4.56). The LQ controller is represented schematically in Figure 4.4. To simplify the discussion, we will assume that $r(k)$ is described as integrated white noise from this point

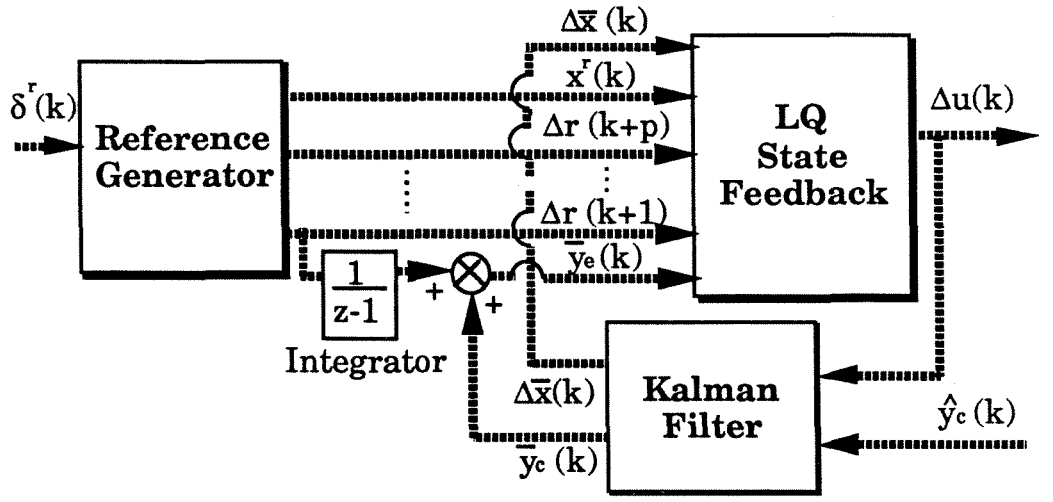


Figure 4.4. LQG Controllers with General Reference Inputs

on.

**$H_2$-Optimal Controller: Kalman Filter + LQ State Feedback**

The $H_2$-optimal controller for the given problem is a combination of the MR Kalman filter and the LQ state feedback compensator written as follows:

$$\begin{aligned}\Delta\bar{X}(k) &= (\Phi - K_G\Xi\Phi - \Gamma_u L_{LQ} + K_G\Xi\Gamma_u L_{LQ})\Delta\bar{X}(k-1) \\ &- (I - K_G\Xi)\Gamma_u L_{LQ}\Gamma_r r(k-1) + K_G\hat{y}_c(k) \qquad (4.59)\\ \Delta u(k) &= -L_{LQ}\left\{\Delta\bar{X}(k) + \Gamma_r r(k)\right\} \qquad (4.60)\end{aligned}$$

where $\Gamma_r = \begin{bmatrix} 0 \\ -I \end{bmatrix}$.

## 4.3.4 Constraint Handling: Extended Kalman Filter

In the events of input saturation or mode switching, the controller (4.59)-(4.60) can exhibit significant "wind-up" as $\Delta u(k) \neq -L_{LQ}\left(\Delta\bar{X}(k) + \Gamma_r r(k)\right)$. The phenomenon of wind-up can render detrimental consequences including severe performance deterioration and instability. The simplest anti-windup scheme for the LQG controllers

is the Extended Kalman filter in which (4.59) is replaced by

$$\Delta\bar{X}(k) = (\Phi - K_G\Xi\Phi)\Delta\bar{X}(k-1) + (I - K_G\Xi)\Gamma_u\Delta u_{true}(k-1) + K_G\hat{y}_c(k) \quad (4.61)$$

and $\Delta u_{true}$ represents the "true" input to the system. In the presence of input constraints, $\Delta u_{true}(k)$ can be chosen as $u_{sat} - u_{true}(k-1)$, which is the projection of $u_{true}(k-1) - L_{LQ}\Delta\bar{X}^e$ ( $\Delta\bar{X}^e \triangleq \Delta\bar{X}(k) + \Gamma_r r(k)$ ) onto the constrained input space of $u(k)$.

For multivariable systems, however, $\Delta u_{true}(k)$ calculated by projecting $u_{true}(k-1) - L_{LQ}\Delta\bar{X}^e(k)$ onto the constrained input space of $u(k)$ is not optimal in general and can cause significant performance deterioration. This is because input constraints can change the direction of the input and make the loop gains significantly different from those in the absence of constraints, especially for ill-conditioned systems combined with a directionally sensitive controller. A simple fix to circumvent this problem is to make the true input $u_{true}$ be in the same direction as $u(k)(\triangleq u_{true}(k-1) - L_{LQ}\Delta\bar{X}^e(k))$ (see Figure 4.5). The following directionality correction scheme can be used to accomplish this ([19]):

$$u_{true}(k) = \begin{cases} u_{true}(k-1) - L_{LQ}\Delta\bar{X}^e(k) \text{ when } \|(u_{true}(k-1) - L_{LQ}\Delta\bar{X}^e(k))/u_{sat}\|_\infty \leq 1 \\ \frac{(u_{true}(k-1) - L_{LQ}\Delta\bar{X}^e(k))}{\|(u_{true}(k-1) - L_{LQ}\Delta\bar{X}^e(k))/u_{sat}\|_\infty} \text{ when } \|(u_{true}(k-1) - L_{LQ}\Delta\bar{X}^e(k))/u_{sat}\|_\infty > 1 \end{cases} \quad (4.62)$$

where $u_{sat}$ is $u_{true}(k-1) + \Delta u_{sat}(k)$ and $[\cdot]/[\cdot]$ is the element-by-element divsion operator. The extended Kalman filter with the directionality correction scheme is shown in Figure 4.6.

Various output constraints (constraints on $y_c$) must be handled in *ad hoc* ways (*e.g.*, mode switching). The output constraints can be addressed more directly in the subsequently discussed MPC.

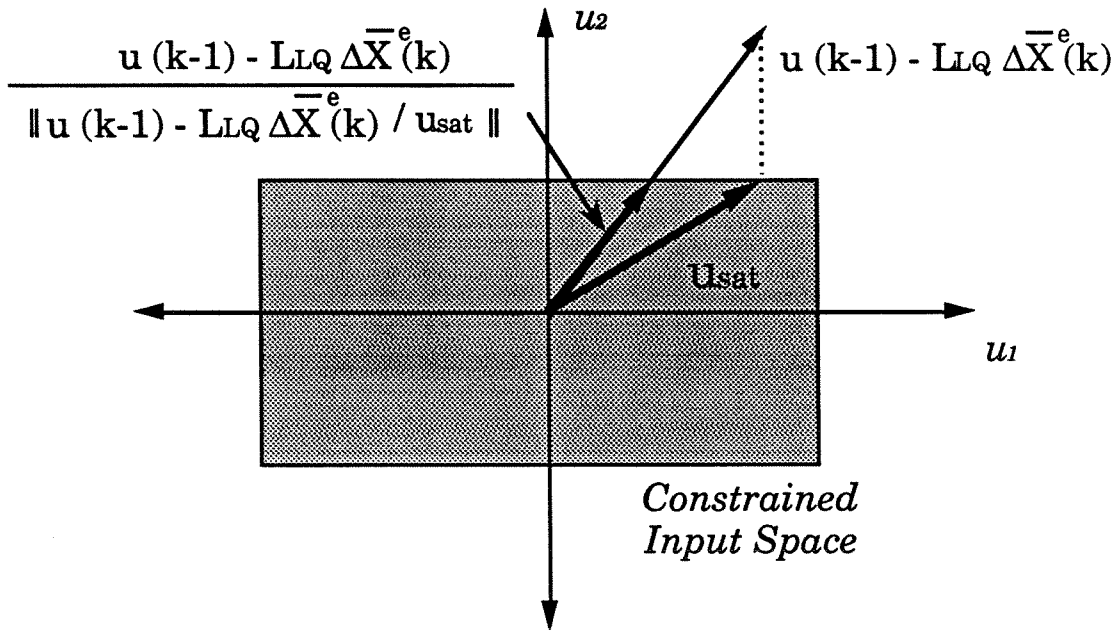


Figure 4.5. Directionality Change in Inputs Due to Input Constraints for Systems with Two Inputs

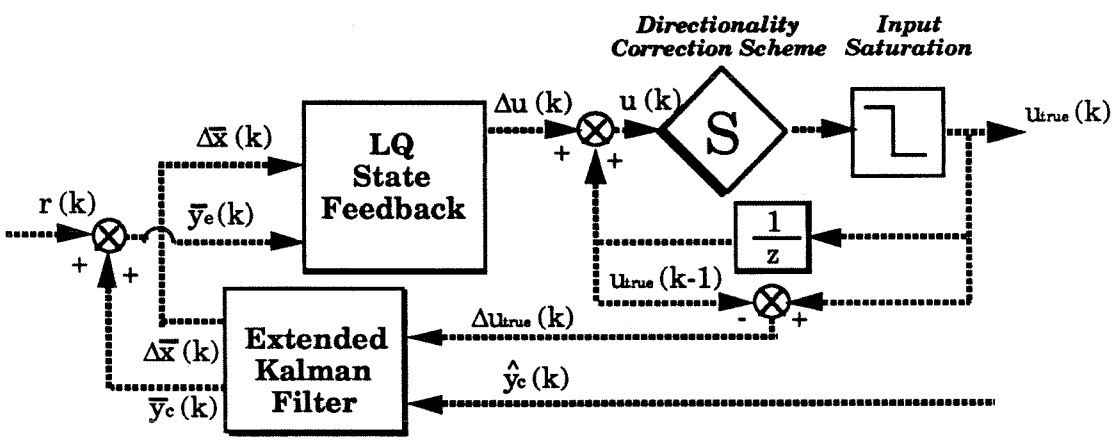


Figure 4.6. Extended Kalman Filter with Directionality Correction Scheme

### 4.3.5 Robust Design/Tuning

As mentioned before, a serious drawback of LQG design from industrial perspective has been the overabundance of indirect, nonintuitive design paramaters and a lack of simple, intuitive on-line tuning parameters. The purpose of this section is to equip the LQG controllers with a parsimonious set of tuning parameters and develop simple, intuitive tuing rules for this set of parameters.

#### Closed-Loop Relationships

It is easy to derive the following closed-loop relationships between various external inputs / system states and their estimates:

$$\begin{bmatrix} \Delta X(k) \\ \Delta \bar{X}(k) \end{bmatrix} = \begin{bmatrix} \Phi & -\Gamma_u L_{LQ} \\ K_G \Xi \Phi & \Phi - K_G \Xi \Phi - \Gamma_u L_{LQ} \end{bmatrix} \begin{bmatrix} \Delta X(k-1) \\ \Delta \bar{X}(k-1) \end{bmatrix} + \begin{bmatrix} \Gamma_d & 0 & -\Gamma_u L_{LQ} \Gamma_r \\ K_G \Xi \Gamma_d & K_G & -\Gamma_u L_{LQ} \Gamma_r \end{bmatrix} \begin{bmatrix} \Delta d(k-1) \\ v_c(k) \\ r(k) \end{bmatrix} \tag{4.63}$$

Subtracting the second equation from the first one, we obtain

$$\begin{bmatrix} \Delta X(k) \\ \Delta X(k) - \Delta \bar{X}(k) \end{bmatrix} = \begin{bmatrix} \Phi & -\Gamma_u L_{LQ} \\ 0 & \Phi - K_G \Xi \Phi \end{bmatrix} \begin{bmatrix} \Delta X(k-1) \\ \Delta X(k-1) - \Delta \bar{X}(k-1) \end{bmatrix} + \begin{bmatrix} \Gamma_d & 0 & -\Gamma_u L_{LQ} \Gamma_r \\ (K_G \Xi - I)\Gamma_d & -K_G & 0 \end{bmatrix} \begin{bmatrix} \Delta d(k-1) \\ v_c(k) \\ r(k) \end{bmatrix} \tag{4.64}$$

The closed-loop transfer function from $\begin{bmatrix} (\check{\Delta d})^T(z) & \check{v_c}^T(z) & \check{r}^T(z) \end{bmatrix}^T$ to $\check{y_c}(z)$ can be expressed as follows (the notation $(\check{\cdot})(z)$ represents the z-transform of the signal):

$$\check{y_e}(z) = \left[\begin{array}{cc|ccc} \Phi - \Gamma_u L_{LQ} & \Gamma_u L_{LQ} & \Gamma_d & 0 & -\Gamma_u L_{LQ}\Gamma_r \\ 0 & \Phi - K_G \Xi \Phi & (K_G\Xi - I)\Gamma_d & -K_G & 0 \\ \hline \Xi & 0 & 0 & 0 & 0 \end{array}\right] \begin{bmatrix} (\check{\Delta d})(z) \\ z\check{v_c}(z) \\ z\check{r}(z) \end{bmatrix} \tag{4.65}$$

where

$$\left[\begin{array}{c|c} A & B \\ \hline C & D \end{array}\right] \equiv C(zI - A)^{-1}B + D \tag{4.66}$$

The following insights on the closed-loop stability, performance and robustness can be drawn from the above equation:

1. *Closed-Loop Stability*

   The eigenvalues of the closed-loop matrix are those of $\Phi - \Gamma_u L_{LQ}$ and $\Phi - K\Xi\Phi$. Hence, the closed-loop system is stable if and only if all eigenvalues of $\Phi - \Gamma_u L_{LQ}$ (*i.e.*, regulator poles) and those of $\Phi - K_G\Xi\Phi$ (*i.e.*, observer poles) lie strictly inside the unit disk. The observer/regulator poles are guaranteed to lie inside the unit disk since $K_G$ and $L_{LQ}$ are obtained from stabilizing solutions of their respective Riccati equations.

2. *Asymptotic Disturbance Rejection Property*

   The closed-loop system rejects "persistent" disturbances (when $d$ is integrated white noise) and follows step setpoint changes with no offset as long as the observer/regulator poles are placed in the unit disk. This can be seen from the closed-loop relationships between $\Delta d(k)$ and $y_c(k)$: $y_c(k)$ is simply expressed as a white-noise passed through stable (closed-loop) dynamics.

3. *Sensitivity and Robustness*

   The closed-loop expressions provide insights and guidelines for closed-loop per-

formance and robustness as well.

- Note that the observer dynamics affect the closed-loop transfer function from disturbance ($\Delta d(k)$) and measurement noise ($v$), but not the closed-loop transfer function from the output reference vector ($\Delta r(k)$). On the other hand, the regulator dynamics affect all the closed-loop tranfer functions.

- The closed-loop transfer function from $-\check{v}_c(z)$ to $\check{y}(z)$ can be expressed as

$$H = \Xi(z - \Phi + \Gamma_u L_{LQ})^{-1}\Gamma_u L_{LQ}(z - \Phi + K_G\Xi\Phi)^{-1}K_G(zI) \qquad (4.67)$$

  The function $H$ is called "complementary sensitivity function" and has a direct relevance to the closed-loop system's sensitivity and robustness. For example, the complement of $H$ (*i.e.*, $I - H$) is called "sensitivity function" and expresses the relationship between open-loop and closed-loop responses of the controlled variables to disturbances. Note that the state-feedback gain ($L_{LQ}$) and the filter gain ($K_G$) both affect the complementary sensitivity function.

One major difficulty for LQG design from robustness perspective is that there is no transparent rule on how the traditional LQG design parameters ($\Lambda_{y_e}, \Lambda_{\Delta u}, Q_d, Q_r$ and $R_c$) must be chosen in order to obtain a desired complementary sensitivity function (which has a more transparent connection with closed-loop performance and robustness [20]). Consequently, design must be based on intuition, experience, and painstaking trial and errors. In addition, on-line tuning of these traditional parameters require solving Riccati equations every time some of the parameters are changed. Motivated by these considerations, we next look for a way of combining all the traditional design parameters into a simple set of intuitive, on-line tuneable parameters. It turns out that, under reasonable assumptions on system disturbances and measurement noise,

we can find such a set of parameters for LQG controllers.

## Integrated White Noise Output Disturbances with White Measurement Noise

In many chemical systems, disturbances and measurement noise are well described as integrated white noise (*i.e.*, random step functions whose magnitudes are normally distributed and time-occurrence follows Poisson distribution) and white-noise entering each output indepedently respectively. The model for such a system is

$$\begin{bmatrix} \Delta x(k) \\ \Delta d(k) \\ y_c(k) \end{bmatrix} = \begin{bmatrix} A_{11} & 0 & 0 \\ 0 & 0 & 0 \\ C_c A_{11} & I & I \end{bmatrix} \begin{bmatrix} \Delta x(k-1) \\ \Delta d(k-1) \\ y_c(k-1) \end{bmatrix} \tag{4.68}$$

$$+ \begin{bmatrix} 0 \\ I \\ 0 \end{bmatrix} \Delta d'(k-1) + \begin{bmatrix} B_u \\ 0 \\ C_c B_u \end{bmatrix} \Delta u(k-1) \tag{4.69}$$

$$\hat{y}_c(k) = \begin{bmatrix} 0 & 0 & I \end{bmatrix} \begin{bmatrix} \Delta x(k) \\ \Delta d(k) \\ y_c(k) \end{bmatrix} + v_c(k) \tag{4.70}$$

where $\Delta d'$ and $v_c$ are white noise with following covariance matrices:

$$E\{\Delta d' \Delta d'^T\} = \text{diag}(q_1, \cdot, q_n) \tag{4.71}$$

$$E\{\Delta v_c \Delta v_c^T\} = \text{diag}(r_1, \cdot, r_n) \tag{4.72}$$

$n$ is the number of controlled outputs. The system is represented in terms of block diagram in Figure 4.7.

The system described through (4.68)-(4.70) can be shown to be equivalent to the

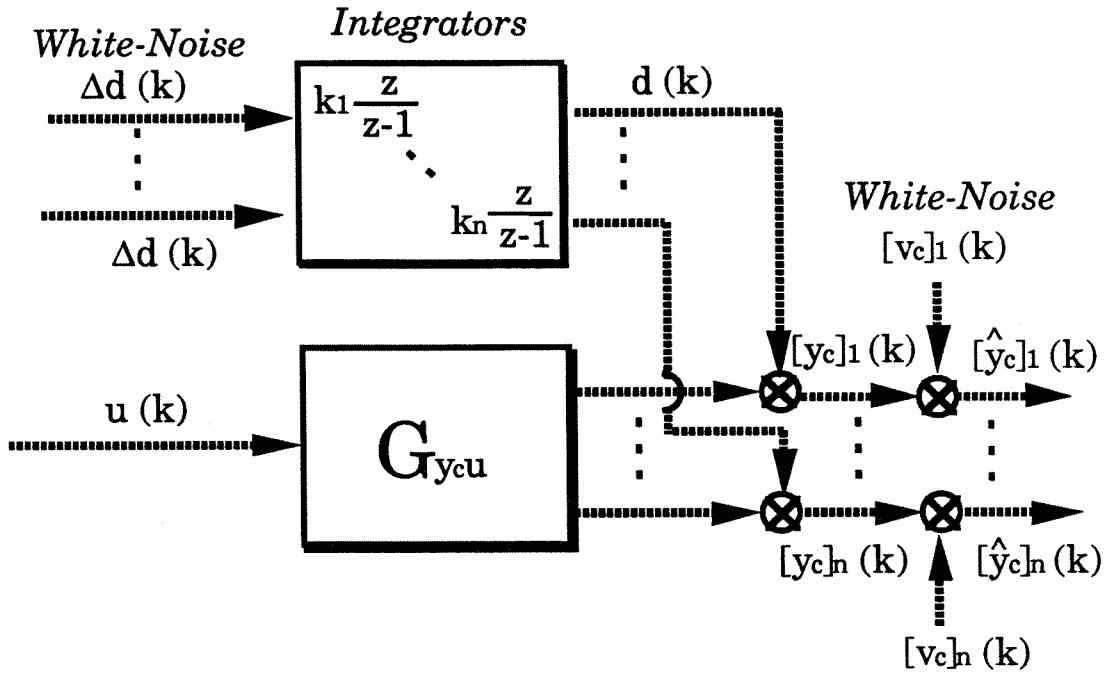


Figure 4.7. System with Integrated White Noise Disturbances and White Measurement Noise Entering Each Ouput Independently

following reduced-order system:

$$\begin{bmatrix} \Delta x(k) \\ y_c(k) \end{bmatrix} = \begin{bmatrix} A_{11} & 0 \\ C_c A_{11} & I \end{bmatrix} \begin{bmatrix} \Delta x(k-1) \\ y_c(k-1) \end{bmatrix} \tag{4.73}$$

$$+ \begin{bmatrix} 0 \\ I \end{bmatrix} \Delta d(k-1) + \begin{bmatrix} B_u \\ C_c B_u \end{bmatrix} \Delta u(k-1) \tag{4.74}$$

$$\hat{y}_c(k) = \begin{bmatrix} 0 & I \end{bmatrix} \begin{bmatrix} \Delta x(k) \\ y_c(k) \end{bmatrix} + v_c(k) \tag{4.75}$$

The following expression for $K_G$ shows that the optimal filter gain for the above system is parametrized in terms of an n-dimensional real vector, each element of which lies in $(0, 1]$.

$$K_G = \begin{bmatrix} 0 \\ F \end{bmatrix} \tag{4.76}$$

where

$$F = \begin{bmatrix} f_1 & & \\ & \ddots & \\ & & f_n \end{bmatrix} \tag{4.77}$$

$$f_i = \frac{\tilde{q}_i + \sqrt{\tilde{q}_i^2 + 4\tilde{q}_i}}{\tilde{q}_i + \sqrt{\tilde{q}_i^2 + 4\tilde{q}_i} + 2} \tag{4.78}$$

$$\tilde{q}_i = q_i/r_i \qquad \text{for } 1 \leq i \leq n \tag{4.79}$$

We immediately see that $0 < f_i \leq 1$ and

$$f_i \rightarrow 0 \text{ as } \tilde{q}_i \rightarrow 0 \tag{4.80}$$

$$f_i \rightarrow 1 \text{ as } \tilde{q}_i \rightarrow \infty \tag{4.81}$$

The complementary sensitivity functon matrix $H$ is expressed as

$$H = \Xi(z - \Phi + \Gamma_u L_{LQ})^{-1}\Gamma_u L_{LQ}(z - \Phi + K_G \Xi\Phi)^{-1}K_G(zI) \tag{4.82}$$

Simple calculation shows that, for the system (4.73)-(4.75)

$$(z - \Phi + K_G\Xi\Phi)^{-1}(zI) = \begin{bmatrix} 0 \\ (z - I + F)^{-1}F(zI) \end{bmatrix} \tag{4.83}$$

For convenience, denote $(z - \Phi + \Gamma_u L_{LQ})^{-1}\Gamma_u L_{LQ}$ as

$$(z - \Phi + \Gamma_u L_{LQ})^{-1}\Gamma_u L_{LQ} = \begin{bmatrix} (G_{LQ})_{11} & (G_{LQ})_{12} \\ (G_{LQ})_{21} & (G_{LQ})_{22} \end{bmatrix} \tag{4.84}$$

Then, straightforward algebra leads to

$$H = (G_{LQ})_{22}(z - I + F)^{-1}F(zI) \tag{4.85}$$

$(G_{LQ})_{22}$ is interpreted as the complementary sensitivity function when measurements are perfect (just replace F with an identity matrix). For minimum-phase systems with zero input weight ( $\Lambda_{\Delta u} = 0$), it can be shown that

$$(G_{LQ})_{22} = \frac{1}{z}I \tag{4.86}$$

Hence, the resulting complementary sensitivity function for this case is

$$H = \mathrm{diag}(\frac{f_1}{z-(1-f_1)}, \cdots, \frac{f_n}{z-(1-f_n)}) \tag{4.87}$$

and the closed-loop response of the $i^{\text{th}}$ output to a disturbance is described as a first-order system with time constant of $-\frac{T}{\ln(\sqrt{1-f_i})}$ where $T$ is the sampling time. Even for nonminimum-phase systems, we see that $(z-I+F)^{-1}F(zI)$ acts as a first-order low-pass filter that detunes the "ideal (perfect measurement)" complementary sensitivity function.

## Double-Integrated White Noise Output Disturbances with White Measurement Noise

For systems with integrators or other stable "slow" dynamics (relative to the desired closed-loop bandwidth), disturbances and measurement noise are often described as *double*-integrated white-noise and white-noise entering each output indepedently re-

spectively. The model for such a system is

$$\begin{bmatrix} \Delta x(k) \\ \Delta d(k) \\ y_c(k) \end{bmatrix} = \begin{bmatrix} A_{11} & 0 & 0 \\ 0 & I & 0 \\ C_c A_{11} & I & I \end{bmatrix} \begin{bmatrix} \Delta x(k-1) \\ \Delta d(k-1) \\ y_c(k-1) \end{bmatrix} + \begin{bmatrix} B_u \\ 0 \\ C_c B_u \end{bmatrix} \Delta u(k-1) + \begin{bmatrix} 0 \\ I \\ 0 \end{bmatrix} \Delta d'(k-1) \tag{4.88}$$

$$\hat{y}_c(k) = \begin{bmatrix} 0 & 0 & I \end{bmatrix} \begin{bmatrix} \Delta x(k) \\ \Delta d(k) \\ y_c(k) \end{bmatrix} + v_c(k) \tag{4.89}$$

where $\Delta d'$ and $v_c$ are white noise with following covariance matrices:

$$E\{\Delta d' \Delta d'^T\} = \text{diag}(q_1, \cdot, q_n) \tag{4.90}$$

$$E\{\Delta v_c \Delta v_c^T\} = \text{diag}(r_1, \cdot, r_n) \tag{4.91}$$

Again, $n$ is the number of controlled outputs. The system is represented in terms of block diagram in Figure 4.8.

The optimal filter gain $K_G$ for the system is also parametrized in terms of an n-dimension real vector, each element of which lies in $(0, 1]$.

$$K_G = \begin{bmatrix} 0 \\ F_b \\ F_a \end{bmatrix} \tag{4.92}$$

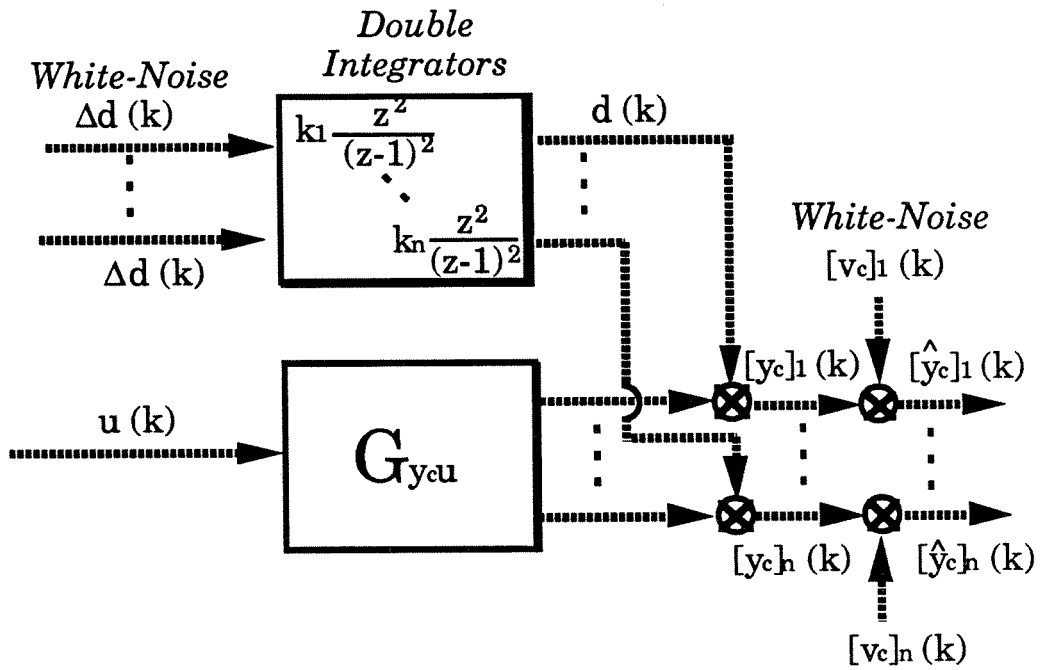


Figure 4.8. System with Double-Integrated White Noise Disturbances and White Measurement Noise Entering Each Ouput Independently

where

$$F_b = \begin{bmatrix} (f_b)_1 & & \\ & \ddots & \\ & & (f_b)_n \end{bmatrix} \tag{4.93}$$

$$F_a = \begin{bmatrix} (f_a)_1 & & \\ & \ddots & \\ & & (f_a)_n \end{bmatrix} \tag{4.94}$$

$$(f_b)_i = \frac{(f_a)_i^2}{2-(f_a)_i} \tag{4.95}$$

$$(f_a)_i = \frac{\tilde{b}_i}{\tilde{c}_i + 1} \tag{4.96}$$

$$\tilde{c}_i = \frac{\tilde{b}_i^2}{\tilde{q}_i} - 1 \tag{4.97}$$

$$\tilde{b}_i = \left( \frac{\tilde{q}_i^2}{2} + \sqrt{\frac{\tilde{q}_i^2}{4} + 4\tilde{q}_i} + \sqrt{-4\tilde{q}_i + \left( \frac{-\tilde{q}}{2} - \sqrt{\frac{\tilde{q}_i^2}{4} + 4\tilde{q}_i} \right)^2} \right) \Big/ 2 \quad (4.98)$$

$$\tilde{q}_i = q_i / r_i \qquad \text{for } 1 \leq i \leq n \quad (4.99)$$

Again, we immediately see that $0 < f_i \leq 1$ and

$$f_i \rightarrow 0 \text{ as } \tilde{q}_i \rightarrow 0 \quad (4.100)$$

$$f_i \rightarrow 1 \text{ as } \tilde{q}_i \rightarrow \infty \quad (4.101)$$

We next relate the complementary sensitivity functon matrix $H$ with $(f_i)_a$. Recall that $H$ is expressed as

$$H = \Xi(z - \Phi + \Gamma_u L_{LQ})^{-1} \Gamma_u L_{LQ} (z - \Phi + K_G \Xi \Phi)^{-1} K_G(zI) \quad (4.102)$$

Simple calculation shows that, for the system (4.88)-(4.89)

$$(z - \Phi + K_G \Xi \Phi)^{-1} K_G(zI) = \begin{bmatrix} 0 \\ \begin{bmatrix} F_b z^2 - F_b z \\ F_a z^2 - (F_a - F_b) z \end{bmatrix} (z^2 - (2I - F_a - F_b)z + (I - F_a))^{-1} \end{bmatrix} \quad (4.103)$$

For convenience, denote $(z - \Phi + \Gamma_u L_{LQ})^{-1} \Gamma_u L_{LQ}$ as

$$(z - \Phi + \Gamma_u L_{LQ})^{-1} \Gamma_u L_{LQ} = \begin{bmatrix} (G_{LQ})_{11} & (G_{LQ})_{12} & (G_{LQ})_{13} \\ (G_{LQ})_{21} & (G_{LQ})_{22} & (G_{LQ})_{23} \\ (G_{LQ})_{31} & (G_{LQ})_{32} & (G_{LQ})_{33} \end{bmatrix} \quad (4.104)$$

Then, straightforward algebra leads to

$$H = \begin{bmatrix} (G_{LQ})_{32} & (G_{LQ})_{33} \end{bmatrix} \begin{bmatrix} F_b z^2 - F_b z \\ F_a z^2 - (F_a - F_b) z \end{bmatrix} (z^2 I - (2I - F_a - F_b)z + (I - F_a))^{-1} \tag{4.105}$$

For minimum-phase systems with zero input weight ( $\Lambda_{\Delta u} = 0$), it can be shown that

$$\begin{bmatrix} (G_{LQ})_{32} & (G_{LQ})_{33} \end{bmatrix} = \frac{1}{z} \begin{bmatrix} I & I \end{bmatrix} \tag{4.106}$$

Hence, the resulting complementary sensitivity function for this case is

$$\text{diag}\left( \frac{((f_a)_1 + (f_b)_1)z - (f_a)_1}{z^2 - (2 - (f_a)_1 - (f_b)_1)z + (1 - (f_a)_1)}, \cdots, \frac{((f_a)_n + (f_b)_n)z - (f_a)_n}{z^2 - (2 - (f_a)_n - (f_b)_n)z + (1 - (f_a)_n)} \right)$$

and the closed-loop response of the $i^{\text{th}}$ output is described as a second-order system poles of which are directly affected by the choice of $(f_a)_i$. Note that

$$h_i \to \frac{2z - 1}{z^2} \text{ as } (f_a)_i \to 1 \tag{4.107}$$

With the above complementary sensitivity function, the closed-loop system rejects "ramp" disturbances perfectly after one sampling unit. One may desire the closed-loop response to be of second order with real poles; in this case, the following relationship between $(f_a)_i$ and $(f_b)_i$ can be used instead of (4.95):

$$(f_b)_i = 2 - (f_a)_i - 2\sqrt{1 - (f_a)_i} \tag{4.108}$$

When the above relationship is used, the closed-loop system is a second order system with both time constants $-T/\ln(\sqrt{1 - (f_a)_i})$.

For nonminimum-phase systems and/or nonzero input weights, the tuning parameters $(f_a)_i$s can still be used to detune $(1 - \frac{1}{z})(G_{LQ})_{32} + (G_{LQ})_{33}$, the ideal comple-

mentary sensitivity function, in an intuitive manner.

## Discussion on More General Disturbances

The two types of disturbances that we were able to parametrize the optimal filter gain for are quite general from a practical standpoint. In addition, for most chemical processes, exact modelling of disturbances is impossible; only its asymptotic nature may be known. For instance, integrated white noise disturbances that enter the outputs through overdamped, but "fast" dynamics (relative to the desired closed-loop bandwidth) can be well approximated as integrated white noise. On the other hand, step disturbances that enter the outputs through overdamped,"slow" dynamics (relative to the desired closed-loop bandwidth) are well approximated as double-integrated white noise. For most chemical systems, disturbances are one of these types and the proposed tuning rules can be used.

For nondecoupled disturbances and disturbances of more general dynamics, we have not been able to find a parametrization for the optimal filter gain that is suitable for on-line tuning. However, one may sacrifice the "optimality" (which is valid only when the stochastic assumptions on the signals are perfectly satisfied) and combine the LQ controller with an estimator equipped with tuning parameters that determine the complementary sensitivity function in a transparent manner. This motivation will be explored in the subsequent section in the context of a technique called Internal Model Control.

## Robust Design/Tuning Rules

In summary, the proposed LQG tuning rule involves two sets of tuning parameters:

1. $f_i$ or $(f_a)_i$ affects the closed-loop response of the $i^{\text{th}}$ output and lies in $(0, 1]$. These parameters are most suitable for on-line tuning. One can start with $(f_a)_i = 0$ which implies open-loop, and move toward $(f_a)_i = 1$ until performance

starts deteriorating.

2. $\Lambda_{\Delta u}$ can be set to essentially zero for SISO systems or well-conditioned (*i.e.*, directionally insensitive) MIMO systems. For ill-conditioned systems, however, setting $\Lambda_{\Delta u}$ yields a directionally sensitive controller (*e.g.*, inverse-based controller), and detuning the closed-loop response of each output independently through $f_i$ may not lead to a desirable closed-loop reponse, especially in the presence of input uncertainty [60]. For these cases, a nonzero $\Lambda_{\Delta u}$ makes the resulting control system less sensitive to directionality. Since changing $\Lambda_{\Delta u}$ requires resolving a Riccati equation, it is more practical to determine $\Lambda_{\Delta u}$ off-line. A procedure to determine $\Lambda_{\Delta u}$ analytically is given in Section 4.4 where a tuning procedure for IMC controllers is presented.

## 4.4 Internal Model Control (IMC)

In an effort to provide general LQG controllers with design/tuning parameters that have a transparent connection with system robustness, we tailor the LQG design method and propose a techique similar to Internal Model Control proposed by Garcia and Morari [24]. At this point, the proposed technique is applicable only to open-loop stable systems, although extensions to open-loop unstable systems should be possible. The model we use for control system design is the modified state-space difference model of (4.24)-(4.25) that we used for the LQG design.

### 4.4.1 Minimization Objective

In the proposed IMC design method, we first design the LQG controller with the following minimization objective:

$$\sum_{i=1}^{q}\sum_{k=0}^{\infty}\left(y_e^T(k)\Lambda_{y_e}y_e(k)+\Delta u^T(k)\Lambda_{\Delta u}\Delta u(k)\right)_i \tag{4.109}$$

where $(\cdot)_i$ represents that $y_e(k)$ and $\Delta u(k)$ are those resulting from the input

$$\begin{bmatrix} \Delta d \\ \Delta r \\ v_c \end{bmatrix}_i = \begin{bmatrix} Q_d & & \\ & Q_r & \\ & & 0 \end{bmatrix} \delta_i \tag{4.110}$$

$\delta_i$ is a unit impulse entering the $i^{\text{th}}$ channel at $t = 0$. As before, $q = (\dim\{d\} + \dim\{r\} + \dim\{v_c\})$. The correponding choices of $W_w$ and $W_p$ for the standard $H_2$-optimal control discussed in Chapter 2 problem are as follows:

$$W_w = \begin{bmatrix} \frac{z}{z-1}Q_d^{1/2} & & \\ & \frac{z}{z-1}Q_r^{1/2} & \\ & & 0 \end{bmatrix} \tag{4.111}$$

$$W_p = \begin{bmatrix} \frac{z-1}{z}\Lambda_{\Delta u}^{1/2} & \\ & \Lambda_{y_e}^{1/2} \end{bmatrix} \tag{4.112}$$

### 4.4.2 Detuning for Robustness

Once the LQG controller based on the above objective is designed, the next step is to detune the closed-loop in order to obtain a complementary sensitivity function that is desirable from the robustness viewpoint. The main question that arises then is how to best accompish this "detuning."

Consider the block diagram of Figure 4.9(a) that represents the closed-loop system with the LQG optimal controller. One can add and subtract the transfer function block $G_{y_cu}$ and obtain the diagram of Figure 4.9(b). Note that the closed-loop transfer function from $v_c$ to $y_c$ is $-G_{y_cu}Q_{IMC}$. Hence, $G_{y_cu}Q_{IMC}$ represents the "ideal" complementary sensitivity function (*i.e.*, the optimal complementary sensitivity function in the absence of measurement noise and modelling errors) which must be detuned for robustness. A natural way of detuning is to add a filter block $F_{IMC}$ as shown in

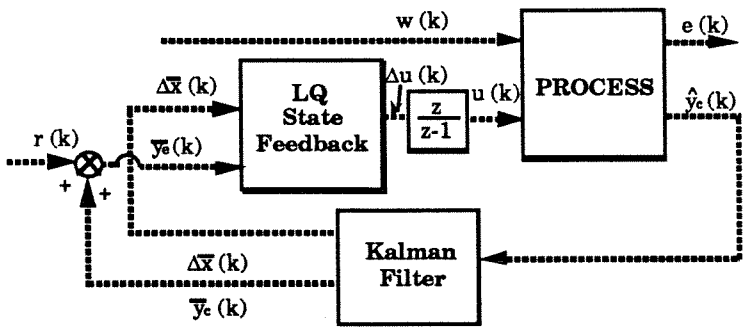


(a)

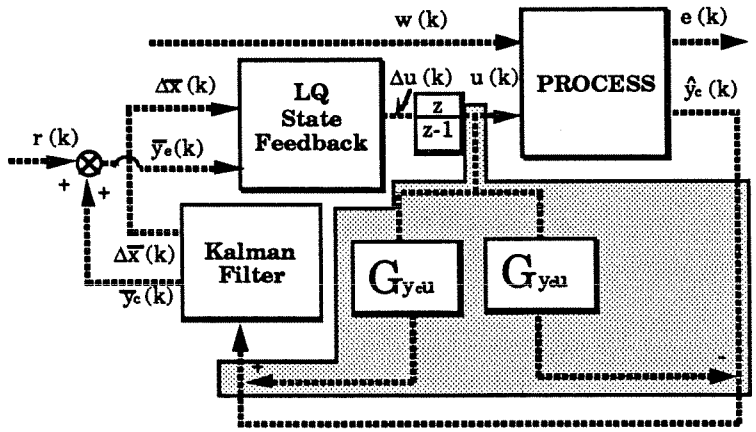


(b)

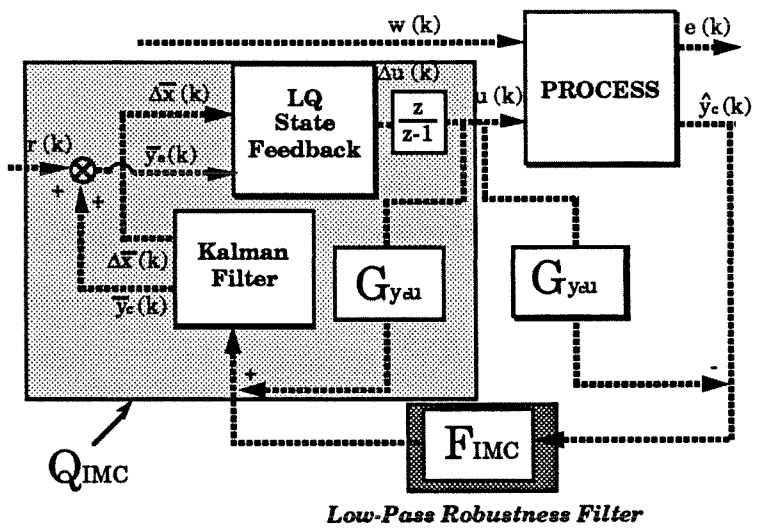


(c)

Figure 4.9. IMC Detuning for Robustness and Noise-Sensitivity Reduction

Figure 4.9(c). The resulting complementary sensitivity function is $G_{y_cu}Q_{IMC}F_{IMC}$. Hence, $F_{IMC}$ detunes the ideal complementary sensitivity function in a user chosen manner. Note that the only requirement on $F_{IMC}$ for internal stability is that it is stable itself. For the case where $G_{y_cu}$ has a stable, causal right inverse and $\lambda_{\Delta u} = 0$. $Q_{IMC} = (G_{y_cu})_r^{-1}$ and $F_{IMC}$ is indeed the complementary sensitivity function.

### 4.4.3 State Space Formula for IMC Controller

The optimal estimator for the given process and disturbances is the following Kalman filter:

$$\begin{aligned}\Delta\bar{X}(k) &= \Phi\Delta\bar{X}(k-1) + \Gamma_u\Delta u(k-1) \\ &+ K_{IMC}[\hat{y}_c^f(k) - \Xi\{\Phi\Delta\bar{X}(k-1) + \Gamma_u\Delta u(k-1)\}] \qquad (4.113)\end{aligned}$$

where

$$K_{IMC} = \Sigma_{IMC}\Xi^T\{\Xi\Sigma_{IMC}\Xi^T\}^{-1} \qquad (4.114)$$

$\Sigma_{IMC}$ represents the unique stabilizing solution (*i.e.*, the solution that leads to a stable $\Phi - K_{IMC}\Xi\Phi$) to the following Algebraic Riccati Equation (ARE):

$$\Sigma_{IMC} = \Phi\Sigma_{IMC}\Phi^T - \Phi\Sigma_{IMC}\Xi^T\{\Xi\Sigma_{IMC}\Xi^T\}^{-1}\Xi\Sigma_{IMC}\Phi^T + \Gamma_d Q_d \Gamma_d^T \qquad (4.115)$$

The optimal state feedback is same as before. The $H_2$-optimal controller for the given problem is a combination of the Kalman filter and the LQ state feedback compensator written as follows:

$$\begin{aligned}\Delta\bar{X}(k) &= (\Phi - K_{IMC}\Xi\Phi - \Gamma_u L_{LQ} + K_{IMC}\Xi\Gamma_u L_{LQ})\Delta\bar{X}(k-1) \\ &- (I - K_{IMC}\Xi)\Gamma_u L_{LQ}\Gamma_r r(k-1) + K_{IMC}\hat{y}_c^f(k) \qquad (4.116) \\ \Delta u(k) &= -L_{LQ}\left\{\Delta\bar{X}(k) + \Gamma_r r(k)\right\} \qquad (4.117)\end{aligned}$$

Next we must augment this controller with the robustness filter $F_{IMC}$. The realization of the transfer function $G_{y_c u}$ can be written as follows:

$$\begin{bmatrix} \Delta\bar{x}^u(k) \\ \bar{y}_c^u(k) \end{bmatrix} = \begin{bmatrix} A & 0 \\ C_c A & I \end{bmatrix} \begin{bmatrix} \Delta\bar{x}^u(k-1) \\ \bar{y}_c^u(k-1) \end{bmatrix} + \begin{bmatrix} C_c \\ C_c B_u \end{bmatrix} \Delta u(k-1) \quad (4.118)$$

$$\bar{y}_c^u(k) = \begin{bmatrix} 0 & I \end{bmatrix} \begin{bmatrix} \Delta\bar{x}^u(k) \\ \bar{y}_c^u(k) \end{bmatrix} \quad (4.119)$$

In addition, let the realization of $F_{IMC}$ be written as

$$\bar{x}^f(k) = A^f \bar{x}^f(k-1) + B^f(\hat{y}_c(k) - \bar{y}_c^u(k)) \quad (4.120)$$

$$\hat{y}_{IMC}^f(k) = C^f \bar{x}^f(k) \quad (4.121)$$

Now, we can express $y_c^f$ as

$$\hat{y}_c^f = C^f \bar{x}^f(k) + \bar{y}_c^u(k) \quad (4.122)$$

$$= C^f \left( A^f \bar{x}^f(k-1) + B^f(\hat{y}_c(k) - \bar{y}_c^u(k)) \right) + \bar{y}_c^u(k) \quad (4.123)$$

$$= C^f A^f \bar{x}^f(k-1) + (I - C^f B^f)\bar{y}_c^u(k) + C^f B^f \hat{y}_c(k) \quad (4.124)$$

$$= C^f A^f \bar{x}^f(k-1) + (I - C^f B^f)\left(C_c A \Delta\bar{x}^u(k-1) + \bar{y}_c^u(k-1) + C_c B_u \Delta u(k-1)\right)$$

$$+ C^f B^f \hat{y}_c(k) \quad (4.125)$$

The "undetuned" LQG estimator has the realization

$$\begin{bmatrix} \Delta\bar{x}(k) \\ \bar{y}_c(k) \end{bmatrix} = \begin{bmatrix} A & 0 \\ C_c A & I \end{bmatrix} \begin{bmatrix} \Delta\bar{x}(k-1) \\ \bar{y}_c(k-1) \end{bmatrix} + \begin{bmatrix} B_u \\ C_c B_u \end{bmatrix} \Delta u(k-1)$$

$$+ K_{IMC} \left( \hat{y}_c^f(k) - \begin{bmatrix} C_c A & I \end{bmatrix} \begin{bmatrix} \Delta\bar{x}(k-1) \\ \bar{y}_c(k-1) \end{bmatrix} - C_c B_u \Delta u(k-1) \right) \quad (4.126)$$

Combining (4.125) and (4.126),

$$\begin{aligned}
\begin{bmatrix} \Delta\bar{x}(k) \\ \bar{y}_c(k) \end{bmatrix} &= \left( \begin{bmatrix} A & 0 \\ C_cA & I \end{bmatrix} - K_{IMC} \begin{bmatrix} C_cA & I \end{bmatrix} \right) \begin{bmatrix} \Delta\bar{x}(k-1) \\ \bar{y}_c(k-1) \end{bmatrix} \\
&+ \left( \begin{bmatrix} B_u \\ C_cB_u \end{bmatrix} - K_{IMC}C_cB_u \right) \Delta u(k-1) \\
&+ K_{IMC} \left\{ C^f A^f \bar{x}^f(k-1) \right. \\
&+ (I - C^f B^f)\left(C_cA\Delta\bar{x}^u(k-1) + \bar{y}_c^u(k-1) + C_cB_u\Delta u(k-1)\right) \\
&+ \left. C^f B^f \hat{y}_c(k) \right\} \qquad (4.127)
\end{aligned}$$

A general state-space formula for the IMC controller can now be written as follows:

$$\bar{X}^{IMC}(k) = \Phi^{IMC}\bar{X}^{IMC}(k-1) + \Gamma_u^{IMC}\Delta u(k-1) + \Gamma_{y_c}^{IMC}\hat{y}_c(k) \qquad (4.128)$$

$$\Delta\bar{X}^e(k) = \begin{bmatrix} 0 & 0 & 0 & I & 0 \\ 0 & 0 & 0 & 0 & I \end{bmatrix} \bar{X}^{IMC} - \begin{bmatrix} 0 \\ I \end{bmatrix} r(k) \qquad (4.129)$$

$$\Delta u(k) = -L_{LQ}\Delta\bar{X}^e \qquad (4.130)$$

where

$$\bar{X}^{IMC}(k) = \begin{bmatrix} \Delta\bar{x}^u(k) \\ \bar{y}_c^u(k) \\ \bar{x}^f(k) \\ \Delta\bar{x}(k) \\ \bar{y}_c(k) \end{bmatrix} \qquad (4.131)$$

$$\Phi^{IMC} = \begin{bmatrix} \begin{bmatrix} A & 0 \\ C_cA & I \end{bmatrix} & 0 \\ -B^f \begin{bmatrix} C_cA & I \end{bmatrix} & A^f \\ K_{IMC} \begin{bmatrix} (I - C^fB^f)C_cA & I - C^fB^f \end{bmatrix} & K_{IMC}C^fA^f \end{bmatrix}$$

$$\begin{bmatrix} 0 \\ 0 \\ \begin{bmatrix} A & 0 \\ C_cA & I \end{bmatrix} - K_{IMC} \begin{bmatrix} C_cA & I \end{bmatrix} \end{bmatrix} \tag{4.132}$$

$$\Gamma_u^{IMC} = \begin{bmatrix} \begin{bmatrix} B_u \\ C_cB_u \end{bmatrix} \\ -B^f C_c B_u \\ \begin{bmatrix} B_u \\ C_cB_u \end{bmatrix} - K_{IMC} C^f B^f C_c B_u \end{bmatrix} \tag{4.133}$$

$$\Gamma_{y_c}^{IMC} = \begin{bmatrix} \begin{bmatrix} 0 \\ 0 \end{bmatrix} \\ B^f \\ K_{IMC} C^f B^f \end{bmatrix} \tag{4.134}$$

It may be computationally advantageous to implement the above estimator in series since the matrix $\Phi^{IMC}$ has a block-triangular structure.

### 4.4.4 Constraint Handling

For input constraints, the idea of extended Kalman filtering can be applied to the IMC estimator transparently. Hence, in the presence of input constraints or mode switching, the IMC estimator of (4.128) can be replaced by the following estimator:

$$\bar{X}^{IMC}(k) = \Phi^{IMC} \bar{X}^{IMC}(k-1) + \Gamma_u^{IMC} \Delta u_{true}(k-1) + \Gamma_{y_c}^{IMC} \hat{y}_c(k) \tag{4.135}$$

where $\Delta u_{true}$ is the "true" input to the process. Note that this anti-windup mechanism is different from the traditional IMC anti-windup method, which is known to cause sluggish recovery from saturation when the process contains dynamics that are

slow relative to the closed-loop bandwidth [10]. The proposed anti-windup scheme will not have this problem since, unlike in the traditional scheme, all the controller states are correctly updated. This can be seen transparently from Figure 4.10.

When an ill-conditioned MIMO system is subjected to input constraints, the directional correction scheme proposed in Section 4.3.4 can be used. All the output constraints must be handled through *ad hoc* ways such as mode-switching.

### 4.4.5 Robust Design/Tuning of IMC Filter

In this section, we present a method to design the IMC filter directly such that the robust performance requirement is satisfied. The method is based on the frequency-domain robust performance normbounds that can be easily derived using the SSV analysis.

#### Derivation of Robust Performance Norm-Bounds

In this section, we present briefly a method for deriving robust performance norm-bounds on desired transfer function matrices. The following theorem enables the calculation of the "tightest" frequency-domain bounds on the maximum singluar value of a chosen closed-loop transfer function, guaranteeing robust performance [59].

**Theorem 4.2** *Let $M \in \mathcal{C}^{n\times m}$ be written as*

$$M = R_{11} + R_{12}L(I - R_{22}L)^{-1}R_{21} \tag{4.136}$$

*where*

$$R_{11} \in \mathcal{C}^{n\times m}, R_{12} \in \mathcal{C}^{n\times p}, R_{21}, \in \mathcal{C}^{k\times m}, R_{22} \in \mathcal{C}^{k\times p} \text{ and } L \in \mathcal{C}^{p\times k} \tag{4.137}$$

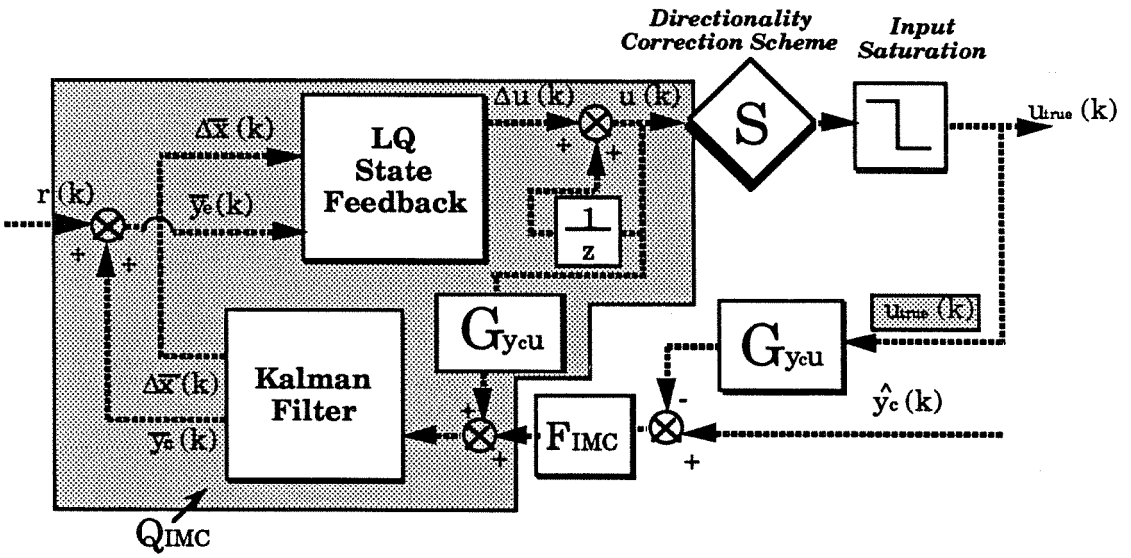


(a) Traditional IMC Anti-Windup

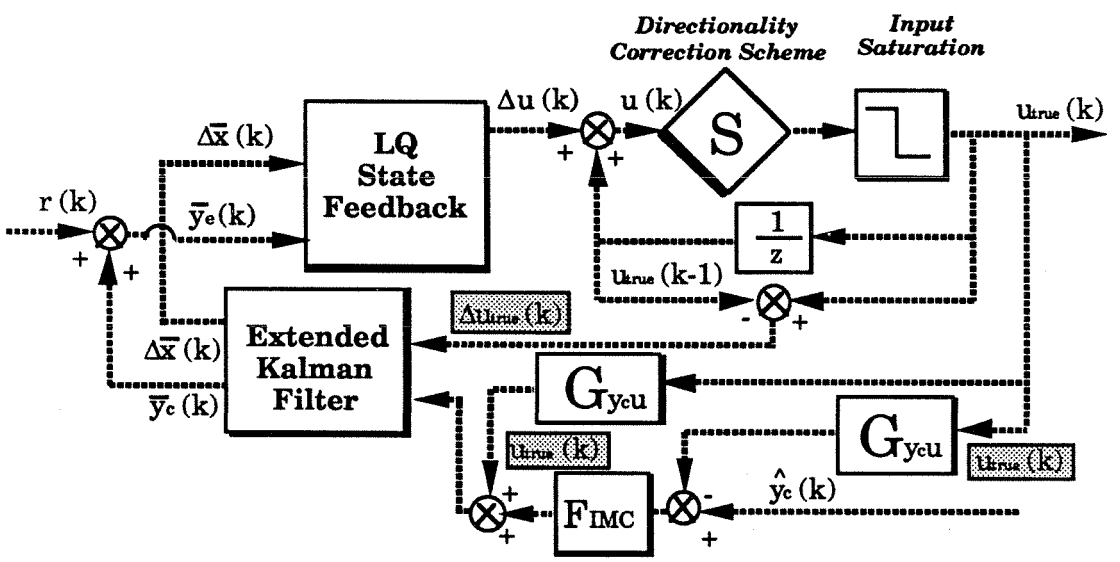


(b) New IMC Anti-Windup

Figure 4.10. Traditional IMC Anti-Windup vs. New IMC Anti-Windup

*Define*

$$f(c_L) = \mu \begin{bmatrix} \mathbf{\Delta} & \\ & \mathbf{\Delta_L} \end{bmatrix} \begin{bmatrix} R_{11} & R_{12} \\ c_L R_{21} & c_L R_{22} \end{bmatrix} \tag{4.138}$$

*where*

$$\begin{aligned} \mathbf{\Delta} &= \left\{ \Delta : \Delta = \begin{bmatrix} \Delta & & \\ & \ddots & \\ & & \Delta_\ell \end{bmatrix} ; \sum_{i=1}^{\ell} m_i = m \quad \sum_{i=1}^{\ell} n_i = n, \quad \Delta_i \in \mathcal{C}^{m_i \times n_i} \right\} \\ \mathbf{\Delta_L} &= \left\{ \Delta : \Delta \in \mathcal{C}^{p \times k} \right\} \\ & c_L \in \mathcal{R}^+ \end{aligned} \tag{4.139}$$

*Assume*

$$\mu_\Delta(R_{11}) < 1 \quad \text{and} \quad \det(I - R_{22}L) \neq 0 \tag{4.140}$$

*then*

$$\mu_\Delta(M) < 1 \tag{4.141}$$

*if*

$$\bar{\sigma}(L) < c_L^* \tag{4.142}$$

*where* $c_L^*$ *solves* $f(c_L^*) = 1$.

**Proof** see Skogestad & Morari [59]. ■

Theorem 4.2 suggests that the norm bound on $L$ guaranteeing robust performance can be obtained by parametrizing the closed-loop system in terms of $L$ and choosing the frequency-dependent scaling factor $c_L^*(\omega)$ such that $f(c_L^*(\omega)) = 1 \; \forall \omega$. $c_L^*(\omega)$ is the *tightest* norm bound of $L$ in the sense that, for each $c_L(\omega) > c_L^*(\omega)$ for some $\omega$, there exists at least one $L$ such that $\bar{\sigma}(L(j\omega)) = c_L(\omega)$ and $\sup_\omega f(c_L(\omega)) \geq 1$.

**Comments on Theorem 4.2:**

1. $f(c_L)$ is a non-decreasing function of $c_L$. Thus the scaling factor $c_L^*$ can be easily found through a simple search-procedure (*e.g.*, bisection method).

2. Because $f_{c_L}$ is monotonically increasing function of $c_L$, the requirement for $c_L^* > 0$ is that $\mu < 1$ for $L = 0$.

3. There may exist many sets of $J, L$ parametrizing $K$. The norm bounds on different $L$'s can be combined over different frequency ranges. For example, suppose that both $L_1$ and $L_2$ parametrize $K$. Then, robust performance is met if, for each $\omega$, $\bar{\sigma}(L_1(j\omega)) < c_{L_1}^*(\omega)$ or $\bar{\sigma}(L_2(j\omega)) < c_{L_2}^*(\omega)$.

4. Condition (4.142) is only sufficient for robust performance as robust performance must be guaranteed for every $L$ (as opposed to a particular $L$), which satisfies $0 \leq \bar{\sigma}(L)(\omega) < c_L^*(\omega)$. $\mu_\Delta(R_{11}) < 1$ requires that $f(c_L) < 1$ for $c_L = 0$.

5. Tightest bounds can be obtained if we restrict $L$ to be a scalar-times-identity matrix. Then, the $\mu$ can be calculated with respect to $\mathbf{\Delta_L} = \left\{\delta I^{p\times k} : \delta \in \mathcal{C}\right\}$.

## Using Robust Performance Normbounds for Design of IMC Filter

We can use the above method in designing the IMC filter for robust performance. Figure 4.11(a) shows a block diagram for general robust performance problems. We can parametrize the closed-loop system in terms of $F_{IMC}$ as shown in Figure 4.11(b) and derive the robust performance norm-bound on $F_{IMC}$. One problem is that the bound on $\bar{\sigma}(F_{IMC}(j\omega)$ will not be feasible (*i.e.*, drop to zero) in the low frequency region since $F_{IMC} = 0$ implies open-loop (see the second comment on Theorem 4.2). An immediate way to overcome this problem is to reparametrize the closed-loop in terms of $I - F_{IMC}$ as shown in Figure 4.11(c) and to derive the robust performance norm-bound on $I - F_{IMC}$. The bound on $\bar{\sigma}(I - F_{IMC}(j\omega))$ should be feasible in the low frequency region, but will often be infeasible in the high frequency region where detuning is required for robust stability ($I - F_{IMC} = 0$ implies no detuning).

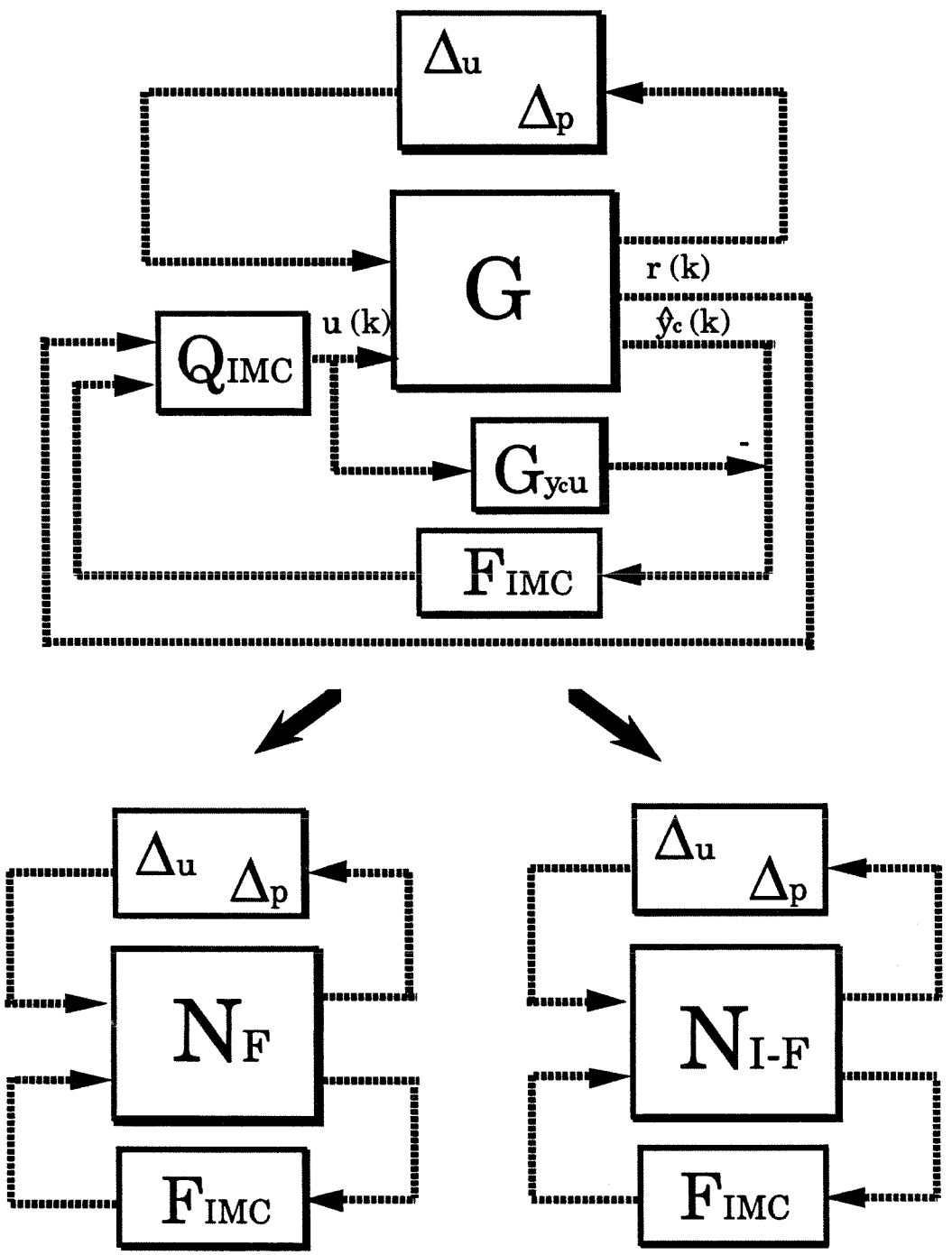


Figure 4.11. General Method for Deriving Norm-Bounds on $F_{IMC}$ and $I - F_{IMC}$

Hence, the bound on $\bar{\sigma}(F_{IMC}(j\omega))$ must be combined with that on $\bar{\sigma}(I - F_{IMC}(j\omega))$ in designing $F_{IMC}$. More specifically, if $F_{IMC}$ is designed such that either of the bounds is satisfied at each frequency, then we may conclude that robust performance is achieved.

### Robust Design/Tuning Rules

In summary of the foregoing discussion, we propose the following design/tuning rules for IMC controllers:

1. As mentioned before, a nonzero input weight can reduce the directional sensitivity of the LQ controller for an ill-conditioned system. Hence, the input weight $\Lambda_{\Delta u}$ (chosen as a constant-times-identity matrix for simplicity) is gradually increased until the resulting robust performance norm-bounds on $F_{IMC}$ and $I - F_{IMC}$ start deteriorating.

2. The robust performance norm-bounds on $F_{IMC}$ and $I - F_{IMC}$ are used to design $F_{IMC}$ satisfying robust performance, if possible. Otherwise, a more elaborate design such as $\mu$-Synthesis may be necessary.

3. Equipping the $F_{IMC}$ with on-line tuning parameters that directly affect the speed of the closed-loop response (*e.g.*, pole locations) can add further flexibility of the control system.

## 4.4.6 Relationship with LQG and Traditional IMC

To clarify the relationship between LQG and IMC, we reconsider the two special types of disturbance/noise for which we were able to parametrize the optimal estimator with a real parameter vector and establish a connection between the two techniques.

## Integrated White Noise Disturbance in Each Output with White Measurement Noise

Recall that, for LQG controllers, the complementary sensitivity function was expressed as

$$H_{LQG} = (G_{LQ})_{22}(z - I + F)^{-1}F(zI) \tag{4.143}$$

On the other hand, for IMC controllers, the complementary sensitivity function is

$$H_{IMC} = G_{y_cu}Q_{IMC}F_{IMC} \tag{4.144}$$

It can be easily seen by letting $F = I$ that the "undetuned" complementary sensitivity function $G_{y_cu}Q_{IMC}$ is $(G_{LQ})_{22}$. Hence, $F_{IMC}$ that leads to an IMC controller equivalent to the LQG controller is simply the following diagonal first-order filter.

$$F_{IMC} = (z - I + F)^{-1}F(zI) \tag{4.145}$$

## Double-Integrated White Noise Disturbance on Each Output with White Measurement Noise

The complementary sensitivity function for LQG controllers is

$$H_{LQG} = \begin{bmatrix} (G_{LQ})_{32} & (G_{LQ})_{33} \end{bmatrix} \begin{bmatrix} F_b z^2 - F_b z \\ F_a z^2 - (F_a - F_b)z \end{bmatrix} (z^2-(2I-F_a-F_b)z+(I-F_a))^{-1} \tag{4.146}$$

On the other hand, for IMC controllers, the complementary sensitivity function is

$$H_{IMC} = G_{y_cu}Q_{IMC}F_{IMC} \tag{4.147}$$

$$= \begin{bmatrix} (G_{LQ})_{32} & (G_{LQ})_{33} \end{bmatrix} \begin{bmatrix} \frac{z-1}{z}I \\ I \end{bmatrix} F_{IMC} \tag{4.148}$$

$F_{IMC}$ that leads to an IMC controller equivalent to the LQG controller is

$$F_{IMC} = \left( \begin{bmatrix} (G_{LQ})_{32} & (G_{LQ})_{33} \end{bmatrix} \begin{bmatrix} \frac{z-1}{z} I \\ I \end{bmatrix} \right)^{-1} \begin{bmatrix} (G_{LQ})_{32} & (G_{LQ})_{33} \end{bmatrix} \begin{bmatrix} F_b z^2 - F_b z \\ F_a z^2 - (F_a - F_b) z \end{bmatrix} (z^2 I - (2I - F_a - F_b)z + (I - F_a))^{-1} \quad (4.149)$$

In general, such a filter would be extremely complex and is a function of $L_{LQ}$ as well as $F_a$ and $F_b$. The only exception is the case of a minimum-phase system with zero input weight. For this case,

$$\begin{bmatrix} (G_{LQ})_{32} & (G_{LQ})_{33} \end{bmatrix} = \frac{1}{z} \begin{bmatrix} I & I \end{bmatrix} \quad (4.150)$$

and the expression (4.117) reduces to

$$F_{IMC} = \frac{z}{2z-1} \left( (F_a + F_b)z^2 - F_a z \right) \left( z^2 I - (2I - F_a - F_b)z + (I - F_a) \right)^{-1} \quad (4.151)$$

Using similar arguments, one can show that, for general disturbances, $F_{IMC}$ leading to an IMC controller equivalent to its correponding LQG controller is very complex and is a function of $L_{LQ}$ as well as $K_G$.

The proposed IMC technique differs from the standard IMC technique [50] in that the IMC controllers are interpreted as state-observer based compensators and that its formulation allows for the flexibility of including a nonzero input weight in the objective function. Standard IMC is developed in an input/output setting and $Q_{IMC}$ is calculated directly assuming a zero input weight. The flexibility of including a nonzero input weight can be important for ill-conditioned systems for which inverse-based controllers are not desirable from a robust viewpoint.

## 4.5 Model Predictive Control (MPC)

For the LQG and IMC controllers, input constraints are handled through an extended estimator combined with a directionality correction scheme. These constraint handling schemes are simple and intuitive, but are *ad hoc* and suboptimal. In addition, various output constraints must be handled in heuristic ways (*e.g.*, mode switching). Motivated by these considerations, we develop in this section a Model Predictive Control technique that can incorporate various constraints in a direct manner. Before we begin our discussion on MPC, we would like to remark that the proposed technique represents a significant step forward for MPC. The new interpretation of MPC controllers as a combination of a state observer and a compensator (constant linear state feedback for unconstrained cases and nonlinear state feedback for cases) enables more transparent analysis of the control system and flexible, intuitive design and tuning as well.

### 4.5.1 Minimization Objective

Consider the same disturbances as in (4.38). The minimization objective of MPC is based on a finite moving time horizon: Minimize at each $t = k$ the function

$$\sum_{i=1}^{q} \sum_{t=k}^{k+p} \left( y_e^T(t) \Lambda_{y_e} y_e(t) + \Delta u^T(t) \Lambda_{\Delta u} \Delta u(t) \right)_i \tag{4.152}$$

$p$ is called "prediction horizon," and often used as a tuning parameter in traditional MPC techniques. The main motivation for adopting the finite-moving-horizon-based objective function is that on-line constrained optimization can be performed to calculate the best controller moves in the presence of input/output constraints. This is discussed in Section 4.5.3.

### 4.5.2 Optimal Control Design

The separation principle still applies for the MPC in the absence of constraints. Hence, we can design the state estimator and the compensator separately and combine them to obtain the optimal control system.

**Optimal Estimator: Kalman Filter**

Since disturbances to the system have not changed, the optimal estimator remains the same as before: the Kalman filter of (4.42).

**Optimal Compensator: MPC State Feedback**

To obtain the optimal state feedback for the objective (4.152), we develop the following prediction equation (note that it is optimal to set $\Delta d(q) = 0$ for $q \geq k$ since it is zero-mean white noise):

$$\bar{\mathcal{Y}}_e^p(k+1|k) = \bar{\mathcal{Y}}_c^p(k+1|k) - \mathcal{R}^p(k+1|k) \tag{4.153}$$

$$\bar{\mathcal{Y}}_c^p(k+1|k) = \mathcal{S}^x \Delta x(k) + \mathcal{I}^p y_c(k) + \mathcal{S}^{\mathcal{U}} \Delta \mathcal{U}(k) \tag{4.154}$$

where

$$\bar{\mathcal{Y}}_e^p(k+1|k) = \begin{bmatrix} \bar{y}_e(k+1|k) \\ \bar{y}_e(k+2|k) \\ \vdots \\ \bar{y}_e(k+p|k) \end{bmatrix} \qquad \bar{\mathcal{Y}}_c^p(k+1|k) = \begin{bmatrix} \bar{y}_c(k+1|k) \\ \bar{y}_c(k+2|k) \\ \vdots \\ \bar{y}_c(k+p|k) \end{bmatrix}$$

$$\Delta \mathcal{U}^m(k) = \begin{bmatrix} \Delta u(k) \\ \Delta u(k+1) \\ \vdots \\ \Delta u(k+m-1) \end{bmatrix} \qquad \mathcal{R}^p(k+1|k) = \begin{bmatrix} r(k+1|k) \\ r(k+2|k) \\ \vdots \\ r(k+p|k) \end{bmatrix}$$

$$\mathcal{I}^p = \begin{bmatrix} I_{\dim\{y_c\}} \\ I_{\dim\{y_c\}} \\ \vdots \\ I_{\dim\{y_c\}} \end{bmatrix} \qquad \mathcal{S}^x = \begin{bmatrix} C_cA \\ C_cA^2 + C_cA \\ \vdots \\ \sum_{j=1}^{p} C_cA^j \end{bmatrix}$$

$$\mathcal{S}^{\mathcal{U}} = \begin{bmatrix} C_cB_u & 0 & \cdots & 0 \\ C_cAB_u + C_cB_u & C_cB_u & \cdots & 0 \\ \vdots & \vdots & \ddots & \vdots \\ \sum_{j=1}^{p} C_cA^{j-1}B_u & \sum_{j=1}^{p-1} C_cA^{j-1}B_u & \cdots & \sum_{j=1}^{p-m+1} C_cA^{j-1}B_u \end{bmatrix} \tag{4.155}$$

$\bar{y}_e(k+q|k,j)$ represents the prediction of $y_e(k+q)$ based on the measurements at $t = k$. We also allowed the flexibility of specifying the number of input moves, $m$, differently from the output prediction horizon $p$ (*i.e.*, $1 \leq m \leq p$). In the LQG design, we assumed that $r$ is described as integrated white noise. An analogous treatment would be to set $\mathcal{R}^p(k+1|k) = r(k)\mathcal{I}^p$. By incorporating information on the *future* reference changes into the prediction equation, MPC can handle more general types of reference inputs *without* increasing the system order.

Simple least-square solution calculation shows that the optimal state feedback law for the objective (4.152) is as follows:

$$\Delta u(k) = -L_{MPC} \begin{bmatrix} \Delta x(k) \\ y_c(k) \end{bmatrix} + K_{MPC}\mathcal{R}^p(k+1|k) \tag{4.156}$$

where

$$L_{MPC} = -K_{MPC} \begin{bmatrix} \mathcal{S}^x & \mathcal{I}^p \end{bmatrix} \tag{4.157}$$

$$K_{MPC} = \begin{bmatrix} I & 0 & \cdots & 0 \end{bmatrix} \left( (\mathcal{S}^{\mathcal{U}})^T \tilde{\Lambda}_{y_e}^T \tilde{\Lambda}_{y_e} \mathcal{S}^{\mathcal{U}} + \tilde{\Lambda}_{\Delta u}^T \tilde{\Lambda}_{\Delta u} \right)^{-1} (\mathcal{S}^{\mathcal{U}})^T \tilde{\Lambda}_{y_e}^T \tilde{\Lambda}_{y_e} \tag{4.158}$$

where $\tilde{\Lambda}_{y_e} = \text{diag}(\overbrace{\Lambda_{y_e}, \cdots, \Lambda_{y_e}}^{p})$ and $\tilde{\Lambda}_{\Delta u}$ is defined in the same way. The compensator is stable if and only if all eigenvalues of $(\Phi - \Gamma_{\Delta u} L_{MPC})$ lie inside the unit disk. Assuming the reference vector is a step function,

$$\Delta u(k) = -L_{MPC} \left\{ \begin{bmatrix} \Delta x(k) \\ y_c(k) \end{bmatrix} - \begin{bmatrix} 0 \\ r(k) \end{bmatrix} \right\} \tag{4.159}$$

which is same control law as the LQ regulator with $L_{LQ}$ replaced by $L_{MPC}$. By definition, $L_{MPC} \to L_{LQ}$ as $p, q \to \infty$ for minimum-phase systems since $L_{MPC}$ is guaranteed to be a stabilizing control law in this case (one would need weighting on $\Delta u$ at $t = \infty$ to guarantee stability for nonminimum-phase systems).

**Optimal "Unconstrained" MPC: Kalman Filter + MPC State Feedback**

The optimal unconstrained controller is the combination of the Kalman filter and MPC state feedback:

$$\Delta u(k) = -L_{MPC} \begin{bmatrix} \Delta \bar{x}(k) \\ \bar{y}_c(k) \end{bmatrix} + K_{MPC} \mathcal{R}^p(k+1|k) \tag{4.160}$$

### 4.5.3 Constraint Handling: On-Line Quadratic Programming

The main advantage of MPC is that constraints can be incorporated directly into the controller formulation. In the presence of the constraints described through (2.70)-(2.72), the MPC state feedback is replaced by an on-line optimizer that calculates at every $t = k$ the optimal control moves (not violating the given constraints) for the specified number of steps ahead and implements the first move. The optimization can be written as follows:

$$\min_{\Delta \mathcal{U}^m(k)} \sum_{t=k}^{k+p} \left( \bar{y}_e^T(t) \Lambda_{y_e} \bar{y}_e(t) + \Delta u^T(t) \Lambda_{\Delta u} \Delta u(t) \right) \tag{4.161}$$

such that

$$u_{low}(k+q) \leq u(k,j+q) \leq u_{high}(k+q) \quad 0 \leq q \leq m-1 \tag{4.162}$$

$$|\Delta u(k+q)| \leq \Delta u_{max}(k+q) \quad 0 \leq q \leq m-1 \tag{4.163}$$

$$(y_c)_{low}(k+q) \leq y_c(k,j+q) \leq (y_c)_{high}(k+q) \quad 1 \leq q \leq p \tag{4.164}$$

Of course, if $m \leq p-1$, then we constrain $\Delta u(k+q)$ to be zero for $m \leq q \leq p-1$.

The above optimzation problem can be formulated into the following standard Quadratic Programming problem:

$$\min_{\Delta \mathcal{U}^m(k)} \quad \left\{ ||\tilde{\Lambda}_{y_e}^{1/2}(\bar{\mathcal{Y}}_e^p(k,j+1|k,j) - \mathcal{R}^p(k+1|k))||^2 + ||\tilde{\Lambda}_{\Delta u}^{1/2} \Delta \mathcal{U}^m(k)||^2 \right\} \tag{4.165}$$

$$\text{s.t.} \quad \mathcal{C}^u \Delta \mathcal{U}^m(k) \geq \mathcal{C}(k+p|k) \tag{4.166}$$

$$\mathcal{C}^u(k+p|k) = \begin{bmatrix} -\mathcal{I}_L \\ \mathcal{I}_L \\ -\mathcal{I}_D \\ \mathcal{I}_D \\ -S^{\mathcal{U}} \\ S^{\mathcal{U}} \end{bmatrix} \tag{4.167}$$

$$\mathcal{I}_L = \underbrace{\begin{bmatrix} I_{\dim\{u\}} & 0 & \cdots & 0 \\ I_{\dim\{u\}} & I_{\dim\{u\}} & \cdots & 0 \\ \vdots & \vdots & \ddots & \vdots \\ I_{\dim\{u\}} & I_{\dim\{u\}} & \cdots & I_{\dim\{u\}} \end{bmatrix}}_{m}$$

$$\mathcal{I}_D = \underbrace{\begin{bmatrix} I_{\dim\{u\}} & 0 & \cdots & 0 \\ 0 & I_{\dim\{u\}} & \cdots & 0 \\ \vdots & \vdots & \ddots & \vdots \\ 0 & 0 & \cdots & I_{\dim\{u\}} \end{bmatrix}}_{m} \tag{4.168}$$

$$\mathcal{C}(k+p|k) = \begin{bmatrix} u(k-1) - u_{high}(k) \\ \vdots \\ u(k-1) - u_{high}(k+m-1) \\ u_{low}(k) - u(k-1) \\ \vdots \\ u_{low}(k+m-1) - u(k-1) \\ -\Delta u_{max}(k) \\ \vdots \\ -\Delta u_{max}(k+m-1) \\ -\Delta u_{max}(k) \\ \vdots \\ -\Delta u_{max}(k, j+q-1) \\ \mathcal{S}^x \Delta\bar{x}(k) + \mathcal{I}^p \bar{y}_c(k) - \mathcal{Y}^p_{high}(k+1|k) \\ -\mathcal{S}^x \Delta\bar{x}(k) - \mathcal{I}^p \bar{y}_c(k) + \mathcal{Y}^p_{low}(k+1|k) \end{bmatrix} \tag{4.169}$$

where $\mathcal{Y}^p_{high}/\mathcal{Y}^p_{low}$ represent upper/lower bounds on $\mathcal{Y}^p_c$:

$$\mathcal{Y}^p_{high}(k+1|k) = \begin{bmatrix} ((y_c)_{high}(k+1))^T & ((y_c)_{high}(k+2))^T & \cdots & ((y_c)_{high}(k+p))^T \end{bmatrix}^T \tag{4.170}$$

$$\mathcal{Y}^p_{low}(k+1|k) = \begin{bmatrix} ((y_c)_{low}(k+1))^T & ((y_c)_{low}(k+2))^T & \cdots & ((y_c)_{low}(k+p))^T \end{bmatrix}^T \tag{4.171}$$

The optimization can be solved by the standard Quadratic Programming (QP). For

details on the solution procedures, the readers are referred to Garcia & Morshedi [25] and Ricker [56].

### 4.5.4 Robust Design/Tuning

MPC controllers are equipped with many potential design/tuning parameters. The traditional tuning parameters include:

1. Prediction Horizon ($p$)
2. Number of Calculated Control Moves ($m$)
3. Output/Input Weights ($\Lambda_{y_e}$ and $\Lambda_{\Delta u}$)
4. Constraints on $\Delta u$.

With the introduction of a general state observer to MPC, we have added more of these indirect parameters such as noise covariance matrices. In spite of the abundance of tuning parameters, tuning MPC controllers is not known to be an easy task. The main reason is that none of the tuning parameters have transparent connection with closed-loop performance and robustness.

In the new framework, we recommend the following set of tuning rules:

1. Decide on the prediction horizon and number of control moves such that the resulting $\Phi - L_{MPC}\Gamma_u\Phi$ has all its eigenvalues strictly inside the unit disk. In general, we recommend that the prediction horizon, $p$, be chosen longer than the desired settling time and the number of input moves, $m$, be chosen as close to $p$ as possible (within computational limits).

2. Assuming the inputs and outputs are scaled correctly, choose $\Lambda_{y_e}$ to be an identity matrix and $\Lambda_{\Delta u}$ to be a scalar-times-identity matrix. For SISO systems or well-conditioned MIMO systems, choose the scalar for the input weight just large enough to satisfy the stability criterion. For ill-condtioned MIMO systems,

choose the scalar somewhat larger; a good method to decide on the scalar is to derive robust performance norm-bounds on $F_{IMC}$ and $I - F_{IMC}$ for each tested value of the scalar and choose the value at which the bounds start deteriorating. Further on-line adjustments may be made later.

3. For case where disturbances and measurement noise are described as integrated (or double-integrated) white noise and white noise respectively, use the parameter $F$ (or $F_a$) for the state estimator to adjust the speed of the closed-loop response. For cases of more general disturbances, use the IMC estimator described in Section 4.4.3 instead of the Kalman filter to obtain the state estimates, $\Delta\bar{x}$ and $\Delta\bar{y}_c$ for the prediction equation. The IMC filter may be designed off-line using the robust performance norm-bounds and further adjusted on-line.

We do not recommend using constraints on $\Delta u$ as tuning parameters because this makes the controller necessarily nonlinear and analysis of such a controller is very difficult. The tuning procedure outlined above should simplify the tuning for MPC controllers immensely as all the parameters are intuitive and their effects are well understood.

### 4.5.5 Relationship with Dynamic Matrix Control

The proposed MPC technique is completely equivalent to the standard Dynamic Matrix Control (DMC) technique [15] when the state estimator is designed for the following systems:

$$\begin{bmatrix} \Delta x(k) \\ \Delta d(k) \\ y_c(k) \end{bmatrix} = \begin{bmatrix} A_{11} & 0 & 0 \\ 0 & 0 & 0 \\ C_c A_{11} & I & I \end{bmatrix} \begin{bmatrix} \Delta x(k-1) \\ \Delta d(k-1) \\ y_c(k-1) \end{bmatrix} \tag{4.172}$$

$$+ \begin{bmatrix} 0 \\ I \\ 0 \end{bmatrix} \Delta d'(k-1) + \begin{bmatrix} B_u \\ 0 \\ C_c B_u \end{bmatrix} \Delta u(k-1) \tag{4.173}$$

$$\hat{y}_c(k) = \begin{bmatrix} 0 & 0 & I \end{bmatrix} \begin{bmatrix} \Delta x(k) \\ \Delta d(k) \\ y_c(k) \end{bmatrix} \tag{4.174}$$

Hence, DMC assumes that system disturbances are described through integrated white noise entering each output independently. In addition, it assumes that the measurements are noise-free. These assumptions, especially the first assumption, can lead to poor performance regardless of the choice of tuning parameters.

## 4.6 $\mu$-Synthesis

In Chapter 3, we mentioned that there exists no general method of solving the optimization problem

$$\inf_{K \in \mathcal{K}_s} \sup_{\omega} \inf_{D(\omega) \in \mathcal{D}_{rp}} \bar{\sigma} \left[ D(\omega)\, \mathcal{F}_l(G, K)|_{s=j\omega}\, D^{-1}(\omega) \right] \tag{4.175}$$

As a partial solution to the problem, Doyle [17] suggested a method called "$\mu$-Synthesis." For the sake of completeness, we review this design method and point out some of the practical barriers for the method.

### 4.6.1 Algorithm

$\mu$-Synthesis is an iterative procedure to obtain a suboptimal solution to the optimization problem (4.175). The algorithm can be summarized as follows:

**Step 1** Initialize the D-scaling by choosing a unimodular $D_0 \in \mathcal{D}_{rp}^s$ where

$$\mathcal{D}_{rp}^s = \left\{ D \in \mathcal{RH}_\infty : D^{-1} \in \mathcal{RH}_\infty, D(j\omega) \in \mathcal{D}_{rp} \forall \omega \right\} \tag{4.176}$$

Often, the identity matrix is a good choice when no information is available on how best to choose $D_0$.

**Step 2** Using the standard $H_\infty$-optimal design method (Doyle *et al.* [18]), find $K \in \mathcal{K}_s$ that minimizes

$$\sup_\omega \bar{\sigma} \left[ D_0 \mathcal{F}_\ell(G, K) D_0^{-1} \Big|_{s=j\omega} \right] \tag{4.177}$$

**Step 3** For a selected set of frequencies $W$, find $D(\omega) \in \mathcal{D}_{rp}$ that minimizes

$$\bar{\sigma} \left[ D(\omega) \left( D_0 \mathcal{F}_\ell(G, K) D_0^{-1} \right) \Big|_{s=j\omega} D^{-1}(\omega) \right] \tag{4.178}$$

**Step 4** Let $\tilde{D}(\omega) = D(\omega) * D_0(j\omega)$ for each $\omega \in W$. Then, find a new $D_0 \in \mathcal{D}_{rp}^s$ such that $D_0(j\omega) = U(\omega)\tilde{D}(\omega) \ \ \forall \omega \in W$ where $U(\omega)$ is any unitary matrix.

**Step 5** Go back to Step 2 and repeat the procedure until $\tilde{D}(\omega)$ does not change significantly from the last iteration for all $\omega \in W$.

### 4.6.2 Practical Barriers

It is important to note that (4.175) is nonconvex with respect to $(Q, D(\omega))$, and hence, the procedure does not guarantee convergence to the global minimum. However, it is the only design method available, the objective of which is to explicitly minimize the upperbound of the Structured Singular Value for robust performance. The following numerical problems can make application of this powerful design method difficult.

1. Step 2 is a very involved, iterative optimization. Our experience with the available software shows that the algorithm is unreliable for a certain class of systems.

2. Step 4 introduces error since $D$-scale is approximated only at a *finite* number of frequencies. This error can cause the algorithm to diverge.

In addition, $\mu$-Synthesis design yields a controller with no on-line tuning parameters. This implies that the design engineer must have access to an uncertainty model that is accurate quantitatively as well as qualitatively. Unfortunately, this is seldom the case for most chemical processes.

### 4.6.3 Constraint-Handling

In the presence of input constraints and mode-switching, a controller designed via $\mu$-Synthesis can show significant performance deterioration if implemented as is. For $\mu$-Synthesis controllers, there does not exist a simple anti-windup compensation scheme like the extended Kalman filtering. However, recent work by Campo [10] provided a theoretical basis for synthesizing anti-windup, bumpless transfer schemes for general multivariable controllers. The technique guarantees the recovery of the original linear performance when the input matches the controller output exactly, and aims at "quick" recovery from saturation or mode switching by minimizing the "memory" (expressed through the hankel norm) of the control system. For details, readers are referred to Campo [10].

## 4.7 Numerical Example: Heavy Oil Fractionator

In this section, we apply the proposed IMC design method to a heavy oil fractionating column. The schematic diagram of the fractionating column is shown in Figure 4.12. The control system design problem (shown in Figure 4.13) is a simplified version of that presented in *The Shell Process Control Workshop* (so called "Shell Control Problem") [54].

### 4.7.1 Problem Statement

The control problem we consider is shown in Figure 4.13. The transfer function models are given as follows:

$$G_{y_c u} = \begin{bmatrix} 4.05\frac{e^{-27s}}{50s+1} & 1.77\frac{e^{-28s}}{60s+1} \\ 5.39\frac{e^{-18s}}{50s+1} & 5.72\frac{e^{-14s}}{14s+1} \end{bmatrix} \tag{4.179}$$

$$G_{y_c d} = \begin{bmatrix} 1.20\frac{e^{-27s}}{45s+1} & 1.44\frac{e^{-27s}}{40s+1} \\ 1.52\frac{e^{-15s}}{25s+1} & 1.83\frac{e^{-15s}}{20s+1} \end{bmatrix} \tag{4.180}$$

$$G_{y_s u} = \begin{bmatrix} 3.66\frac{e^{-2s}}{9s+1} & 1.65\frac{e^{-20s}}{30s+1} \\ 5.92\frac{e^{-11s}}{12s+1} & 2.54\frac{e^{-12s}}{27s+1} \\ 4.13\frac{e^{-5s}}{8s+1} & 2.38\frac{e^{-7s}}{19s+1} \\ 4.06\frac{e^{-8s}}{13s+1} & 4.18\frac{e^{-4s}}{33s+1} \end{bmatrix} \tag{4.181}$$

$$G_{y_s d} = \begin{bmatrix} 1.16\frac{1}{11s+1} & 1.27\frac{1}{6s+1} \\ 1.73\frac{1}{5s+1} & 1.79\frac{1}{19s+1} \\ 1.31\frac{1}{2s+1} & 1.26\frac{1}{22s+1} \\ 1.19\frac{1}{19s+1} & 1.17\frac{1}{24s+1} \end{bmatrix} \tag{4.182}$$

$$\Theta = I \tag{4.183}$$

$\Theta$ represents measurement delays and it is identity in this case. We can factor out the time delays in $G_{y_c u}$ and $G_{y_c d}$ as measurement delays, $\Theta$, and consider the equivalent control problem where

$$G_{y_c u} = \begin{bmatrix} 4.05\frac{1}{50s+1} & 1.77\frac{e^{-s}}{60s+1} \\ 5.39\frac{e^{-4s}}{50s+1} & 5.72\frac{1}{14s+1} \end{bmatrix} \tag{4.184}$$

$$G_{y_c d} = \begin{bmatrix} 1.20\frac{1}{45s+1} & 1.44\frac{1}{40s+1} \\ 1.52\frac{e^{-s}}{25s+1} & 1.83\frac{e^{-s}}{20s+1} \end{bmatrix} \tag{4.185}$$

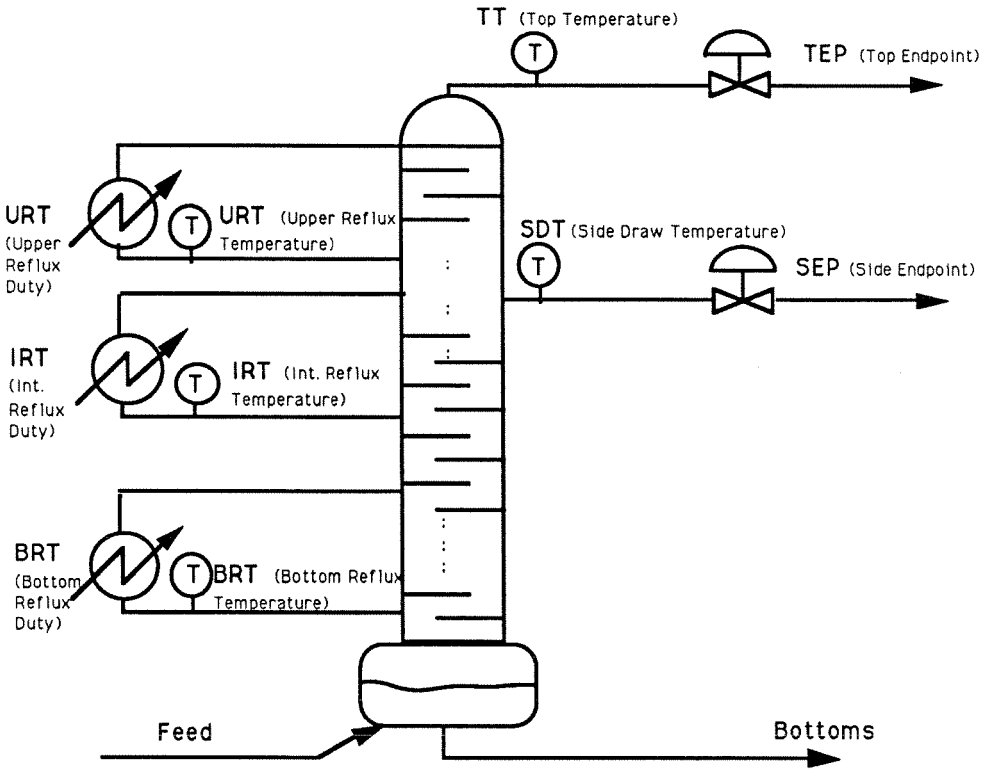


Figure 4.12. Schematic Diagram of a Heavy Oil Fractionator

$$\Theta = \begin{bmatrix} e^{-27s} & \\ & e^{-14s} \end{bmatrix} \tag{4.186}$$

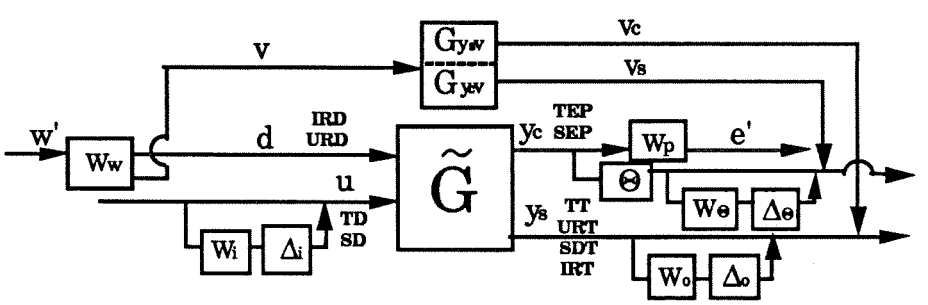


Figure 4.13. Control Problem in the Heavy Oil Fractionator

Since no specific sampling limitation was provided in the Shell Control Problem, we assume that both $\hat{y}_c$ and $\hat{y}_s$ can be measured continuously.

We consider a simple measurement noise, that affects all temperature measurements in the same manner. Furthermore, it is assumed that the measurement noise associated with the primary measurements is negligible. Hence, we choose

$$G_{\hat{y}_s v} = \begin{bmatrix} 1 \\ 1 \\ 1 \\ 1 \end{bmatrix} \quad G_{\hat{y}_c v} = \begin{bmatrix} 0 \\ 0 \end{bmatrix} \tag{4.187}$$

One physical source of such measurement error is the pressure variation in the column that often has a much stronger influence on the temperatures than the compositions. The following performance specification and noise model is used:

$$W_d = \begin{bmatrix} I & 0 & 0 \\ 0 & 0 & 0 \\ 0 & 0 & 0.25\frac{s+1}{0.25s+1} \end{bmatrix} \quad W_p = \begin{bmatrix} 0.35\frac{30s+1}{10s+0.0001} I & 0 \\ 0 & 0 \end{bmatrix} \tag{4.188}$$

Hence, we are not including any reference change and input penalty term. (4.188) requires almost no offset (attenuation of all signals by a factor of 3500) at steady-state and attenuation of all signals of frequency smaller than 0.1 rad/min. In addition, it requires that the measurement noise at frequency higher than 10 rad/min is not amplified (see Figure 4.14).

The uncertainty we consider is described in Figure 4.13. $\mathbf{\Delta_i}$,$\mathbf{\Delta_\Theta}$, and $\mathbf{\Delta_o}$ are best viewed as the uncertainty associated with actuators, primary measurements, and secondary measurements respectively. We use the following uncertainty weights:

$$W_i = W_o = 0.1\frac{2s+1}{0.1s+1} I; \quad W_\Theta = 0.1\frac{5s+1}{0.25s+1} I \tag{4.189}$$

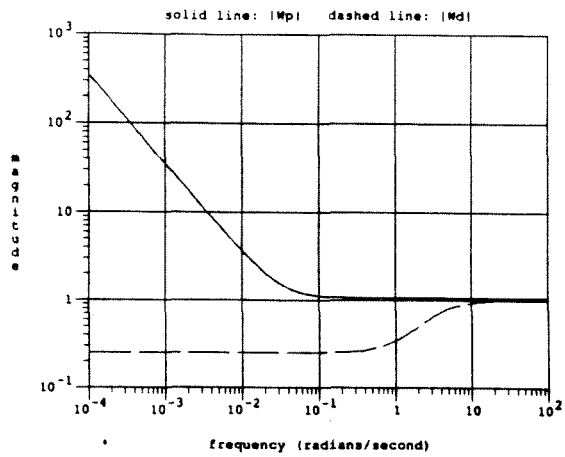


Figure 4.14. Magnitudes of Disturbance/Noise, Performance Weights

The magnitudes of $W_i, W_o$, and $W_\Theta$ are plotted in Figure 4.15. (4.189) allows 10% error in all the actuators and measurements in the low frequency region. (4.189) also allows time delay errors of approximately 1 minute in the primary measurements ($c_D$) and approximately 1/2 minute in the secondary measurements and actuators.

Our objective is to design a control system achieving robust performance.

## 4.7.2 Preliminary Analysis

Let us first check if it is possible to achieve *nominal* performance with a control system using the composition measurements alone. When the time delays are approximated by second order Padé elements, the achievable $H_\infty$-norm for nominal closed-loop performance is greater than 1, which implies that it is impossible to design a controller meeting the performance specification with composition measurements alone, even in the absence of model uncertainty. This is due to the significant delays in the measurements; we must utilize the temperature measurements, which have no deadtime

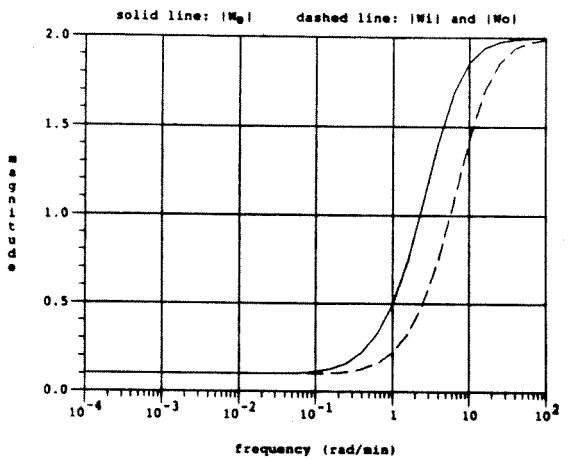


Figure 4.15. Magnitudes of Actuator/Measurement Uncertainty Weights

associated with them. There are four temperature measurements available. Since the number of the disturbances we are concerned with is only two ($IRD$ and $URD$), two measurements are sufficient for the design of an inferential controller yielding a perfect nominal performance (*i.e.*, in the absence of uncertainty and measurement noise). Hence, our objective becomes to select two temperatures among the four available ones and design a control system achieving robust performance. We have the following six possible choices for temperature-pair measurements:

$$y_m^1 = \begin{pmatrix} TT \\ URT \end{pmatrix} \quad y_m^2 = \begin{pmatrix} TT \\ SDT \end{pmatrix} \quad y_m^3 = \begin{pmatrix} TT \\ IRT \end{pmatrix}$$

$$y_m^4 = \begin{pmatrix} URT \\ SDT \end{pmatrix} \quad y_m^5 = \begin{pmatrix} URT \\ IRT \end{pmatrix} \quad y_m^6 = \begin{pmatrix} SDT \\ IRT \end{pmatrix}$$

Let us next look at the possibility of designing an output estimation based IMC controller achieving robust performance using the temperature measurements alone.

| Measurement Set | $\max_{\Delta_u \in \mathbf{\Delta_u}} \bar{\sigma}(F_{c'd'}(\Delta_u, \tilde{Q}, E))_{\omega=0}$ |
|---|---|
| $s_1$ | $3.688 \times 10^3$ |
| $s_2$ | $1.951 \times 10^3$ |
| $s_3$ | $1.993 \times 10^3$ |
| $s_4$ | $2.233 \times 10^3$ |
| $s_5$ | $7.511 \times 10^3$ |
| $s_6$ | $\approx \infty$ |

The Worst-Case Steady-State Performance with Inferential Controllers for All Measurement Sets

Since $G_{y_c u}$ is minimum-phase and square, we choose $Q_{IMC} = G_{y_c u}^{-1}$. In addition, because $G_{y_s d}$ is minimum-phase and square, the following output estimator gives perfect estimation of $y_c$ in the absence of modelling error and measurement noise:

$$\bar{y}_c = G_{y_c d} G_{y_s d}^{-1} (\hat{y}_s - G_{y_s u} u) + G_{y_c u} u \tag{4.190}$$

$$= G_{y_c d} G_{y_s d}^{-1} \hat{y}_s + \left( G_{y_c u} - G_{y_c d} G_{y_s d}^{-1} G_{y_s u} \right) u \tag{4.191}$$

Nonproper transfer functions are approximated with proper transfer functions by adding poles at a high frequency (*i.e.*, $\omega = 1000$). Table 4.1 shows the worst possible steady-state performance ($\max_{\Delta_u \in \mathbf{\Delta_u}} \bar{\sigma}(\mathcal{F}_{y_c w}(0))$). We observe that, for all measurment candidates, this is far greater than 1 due to the model uncertainty and the stringent performance specification at steady-state (*i.e.*, attenuation of all signals by a factor of 3500). Actually, the measurement set yielding the best steady-state performance ($s_2$) is only slightly better than the open-loop ( $1.951 \times 10^3$ vs. $1.060 \times 10^4$). This analysis lets us conclude that we must utilize both the composition and temperature measurements in output estimation. In the next section, we examine the viability of designing an IMC controller based on the output estimator which utilizes both the temperature and composition measurements.

### 4.7.3 Measurement Selection and Design of an Output Estimation Based IMC Controller

In this section, we examine the possibility of designing an IMC controller achieving robust performance based on an output estimator that uses the composition measurements as well as the temperature measurements. For the output estimator design, we follow the method introduced in Section 4.2.3. For the main estimator, we use the nominally "perfect" estimator of (4.190). In addition, we augment the main estimator with an auxiliary estimator, which is designed to yield the following decoupled first order response from the estimation error, $\hat{y}_c - \bar{y}_c^{sm}$, to the correction term, $\bar{y}_c^{pm}$:

$$\bar{y}_c^{pm} = \begin{bmatrix} \frac{1}{26s+1} & \\ & \frac{1}{13.37s+1} \end{bmatrix} (\hat{y}_c - \bar{y}_c^{sm}) \tag{4.192}$$

Note that time constants are chosen as $\frac{3\delta_i}{\pi}$.

Next the norm bounds on $[I - F_{IMC}(j\omega)]$ and $F_{IMC}(j\omega)$ are derived. The bounds for all six measurements are shown in Figure 4.16. We observe that the bounds for $y_m^2$ are superior to those for all other measurements. Indeed, $y_m^2$ and $y_m^3$ are the only measurement sets which yield "feasible" sets of bounds. The following simple filter satisfies one of the bounds on $\bar{\sigma}(I - F_{IMC}(j\omega))$ and $\bar{\sigma}(F_{IMC}(j\omega))$ for $y_m^2$ at every frequency (see Figure 4.17):

$$F_{IMC} = \frac{1}{1.0s+1} I \tag{4.193}$$

A diagonal first order filter $F_{IMC}$ is designed for each measurement set so that it fits the bounds (shown in Figure 4.16) as much as possible. Figure 4.18 shows the plots of the Structured Singular Values for robust performance for all measurement sets with the designed filters. The $\mu$-plot for $y_m^2$ confirms that robust performance is indeed achieved for $y_m^2$. Although $y_m^3$ also satisfies the robust performance condition, the $\mu$-plots clearly show that the performance of $y_m^2$ is superior to that for $y_m^3$ at all

frequencies.

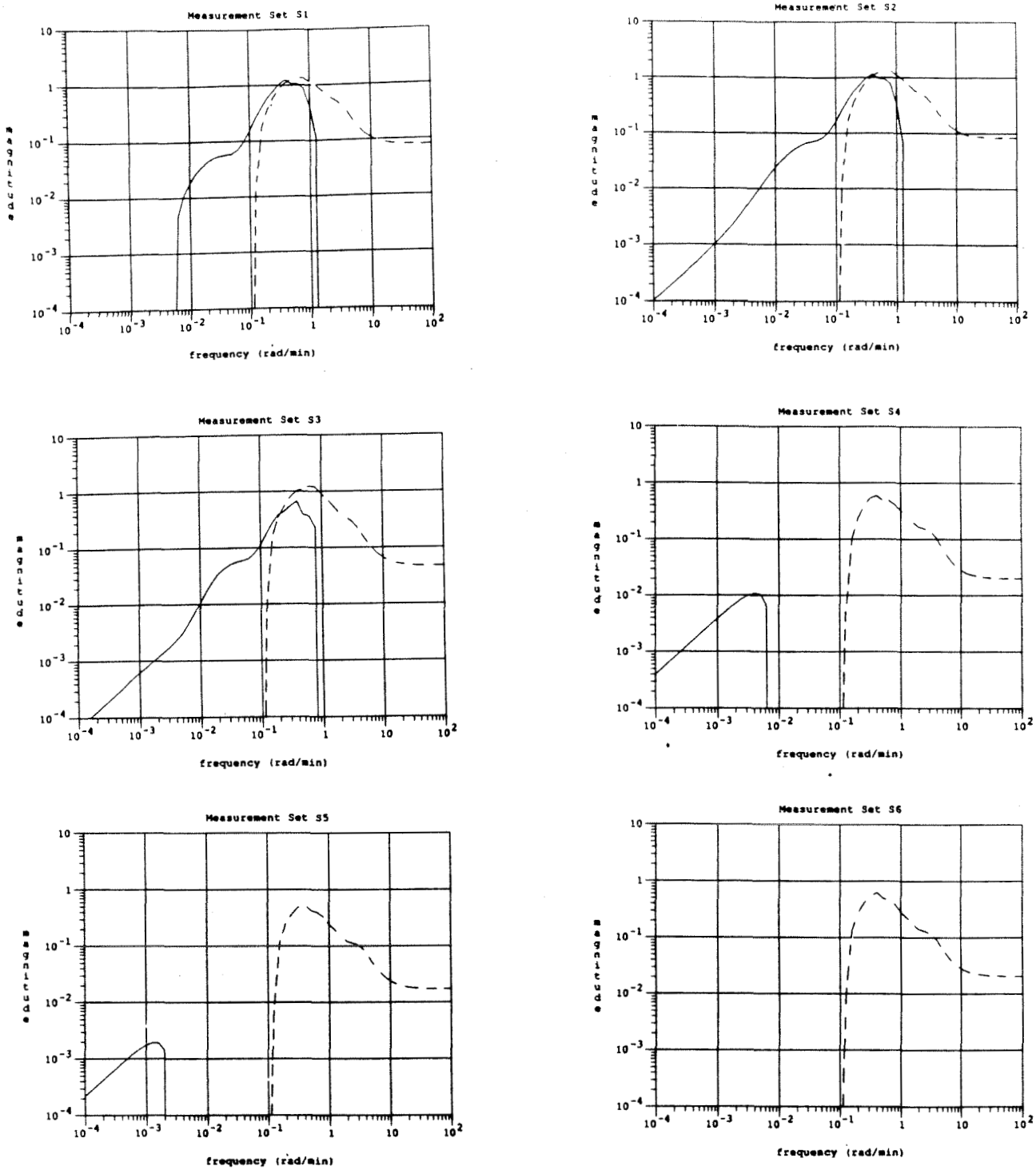


Figure 4.16. Robust Performance Bounds on $\bar{\sigma}(I - F_{IMC}(j\omega))$ and $\bar{\sigma}(F_{IMC}(j\omega))$

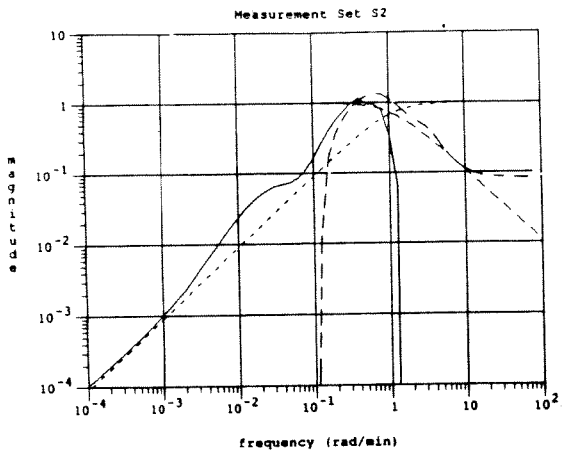


Figure 4.17. Meeting the Robust Performance Bounds for $y_m^2$ with $F_{IMC} = \frac{1}{1.0s+1} I$

# Appendix 4.A: Minimizing the Error Due to Uncontrollable Subspace

In Section 4.3.3, we state that the matrix $C_c(I - A)^{-1}B_u$ must have full row rank in order to design the LQ state feedback controller achieving the integral action. When this condition is not met, we must reduce the number of controlled variables. The optimal way (in the sense of the Frobenious norm of the matrix relating disturbances to the steady state errors) of doing this is to replace $y_e$ with $y_e^*$, that is the projection of $y_e$ into the controllable subspace $X$. The projection of $y_c$ into the space $X$ can be easily calculated by the following formula:

$$y_e^* = P_X^+ y_e = G_{y_e u}(G_{y_e u}^T G_{y_e u})^{-1} G_{y_e u}^T y_e \tag{4.194}$$

One can simply replace $\Lambda_{y_e}$ with $\Lambda_{y_e^*} = (P_X^+)^T \Lambda_{y_e} P_X^+$ in calculating the optimal feedback gain. This is equivalent to reducing the dimension of $y_e$ optimally in order to make the LQ design feasible.

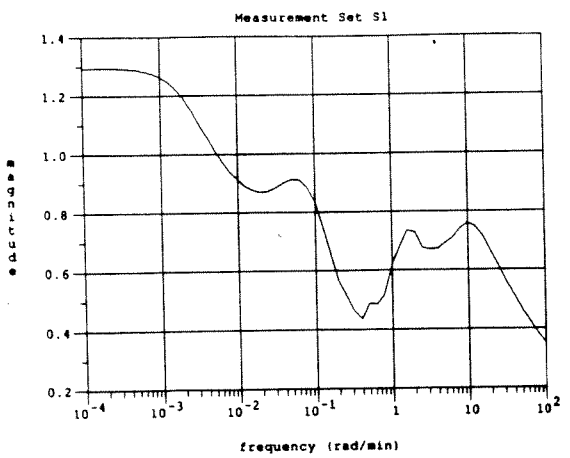


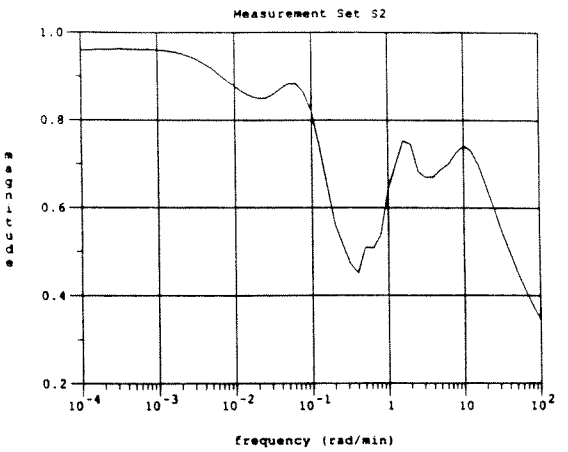


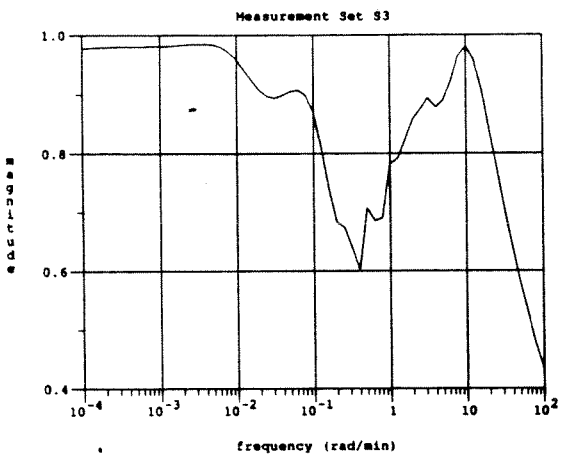


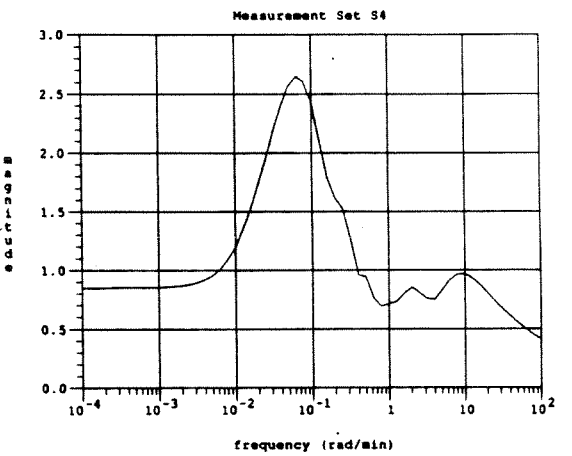


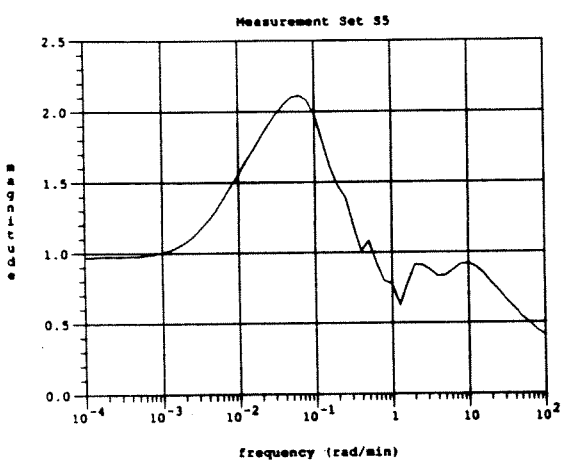


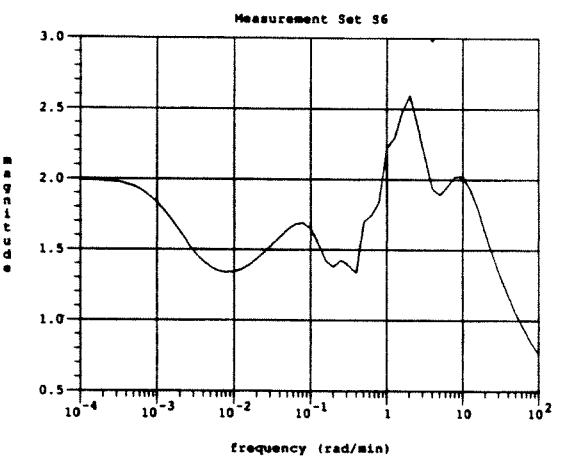


Figure 4.18. Structured Singular Values for Robust Performance

# Chapter 5

# State Estimation Based Inferential Control System Design

## 5.1 Overview

The topic of this chapter is *state estimation based* inferential control system design. In contrast to the approach taken in Chapter 4 where an independently designed output estimator and a conventional feedback controller are combined into an inferential control system, a control system that calculates the input moves directly from secondary measurements is to be designed using a first principles or empirically identified model in this chapter. Hence, for the control techniques developed in this chapter, we relax the assumption of the primary measurements' availability at a uniform, desirable sampling rate. The introduced techniques can incorporate multi-rate sampled secondary measurements as well as potentially unreliable primary measurements. When compared to the two step design approach of Chapter 4, the direct approach has the potential advantage of higher achievable performance. However, it has the disadvantage that it requires a full dynamic model relating the manipulated variables/disturbances and primary/secondary variables.

As in Chapter 4, our main objective is to devise an *inferential* control technique that can offer true "multi-variable" performance and has desirable operational characteristics like PID controllers. The operational characteristics of our main concern are flexible, intuitive on/off-line tuning and straightforward handling of constraints

and actuator/sensor failures. For sensor failures, we are particularly concerned with those of unreliable primary measurements. A desirable failure tolerance property for primary measurements may be stated as follows:

> A failure of a primary measurement does not affect the closed-loop responses of the other primary variables and the primary variables corresponding to the failed measurement maintains an "acceptable" behavior.

We will refer to this measurement failure property as "Decentralized Failure Tolerance (DFT)."

Given the formulation for measurement selection in Chapter 3, the most straightforward approach is to design the controller that minimizes the "worst-case" $H_\infty$-norm of the closed-loop system from weighted external inputs to weighted controlled outputs. As we mentioned in Chapter 4, the problem of synthesizing the controller minimizing the "worst-case" error has not been solved even for SR (or continuous-time) systems. As an alternative, we described a synthesis procedure called $\mu$-Synthesis that combines the $H_\infty$-optimal design with $\mu$-analysis in an iterative manner. However, there are several theoretical drawbacks that prevent the extension of the technique to multi-rate sampled-data systems. Some of the theoretical barriers include

1. Lack of $H_\infty$-optimal solution for general multi-rate sampled-data systems.

2. Nonapplicability of frequency-domain $\mu$-analysis to time-varying continuous-time or shift-varying discrete-time systems without resorting to approximations or conservativeness.

3. Lack of general framework to address the issue of failure tolerance to the synthesis procedure.

Although progress is made in this area [33,23], it will be awhile before these theoretical issues are resolved completely.

In addition to the theoretical barriers, there are often overlooked practical barriers for the practical application of $\mu$-Synthesis. $\mu$-Synthesis is basically an off-line design method with no on-line tuning parameters. The method requires a mathematical model of system uncertainty and choosing frequency-domain weighting functions for external inputs and outputs. When the uncertainty model and chosen weighting functions do not reflect the model/plant mismatches and performance objectives for real systems correctly, the control system can lead to less-than-acceptable performance. Since there is no way of adjusting the controller on-line, the design must be abandoned and a new design must be carried out based on a different uncertainty model and/or weighting functions. For chemical processes, most engineers have access neither to an accurate, nonconservative, uncertainty model nor to expertise required for proper selection of weighting functions without extensive trial and errors. Upon these considerations, we seek alternatives in this chapter.

We develop this chapter in a parallel fashion to Chapter 4. We first introduce a modified state space model that is suitable for designing controllers with integral action. Then, design of the optimal state estimator for a multi-rate sampled-data system under general stochastic assumptions about the external input signals is discussed. When combined with the LQ feedback regulator, this gives the $H_2$-optimal controller (as defined in Chapter 2). For systems with failure-prone primary measurements, we also discuss design of a suboptimal, cascaded state estimator that can lead to a control system with the DFT property. In order to provide a basis for simple, intuitive design and tuning for robustness, we extend the state space IMC technique presented in Chapter 4 to our inferential control problem.

Extension of the output based MPC technique introduced in Chapter 4 to multi-rate sampled-data systems is straightforward. We simply use the state estimates from either the optimal state estimator or the IMC estimator to develop prediction for future outputs. The proposed MPC technique accomplishes the goal we set out.

It incorporates the full model information and has enough degrees of freedom to give true "multi-variable" performance and robustness. Yet, the controllers have many desirable operational properties such as flexible, intuitive on-line tuning, straightforward input/output constraint handling, and tolerance to actuator/sensor failures.

The chapter concludes with an application to a high-purity distillation column. The merits of the proposed techniques during various nonideal operating modes are demonstrated as well as their performance during an ideal operating mode.

## 5.2 Linear Quadratic Gaussian (LQG)

### 5.2.1 Process Model

The following state-space difference equation can be used to describe a general linear multi-rate sampled-data system:

**Process:**

$$x(k,j) = Ax(k,j-1) + B_u u(k,j-1) + B_d d(k,j-1) \tag{5.1}$$

$$y_c(k,j) = C_c x(k,j) \tag{5.2}$$

$$y_s(k,j) = C_s x(k,j) \tag{5.3}$$

**Controlled Variables:**

$$y_e(k,j) = C_c x(k,j) - r(k,j) \tag{5.4}$$

**Measurements:**

$$\begin{bmatrix} \hat{y}_{c_{\theta_c}}(k,j) \\ \hat{y}_{s_{\theta_s}}(k,j) \end{bmatrix} = \begin{bmatrix} C_c(j)x(k,j-\theta_c) \\ C_s(j)x(k,j-\theta_s) \end{bmatrix} + \begin{bmatrix} v_c(k,j) \\ v_s(k,j) \end{bmatrix} \tag{5.5}$$

$C_c(j)$ and $C_s(j)$ are $C_c$ and $C_s$ with the elements of all rows corresponding to the measurements unavailable at $j^{\text{th}}$ sampling instant set to zeros. It is assumed that $(A, B_u)$ is a stabilizable pair and $\left(\begin{bmatrix} C_c \\ C_s \end{bmatrix}, A\right)$ is a detectable pair. $\theta_c$ and $\theta_s$ are the measurement delays (in terms of STU) of the primary and secondary measurements respectively.

By performing some simple algebraic manipulation, we can put (5.1)-(5.5) into the following standard state-space form:

$$X(k,j) = \Phi' X(k,j-1) + \Gamma_u u(k,j-1) + \Gamma_d d(k,j-1) \tag{5.6}$$

$$\hat{Y}(k,j) = \Xi(j) X(k,j) + V(k,j) \tag{5.7}$$

where

$$X(k,j) = \begin{bmatrix} x(k,j) \\ y_c(k,j) \\ y_{c_1}(k,j) \\ \vdots \\ y_{c_{\theta_c}}(k,j) \\ y_s(k,j) \\ y_{s_1}(k,j) \\ \vdots \\ y_{s_{\theta_s}}(k,j) \end{bmatrix} \quad \hat{Y}(k,j) = \begin{bmatrix} \hat{y}_{c_{\theta_c}}(k,j) \\ \hat{y}_{s_{\theta_s}}(k,j) \end{bmatrix} \quad V(k,j) = \begin{bmatrix} V_c(k,j) \\ V_s(k,j) \end{bmatrix} \tag{5.8}$$

$$\Phi' = \left[\begin{array}{c|cccccc|cccc} A & 0 & 0 & \cdots & 0 & 0 & 0 & 0 & \cdots & 0 & 0 \\ C_cA & 0 & 0 & \cdots & 0 & 0 & 0 & 0 & \cdots & 0 & 0 \\ 0 & I & 0 & \cdots & 0 & 0 & 0 & 0 & \cdots & 0 & 0 \\ 0 & 0 & I & 0 & \cdots & 0 & 0 & 0 & \cdots & 0 & 0 \\ \vdots & \vdots & \ddots & \ddots & \ddots & \vdots & \vdots & \vdots & \vdots & \vdots & \vdots \\ 0 & 0 & 0 & \cdots & I & 0 & 0 & 0 & \cdots & 0 & 0 \\ C_sA & 0 & 0 & \cdots & 0 & 0 & 0 & 0 & \cdots & 0 & 0 \\ 0 & 0 & 0 & \cdots & 0 & 0 & I & 0 & \cdots & 0 & 0 \\ 0 & 0 & 0 & \cdots & 0 & 0 & 0 & I & 0 & \cdots & 0 \\ \vdots & \vdots & \vdots & \vdots & \vdots & \vdots & \vdots & \ddots & \ddots & \ddots & \vdots \\ 0 & 0 & 0 & 0 & 0 & 0 & 0 & 0 & \cdots & I & 0 \end{array}\right] \tag{5.9}$$

$$\Gamma_u = \begin{bmatrix} B_u \\ C_cB_u \\ 0 \\ \vdots \\ \vdots \\ 0 \\ C_sB_u \\ 0 \\ \vdots \\ \vdots \\ 0 \end{bmatrix} \qquad \Gamma_d = \begin{bmatrix} B_d \\ C_cB_d \\ 0 \\ \vdots \\ \vdots \\ 0 \\ C_sB_d \\ 0 \\ \vdots \\ \vdots \\ 0 \end{bmatrix} \tag{5.10}$$

$$\Xi(j) = \begin{bmatrix} \Xi_c(j) \\ \Xi_s(j) \end{bmatrix} = \left[\begin{array}{c|ccc|ccc} 0 & 0 & 0 & \cdots & H_c(j) & 0 & 0 & \cdots & 0 \\ 0 & 0 & 0 & \cdots & 0 & 0 & 0 & \cdots & H_s(j) \end{array}\right] \tag{5.11}$$

$$H_c(j) = \begin{bmatrix} (h_1)_c(j) & & \\ & \ddots & \\ & & (h_\ell)_c(j) \end{bmatrix} \tag{5.12}$$

$$H_s(j) = \begin{bmatrix} (h_1)_s(j) & & \\ & \ddots & \\ & & (h_\ell)_s(j) \end{bmatrix} \tag{5.13}$$

$$(h_i)_c(j) = \begin{cases} 1 \text{ if } i^{\text{th}} \text{ primary measurement is available at } j^{\text{th}} \text{ sampling instant} \\ 0 \text{ otherwise} \qquad 1 \leq i \leq \dim\{y_c\} \end{cases} \tag{5.14}$$

$$(h_i)_s(j) = \begin{cases} 1 \text{ if } i^{\text{th}} \text{ secondary measurement is available at } j^{\text{th}} \text{ sampling instant} \\ 0 \text{ otherwise} \qquad 1 \leq i \leq \dim\{y_s\} \end{cases} \tag{5.15}$$

It is assumed, for convenience of notation, that all measurements are synchronized at $j = 0$ implying that $\Xi(0)$ has full row rank. For simplicity of exposition, we assume from this point on that the measurement delays $\theta_c$ and $\theta_s$ are zero. However, all results obtained in this chapter are applicable without modification to cases where these delays are not zero.

For the reasons explained in Chapter 4, it is convenient to express the model in terms of the changes in the inputs. For this purpose, we subtract the equation (5.6) at $t = (k, j-1)$ from that at $t = (k, j)$ to obtain the following modified state-space representation of the system:

$$\Delta X(k,j) = \Phi \Delta X(k,j-1) + \Gamma_u \Delta u(k,j-1) + \Gamma_d \Delta d(k,j-1) \tag{5.16}$$

$$\hat{Y}(k,j) = \Xi(j)\Delta X(k,j) + V(k,j) \tag{5.17}$$

where

$$\Delta X(k,j) = \begin{bmatrix} \Delta x(k,j) \\ y_c(k,j) \\ y_s(k,j) \end{bmatrix}$$

$$\Phi = \begin{bmatrix} A & 0 & 0 \\ C_c A & I & 0 \\ C_s A & 0 & I \end{bmatrix} \tag{5.18}$$

$\Delta$ variable represents the change in the variable from the previous sampling time (*e.g.*, $\Delta x(k,j) = x(k,j) - x(k,j-1)$).

**Theorem 5.1 : Detectability of Multi-Rate Sampled-Data System**

*The system (5.16)-(5.17) is detectable if and only if*

$$\left( \begin{bmatrix} C_c \\ C_s \end{bmatrix}, A \right) \text{ is a detectable pair.} \tag{5.19}$$

**Proof** See Appendix 5.B. ■

In addition, from Section 4.3.1, $\left( \begin{bmatrix} A & 0 \\ C_c A & I \end{bmatrix}, \begin{bmatrix} B_u \\ C_c B_u \end{bmatrix} \right)$ is a stabilizable pair if and only if $(B_u, A)$ is a stabilizable pair and $\mathrm{Ker}\{(C_c(I-A)^{-1}B_u)^T\} = \emptyset$. We are not concerned with the stabilizability of the whole system (*i.e.*, the stabilizability of $(\Phi, \Gamma_u)$) since our performance objective does not include the errors in the secondary variables. In other words, we do not require that the integrators on the states $y_s$ to be stabilized since offsets in $y_s$ do not cause any problem.

### 5.2.2 Minimization Objective

Let us consider the following inputs to the system:

$$\begin{bmatrix} \Delta d \\ \Delta r \\ \begin{bmatrix} v_c \\ v_s \end{bmatrix} \end{bmatrix}_{i\ell} = \begin{bmatrix} Q_d & & \\ & Q_r & \\ & & R \end{bmatrix} [\delta_i]_\ell \tag{5.20}$$

where $[\delta_i]_\ell$ is a unit impulse entering the $i^{\text{th}}$ channel at $t = (0, \ell)$. The objective function is as follows:

$$\sum_{\ell=0}^{N-1} \sum_{i=1}^{q} \sum_{t=(0,0)}^{\infty} \left( y_e^T(t) \Lambda_{y_e} y_e(t) + \Delta u^T(t) \Lambda_{\Delta u} \Delta u(t) \right)_{i\ell} \tag{5.21}$$

where $q = (\dim\{d\} + \dim\{r\} + \dim\{v_c\} + \dim\{v_s\})$. The subscript $(\cdot)_{i\ell}$ represents that $y_c(t)$ and $\Delta u(t)$ are those resulting from the input $[\cdot]_{i\ell}$. In the stochastic framework, the objective is interpreted as minimization of the steady-state variances of $y_e$ and $\Delta u$ (weighted through $\Lambda_{y_e}^{1/2}$ and $\Lambda_{\Delta u}^{1/2}$ respectively) when $\Delta d$ and $V$ are white noise with covariance matrices of $Q_d$ and $R$ respectively. The above objective also assumes that $\Delta r$ is a white noise; however, all techniques in this chapter can be trivially extended to more general types of reference inputs and this will be discussed in detail.

### 5.2.3 Optimal Control Design

Invoking the separation principle, the $H_2$-optimal controller is the combination of the optimal state estimator and the LQ regulator.

**Optimal Estimator: MR Kalman Filter**

The optimal estimator for the given process and disturbances is the following Kalman

filter:

$$\begin{aligned}\Delta\bar{X}(k,j) &= \Phi\Delta\bar{X}(k,j-1)+\Gamma_u\Delta u(k,j-1)\\ &+ K_G(j)[\hat{Y}(k,j)-\Xi(j)\{\Phi\Delta\bar{X}(k,j-1)+\Gamma_u\Delta u(k,j-1)\}] \quad (5.22)\end{aligned}$$

where

$$K_G(j)=\Sigma_s(j)\Xi^T(j)\{\Xi(j)\Sigma_s(j)\Xi^T(j)+R\}^{-1} \quad (5.23)$$

$\Sigma_s(j)$ represents the steady-state solution to the following periodically time varying (PTV) Riccati equation:

$$\begin{aligned}\Sigma(k,j+1) &= \Phi\Sigma(k,j)\Phi^T-\Phi\Sigma(k,j)\Xi^T(j)\{\Xi(j)\Sigma(k,j)\Xi^T(j)+R\}^{-1}\Xi(j)\Sigma(k,j)\Phi^T\\ &+ \Gamma_d Q_d\Gamma_d^T \quad (5.24)\end{aligned}$$

Because the above Riccati difference equation is PTV, its steady-state solution $\Sigma_s$ is also PTV.

**Definition 5.1 A Stabilizing Solution to PTV Riccati Equation**

*A steady-state solution to the PTV Riccati equation (5.24) is called*

1. *a "stabilizing solution" if the matrix* $\prod_{j=0}^{N-1}(\Phi-K_G(j)\Xi(j)\Phi)$ *has all its eigenvalues (called "observer eigenvalues") strictly inside the unit disk.*
2. *a "strong solution" if all the eigenvalues lie within the closed unit disk.*

There are two ways to obtain the stabilizing $\Sigma_s(j)$. One way is to convert the PTV system to a shift invariant (SI) system by changing the time scale from $\tau_S$ to $\tau_B$. This method allows us to obtain the stabilizing solution by solving an algebraic Riccati equation and is discussed in detail in Appendix 5.A.

The other way is to iterate on the PTV Riccati difference equation until $\Sigma(k+1,j)\approx\Sigma(k,j)\ \ \forall j$. The following conditions (in addition to the detectablity of

$(\Xi(j), \Phi)$ guarantee the convergence of the Riccati difference equation (5.24) to a stabilizing solution:

1. $\Sigma(0,0) \geq 0$ and $R > 0$.

2. $(\Phi, \Gamma_d Q_d^{1/2})$ is a stabilizable pair.

The former condition requires a positive semidefinite initial error covariance matrix and nonsingular measurement noise. The latter condition states that all unstable dynamics of the system should be excited through the state excitation noise $\Delta d$. If this condition is not satisfied, the obtained filter gain may lead to bias in the estimates when there are disturbances other than those modelled and/or mismatches between the model and the real system. A simple way to get around this problem is to add more disturbances that can account for modelling errors, *etc.*

The assumption of nonsingular $R$ is necessary to prevent the matrix $(\Xi(j)\Sigma(k,j)\Xi^T(j) + R)$ from becoming singular. The matrix can become singular because $\Xi(j)$ can contain rows of zeros. If the solution to the singular problem is desired, the following step has to be taken:

> "Condensate" the measurement matrix $\Xi(j)$ meaning $\Xi(j)$ is made to have full row rank by deleting all rows that contain only zero elements or, more generally, that are linearly dependent.

If we denote the "condensated" $\Xi(j)$ as $\Xi^c(j)$, the stabilizability of $(\Phi, \Gamma_d Q_d^{1/2})$ guarantees that the matrix $\left(\Xi^c(j)\Sigma(k,j)(\Xi^c(j))^T\right)$ is nonsingular.

**Optimal Compensator: LQ State Feedback**

The optimal state feedback compensator for the given objective (5.21) is as follows:

$$\Delta u(k,j) = -L_{LQ} \begin{bmatrix} \Delta x(k,j) \\ y_e(k,j) \\ y_s(k,j) \end{bmatrix} \tag{5.25}$$

$$= -L_{LQ}\left(\begin{bmatrix} \Delta x(k,j) \\ y_c(k,j) \\ y_s(k,j) \end{bmatrix} - \begin{bmatrix} 0 \\ r(k,j) \\ 0 \end{bmatrix}\right) \tag{5.26}$$

where

$$L_{LQ} = \left[\ (\Gamma_u^T \Psi_s \Gamma_u + \Lambda_{\Delta u})^{-1} \Gamma_u^T \Psi_s \Phi \ \middle|\ \mathcal{O}_{\dim\{y_s\}}\ \right] \tag{5.27}$$

$\Psi_s$ is the solution to the following algebraic Riccati equation (ARE):

$$\Psi = \tilde{\Phi}^T \Psi \tilde{\Phi} - \tilde{\Phi}^T \Psi \tilde{\Gamma}_u (\tilde{\Gamma}_u^T \Psi \tilde{\Gamma}_u + \Lambda_{\Delta u})^{-1} \tilde{\Gamma}_u^T \Psi \tilde{\Phi} + \mathrm{diag}\left[\mathcal{O}_{\dim\{x\}}, \Lambda_{y_e}\right] \tag{5.28}$$

where $\tilde{\Phi}$ is the $(\dim\{x\}+\dim\{y_c\}) \times (\dim\{x\}+\dim\{y_c\})$ subblock of $\Phi$ starting from the top-left corner. $\tilde{\Gamma}_u$ are the first $\dim\{x\} + \dim\{y_c\}$ rows of $\Gamma_u$. The ARE (5.28) does not have a stabilizing solution unless $(\tilde{\Phi}, \tilde{\Gamma}_u)$ is a stabilizable pair. The condition $\mathrm{Ker}\{(C_c(I-A)^{-1}B_u)^T\} = \emptyset$ (which is required for the stabilizability) is not satisfied if $C_c(I-A)^{-1}B_u$ does not have full row rank (for example, $\dim\{y_c\} > \dim\{u\}$). As explained in Section 4.3.3, the number of primary variables must be reduced first in this case by projecting $y_c$ onto the controllable subspace in order for the LQ design to be feasible.

The reason why we exclude the states $y_s$ from our calculation is that we are not interested in the performance of $y_s$. The computation of the optimal state feedback with these states left in will require an unnecessarily large number of manipulated variables since the stabilizability of $(\Phi, \Gamma_u)$ requires that $\left(\begin{bmatrix} C_c \\ C_s \end{bmatrix}(I-A)^{-1}B_u\right)$ has full row rank because of the additional integrators on the states $y_s$.

The above control law is valid for step reference inputs. For more general types of reference inputs, we need to use augmented states in calculating the control moves as discussed in Section 4.3.3.

**$H_2$-Optimal Controller: MR Kalman Filter + LQ State Feedback**

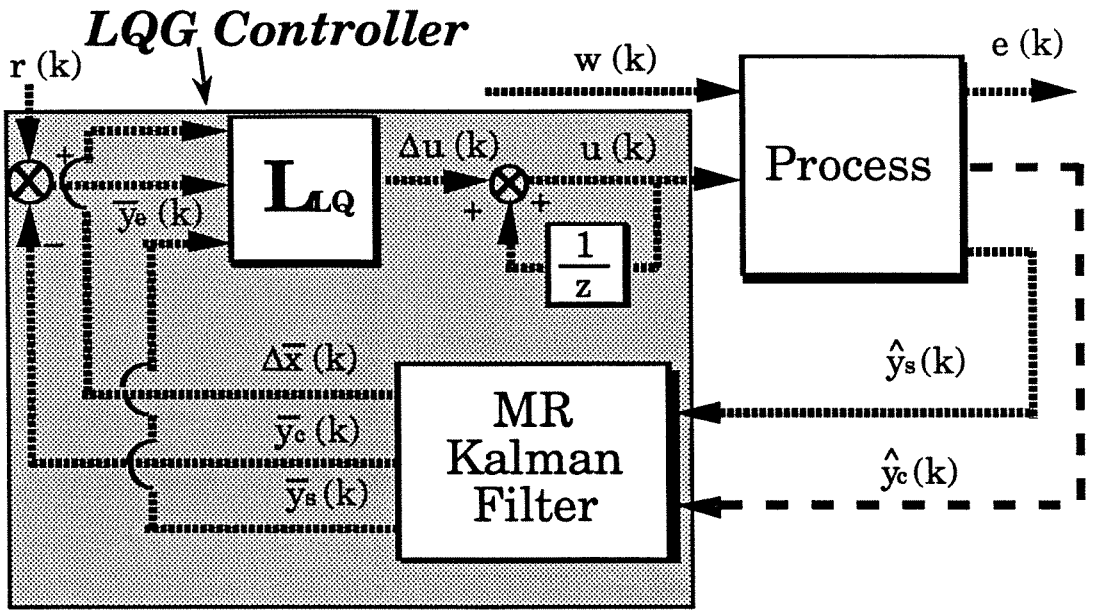


Figure 5.1. LQG Controller for MR Sampled-Data Systems

The $H_2$-optimal controller for the given problem is a combination of the MR Kalman filter and the LQ state feedback compensator written as follows:

$$\begin{aligned}\Delta\bar{X}(k,j) &= (\Phi - K_G(j)\Xi(j)\Phi - \Gamma_u L_{LQ} + K_G(j)\Xi(j)\Gamma_u L_{LQ})\Delta\bar{X}(k,j-1) \\ &- (I - K^G(j)\Xi(j))\Gamma_u L_{LQ}\Gamma_r r(k,j-1) + K_G(j)\hat{Y}(k,j) \qquad (5.29)\\ \Delta\bar{X}^e(k,j) &= \bar{X}(k,j) + \Gamma_r r(k,j) \qquad (5.30)\\ \Delta u(k,j) &= -L_{LQ}\Delta\bar{X}^e(k,j) \qquad (5.31)\end{aligned}$$

where

$$\Gamma_r = \begin{bmatrix} 0 \\ -I \\ 0 \end{bmatrix} \qquad (5.32)$$

The control system is described pictorially in Figure 5.1.

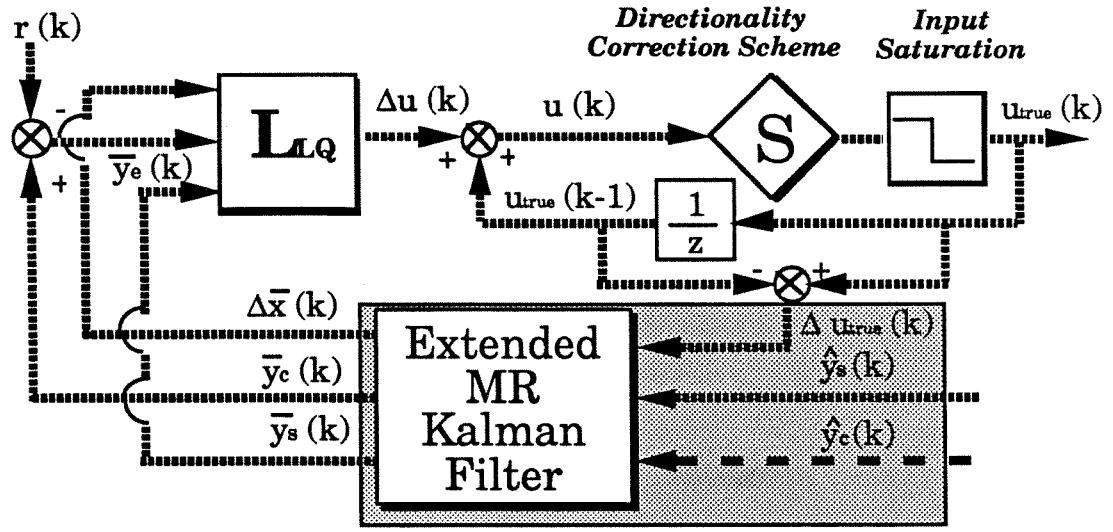


Figure 5.2. Extended MR Kalman Filter with Directionality Correction Scheme

### 5.2.4 Constraint Handling: Extended Kalman Filter

In the presence of input constraints (constraints on $u$ and $\Delta u$), the controller (5.29)-(5.31) can show significant "wind-up" as $\Delta u(k,j) \neq -L_{LQ}\Delta\bar{X}^e(k,j)$. The simplest anti-windup scheme is the Extended Kalman filter where (5.29) is replaced by

$$\begin{aligned}\Delta\bar{X}(k,j) &= (\Phi - K_G(j)\Xi(j)\Phi)\Delta\bar{X}(k,j-1) + (I - K_G(j)\Xi(j))\Gamma_u\Delta u_{true}(k,j-1) \\ &+ K_G\hat{Y}(k,j) \end{aligned} \tag{5.33}$$

and $\Delta u_{true}$ represents the "true" input to the system, which is the projection of $u_{true}(k,j-1) - L_{LQ}\Delta\bar{X}^e(k,j)$ onto the constrained input space of $u(k,j)$. For ill-conditioned MIMO systems, the directionality correction scheme discussed in Section 4.3.4 can be used in conjunction with the Extended Kalman filter. The anti-windup scheme is described pictorially in Figure 5.2.

A drawback of LQG controllers is that the output constraints (constraints on $y_c$) are handled in *ad hoc* ways (*e.g.*, mode switching). The MPC technique, discussed subsequently, addresses various types of constraints explicitly through on-line opti-

mization.

### 5.2.5 Failure Tolerance: Cascaded Kalman Filter

The MR Kalman filter is "optimal" when all the measurements are available. However, when any of the primary measurements fails, the performance can deteriorate severely and can even lead to instability. In order to incorporate the failure tolerance property (ideally, the DFT property discussed earlier), we suggest to replace the MR Kalman filter with the cascaded Kalman filter shown in Figure 5.3(b). For the design of the cascaded filter, we partition the R matrix as follows:

$$R = \begin{bmatrix} R_c & 0 \\ 0 & R_s \end{bmatrix} \tag{5.34}$$

Hence, we assume that $v_c$ and $v_s$ are uncorrelated. Not only are most measurement noises independent, but it is also impractical to model measurement noises accounting for their correlation. Therefore, almost all control problems would satisfy the assumption. The cascaded estimator is composed of two parts: the main estimator using the "reliable" secondary measurements and the auxiliary estimator using the "unreliable" primary measurements. The notation $\{\cdot\}^{sm}$ and $\{\cdot\}^{pm}$ will be used to imply that the variables or matrices under consideration are relevant to the main and auxiliary estimators respectively.

**Design of Main Estimator**

The main estimator is to be designed to depend only on the "reliable" secondary measurements. Hence, we construct the optimal state estimator for system (5.16) with the measurements

$$\hat{y}_s(k,j) = \Xi_s(j)\Delta X(k,j) + v_s(k,j) \tag{5.35}$$

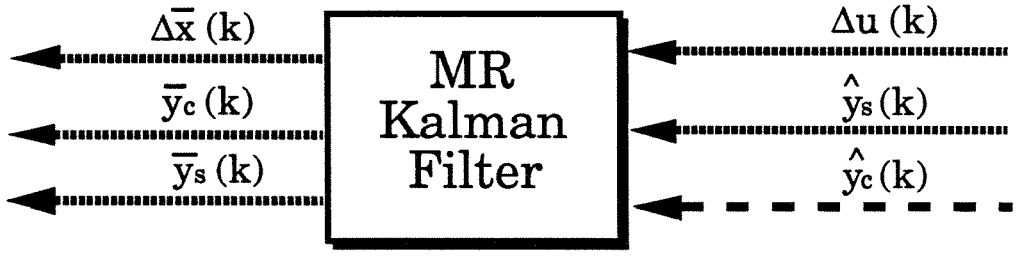


(a) Multi-Rate Kalman Filter

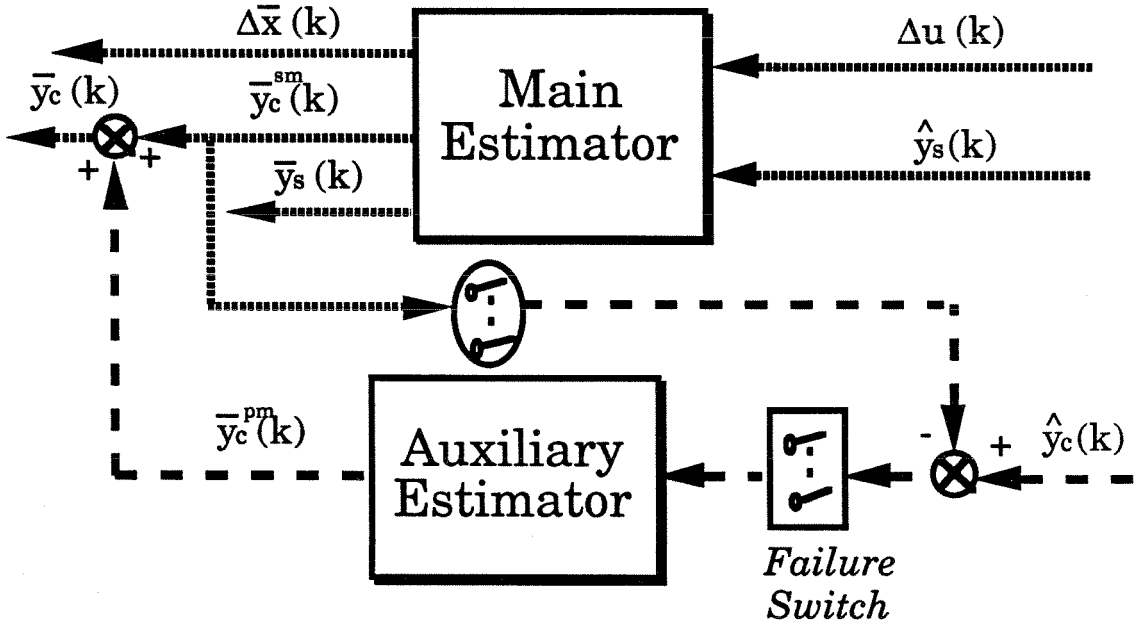


(b) Cascaded Kalman Filter

Figure 5.3. MR Kalman Filter vs. Failure-Tolerant Cascaded Kalman Filter

where $\Xi_s(j) = \begin{bmatrix} 0 & 0 & H_s(j) \end{bmatrix}$. The optimal estimator for system (5.16), (5.35) is of the form:

$$\begin{aligned} \Delta\bar{X}^{sm}(k,j) &= \Phi\Delta\bar{X}^{sm}(k,j-1) + \Gamma_u\Delta u(k,j-1) \\ &+ K_G^{sm}(j)[\hat{y}_s(k,j) - \Xi_s(j)\{\Phi\Delta\bar{X}(k,j-1) + \Gamma_u\Delta u(k,j-1)\}] \end{aligned} \tag{5.36}$$

and the optimal filter gain is given by:

$$K_G^{sm}(j) = \Sigma_s^{sm}(j)(\Xi_s)^T(j)\{\Xi_s(j)\Sigma_s^{sm}(j)(\Xi_s)^T(j) + R_s\}^{-1} \tag{5.37}$$

$\Sigma_s^{sm}(j)$ represents the steady-state solution to the following PTV Riccati equation:

$$\begin{aligned} \Sigma^{sm}(k,j+1) &= \Phi\Sigma^{sm}(k,j)\Phi^T \\ &- \Phi\Sigma^{sm}(k,j)(\Xi_s)^T(j)\{\Xi_s(j)\Sigma^{sm}(k,j)(\Xi_s)^T(j) + R_s\}^{-1}\Xi_s(j)\Sigma^{sm}(k,j)\Phi^T \\ &+ \Gamma_d Q_d \Gamma_d^T \end{aligned} \tag{5.38}$$

Note that (5.38) can be written as an algebraic Riccati equation (ARE) if all secondary variables are sampled at a uniform rate.

One difficulty is that $(\Xi_s(j), \Phi)$ is not a detectable pair. The integrators on the states $y_c$ cannot be observed through the measurements $\hat{y}_s$. However, we can still find the optimal filter gain under the following assumptions:

*Assumption 1* $(C_s, A)$ is a detectable pair.

*Assumption 2* $\mathrm{Ker}\{C_s(I-A)^{-1}B_d\} \subset \mathrm{Ker}\{C_c(I-A)^{-1}B_d\}$.

*Assumption 3* $\Sigma^{sm}(0,0) \geq 0$ and $R > 0$.

The PTV Riccati equation (5.38) under the above assumptions has the following

property:

*Property 1* $\lim_{k\to\infty} \Sigma^{sm}(k,j) \triangleq \Sigma_s^{sm}(j) = \tilde{\Sigma}_s^{sm}(j) + \begin{bmatrix} 0 & 0 & 0 \\ 0 & \Sigma_{22}^{sm} & 0 \\ 0 & 0 & 0 \end{bmatrix}$.

*Property 2* $\tilde{\Sigma}_s^{sm}(j)$ does not depend on the initial condition $\Sigma^{sm}(0,0)$.

The above results call for some clarification.

1. The first assumption is reasonable, since it is required to maintain closed-loop stability even when all the primary measurements fail.

2. The second assumption says that all disturbances ($d$) affecting the primary variables $y_c$ should be observable from the secondary measurements. Assuming all disturbances are linearly independent (*i.e.*, $Q_d$ has a full rank), this is clearly required for the convergence of the Riccati equation (5.38), since we cannot estimate $y_c$ perfectly at steady state otherwise. If $\dim\{d\} > \dim\{y_s\}$, the assumption is violated. In this case, the number of disturbances must be reduced by projecting $d$ onto the observable space; this is discussed in Appendix 5.C.

3. The second property implies that the optimal gain $K_G^{sm}(j)$ does not depend on the initial condition $\Sigma_{22}^{sm}$ since this part of $\Sigma_s^{sm}(j)$ does not show up in the expression for $K_G^{sm}$.

In addition to the three assumptions, if $\left( \begin{bmatrix} A & 0 \\ C_s A & 0 \end{bmatrix}, \begin{bmatrix} B_u \\ C_s B_u \end{bmatrix} Q_d^{1/2} \right)$ is a stabilizable pair (*i.e.*, all unstable modes are excited by disturbance), $K_G^{sm}(j)$ calculated from $\tilde{\Sigma}_s^{sm}(j)$ leads to $n$ observer eigenvalues at $(1,0)$ and the rest strictly inside the unit disk where $n$ is the dimension of $y_c$. The $n$ eigenvalues correspond to the integrators on $y_c$ that are in the unobservable subspace and cannot be moved regardless of the choice of the filter gain. Hence, $\tilde{\Sigma}_s^{sm}(j)$ is a strong solution, but not a stabilizing solution. A consequence is that, when the assumption

of $\mathrm{Ker}\{C_s(I-A)^{-1}B_d\} \subset \mathrm{Ker}\{C_c(I-A)^{-1}B_d\}$ is not satisfied, the estimate of $y_c$ will exhibit bias. In practice, the assumption is almost always not satisfied because of unknown disturbances and insufficient number of measurements. Another factor that can cause bias in the estimates is model uncertainty. An implication is that the main estimator alone will lead to steady-state offsets in practice. We overcome this problem by cascading the main estimator with an auxiliary estimator that uses the primary measurements.

**Design of Auxiliary Estimator**

The auxiliary estimator is designed for the following system:

$$\begin{bmatrix} w(k,j) \\ y_c^{pm}(k,j) \end{bmatrix} = \begin{bmatrix} A^e & 0 \\ C^e & I \end{bmatrix} \begin{bmatrix} w(k,j-1) \\ y_c^{pm}(k,j-1) \end{bmatrix} + \begin{bmatrix} B^e \\ D^e \end{bmatrix} w'(k,j) \tag{5.39}$$

$$\hat{y}_c^{pm}(k,j) \triangleq \hat{y}_c(k,j) - \Xi_c(j)\bar{X}^{sm}(k,j) \tag{5.40}$$

$$= \begin{bmatrix} 0 & H_c(j) \end{bmatrix} \begin{bmatrix} w(k,j) \\ y_c^{pm}(k,j) \end{bmatrix} + v_c(k,j) \tag{5.41}$$

where $w'(k,j)$ is a white noise with covariance matrix $Q_{w'}$. Physically, $y_c^{pm}$ represents the error between $y_c$ and the estimate of $y_c$ in the main estimator ($\bar{y}_c^{sm}$). This error may arise from various factors such as unmodelled disturbances, modelling errors, and insufficient number of measurements. Note that, in the above formulation, $\Delta y_c^{pm}$, the change in $y_c^{pm}$ from the previous sampling time, is modelled as a white noise passed through dynamics $B^e(zI-A^e)^{-1}C^e+D^e$. The optimal estimator for the above system is

$$\begin{bmatrix} \bar{w}(k,j) \\ \bar{y}_c^{pm}(k,j) \end{bmatrix} = \begin{bmatrix} A^e & 0 \\ C^e & I \end{bmatrix} \begin{bmatrix} \bar{w}(k,j-1) \\ \bar{y}_c^{pm}(k,j-1) \end{bmatrix} + K_G^{pm}(j) \left( \hat{y}_c^{pm}(k,j) - H_c(j) \begin{bmatrix} C^e & I \end{bmatrix} \begin{bmatrix} \bar{w}(k,j-1) \\ \bar{y}_c^{pm}(k,j-1) \end{bmatrix} \right) \tag{5.42}$$

$$K_G^{pm}(j) = \Sigma_s^{pm}(j)(\Xi^e)^T(j)\left\{\Xi^e(j)\Sigma_s^{pm}(j)(\Xi^e)^T(j) + R_c\right\}^{-1} \tag{5.43}$$

where

$$\Xi^e = \begin{bmatrix} 0 & H_c(j) \end{bmatrix} \tag{5.44}$$

$\Sigma_s^{pm}(j)$ is the steady-state periodic solution to the PTV Riccati equation

$$\begin{aligned} \Sigma^{pm}(k,j+1) &= \Phi^e\Sigma^{pm}(k,j)(\Phi^e)^T \\ &- \Phi^e\Sigma^{pm}(k,j)(\Xi^e)^T(j)\{\Xi^e(j)\Sigma^{pm}(k,j)(\Xi^e)^T(j) + R_c\}^{-1}\Xi^e(j)\Sigma^{pm}(k,j)(\Phi^e)^T \\ &+ \Gamma^e Q_{w'}(\Gamma^e)^T \end{aligned} \tag{5.45}$$

and

$$\Phi^e = \begin{bmatrix} A^e & 0 \\ C^e & I \end{bmatrix} \qquad \Gamma^e = \begin{bmatrix} B^e \\ D^e \end{bmatrix} \tag{5.46}$$

Partition $K_G^{sm}$ and $K_G^{pm}$ as follows:

$$K_G^{sm}(j) = \begin{bmatrix} (K_G^{sm})^x(j) \\ (K_G^{sm})^{y_c}(j) \\ (K_G^{sm})^{y_s}(j) \end{bmatrix}; \qquad K_G^{pm}(j) = \begin{bmatrix} (K_G^{pm})^w(j) \\ (K_G^{sm})^{y_c}(j) \end{bmatrix} \tag{5.47}$$

The main and auxiliary filter may be combined into a single estimator as follows:

$$\begin{aligned} \bar{X}^{cas}(k,j) &= \Phi^{cas}\bar{X}^{cas}(k,j-1) + \Gamma_u^{cas}\Delta u(k,j-1) \\ &+ K^{cas}(j)\left[\hat{Y}(k,j) - \Xi^{cas}(j)\left\{\Phi^{cas}\bar{X}^{cas}(k,j-1) - \Gamma_u^{cas}\Delta u(k,j-1)\right\}\right] \end{aligned} \tag{5.48}$$

where

$$\bar{X}^{cas} = \begin{bmatrix} \bar{X}^{sm} \\ \bar{w} \\ \bar{y}_c^{sm} + \bar{y}_c^{pm} \\ \bar{y}_s^{sm} \end{bmatrix} \tag{5.49}$$

$$\Phi^{cas} = \begin{bmatrix} A & 0 & 0 & 0 \\ 0 & A^e & 0 & 0 \\ C_c A & C^e & I & 0 \\ C_s A & 0 & 0 & I \end{bmatrix} \qquad \Gamma_u^{cas} = \begin{bmatrix} B_u \\ 0 \\ C_c B_u \\ C_s B_u \end{bmatrix} \tag{5.50}$$

$$\Xi^{cas}(j) \triangleq \begin{bmatrix} \Xi_c^{cas}(j) \\ \Xi_s^{cas}(j) \end{bmatrix} = \begin{bmatrix} 0 & 0 & H_c(j) & 0 \\ 0 & 0 & 0 & H_s(j) \end{bmatrix} \tag{5.51}$$

$$K^{cas}(j) = \begin{bmatrix} 0 \\ (K_G^{pm})^w(j) \\ (K_G^{pm})^{y_c}(j) \\ 0 \end{bmatrix} \left| \left( I - \begin{bmatrix} 0 \\ 0 \\ (K_G^{pm})^{y_c}(j) \\ 0 \end{bmatrix} \Xi_c^{cas}(j) \right) \begin{bmatrix} (K_G^{sm})^x(j) \\ 0 \\ (K_G^{sm})^{y_c}(j) \\ (K_G^{sm})^{y_s}(j) \end{bmatrix} \right. \tag{5.52}$$

The LQ feedback must be calculated for the extended system (including the states $w$) as well.

In practice, it is almost impossible to model accurately the error between the estimate of $y_c$ and the actual $y_c$. Often, the following two simple models lead to adequate results and have the advantages of not having to solve a PTV Riccati equation and yielding an auxiliary estimator equipped with a set of intuitive on-line tuning parameters:

- **Case I: Integrated White Noise Errors:**

  If we model the error between $\bar{y}_c^{sm}$ and the actual $y_c$ as random steps, the system

(5.39)-(5.41) simplifies to

$$y_c^{pm}(k,j) = y_c^{pm}(k,j-1) + w'(k,j) \tag{5.53}$$

$$\hat{y}_c^{pm}(k,j) = H_c(j)y_c^{pm}(k,j) + v_c(k,j) \tag{5.54}$$

In order to achieve a desirable failure tolerance property, we restrict our design such that the failure of one primary measurement (a component of $\hat{y}_c^{pm}$) does not affect the estimates of the other components of $y_c$. Then, if the compensator is designed to be noninteracting, we achieve the DFT property. For this purpose, we constrain the choice of $Q_{w'}$ and $R_c$ to be *diagonal* so that the resulting $K_G^{pm}$ will be diagonal as well. For diagonal $Q_{w'}$ and $R_c$, it can be shown that

$$K_G^{pm}(j) = \text{diag}[f_1(j), \cdots, f_n(j)] \tag{5.55}$$

where

$$f_i(j) = \begin{cases} f_i & \text{if } i^{\text{th}} \text{ measurement is available at } j^{\text{th}} \text{ sampling instant.} \\ 0 & \text{if } i^{\text{th}} \text{ measurement is unavailable at } j^{\text{th}} \text{ sampling instant.} \end{cases} \tag{5.56}$$

Since the $i^{\text{th}}$ element of the vector multiplying $K_G^{pm}(j)$ in (5.42) is zero whenever $f_i(j) = 0$, one can simply implement $K_G^{pm} = \text{diag}[f_i, \cdots, f_n]$. $f_i$ is a constant between 0 and 1 (see Section 4.3 of Chapter 4 for the exact relationship between $f_i$ and the signal-to-noise ratio) and can be used as on-line tuning parameters.

Defining $\bar{X} = \bar{X}^{sm} + \begin{bmatrix} 0 \\ \bar{y}_c^{pm} \\ 0 \end{bmatrix}$, straightforward algebra shows that the cascaded estimator can be put into the same structure as the MR Kalman filter (5.22)

with $K_G(j)$ replaced by $K_G^{cas}(j)$ where

$$K_G^{cas}(j) = \left[ \begin{array}{c|c} \begin{array}{c} 0 \\ K_G^{pm}(j) \\ 0 \end{array} & \left( I - \begin{array}{c} 0 \\ K_G^{pm}(j) \\ 0 \end{array} \Xi_c(j) \right) K_G^{sm}(j) \end{array} \right] \tag{5.57}$$

where $\Xi_c(j) = \left[ \begin{array}{ccc} 0 & H_c(j) & 0 \end{array} \right]$.

- **Case II: Double-Integrated White Noise Errors:**

  If we model the error between the estimate of $y_c$ ($\bar{y}_c^{sm}$) and the actual $y_c$ as random ramps (double-integrated white noise), the system (5.39)-(5.41) becomes

$$\left[ \begin{array}{c} y_c^{pm}(k,j) \\ w(k,j) \end{array} \right] = \left[ \begin{array}{cc} I & I \\ 0 & I \end{array} \right] \left[ \begin{array}{c} y_c^{pm}(k,j-1) \\ w(k,j-1) \end{array} \right] + \left[ \begin{array}{c} 0 \\ I \end{array} \right] w'(k,j) \tag{5.58}$$

$$\hat{y}_c^{pm}(k,j) = \left[ \begin{array}{cc} H_c(j) & 0 \end{array} \right] \left[ \begin{array}{c} y_c^{pm}(k,j) \\ w(k,j) \end{array} \right] + v_c(k,j) \tag{5.59}$$

  Again, to achieve the DFT property, we restrict the choice of $Q_{w'}$ and $R_c$ to be *diagonal* so that the resulting $K_G^{pm}$ be diagonal as well. For diagonal $Q_{w'}$ and $R_c$, it can be shown that

$$K_G^{pm}(j) = \text{diag}\left\{ [f_a]_1(j), \cdots, [f_a]_n(j), [f_b]_1(j), \cdots, [f_b]_n(j) \right\} \tag{5.60}$$

  where

$$[f_a]_i(j) = \begin{cases} f_i & \text{if } i^{\text{th}} \text{ measurement is available at } j^{\text{th}} \text{ sampling instant.} \\ 0 & \text{if } i^{\text{th}} \text{ measurement is unavailable at } j^{\text{th}} \text{ sampling instant.} \end{cases} \tag{5.61}$$

  and

$$[f_b]_i(j) = \frac{[f_a]_i^2(j)}{2 - [f_a]_i(j)} \tag{5.62}$$

$[f_a]_i$ is a constant between 0 and 1 (see Section 4.3 of Chapter 4 for the exact relationship between $f_i$ and the signal-to-noise ratio). As before, for implementation,

$$K_G^{pm}(j) = \text{diag}\{[f_a]_1, \cdots, [f_a]_n, [f_b]_1, \cdots, [f_b]_n\} \quad \forall j \tag{5.63}$$

$(f_a)_i$ can be used as on-line tuning parameters.

In the event of a failure of a primary measurement, the parameter auxiliary filter gain $f_i$ (or $[f_a]_i$) corresponding to the failed measurement is simply set to zero (see Figure 5.3(b)).

It can be shown easily that $K_G^{cas}(j)$ calculated from the strong solution $\Sigma_s^{sm}(j)$ and the stabilizing solution $\Sigma_s^{pm}(j)$ places all the observer poles strictly inside the unit disk. The cascaded estimator constructed under the above two models is generally suboptimal since $\hat{y}_c$ is used to update only the states $y_c$ (and $w$ for Case II) and not $\Delta x$ and $y_s$. However, this performance degradation is insignificant especially when the primary measurements are accompanied by large sampling delays since, for these cases, the primary measurements can be used only to correct for the "low frequency" errors in the estimates. Our numerical experience reveals that the cascaded estimator indeed performs almost as well as the optimal MR filter for most practical problems. On the other hand, it is preferred to the MR Kalman filter for its superior failure-tolerance property.

## 5.3 Internal Model Control (IMC)

LQG controllers for multi-rate sampled-data systems have many design/tuning parameters that must be chosen properly for good performance and robustness. These parameters are not related to the system performance and robustness in a direct, intuitive manner. This presents a great difficulty for engineers since not only are most of the parameters (such as noise covariance matrices and input weights) not readily

on-line adjustable, but it is also unclear how they should be changed in order to improve the robustness characteristics. Motivated by these considerations, we extend the state-space Internal Model Control technique (discussed in Chapter 4) to multirate sampled-data systems with secondary measurements. The technique aims at replacing the nonintuitive design/tuning parameters for LQG controllers with those that have a transparent connection with frequency response of the closed-loop system.

### 5.3.1 Minimization Objective

Let us consider the same disturbances as in (5.20), but assume that there is no measurement noise ($Q_{v_c} = Q_{v_s} = 0$). The objective is to minimize the following quadratic index:

$$\sum_{\ell=0}^{N-1}\sum_{i=1}^{q}\sum_{t=(0,0)}^{\infty}\left(y_c^T(t)\Lambda_{y_e}y_c(t) + \Delta u^T(k)\Lambda_{\Delta u}\Delta u(k)\right)_{i\ell} \tag{5.64}$$

where $q = (\dim\{d\} + \dim\{r\})$. The corresponding weights $W_w$ and $W_p$ in Chapter 2 are as follows:

$$W_w = \begin{bmatrix} \frac{z}{z-1}Q^{1/2} & & \\ & \frac{z}{z-1}Q_r^{1/2} & \\ & & 0 \end{bmatrix} \tag{5.65}$$

$$W_p = \begin{bmatrix} \frac{z-1}{z}\Lambda_{\Delta u}^{1/2} & \\ & \Lambda_{y_e}^{1/2} \end{bmatrix} \tag{5.66}$$

### 5.3.2 Detuning for Robustness

Since the controller is designed assuming no measurement noise, the resulting controller can be quite sensitive measurement noise and model uncertainty. Hence, we must detune the closed-loop in order to obtain a complementary sensitivity function that is desirable from the robustness viewpoint. Again, it is desirable from viewpoint

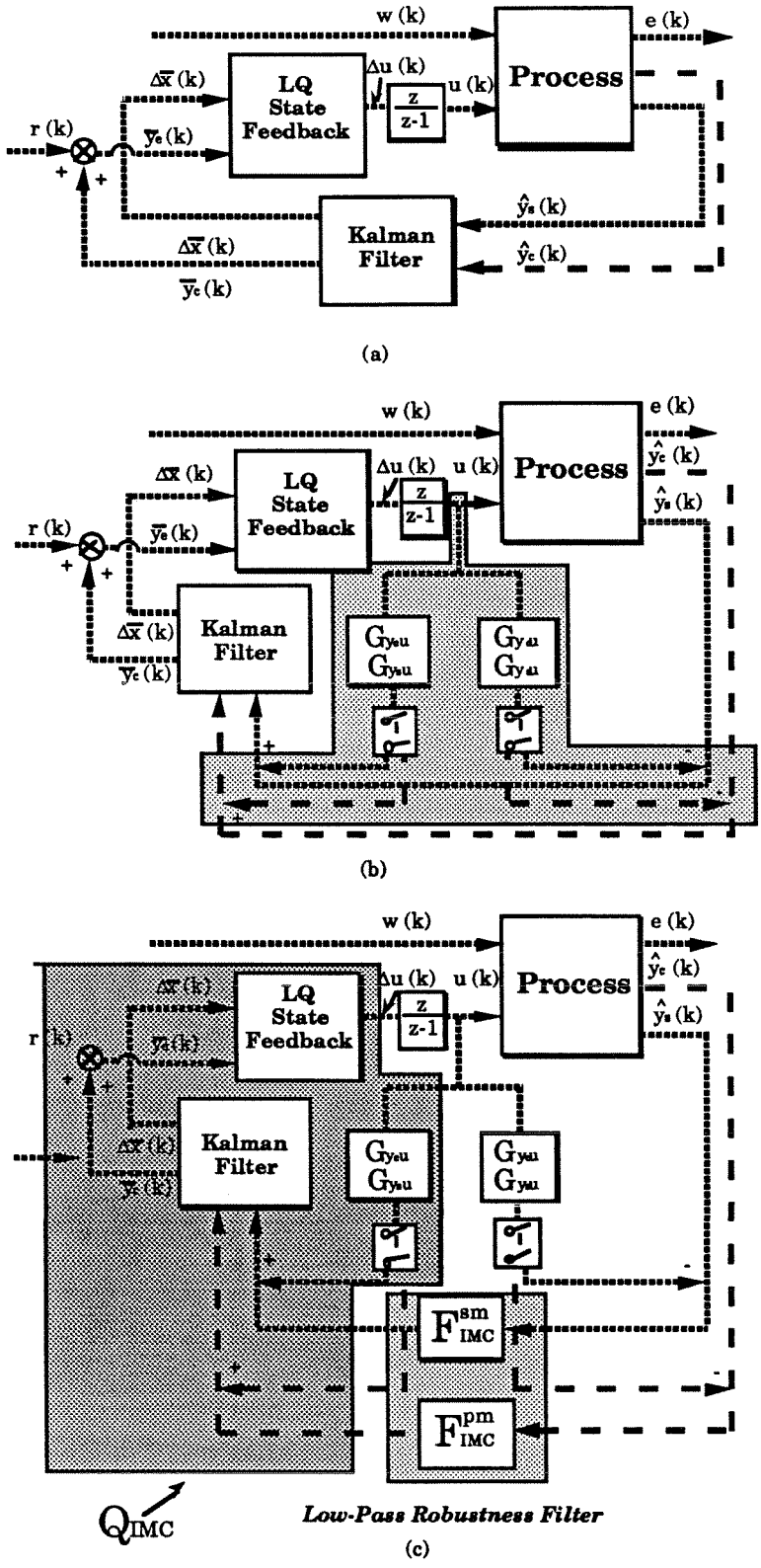


Figure 5.4. IMC Detuning for MR Systems with MR Kalman Filter

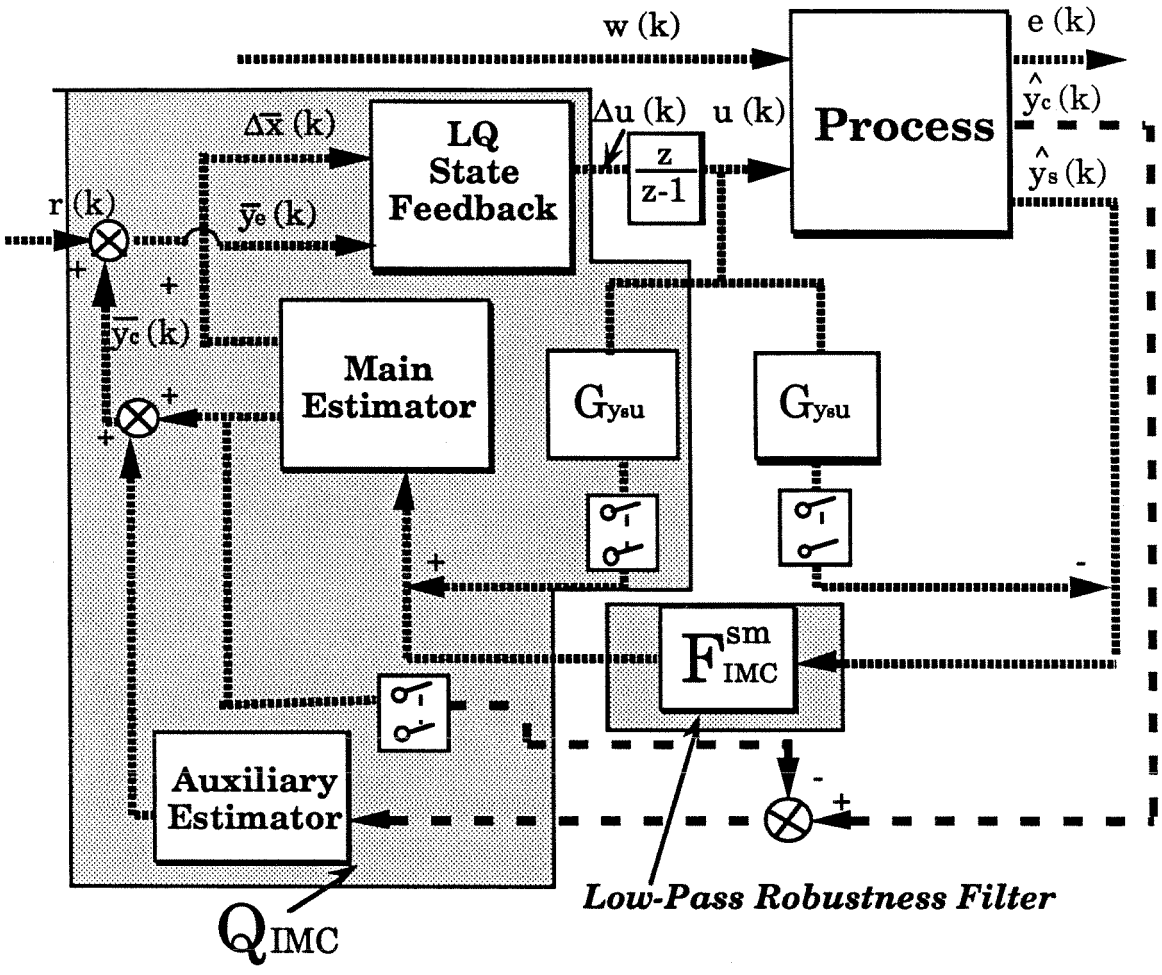


Figure 5.5. IMC Detuning for Multi-Rate Sampled-Data Systems with Cascaded Kalman Filter

of robustness to detune the complementary sensitivity function directly.

Consider the block diagram of Figure 5.4(a). It represents the closed-loop system with the LQG optimal controller. One can add and subtract the block $G_{\hat{y}_s u}$ and $G_{\hat{y}_c u}$ and obtain the diagram of Figure 5.4(b). $G_{\hat{y}_s u}$ and $G_{\hat{y}_c u}$ are operators relating the input move $u$ to the secondary and primary measurements, $\hat{y}_s$ and $\hat{y}_c$ respectively. They may not be shift-invariant operators due to the presence of the multi-rate samplers and hence transfer function representations for these operators may not exist. Note that the closed-loop operator from $[v_s^T, v_c^T]^T$ to $y_s$ is $-G_{y_s u} \circ Q_{IMC}$. Hence, $G_{y_s u} \circ Q_{IMC}$ represents the "ideal" complementary sensitivity opeator (*i.e.*,

the optimal complementary sensitivity operator in the absence of measurement noise and modelling errors) which must be detuned for robustness. A natural way of detuning is to add diagonal low-pass filter blocks $F_{IMC}^{sm}(j)$ and $F_{IMC}^{pm}(j)$ as shown in Figure 5.4(c). Each diagonal element of $F_{IMC}^{sm}(j)$ and $F_{IMC}^{pm}(j)$ is a low-pass filter that runs at the rate corresponding to the sampling time of its respective measurement. The resulting complementary sensitivity operator is $G_{y_cu} \circ Q_{IMC} \circ F_{IMC}$ where $F_{IMC} = \text{diag}\,[F_{IMC}^{sm}(j), F_{IMC}^{pm}(j)]$. Hence, $F_{IMC}$ detunes the ideal complementary sensitivity operator in a user chosen manner. The only requirement on $F_{IMC}^{sm}$ and $F_{IMC}^{pm}$ for internal stability is that they should be stable themselves.

When the cascaded Kalman filter is used instead of the MR Kalman filter, the auxiliary filter is already equipped with intuitive tuning parameters ($f_i$ or $(f_a)_i$). Hence, the IMC filter block is needed only for the secondary measurements as shown in Figure 5.5, simplifying the controller structure. Since, for most practical cases, the cascaded Kalman filter is preferred to the MR Kalman filter, we will limit our discussion to control systems with the cascaded Kalman filters from this point on.

Let us concentrate for a moment on the closed-loop characteristics of a single-rate (SR) system with secondary measurements only. Then the transfer function from $d$ to $y_c$ can be written as

$$\mathcal{F}_{y_cd} = G_{y_cd} - G_{y_cu} Q_{IMC} F_{IMC} G_{y_sd} \tag{5.67}$$

Unlike the output estimation based inferential control systems studied in Chapter 4, the transfer function $I - F_{IMC}^{sm}$ does not represent the transfer function between the open-loop and closed-loop effects of the disturbances on the controlled variables (*i.e.*, the usual sense of "sensitivity function") even for the ideal case where $Q_{IMC}$ is designed to give perfect control (*i.e.*, $Q_{IMC} = G_{y_cu}^{-1} G_{y_cd} (G_{y_sd})^{-1}$). In other words,

$$\mathcal{F}_{y_cd} \neq (I - F_{IMC}^{sm}) G_{y_cd} \tag{5.68}$$

even when $Q_{IMC}$ is designed for perfect control. A consequence is that we cannot adjust the speed of the closed-loop response for each controlled variable separately.

### 5.3.3 State Space Formula for IMC Controller

The cascasded Kalman filter with an auxiliary estimator designed for integrated white noise errors (Case I) can be written as:

$$\begin{aligned}\Delta\bar{X}(k,j) &= \Phi\Delta\bar{X}(k,j-1)+\Gamma_u\Delta u(k,j-1)\\ &+ K^{cas}_{IMC}(j)\left[\begin{bmatrix}\hat{y}_c\\ \hat{y}^f_s(k,j)\end{bmatrix}-\Xi(j)\{\Phi\Delta\bar{X}(k,j-1)+\Gamma_u\Delta u(k,j-1)\}\right]\end{aligned} \tag{5.69}$$

where

$$K^{cas}_{IMC}(j) = \left[\begin{array}{c|c} 0 & \left(I-\begin{bmatrix}0\\ K^{pm}_G(j)\\ 0\end{bmatrix}\Xi_c(j)\right)K^{sm}_{IMC}(j)\\ K^{pm}_G & \\ 0 & \end{array}\right] \tag{5.70}$$

$$K^{pm}_G(j) = \begin{bmatrix} f_1(j) & & \\ & \ddots & \\ & & f_n(j)\end{bmatrix} \tag{5.71}$$

$$K^{sm}_{IMC}(j) = \left(\Sigma^{sm*}_{IMC}(j)(\Xi^c_s(j))^T\{\Xi^c_s(j)\Sigma^{sm*}_{IMC}(j)(\Xi^c_s(j))^T\}^{-1}\right)^{uc} \tag{5.72}$$

$\Xi^c_s(j)$ represents "condensated" $\Xi_s(j)$ meaning the rows of $\Xi_s(j)$ that correspond to the measurements unavailable at $j^{\text{th}}$ sampling instant (and therefore contain only zero elements) are deleted. The operator $(\cdot)^{uc}$ implies that the matrix is "uncondensed" meaning columns of zeros are added for the measurements unavailable at $j^{\text{th}}$ sampling time. $\Sigma^{sm*}_{IMC}(j)$ represents the strong solution (*i.e.*, the solution that leads to $\prod_{j=0}^{N-1}(\Phi - K^{sm}_{IMC}(j)\Xi_s(j)\Phi)$ with all eigenvalues inside the unit disk except for the $n$

eigenvalues at $(1,0)$ corresponding to unobservable subspace) to the following PTV Riccati equation:

$$\begin{aligned}\Sigma^{sm}_{IMC}(k,j+1) &= \Phi\Sigma^{sm}_{IMC}(k,j)\Phi^T \\ &- \Phi\Sigma^{sm}_{IMC}(k,j)(\Xi^c_s(j))^T\{\Xi^c_s(j)\Sigma^{sm}_{IMC}(k,j)(\Xi^c_s(j))^T\}^{-1}\Xi^c_s(j)\Sigma^{sm}_{IMC}(k,j)\Phi^T \\ &+ \Gamma_d Q_d \Gamma_d^T \end{aligned} \tag{5.73}$$

The optimal state feedback is the same as before. The $H_2$-optimal controller for the given problem is a combination of the Kalman filter and the LQ state feedback compensator written as follows:

$$\begin{aligned}\Delta\bar{X}(k,j) &= (\Phi - K^{cas}_{IMC}(j)\Xi(j)\Phi - \Gamma_u L_{LQ} + K^{cas}_{IMC}(j)\Xi(j)\Gamma_u L_{LQ})\Delta\bar{X}(k,j-1) \\ &- (I - K^{cas}_{IMC}(j)\Xi(j))\Gamma_u L_{LQ}\Gamma_r r(k,j-1) + K^{cas}_{IMC}(j)\begin{bmatrix}\hat{y}_c(k,j)\\ \hat{y}^f_s(k,j)\end{bmatrix} \end{aligned} \tag{5.74}$$

$$\Delta\bar{X}^e(k,j) = \bar{X}(k,j) + \Gamma_r r(k,j) \tag{5.75}$$

$$\Delta u(k,j) = -L_{LQ}\Delta\bar{X}^e(k,j) \tag{5.76}$$

Next we must augment this controller with the robustness filter $F_{IMC}$. The realization of the transfer function $G_{y_c u}$ can be written as follows:

$$\begin{bmatrix}\Delta\bar{x}^u(k,j)\\ \bar{y}^u_s(k,j)\end{bmatrix} = \begin{bmatrix}A & 0\\ C_sA & I\end{bmatrix}\begin{bmatrix}\Delta\bar{x}^u(k,j-1)\\ \bar{y}^u_s(k,j-1)\end{bmatrix} + \begin{bmatrix}B_u\\ C_sB_u\end{bmatrix}\Delta u(k,j-1) \tag{5.77}$$

$$\hat{y}^u_s(k,j) = \begin{bmatrix}0 & H_s(j)\end{bmatrix}\begin{bmatrix}\Delta\bar{x}^u(k,j)\\ \bar{y}^u_s(k,j)\end{bmatrix} \tag{5.78}$$

In addition, let the realization of $F^{sm}_{IMC}$ be written as

$$\bar{x}^f(k,j) = A^f\bar{x}^f(k,j-1) + B^f(\hat{y}_s(k,j) - \bar{y}^u_s(k,j)) \tag{5.79}$$

$$y^f_{IMC}(k,j) \;=\; C^f \bar{x}^f(k,j) \tag{5.80}$$

We assumed here that all the secondary measurements are available at a uniform sampling rate of STU (*i.e.*, every $j$). With this assumption, $F^{sm}_{IMC}$ is a shift-invariant operator and $haty^u_s(k,j) = \bar{y}^u_s(k,j)$. For general multi-rate sample-data systems, $A^f, B^f, C^f$ and $D^f$ are PTV matrices.

Now, we can express $y^f_s$ as

$$\begin{aligned}
\hat{y}^f_s(k,j) &= C^f \bar{x}^f(k,j) + \bar{y}^u_s(k,j) && (5.81)\\
&= C^f \left( A^f \bar{x}^f(k,j-1) + B^f(\hat{y}_s(k,j) - \bar{y}^u_s(k,j)) \right) + \bar{y}^u_s(k,j) && (5.82)\\
&= C^f A^f \bar{x}^f(k,j-1) + (I - C^f B^f)\bar{y}^u_s(k,j) + C^f B^f \hat{y}_s(k,j) && (5.83)\\
&= C^f A^f \bar{x}^f(k,j-1) + (I - C^f B^f) H_s(j) \, (C_s A \Delta \bar{x}^u(k,j-1)\\
&+ \bar{y}^u_s(k,j-1) + C_s B_u \Delta u(k,j-1)) + C^f B^f \hat{y}_s(k,j) && (5.84)
\end{aligned}$$

The "undetuned" LQG estimator has the realization

$$\begin{aligned}
\begin{bmatrix} \Delta\bar{x}(k,j) \\ \bar{y}_c(k,j) \\ \bar{y}_s(k,j) \end{bmatrix} &= \begin{bmatrix} A & 0 & 0 \\ C_c A & I & 0 \\ C_s A & 0 & I \end{bmatrix} \begin{bmatrix} \Delta\bar{x}(k,j-1) \\ \bar{y}_c(k,j-1) \\ \bar{y}_s(k,j-1) \end{bmatrix} + \begin{bmatrix} C_c \\ C_c B_u \\ C_s B_u \end{bmatrix} \Delta u(k,j-1)\\
&+ K^{cas}_{IMC}(j) \left( \begin{bmatrix} \hat{y}_c(k,j) \\ \hat{y}^f_s(k,j) \end{bmatrix} - \Xi(j) \left\{ \begin{bmatrix} A & 0 & 0 \\ C_c A & I & 0 \\ C_s A & 0 & I \end{bmatrix} \begin{bmatrix} \Delta\bar{x}(k,j-1) \\ \bar{y}_c(k,j-1) \\ \bar{y}_s(k,j-1) \end{bmatrix} \right.\right.\\
&- \left.\left. \begin{bmatrix} B_u \\ C_c B_u \\ C_s B_u \end{bmatrix} \Delta u(k,j-1) \right\} \right) \qquad (5.85)
\end{aligned}$$

Partition $K_{IMC}^{cas}$ as follows:

$$K_{IMC}^{cas}(j) = \left[ \; (K_{IMC}^{cas})^{\hat{y}_c}(j) \;\middle|\; (K_{IMC}^{cas})^{\hat{y}_s^f}(j) \; \right] \tag{5.86}$$

Combining (5.84) and (5.85),

$$\begin{aligned}
\begin{bmatrix} \Delta\bar{x}(k,j) \\ \bar{y}_c(k,j) \\ \bar{y}_s(k,j) \end{bmatrix} &= \left( \begin{bmatrix} A & 0 & 0 \\ C_cA & I & 0 \\ C_sA & 0 & I \end{bmatrix} - K_{IMC}^{cas}(j)\Xi(j) \begin{bmatrix} A & 0 & 0 \\ C_cA & I & 0 \\ C_sA & 0 & I \end{bmatrix} \right) \begin{bmatrix} \Delta\bar{x}(k,j-1) \\ \bar{y}_c(k,j-1) \\ \bar{y}_s(k,j-1) \end{bmatrix} \\
&+ \left( \begin{bmatrix} B_u \\ C_cB_u \\ C_sB_u \end{bmatrix} - K_{IMC}^{cas}(j)\Xi(j) \begin{bmatrix} B_u \\ C_cB_u \\ C_sB_u \end{bmatrix} \right) \Delta u(k-1) \\
&+ (K_{IMC}^{cas})^{\hat{y}_c}(j)\hat{y}_c(k,j) + (K_{IMC}^{cas})^{\hat{y}_s^f}(j) \Big\{ C^f A^f \bar{x}^f(k,j-1) \\
&+ (I - C^f B^f) H_s(j) \left( C_sA\Delta\bar{x}^u(k,j-1) + \bar{y}_s^u(k,j-1) \right. \\
&+ \left. C_sB_u\Delta u(k,j-1) \right) + C^f B^f \hat{y}_s(k,j) \Big\}
\end{aligned} \tag{5.87}$$

A general state-space formula for the IMC controller can be now written as follows:

$$\Delta\bar{X}^{IMC}(k,j) = \Phi^{IMC}\Delta\bar{X}^{IMC}(k,j-1) + \Gamma_u^{IMC}\Delta u(k,j-1) + \Gamma_Y^{IMC}\hat{Y}^{IMC}(k,j) \tag{5.88}$$

$$\bar{X}^e(k,j) = \begin{bmatrix} \Delta\bar{x}(k,j) \\ \bar{y}_c(k,j) \\ 0 \end{bmatrix} + \begin{bmatrix} 0 \\ -I \\ 0 \end{bmatrix} r(k,j) \tag{5.89}$$

$$\Delta u(k,j) = -L_{LQ}\Delta\bar{X}^e(k,j) \tag{5.90}$$

where

$$\Delta\bar{X}^{IMC}(k,j) = \begin{bmatrix} \Delta\bar{x}^u(k,j) \\ \bar{y}_s^u(k,j) \\ \bar{x}^f(k,j) \\ \Delta\bar{x}(k,j) \\ \bar{y}_c(k,j) \\ \bar{y}_s(k,j) \end{bmatrix} \qquad \hat{Y}^{IMC}(k,j) = \begin{bmatrix} \hat{y}_c(k,j) \\ \hat{y}_s(k,j) \end{bmatrix} \tag{5.91}$$

$$\Phi^{IMC} = \begin{bmatrix} \begin{bmatrix} A & 0 \\ C_sA & I \end{bmatrix} & 0 & 0 \\ -B^f H_c(j) \begin{bmatrix} C_sA & I \end{bmatrix} & A^f & 0 \\ (K_{IMC}^{cas})^{\hat{y}_s^f}(j)(I - C^f B^f)H_s(j) \begin{bmatrix} C_sA & I \end{bmatrix} & (K_{IMC}^{cas})^{\hat{y}_s^f}(j)C^f A^f & 0 \\ \begin{bmatrix} A & 0 & 0 \\ C_cA & I & 0 \\ C_sA & 0 & I \end{bmatrix} - K_{IMC}^{cas}(j)\Xi(j) \begin{bmatrix} A & 0 & 0 \\ C_cA & I & 0 \\ C_sA & 0 & I \end{bmatrix} & & \end{bmatrix} \tag{5.92}$$

$$\Gamma_u^{IMC} = \begin{bmatrix} \begin{bmatrix} B_u \\ C_sB_u \end{bmatrix} \\ -B^f C_s B_u \\ \begin{bmatrix} B_u \\ C_cB_u \\ C_sB_u \end{bmatrix} - (K_{IMC}^{cas})^{\hat{y}_s^f}(j)H_s(j)C^f B^f C_s B_u - (K_{IMC}^{cas})^{\hat{y}_c}(j)H_c(j)C_c B_u \end{bmatrix} \tag{5.93}$$

$$\Gamma_Y^{IMC} = \left[\begin{array}{c|c} \begin{bmatrix} 0 \\ 0 \end{bmatrix} & \begin{bmatrix} 0 \\ 0 \end{bmatrix} \\ 0 & B^f \\ (K_{IMC}^{cas})^{\hat{y}_c}(j) & (K_{IMC}^{cas})^{\hat{y}_s^f}(j) C^f B^f \end{array}\right] \tag{5.94}$$

Even though the above formula is useful for analysis purpose, it is computationally advantageous to implement the above estimator sequentially because of the block-triangular structure of the matrix $\Phi^{IMC}$.

### 5.3.4 Constraint Handling

For input constraints, the idea of extended Kalman filtering can be applied to the IMC estimator straightforwardly. Hence, in the presence of input constraints or mode switching, the IMC estimator of (5.88) can be replaced by the following estimator:

$$\Delta\bar{X}^{IMC}(k,j) = \Phi^{IMC}\Delta\bar{X}^{IMC}(k,j-1) + \Gamma_u^{IMC}\Delta u_{true}(k,j-1) + \Gamma_Y^{IMC}\hat{Y}^{IMC}(k,j) \tag{5.95}$$

where $\Delta u_{true}$ is the "true" input to the process. This anti-windup mechanism is different from the traditional IMC anti-windup method, which is known to cause sluggish recovery from saturation when the process contains dynamics that are slow relative to the closed-loop bandwidth [10]. The proposed anti-windup scheme removes this problem since, unlike in the traditional scheme, all the controller states are correctly updated (see Section 4.4 of Chapter 4 for detail).

When an ill-conditioned MIMO system is subjected to input constraints, the directional correction scheme proposed in Section 4.3.4 can be used. All the output constraints must be handled through *ad hoc* ways such as mode-switching.

### 5.3.5 Robust Design/Tuning Rules

In summary of the foregoing discussion, we propose the following design/tuning rules for IMC controllers:

1. As mentioned before, a nonzero input weight can reduce the directional sensitivity of the LQ controller for an ill-conditioned system. Hence, the input weight $\Lambda_{\Delta u}$ (chosen as a constant-times-identity matrix for simplicity) is gradually increased until the resulting robust performance norm-bounds on $F_{IMC}^{sm}$ and $I - F_{IMC}^{sm}$ (that can be derived using the method discussed in Chapter 4) start deteriorating.

2. The robust performance normbounds on $F_{IMC}^{sm}$ and $I - F_{IMC}^{sm}$ are used to design $F_{IMC}^{sm}$ satisfying robust performance, if possible. Otherwise, a more elaborate design such as $\mu$-Synthesis may be necessary.

3. Equipping the $F_{IMC}$ with on-line tuning parameters that directly affect the speed of the closed-loop response (*e.g.*, pole locations) can add further flexibility of the control system. Furthermore, the parameters $f_i(j)$ of the auxiliary estimator can be adjusted on-line to influence the effect of primary measurements on the closed-loop response.

## 5.4 Model Predictive Control (MPC)

In this section, we develop an inferential MPC technique for multi-rate sampled-data systems.

### 5.4.1 Minimization Objective

Consider the same disturbances as in (5.20). The minimization objective of MPC is based on the finite moving time horizon: Minimize at each $t = (k, j)$ the function

$$\sum_{\ell=0}^{N-1} \sum_{i=1}^{q} \sum_{t=(k,j)}^{(k,j+p)} \left( y_c^T(t) \Lambda_{y_e} y_c(t) + \Delta u^T(t) \Lambda_{\Delta u} \Delta u(t) \right)_{i\ell} \tag{5.96}$$

$p$ is called "prediction horizon," and often used as a tuning parameter. The main motivation for adopting the finite-moving-horizon-based objective function is that the on-line constrained optimization can be performed to calculate the best controller moves in the presence of input/output constraints. This is discussed in Section 5.4.3.

### 5.4.2 Optimal Control Design

The separation principle still applies for the MPC in the absence of constraints. Hence, we can design the state estimator and the compensator separately and combine them to obtain the optimal control system.

**Optimal Estimator: MR Kalman Filter**

Since disturbances to the system have not changed, the optimal estimator remains the same as before: the MR Kalman filter of (5.22).

**Optimal Compensator: MPC State Feedback**

To obtain the optimal state feedback for the objective (5.96), we develop the following prediction equation (note that it is optimal to set $\Delta d(k, q) = 0$ for $q \geq j$):

$$\bar{\mathcal{Y}}_e^p(k, j+1|k, j) = \bar{\mathcal{Y}}_c^p(k, j+1|k, j) - \mathcal{R}^p(k, j+1|k, j) \tag{5.97}$$

$$\bar{\mathcal{Y}}_c^p(k, j+1|k, j) = \mathcal{S}^x \Delta x(k, j) + \mathcal{I}^p y_c(k, j) + \mathcal{S}^{\mathcal{U}} \Delta \mathcal{U}^m(k, j) \tag{5.98}$$

where

$$\bar{\mathcal{Y}}_e^p(k,j+1|k,j) = \begin{bmatrix} \bar{y}_e(k,j+1|k,j) \\ \bar{y}_e(k,j+2|k,j) \\ \vdots \\ \bar{y}_e(k,j+p|k,j) \end{bmatrix} \quad \bar{\mathcal{Y}}_c^p(k+1,j|k,j) = \begin{bmatrix} \bar{y}_c(k,j+1|k,j) \\ \bar{y}_c(k,j+2|k,j) \\ \vdots \\ \bar{y}_c(k,j+p|k,j) \end{bmatrix}$$

$$\Delta\mathcal{U}^m(k,j) = \begin{bmatrix} \Delta u(k,j) \\ \Delta u(k,j+1) \\ \vdots \\ \Delta u(k,j+m-1) \end{bmatrix} \quad \mathcal{R}^p(k,j+1|k,j) = \begin{bmatrix} r(k,j+1|k,j) \\ r(k,j+2|k,j) \\ \vdots \\ r(k,j+p|k,j) \end{bmatrix}$$

$$\mathcal{I}^p = \begin{bmatrix} I_{\dim\{y_c\}} \\ I_{\dim\{y_c\}} \\ \vdots \\ I_{\dim\{y_c\}} \end{bmatrix} \quad \mathcal{S}^x = \begin{bmatrix} C_cA \\ C_cA^2 + C_cA \\ \vdots \\ \sum_{j=1}^{p} C_cA^j \end{bmatrix}$$

$$\mathcal{S}^{\mathcal{U}} = \begin{bmatrix} C_cB_u & 0 & \cdots & 0 \\ C_cAB_u + C_cB_u & C_cB_u & \cdots & 0 \\ \vdots & \vdots & \ddots & \vdots \\ \sum_{j=1}^{p} C_cA^{j-1}B_u & \sum_{j=1}^{p-1} C_cA^{j-1}B_u & \cdots & \sum_{j=1}^{p-m+1} C_cA^{j-1}B_u \end{bmatrix} \tag{5.99}$$

$\bar{y}_e(k,j+1|k,j)$ represents the prediction of $y_e(k,j+q)$ based on the measurements at $t=(k,j)$. We incorporated the flexibility of specifying the number of input moves, $m$, differently from the output prediction horizon $p$ (*i.e.*, $1 \leq m \leq p$). If the reference vector $r(k,j)$ is either a step function or is best assumed as a step function (because no information on the future reference changes is available), $\mathcal{R}^p(k,j+p|k,j) = r(k,j)\mathcal{I}^p$. However, through $\mathcal{R}^p(k,j+1|k,j)$, MPC cannot only handle more general types of reference inputs but can also incorporate information on future reference changes

*without* increasing the system order.

The problem of minimizing the objective function (5.96) with the constraint posed by the prediction equation (5.97) can be formulated as a least-square problem and the optimal state feedback law turns out to be as follows:

$$\Delta u(k,j) = -L_{MPC} \begin{bmatrix} \Delta x(k,j) \\ y_c(k,j) \end{bmatrix} + K_{MPC}\mathcal{R}^p(k,j+1|k,j) \tag{5.100}$$

where

$$L_{MPC} = -K_{MPC} \begin{bmatrix} \mathcal{S}^x & \mathcal{I}^p \end{bmatrix} \tag{5.101}$$

$$K_{MPC} = \begin{bmatrix} I & 0 & \cdots & 0 \end{bmatrix} \left((\mathcal{S}^{\mathcal{U}})^T \tilde{\Lambda}_{y_c}^T \tilde{\Lambda}_{y_e} \mathcal{S}^{\mathcal{U}} + \tilde{\Lambda}_{\Delta u}^T \tilde{\Lambda}_{\Delta u}\right)^{-1} (\mathcal{S}^{\mathcal{U}})^T \tilde{\Lambda}_{y_c}^T \tilde{\Lambda}_{y_e} \tag{5.102}$$

where $\tilde{\Lambda}_{y_e} = \text{diag}(\overbrace{\Lambda_{y_e}, \cdots, \Lambda_{y_e}}^{p})$ and $\tilde{\Lambda}_{\Delta u}$ is defined in the same way. The compensator is stable if and only if all eigenvalues of $(\Phi - \Gamma_{\Delta u} L_{MPC})$ lie inside the unit disk. Assuming the reference vector is a step function (*i.e.*, $\mathcal{R}^p(k,j+p|k,j) = r(k,j)\mathcal{I}^p$),

$$\Delta u(k,j) = -L_{MPC} \left\{ \begin{bmatrix} \Delta x(k,j) \\ y_c(k,j) \end{bmatrix} - \begin{bmatrix} 0 \\ r(k,j) \end{bmatrix} \right\} \tag{5.103}$$

This is the same control law as the LQ regulator except that $L_{LQ}$ replaced by $L_{MPC}$. By definition, $L_{MPC} \to L_{LQ}$ as $p, q \to \infty$ for nonsingular $\Gamma_{\Delta u}$. For singular $\Gamma_{\Delta u}$, $L_{MPC}$ can give an unstable control law for nonminimum-phase system even when $p, q \to \infty$. The control system is pictorially described in Figure 5.6.

### 5.4.3 Constraint Handling: On-Line Quadratic Programming

The main advantage of MPC is that constraints can be incorporated directly into the controller formulation. In the presence of the constraints described through (2.70)-(2.72), the MPC state feedback is replaced by an on-line optimizer that calculates

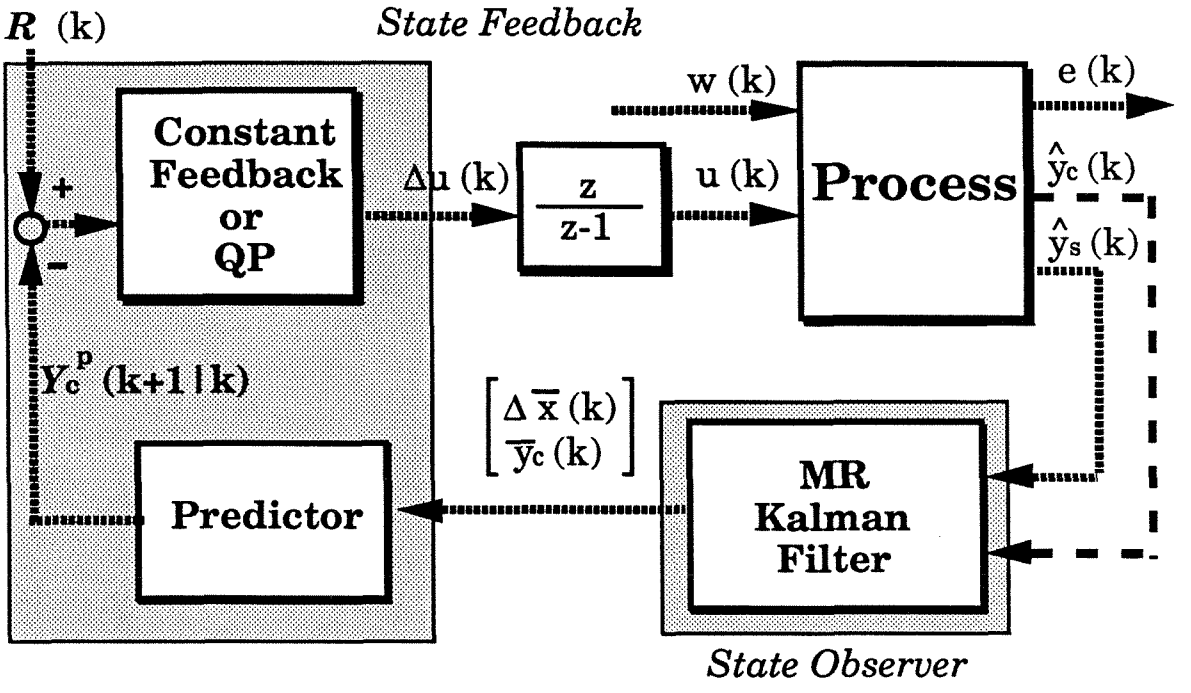


Figure 5.6. State Estimation Based Model Predictive Control for Multi-Rate Sampled-Data Systems

at every $t = (k, j)$ the optimal control moves (not violating the given constraints) within the prediction horizon and implements the first move. The optimization can be written as follows:

$$\min_{\Delta\mathcal{U}(k,j)} \left\{ \sum_{\ell=0}^{N-1} \sum_{i=1}^{d'} \sum_{t=(k,j)}^{(k,j+p)} \left( y_c^T(t) \Lambda_{y_c} y_c(t) + \Delta u^T(t) \Lambda_{\Delta u} \Delta u(t) \right)_{i\ell} \right\} \tag{5.104}$$

such that

$$u_{low}(k, j+q) \leq u(k, j+q) \leq u_{high}(k, j+q) \quad 0 \leq q \leq m-1 \tag{5.105}$$

$$|\Delta u(k, j+q)| \leq \Delta u_{max}(k, j+q) \quad 0 \leq q \leq m-1 \tag{5.106}$$

$$(y_c)_{low}(k, j+q) \leq y_c(k, j+q) \leq (y_c)_{high}(k, j+q) \quad 0 \leq q \leq p \tag{5.107}$$

Of course, if $m \leq p-1$, then we constrain $\Delta u(k, j+q)$ to be zero for $m \leq j \leq p-1$. The optimization can be solved by the standard Quadratic Programming (QP). For details, see Section 4.5.3 of Chapter 4.

### 5.4.4 Failure Tolerance: Cascaded Kalman Filter

To account for unreliable primary measurements, we recommend replacing the optimal MR Kalman filter with the cascaded Kalman filter discussed in section 5.2.5. DFT property is achieved if the MPC state feedback is designed to be completely noninteracting (*i.e.*, the estimate of one primary variable does not affect the other primary variables through control action). In practice, complete DFT property will not be achieved since the presence of the constraints, weights on $\Delta u$, and model/plant mismatch will prevent the MPC compensator from being a completely decoupling compensator. Nevertheless, the cascaded estimator should provide an acceptable failure tolerance property for most practical cases.

### 5.4.5 Robust Design/Tuning

Traditionally, the MPC controllers are tuned with nonintuitive parameters including

1. Prediction Horizon ($p$)
2. Number of Calculated Control Moves ($m$)
3. Output/Input Weights ($\Lambda_{y_e}$ and $\Lambda_{\Delta u}$)
4. Constraints on $\Delta u$

Introduction of a general state observer (*e.g.*, MR Kalman filter) to MPC gives rise to additional indirect robustness tuning parameters including

1. Disturbance Covariance Matrix ($Q_d$)
2. Measurement Noise Covariance Matrix ($R$)

Tuning MPC controllers with the above parameters is a difficult task since none of them have a transparent connection with closed-loop performance and robustness.

Hence, we recommend the following set of tuning rules:

1. Decide on the prediction horizon and number of control moves such that the resulting $\Phi - L_{MPC}\Gamma_u\Phi$ has all its eigenvaules strictly inside the unit disk. In general, we recommend that the prediction horizon be chosen longer than the desired setting time and the number of input moves be chosen as close to the prediction horizon as possible (within computational limit).

2. Choose $\Lambda_{y_e}$ to be an identity matrix and $\Lambda_{\Delta u}$ to be a scalar-times-identity matrix, assuming that the inputs and outputs are scaled correctly. For SISO systems or well-conditioned MIMO systems, choose the input weight to be as small as possible without violating the stability criterion. For ill-condtioned MIMO systems, use a nontrivial scalar for the input weight. A good method to decide on the scalar is to derive the robust performance norm-bounds on $F_{IMC}$ and $I - F_{IMC}$ for each tested value of the scalar and choose the value at which the bounds start deteriorating. Further on-line adjustments may be made later.

3. Use the IMC estimator described in Section 5.3.3 instead of the Kalman filter to obtain the state estimates, $\Delta\bar{x}$ and $\Delta\bar{y}_c$, for the prediction equation. The IMC filter $F^{sm}_{IMC}$ may be designed off-line using the robust performance norm-bounds and further adjusted on-line. For the auxiliary estimator, use the parameters ($f_i$, or $(f_a)_i$) of the filter gain for on-line adjustments.

We do not recommend using constraints on $\Delta u$ as tuning parameters because this makes the controller nonlinear and analysis of such a controller is very difficult. The tuning procedure outlined above should simplify the tuning for MPC controllers immensely as the IMC filter has a direct connection with the frequency-domain characteristics of the complementary sensitivity function.

## 5.5 Numerical Example: High-Purity Distillation Column

We consider the high-purity distillation column shown in Figure 5.7(a). The column is similar to the one described in Appendix A of Morari & Zafiriou [50].

### 5.5.1 Description of Control Problems

The control problem we consider is shown in Figure 5.7(b).

- *Controlled Variables*

  The controlled variables are the bottom and the distillate compositions (denoted by $x_B$ and $y_D$ respectively).

- *Disturbances*

  The main disturbances we consider are the variations in the flowrate ($F$) and the composition ($z_F$).

- *Manipulated Variables*

  The manipulated variables are the reflux flowrate ($L$) and the boil-up ($V$). It is assumed that the responses of the level loops for condensers and reboilers are immediate.

- *Measurements*

  Although the measurement selection is an issue of great importance, we do not treat this problem in this example. Instead, it is assumed that the temperatures of Tray # 10 and Tray # 32 are measured. These locations were selected, based on a compromise between signal-to-noise ratio and sensitivity to uncertainty [41]. Both temperatures are assumed to be measured at one minute intervals. To demonstrate the effect of the sampling rates and delays of the primary measurements on the relative performance and failure tolerance properties of the proposed estimators, we consider the following two cases:

- **Case A: "Fast," Unreliable Primary Measurements**

  The composition measurements ($x_B$ and $y_D$) are available at every one minute with delays of one minute.

- **Case B: "Slow," Unreliable Primary Measurements**

  The composition measurements ($x_B$ and $y_D$) are available at every ten minutes with delays of ten minutes.

- *Model*

We use a 10 state model obtained by performing a model reduction (via balanced realization) on a 41 state full material balance model.

- *Design Parameters*

The following state disturbance covariance matrices and measurement noise covariance matrices were used for the filter designs:

$$Q_d = \begin{bmatrix} 0.001 & 0 \\ 0 & 0.001 \end{bmatrix} \tag{5.108}$$

$$R_c = \begin{bmatrix} 0.000001 & 0 \\ 0 & 0.000001 \end{bmatrix} \qquad R_s = \begin{bmatrix} .01 & 0 \\ 0 & .01 \end{bmatrix} \tag{5.109}$$

$$\Gamma = \begin{bmatrix} 1.0 & 0 \\ 0 & 1.0 \end{bmatrix} \qquad \Lambda = \begin{bmatrix} 0.1 & 0 \\ 0 & 0.1 \end{bmatrix} \tag{5.110}$$

For the auxiliary estimator of the cascaded Kalman filter, the signal-to-noise ratio of identity was assumed. The output horizon $p$ and the input horizon $q$ were chosen to be 30 and 10 respectively. The only constraints we imposed were that $|L| \leq 1.0$ and $|V| \leq 1.0$ at all times.

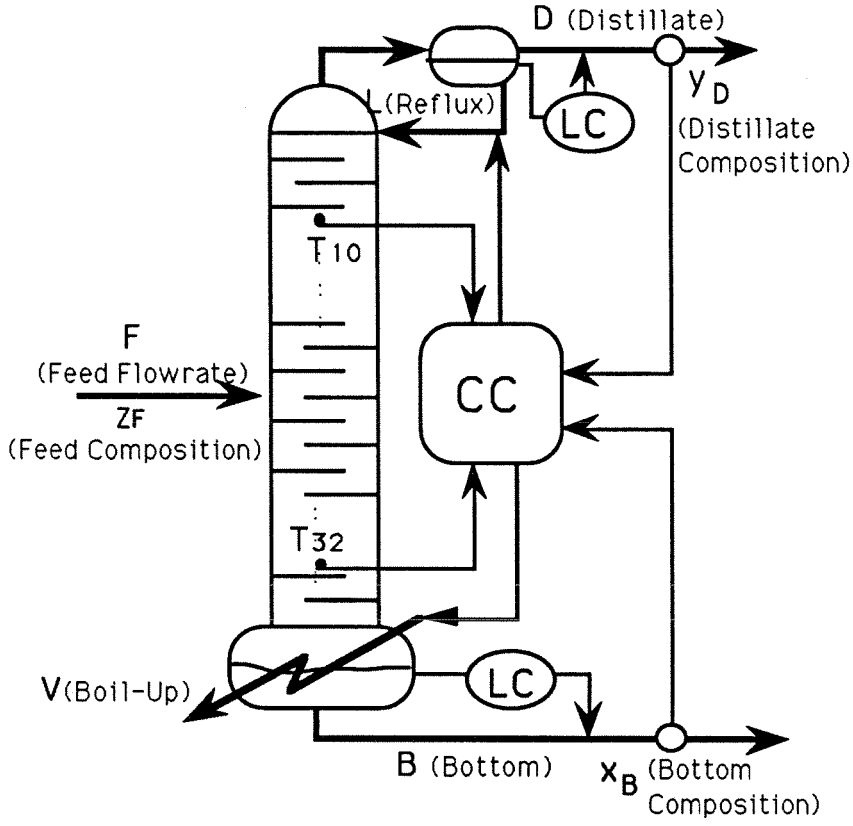


(a) LV High-Purity Column

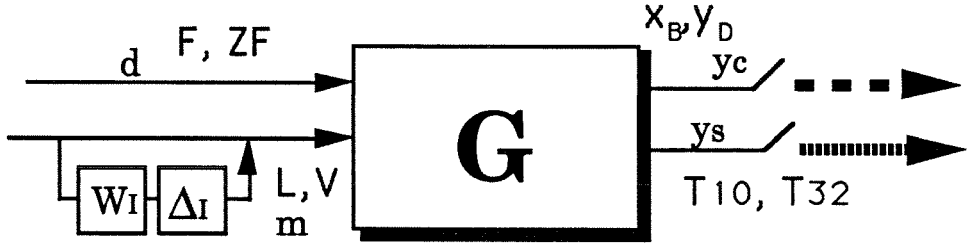


(b) Composition Control Problem

Figure 5.7. LV High-Purity Distillation Column and its Control Problem

### 5.5.2 Results

We simulate the closed-loop response of $x_B$ and $y_D$ to step disturbances in $F$ and $z_F$. $F$ and $z_F$ rise to 0.2 and to 0.1 respectively (corresponding to 20% change of the steady-state values) at $t = 0$, and then, fall to -0.2 and -0.1 at $t = 100$. All simulations were carried out with 20% uncertainty in the flows of $L$ and $V$. Random noises of covariance $R_s$ and $R_c$ were put into the temperature and composition measurements respectively to simulate the measurement noise. The results for Case A and Case B are shown in Figure 5.8 and Figure 5.9 respectively.

**Case A** Comparing the responses shown in Figure 5.8(a), we note that the performance advantage of the MR-Kalman-filter-based MPC over the cascaded-estimator-based MPC is almost negligible. Both controllers drive the compositions to the steady-state operating points without offsets in spite of model/plant mismatch and also give acceptable transient responses. On the other hand, the failure tolerance property of the MR-optimal-estimator-based MPC is far worse than that of the cascade-estimator-based MPC as illustrated in Figure 5.8(b)-(c). In the case of a composition measurement failure, simple adjustments such as setting the innovation term for the failed primary measurement zero is inadequate for the MR optimal estimator.

**Case B** The performance of the MR-optimal-estimator-based MPC and that of the DR-cascade-estimator-based MPC are almost indistinguishable, as shown in Figure 5.9(a). On the contrary to Case A, however, the MR-optimal-estimator-based MPC maintains acceptable performance in the case of a composition measurement failure, as illustrated in Figure 5.9(b)-(c). As the sampling rate and delays of the primary measurements become significant, the dependence of the estimator on these measurements become less, and the distinct performance degradation that we saw for the MR-optimal-estimator-based MPC in Case A

disappears.

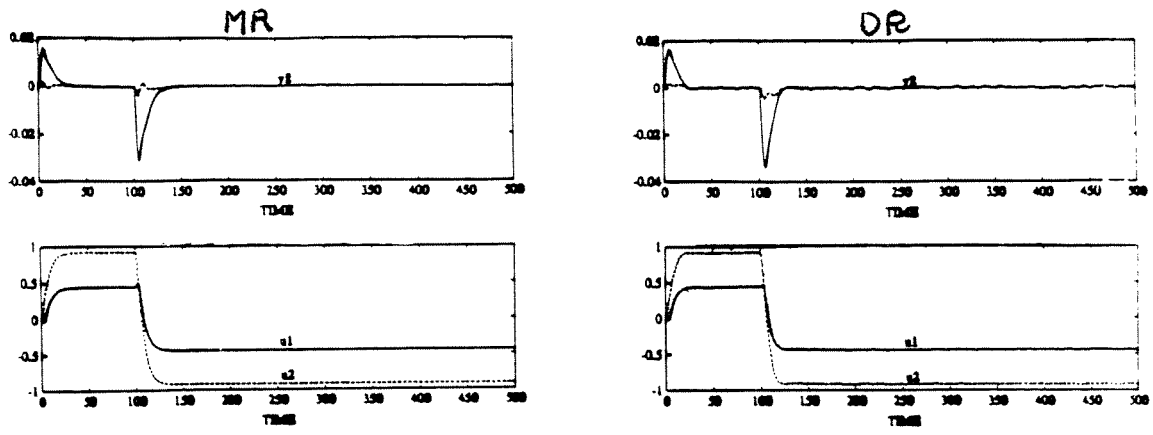


(a) Both Composition Measurements Available

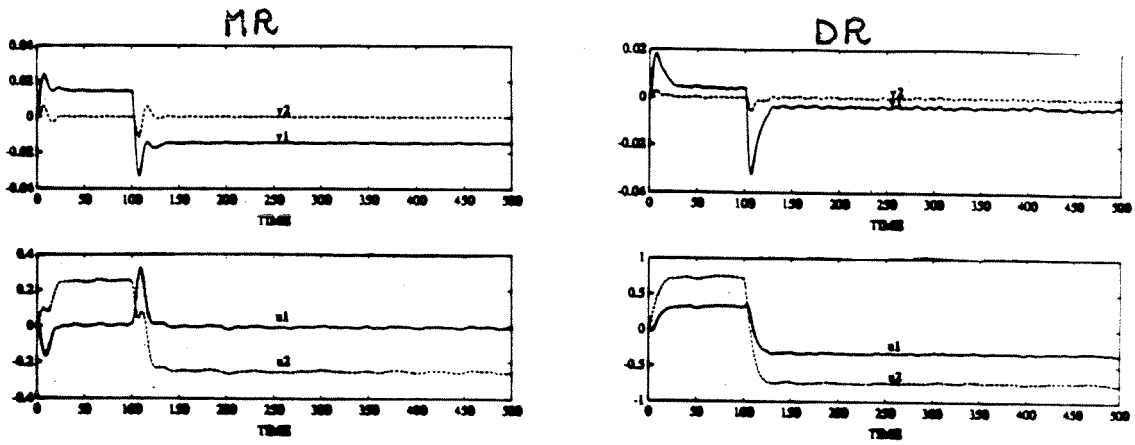


(b) Failure of Bottom Composition ($x_B$) Measurement

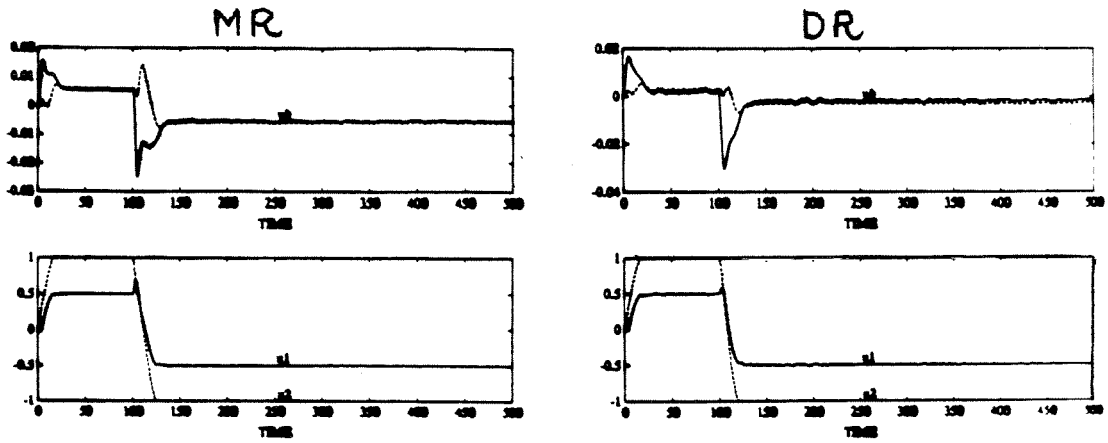


(c) Failure of Top Composition ($y_D$) Measurement

Figure 5.8. Closed-Loop Responses of $x_B$, $y_d$, $L$ and $V$ to Step Disturbances in $F$ and $z_F$ for Case A

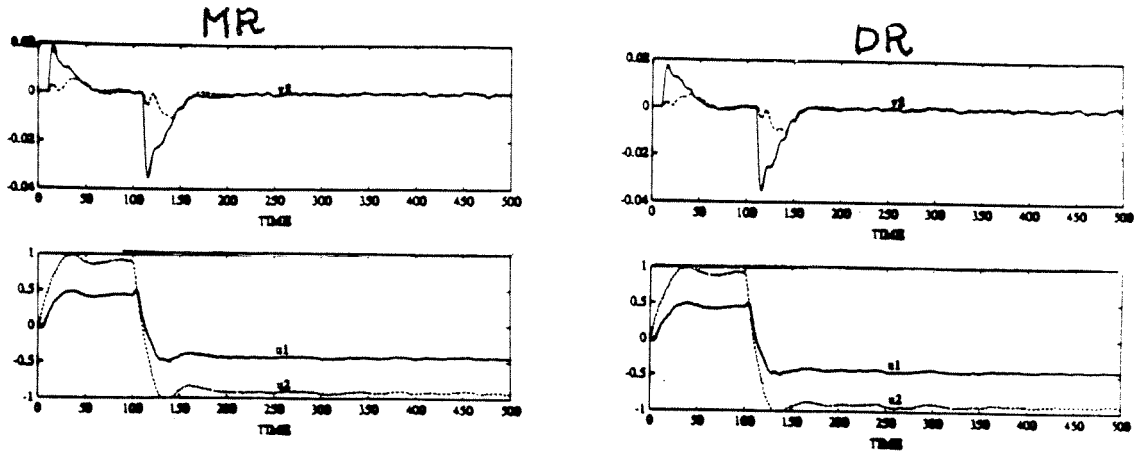


(a) Both Composition Measurements Available

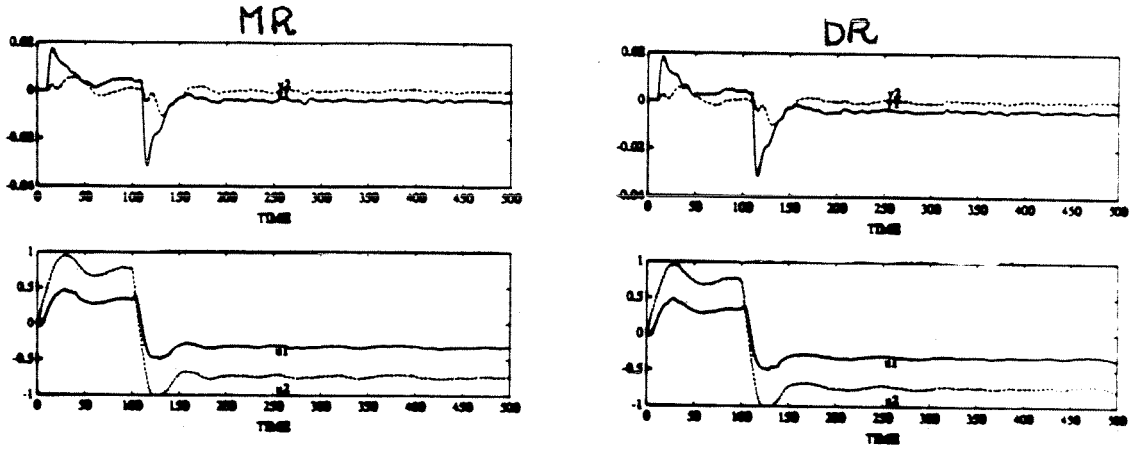


(b) Failure of Bottom Composition ($x_B$) Measurement

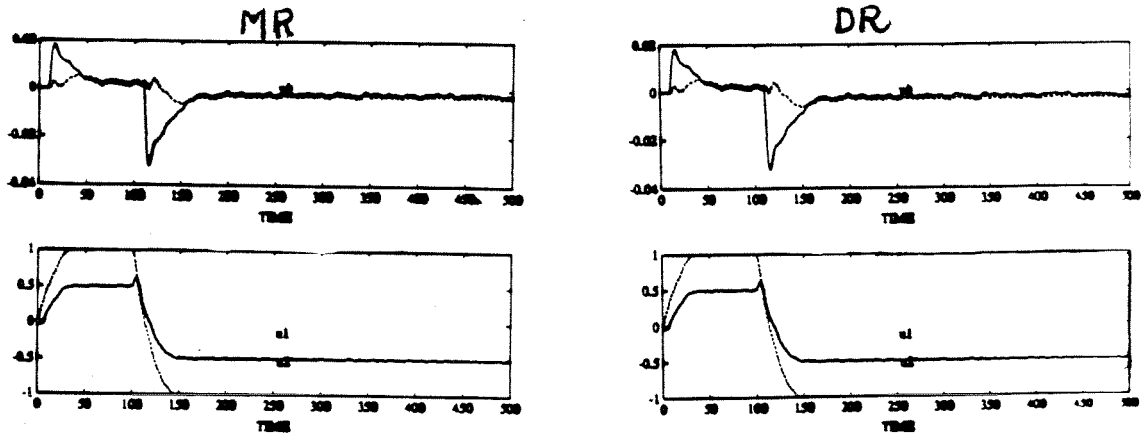


(c) Failure of Top Composition ($y_D$) Measurement

Figure 5.9. Closed-Loop Responses of $x_B$, $y_d$, $L$ and $V$ to Step Disturbances in $F$ and $z_F$ for Case B

# Appendix 5.A: Constructing a SR System for a MR Sampled-Data System

The system expressed through (5.16)-(5.17) is a multi-rate sampled-data system and therefore is shift varying with respect to $\tau_S$, the STU. We can express (5.16)-(5.17) as a SR system with respect to the time unit of $\tau_B$, the BTU. The following is the SR system equivalent to the MR system of (5.16)-(5.17):

$$\Delta X(k,0) = \Phi^{SR}\Delta X(k-1,0) + \Gamma_U^{SR}\Delta U^{SR}(k-1,0) + \Gamma_D^{SR}\Delta D^{SR}(k-1,0) \tag{5.111}$$

$$\hat{Y}^{SR}(k,0) = \Xi^{SR}\Delta X(k,0) + \Upsilon_U^{SR}\Delta U^{SR}(k,0) + \Upsilon_D^{SR}\Delta D^{SR}(k,0) + V^{SR}(k,0) \tag{5.112}$$

where

$$\Delta U^{SR}(k,0) = \begin{bmatrix} \Delta u(k,0) \\ \Delta u(k,1) \\ \vdots \\ \Delta u(k,N-1) \end{bmatrix} \quad \Delta D^{SR}(k,0) = \begin{bmatrix} \Delta d(k,0) \\ \Delta d(k,1) \\ \vdots \\ \Delta d(k,N-1) \end{bmatrix} \tag{5.113}$$

$$\hat{Y}^{SR}(k,0) = \begin{bmatrix} \hat{Y}(k,0) \\ \hat{Y}(k,1) \\ \vdots \\ \hat{Y}(k,N-1) \end{bmatrix} \quad V^{SR}(k,0) = \begin{bmatrix} V(k,0) \\ V(k,1) \\ \vdots \\ V(k,N-1) \end{bmatrix} \tag{5.114}$$

$$\Phi^{SR} = \Phi^N \tag{5.115}$$

$$\Gamma_U^{SR} = \begin{bmatrix} \Phi^{N-1}\Gamma_u & \Phi^{N-2}\Gamma_u & \cdots & \Gamma_u \end{bmatrix} \tag{5.116}$$

$$\Gamma_D^{SR} = \begin{bmatrix} \Phi^{N-1}\Gamma_d & \Phi^{N-2}\Gamma_d & \cdots & \Gamma_d \end{bmatrix} \tag{5.117}$$

$$\Xi^{SR} = \begin{bmatrix} \Xi(0) \\ \Xi(1)\Phi \\ \vdots \\ \Xi(N-1)\Phi^{N-1} \end{bmatrix} \tag{5.118}$$

$$\Upsilon_U^{SR} = \begin{bmatrix} \Xi(0) & 0 & \cdots & 0 \\ 0 & \Xi(1) & \cdots & 0 \\ \vdots & & \ddots & \vdots \\ 0 & 0 & \cdots & \Xi(N-1) \end{bmatrix} \begin{bmatrix} 0 & 0 & \cdots & 0 \\ \Gamma_u & 0 & \cdots & 0 \\ \Phi\Gamma_u & \Gamma_u & \cdots & 0 \\ \vdots & \vdots & \ddots & \vdots \\ \Phi^{N-1}\Gamma_u & \Phi^{N-2}\Gamma_u & \cdots & 0 \end{bmatrix} \tag{5.119}$$

$$\Upsilon_D^{SR} = \begin{bmatrix} \Xi(0) & 0 & \cdots & 0 \\ 0 & \Xi(1) & \cdots & 0 \\ \vdots & & \ddots & \vdots \\ 0 & 0 & \cdots & \Xi(N-1) \end{bmatrix} \begin{bmatrix} 0 & 0 & \cdots & 0 \\ \Gamma_d & 0 & \cdots & 0 \\ \Phi\Gamma_d & \Gamma_d & \cdots & 0 \\ \vdots & \vdots & \ddots & \vdots \\ \Phi^{N-1}\Gamma_d & \Phi^{N-2}\Gamma_d & \cdots & 0 \end{bmatrix} \tag{5.120}$$

The superscript $\{\cdot\}^{SR}$ is used to distinguish the vectors and the matrices used for the SR system. Note from the equations (5.111)-(5.112) that the state excitation noise ($\Gamma_D^{SR}\Delta D^{SR}$) and the measurement noise ($\Upsilon_D^{SR}\Delta D^{SR} + V^{SR}$) are now correlated. Denoting $\Gamma_D^{SR}\Delta D^{SR}$ as $W_X^{SR}$ and $\Upsilon_D^{SR}\Delta D^{SR} + V^{SR}$ as $W_Y^{SR}$ and performing some algebra, one can show that

$$E\left\{ \begin{bmatrix} W_X^{SR}(k,0) \\ W_Y^{SR}(k,0) \end{bmatrix} \begin{bmatrix} (W_X^{SR})^T(k,0) & (W_Y^{SR})^T(k,0) \end{bmatrix} \right\} = \begin{bmatrix} Q^{SR} & T^{SR} \\ (T^{SR})^T & R^{SR} \end{bmatrix} \tag{5.121}$$

where

$$Q^{SR} = \Gamma_D^{SR} \begin{bmatrix} Q_d & & \\ & \ddots & \\ & & Q_d \end{bmatrix} (\Gamma_D^{SR})^T \tag{5.122}$$

$$T^{SR} = \Gamma_D^{SR} \begin{bmatrix} Q_d & & \\ & \ddots & \\ & & Q_d \end{bmatrix} (\Upsilon_D^{SR})^T \tag{5.123}$$

$$R^{SR} = \Upsilon_D^{SR} \begin{bmatrix} Q_d & & \\ & \ddots & \\ & & Q_d \end{bmatrix} (\Upsilon_D^{SR})^T + \begin{bmatrix} R(0) & & \\ & \ddots & \\ & & R(N-1) \end{bmatrix} \tag{5.124}$$

The Riccati equation for the optimal filtering problem of the system (5.111)-(5.112) is as follows:

$$\Sigma^{SR} - \Psi\Sigma^{SR}\Psi^T + \Psi\Sigma^{SR}(\Xi^{SR})^T \left\{\Xi^{SR}\Sigma^{SR}(\Xi^{SR})^T + R^{SR}\right\}^{-1} \Xi^{SR}\Sigma^{SR}\Psi^T - Q^{SR} = 0 \tag{5.125}$$

where

$$\Psi = \Phi^{SR} - T^{SR}(R^{SR})^{-1}\Xi^{SR} \tag{5.126}$$

The unique stabilizing solution to the Riccati equation (5.125) can be obtained through various standard techniques [3,26]. The following Theorem due to Amit [1] relates the solution of (5.125) to the steady-state solution of (5.24):

**Theorem 5.2** *Suppose $\Sigma_*^{SR}$ solves the algebraic Riccati equation (5.125). Let $\Sigma(j)$ be the periodic steady state solution of the Riccati equation (5.24). Then,*

$$\Sigma(0) = \Sigma_*^{SR} \tag{5.127}$$

**Proof** See Amit [1]. ■

Once $\Sigma(0)$ is found, $\Sigma(j), j = 1, \cdots, N-1$ can be easily found by the equation (5.24).

# Appendix 5.B: Proof of Theorem 5.1

The MR system (5.16)-(5.17) is detectable if and only if the SR equivalent system expressed through (5.111)-(5.112) is detectable. The following Lemma is due to Hautus [30]:

**Lemma 5.1** *The system (5.111)-(5.112) is detectable if and only if*

$$\text{rank}\left[\ (\Phi^{SR})^T - \lambda I \ \middle|\ (\Xi^{SR})^T\ \right] = \dim\{\Phi^{SR}\} \quad \forall \lambda \in \mathcal{C},\ \ |\lambda| \geq 1 \tag{5.128}$$

Hence, the MR system (5.16)-(5.17) is detectable if and only if

$$\text{rank}\left[\ (\Phi^N)^T - \lambda I \ \middle|\ (\Xi(0))^T \quad (\Xi(1)\Phi)^T \quad \cdots \quad (\Xi(N-1)\Phi^{N-1})^T\ \right] = \dim\{\Phi\}$$
$$\forall \lambda \in \mathcal{C},\ \ |\lambda| \geq 1 \tag{5.129}$$

The condition (5.129) is trivially satisfied if $\lambda$ is not an eigenvalue of $\Phi^N$. If $\lambda$ is an eigenvalue of $\Phi^N$, $(\Phi)^N$ maps $\text{Ker}\left\{(\Phi^N)^T - \lambda I\right\} = \text{Eig}_{(\Phi^N)^T}(\lambda)$ into itself where

$$\text{Eig}_{\{\cdot\}}(\lambda) = \{v : v = c\bar{v}, c \in \mathcal{R} \text{ and } \bar{v} \text{ is an eigenvector of } \{\cdot\} \text{ corresp. to the eigenvalue } \lambda\} \tag{5.130}$$

**Lemma 5.2**

$$\text{Im}\left\{\left[\ (\Xi(0))^T \quad (\Xi(1)\Phi)^T \quad \cdots \quad (\Xi(N-1)\Phi^{N-1})^T\ \right]\right\} \supset \text{Eig}_{(\Phi^N)^T}(\lambda) \tag{5.131}$$

*if and only if*

$$\text{Im}\left\{(\Xi^c(0))^T\right\} \supset \text{Eig}_{(\Phi^N)^T}(\lambda) \tag{5.132}$$

**Proof** "If" part of the condition is obvious. To prove "only if" part, we note that the synchronous sampling assumption implies that $\mathrm{Im}\left\{(\Xi(0))^T\right\} \supset \mathrm{Im}\left\{(\Xi(n))^T\right\}$, $n = 1, \cdots, N-1$. In addition, an eigenvector of $(\Phi^N)^T$ is an eigenvector of $(\Phi^n)^T$, $n = 1, \cdots, N-1$. Hence, $\mathrm{Im}\left\{(\Xi(n)\Phi^n)^T\right\} \supset \mathrm{Eig}_{(\Phi^N)^T}$ if and only if $\mathrm{Im}\left\{(\Xi(0))^T\right\} \supset \mathrm{Eig}_{(\Phi^N)^T}$ for $n = 1, \cdots, N-1$. This implies that

$$\mathrm{Im}\left\{\left[\begin{array}{cccc} (\Xi(0))^T & (\Xi(1)\Phi)^T & \cdots & (\Xi(N-1)\Phi^{N-1})^T \end{array}\right]\right\} \supset \mathrm{Eig}_{(\Phi^N)^T}(\lambda) \tag{5.133}$$

only if

$$\mathrm{Im}\left\{(\Xi(0))^T\right\} \supset \mathrm{Eig}_{(\Phi^N)^T}(\lambda) \tag{5.134}$$

■

Using the above lemma, we can write

$$\mathrm{rank}\left[\begin{array}{c|ccc} (\Phi^N)^T - \lambda I & (\Xi(0))^T & (\Xi(1)\Phi)^T & \cdots & (\Xi(N-1)\Phi^{N-1})^T \end{array}\right] = \dim\{\Phi\}$$
$$\forall \lambda \in \mathcal{C}, |\lambda| \geq 1 \tag{5.135}$$

$$\Leftrightarrow \quad \mathrm{rank}\left[\begin{array}{c|c} (\Phi^N)^T - \lambda I & (\Xi(0))^T \end{array}\right] = \dim\{\Phi\} \quad \forall \lambda \in \mathcal{C}, \ |\lambda| \geq 1 \tag{5.136}$$

$$\Leftrightarrow \quad \mathrm{rank}\left[\begin{array}{c|c} (\Phi^N)^T - \lambda^N I & (\Xi(0))^T \end{array}\right] = \dim\{\Phi\} \quad \forall \lambda \in \mathcal{C}, \ |\lambda| \geq 1 \tag{5.137}$$

$$\Leftrightarrow \quad \mathrm{rank}\left[\begin{array}{c|c} (\Phi)^T - \lambda I & (\Xi(0))^T \end{array}\right] = \dim\{\Phi\} \quad \forall \lambda \in \mathcal{C}, \ |\lambda| \geq 1 \tag{5.138}$$

The last equivalence is from the fact that $\mathrm{Im}\{(\Phi^N)^T - \lambda^N I\} \equiv \mathrm{Im}\{\Phi^T - \lambda I\}$. This is easy to see since

$$\mathrm{Ker}\left\{(\Phi^N)^T - \lambda^N I\right\} \tag{5.139}$$

$$\equiv \quad \mathrm{Ker}\left\{(\Phi)^T - \lambda I\right\} \tag{5.140}$$

$$\equiv \quad \begin{cases} \{0\} \text{ if } \lambda \text{ is not an eigenvalue of } \Phi. \\ \mathrm{Eig}_{\Phi}(\lambda) \text{ if } \lambda \text{ is an eigenvalue of } \Phi. \end{cases} \tag{5.141}$$

$$\text{rank}\left[\begin{array}{c|c} (\Phi)^T - \lambda I & (\Xi(0))^T \end{array}\right] \tag{5.142}$$

$$= \text{rank}\left[\begin{array}{ccc|cc} A^T - \lambda I & (C_c A)^T & (C_s A)^T & 0 & 0 \\ 0 & I - \lambda I & 0 & I & 0 \\ 0 & 0 & I - \lambda I & 0 & I \end{array}\right] \tag{5.143}$$

$$= \text{rank}\left[\begin{array}{c|cc} A^T - \lambda I & (C_c A)^T & (C_s A)^T \end{array}\right] + \dim(y_c) + \dim(y_s) \tag{5.144}$$

From Lemma 5.1,

$$\text{rank}\left[\begin{array}{c|cc} A^T - \lambda I & (C_c A)^T & (C_s A)^T \end{array}\right] = \dim(A) \tag{5.145}$$

if and only if

$$\left(\left[\begin{array}{c} C_c A \\ C_s A \end{array}\right], A\right) \text{ is a detectable pair.}$$

In addition, one can easily show that $\left(\left[\begin{array}{c} C_c A \\ C_s A \end{array}\right], A\right)$ is a detectable pair if and only if $\left(\left[\begin{array}{c} C_c \\ C_s \end{array}\right], A\right)$ is a detectable pair. Hence,

$$\text{rank}\left[\begin{array}{c|c} (\Phi)^T - \lambda I & (\Xi^c(0))^T \end{array}\right] = \dim(\Phi) = \dim(A) + \dim(y_c) + \dim(y_s) \tag{5.146}$$

if and only if

$$\left(\left[\begin{array}{c} C_c \\ C_s \end{array}\right], A\right) \text{ is a detectable pair.}$$

# Appendix 5.C: Minimizing the Error Due to Unobservable Disturbances

In Section 5.2.5, we state that the Ricatti Equation (5.38) converges to a positive semidefinite symmetric solution only if $\mathrm{Ker}\{C_s(I-A)^{-1}B_d\} \subset \mathrm{Ker}\{C_c(I-A)^{-1}B_d\}$, assuming $Q_{\Delta d}$ has a full rank. When this condition is not satisfied, the optimal way (in the sense of the Frobenious norm of the matrix relating disturbances to steady-state estimation error) to guarantee the convergence is to replace $d$ with $d^*$, that is the projection of $d$ into the observable subspace $Y$. The projection of $d$ into the space $Y$ can be easily calculated by the following formula:

$$d^* = P_Y^+ d = G_{y_s d}^T (G_{y_s d} G_{y_s d}^T)^{-1} G_{y_s d} d \tag{5.147}$$

where $G_{y_s d} = C_s(I-A)^{-1}B_d$. Hence, replacing $Q_{\Delta d}$ with $Q_{\Delta d^*} = P_Y^+ Q_{\Delta d}(P_Y^+)^T$ minimizes the error caused by unobservable disturbances and ensures the convergence of the Riccatti Equation (5.38).

# Chapter 6

# Conclusion and Recommendations

## 6.1 Summary of Contributions

This thesis was motivated by the fact that, in many chemical processes, the measurements of the controlled variables alone do not provide an adequate basis for effective feedback control. Some of the reasons included sampling delays, nonminimum-phase characteristics of the process, poor signal-to-noise ratios of the measurements, and operational unreliability of measurement devices. In the thesis, we have examined two major tasks that are required to obtain a control system utilizing secondary measurements for such processes: measurement selection and inferential control system design.

In Chapter 3, we presented a general measurement selection methodology that can incorporate in a unified manner all the factors that can influence the measurement selection in significant ways. These factors included model uncertainty, signal-to-noise ratios, measurement dynamics, *etc.* The underlying philosophy was to reduce the number of candidates by eliminating those candidates for which no linear time invariant controller exists meeting the required level of robust performance. Based on this philosophy and using the Structured Singular Value theory, a number of numerically efficient screening tools were developed. Some screening tools (called "general screening tools") can be used independently of the controller design methods to be employed subsequently while others (called "design-dependent screening tools") are

tied to specific design approaches. Connections to the previously published measurement selection criteria were clearly drawn and it was shown that the new measurement selection tools has widened scope of applicability and generality. Applications of the proposed tools to a multi-component distillation column and a high-purity distillation column led to intuitive, phyically consistent results.

For inferential control system design, two different approaches were considered: an output estimation based design approach and a state estimation based design approach. The output estimation based design approach involved two independent design tasks: design of an output estimator and that of a feedback controller. While it had the advantage of simpler design tasks and not requiring a full dynamic model relating all external inputs to process variables, it had the disadvantage of lower achievable performance. The state estimation based design approach, on the other hand, had the advantage of yielding an optimal controller guaranteed by the separation principle, but had the disadvantage of always requiring a full dynamic model of the process.

In Chapter 4, the focus was on the output estimation based design. Design of the output estimator was discussed in two different contexts: first, when one has access to a full dynamic (or static) model, and then, when one has access only to records of inputs and outputs of the estimator that are available from simulations or process measurements. For the former case, multi-rate Kalman filter design and $\mu$-Synthesis design were discussed. For the latter case, the estimator design problem was formulated as a regression problem and suitability of various regression techniques was examined. For design of the feedback controller, traditional techniques such as LQG, IMC, and MPC were combined into a control technique that had nice algorithmic properties as well as many operational merits such as straightforward constraint handling and simple, intuitive on-line tuning. The new technique is clearly more general and flexible than any of the traditional techniques since the new technique reduces

to one of the traditional techniques under special assumptions on the external input signals and/or under particular choices of design parameters. A heavy-oil fractionator was used as an example application.

In Chapter 5, the main emphasis was on the state estimation based design. General state estimation techniques (*e.g.*, multi-rate Kalman filtering) used by LQG and finite receding horizon control used by traditional MPC were combined into a control technique that can incorporate general disturbances and multi-rate sampled measurements and has desirable operational characteristics. As in Chapter 4, the concept of classical IMC was extended to equip the control system with on-line tuning parameters that have a direction connection with the speed of the closed-loop responses. Application to a high purity distillation showed very promising results in terms of the control system's closed-loop performance and operational flexibility.

## 6.2 Suggestions for Future Work

For measurement selection, more work can be done under the new philosophy. They include

- **Developement of Tighter Screening Tools**

  Tighter necessary conditions for the existence of a controller achieving robust performance imply screening tools that can eliminate more measurement candidates before going to detailed analyses. In particular, development of a necessary and sufficient condition for the existence of a robustly performing acausal controller for general uncertainty block structures (not just two block cases) would give a nice screening tool. In addition, extension of the methods to include real parameter uncertainty would be beneficial.

- **Number of Measurements**

  Clearly, more measurements imply higher *achievable* performance. However, in

many cases, it may not be necessary to use all the available measurements. In addition, most design methods will lead to performance degradation when too many measurements are employed. It would be beneficial to identify such cases and devise a general rule in choosing the number of measurements.

- **Experimental Verification**

  Although the proposed measurement selection tools were tested on realistic examples, experimental verification would greatly increase their fidelity. Distillation columns seem to be good grounds to test these measurement selection tools.

For inferential control system design, the following topics remain as challenges:

- **Extension of $\mu$-Synthesis to Multi-Rate Sampled Data Systems**

  A major deficiency of the current method is that it cannot incorporate the given uncertainty information explicitly. To extend $\mu$-Synthesis to multi-rate sampled-data systems, $H_\infty$-optimal synthesis problem and nonconservative $\mu$-analysis problem for these systems must be resolved.

- **Regression Based Design of Dynamic Estimators for General Multi-Rate Sampled-Data Systems**

  The regression based estimator design techniques discussed in Chapter 4 is applicable only when all the inputs to the estimator are available at a uniform sampling rate. Extensions of the techniques to general multi-rate sampled data systems would be beneficial.

- **Stability and Robustness Analysis for Constrained MPC Controllers**

  With the new interpretation of MPC controllers as a combination of a linear state observer and a nonlinear state feedback regulator, it may be possible to derive stability or robustness conditions that are simpler than those currently available [64].

- **Experimental Verification**

  Even though simulation study showed that the closed-loop performance of the proposed MPC controller was excellent both for ideal and nonideal operating modes, evaluation of the technique for experimental systems would be beneficial. This study can be done in conjuction with the experimental project suggested for measurement selection.

# Appendix A

# Model Predictive Control Using Step Response Models

## Abstract

We show that unconstrained Model Predictive Control (MPC) based on step response models is identical to linear quadratic optimal output feedback under a particular disturbance and measurement noise assumption. More specifically, MPC in its unconstrained form is equivalent to the optimal state observer (Kalman filter) designed for step disturbances at the output and in the absence of measurement noise, plus linear quadratic state feedback. Analytical results on the state estimation based on step response models allow us to generalize the conventional MPC (which is widely applied in industry) to processes with integrators and to cases with white measurement noise *without* introducing any additional complexity. For the case of an integrated white noise disturbance at the output and white measurement noise, the optimal state estimator is conveniently parametrized in terms of a real parameter vector whose dimension is equal to the number of outputs. A similar parametrization exists for the case of a double-integrated white noise output disturbance. These parametrizations are independent of model complexity and eliminate the need for solving a Riccati equation of potentially very large order and provide natural on-line tuning parameters that can lead to the optimal estimator by proper adjustments. Our analysis shows that the new state-estimation-based MPC is a *direct* extension of conventional

MPC techniques such as Dynamic Matrix Control (DMC) and Internal Model Control (IMC). The new state-space interpretation also points out clearly cases where the conventional MPC will not perform well regardless of tuning, in particular, the cases where disturbances enter the output through slow dynamics.

## A.1 Introduction

Model Predictive Control (MPC) has emerged as a powerful practical control technique during the last decade. Its strength lies in that it uses step response data which are physically intuitive, and that it can handle hard constraints explicitly through on-line optimization. Various MPC techniques such as Dynamic Matrix Control (DMC) [15], Model Algorithmic Control (MAC) [58], and Internal Model Control (IMC) [24] have demonstrated their effectiveness in industrial applications during the past ten years [55,15,14]. One drawback has been that, because most MPC techniques are developed in an unconventional manner using step response models, their generalization to more complex cases has been slow. For example, MPC in its current form is not applicable to integrating systems, which are common in chemical processes.

Lately, there have been efforts to interpret Model Predictive Control in a state-space framework. This not only permits the use of "well-known" state-space theorems, but also allows straightforward generalization to more complex cases such as systems with noisy measurements. Clarke *et al.* developed what is known as "Generalized Predictive Control (GPC)," based on *parametric* input-output models, and showed its connection to LQ optimal control [12,13]. No discussion was given, however, on how to extend the results to the cases of noisy measurements. Recently, Li *et al.* presented a state-space interpretation of MPC based on step response models [42]. However, their generalization to systems with noisy measurements has introduced significant numerical complexity such as the requirement to solve a Riccati equation of potentially very large order (prediction horizon times the number of outputs).

As will be shown in this paper, such additional complexity is unnecessary for most industrial problems.

In this article, we establish a connection between standard MPC and linear quadratic optimal output feedback. Specifically, they are shown to be equivalent under the assumption of random-step (*i.e.*, integrated white noise) disturbances at the output and no measurement noise. Based on the interpretation of the MPC controller as a state observer plus a state feedback regulator, we generalize the conventional MPC to the case where white measurement noise occurs. Contrary to Li's work, however, our approach does not require solving a Riccati equation. Instead, it is shown that the optimal state observer is conveniently parameterized through a real parameter vector whose dimension is the same as the number of outputs. Each element of the parameter vector lies in the interval $(0, 1]$ and therefore can be adjusted on-line. We further extend the results to processes with integrators. Finally, it is shown that the adjustable parameters of the state observer directly affect the speed of the closed-loop response. For stable systems with integrated white noise disturbance at the output, the parameters play the same role as the time constants of the IMC robust filter. We also identify the cases where an IMC controller cannot be made equivalent to a linear quadratic optimal output feedback controller by augmenting it with a simple low-pass filter. Several examples demonstrate that the new state-estimation-based MPC is applicable to a wider range of control problems without introducing further complexity.

## A.2 Modelling the System

In this section, we demonstrate how the step response data can be put in a standard state-space form for stable, integrating, or unstable systems. The representation for stable systems is equivalent to that presented by Li *et al.* (1989). However, the representations for integrating and unstable sytems seem to be new. Throughout this

section, we assume that the stable modes of the system can be described through a finite impulse response (FIR) model, or equivalently the step response coefficients of the "stable part" of the system become constant after a finite number of time steps. Such an assumption may not be perfectly satisfied in practice and an approximation must be made by truncating the step response at a time step from which the outputs change negligibly.

### A.2.1 Stable SISO Systems

Let us suppose that the step response of a stable system is represented as

$$\begin{bmatrix} S_1 & S_2 & \cdots & S_{n-1} & S_n & S_n & \cdots \end{bmatrix} \tag{A.1}$$

where the $k^{\text{th}}$ element represents the response of the output at time $k$ to a unit step input starting at time 0. Then, the step response model of the system can be represented in the following standard state-space form.

$$\tilde{\mathcal{Y}}(k) = M\tilde{\mathcal{Y}}(k-1) + \mathcal{S}\Delta u(k-1) \tag{A.2}$$

$$\tilde{y}(k) = N\tilde{\mathcal{Y}}(k) \tag{A.3}$$

where

$$\tilde{\mathcal{Y}}(k) = [\tilde{y}(k|k), \tilde{y}(k+1|k), \tilde{y}(k+2|k), \cdots, \tilde{y}(k+n-1|k)]^T \tag{A.4}$$

$$M = M^S \equiv \left.\begin{bmatrix} 0 & 1 & 0 & \cdots & 0 & 0 \\ 0 & 0 & 1 & \cdots & 0 & 0 \\ \vdots & \vdots & \ddots & \ddots & \ddots & \vdots \\ 0 & 0 & 0 & \cdots & 0 & 1 \\ 0 & 0 & 0 & \cdots & 0 & 1 \end{bmatrix}\right\} n; \quad \mathcal{S} = \begin{bmatrix} S_1 \\ S_2 \\ \vdots \\ S_{n-1} \\ S_n \end{bmatrix}; \tag{A.5}$$

$$N = [\overbrace{1\ 0\ 0\ \cdots\ 0\ 0}^{n}] \tag{A.6}$$

$\Delta u(k) = u(k) - u(k-1)$ represents the change in the manipulated variable at time $k$. $\tilde{y}(k)$ is the current process output. $\tilde{\mathcal{Y}}(k)$ is a vector containing the dynamic states of the system. Each dynamic state $\tilde{y}(\ell|k)$ has a special interpretation: it is the future process output at time $\ell$ assuming the manipulated variable does not change at present or future (*i.e.*, $\Delta u(k+j) = 0$ for $j \geq 0$). The notation $(\tilde{\cdot})$ is used throughout to emphasize the fact that it is the output from the model, not from the true system. The state-space equation is interpreted as follows: the new projection $\tilde{\mathcal{Y}}(k)$ is the old projection $\tilde{\mathcal{Y}}(k-1)$ shifted up/forward by one element plus the contribution made by the latest input change $\Delta u(k-1)$.

## A.2.2 SISO Systems with Integrators

Let us suppose that the step response of an integrating system is represented as

$$\left[\ S_1\ \ S_2\ \ \cdots\ \ S_{n-1}\ \ S_n\ \ (2S_n - S_{n-1})\ \ (3S_n - 2S_{n-1})\ \ \cdots\ \right] \tag{A.7}$$

Hence, the output increases with a constant slope starting at time $n-1$. Then, the model (A.2)-(A.3) holds for the integrating system when $M^S$ is replaced by $M^I$ where

$$M^I \equiv \left.\begin{bmatrix} 0 & 1 & 0 & \cdots & 0 & 0 \\ 0 & 0 & 1 & \cdots & 0 & 0 \\ \vdots & \vdots & \ddots & \ddots & \ddots & \vdots \\ 0 & 0 & 0 & \cdots & 0 & 1 \\ 0 & 0 & 0 & \cdots & -1 & 2 \end{bmatrix}\right\} n \tag{A.8}$$

Again, the new projection $\tilde{\mathcal{Y}}(k)$ is the old projection $\tilde{\mathcal{Y}}(k-1)$ shifted up by one element (the last element is computed asssuming the output maintains a constant

slope) plus the contribution made by the latest input change $\Delta u(k-1)$.

### A.2.3 Extension to Unstable SISO Systems

We note that the matrix $M$ ($M^S$ or $M^I$) is in companion form [3]. Thus, if the last row of $M$ is $\begin{bmatrix} m_0 & m_1 & \cdots & m_{n-1} \end{bmatrix}$, then the characteristic polynomial of $M^S$ is

$$\lambda^n - m_{n-1}\lambda^{n-1} - m_{n-2}\lambda^{n-2} - \cdots - m_0 = 0 \tag{A.9}$$

For stable systems ($M^S$), the characteristic polynomial and the eigenvalues are

$$\lambda^n - \lambda^{n-1} = 0 \Rightarrow \lambda_1 = \cdots = \lambda_{n-1} = 0; \lambda_n = 1 \tag{A.10}$$

For systems with integrator ($M^I$),

$$\lambda^n - 2\lambda^{n-1} + \lambda^{n-2} = 0 \Rightarrow \lambda_1 = \cdots = \lambda_{n-2} = 0; \lambda_{n-1} = \lambda_n = 1 \tag{A.11}$$

Unstable systems can be modelled in the same framework: the last row of $M$ contains the coefficients of the characteristic polynomial (whose roots include the unstable poles). $S$ contains the step response coefficients until the time when the *stable modes* of the systems have settled plus $m$ additional coefficients where $m$ is the number of unstable poles (excluding the integrator inherent in every step response model). For example, recall that, for an integrating system, we used the step response coefficients of one step beyond the time when the stable modes of the system have settled (*i.e.*, $t = n - 1$).

## A.2.4 MIMO Systems

For MIMO systems, we obtain the same form of model as before:

$$\tilde{\mathcal{Y}}(k) = M\tilde{\mathcal{Y}}(k-1) + \mathcal{S}\Delta u(k-1) \tag{A.12}$$

$$\tilde{y}(k) = N\tilde{\mathcal{Y}}(k) \tag{A.13}$$

The only difference is that $\tilde{y}(k), \tilde{y}(k+1|k)$, *etc.*, are vectors and

$$M = M^S \triangleq \left.\begin{bmatrix} 0 & I_{n_y} & 0 & \cdots & 0 & 0 \\ 0 & 0 & I_{n_y} & \cdots & 0 & 0 \\ \vdots & \vdots & \ddots & \ddots & \ddots & \vdots \\ 0 & 0 & 0 & \cdots & 0 & I_{n_y} \\ 0 & 0 & 0 & \cdots & 0 & I_{n_y} \end{bmatrix}\right\} n \quad \text{for stable systems} \tag{A.14}$$

$$M = M^I \triangleq \left.\begin{bmatrix} 0 & I_{n_y} & 0 & \cdots & 0 & 0 \\ 0 & 0 & I_{n_y} & \cdots & 0 & 0 \\ \vdots & \vdots & \ddots & \ddots & \ddots & \vdots \\ 0 & 0 & 0 & \cdots & 0 & I_{n_y} \\ 0 & 0 & 0 & \cdots & -I_{n_y} & 2I_{n_y} \end{bmatrix}\right\} n \quad \text{for integrating systems} \tag{A.15}$$

$$N = \overbrace{\begin{bmatrix} I_{n_y} & 0 & 0 & \cdots & 0 & 0 \end{bmatrix}}^{n} \tag{A.16}$$

$$\mathcal{S} = \begin{bmatrix} S_1 \\ S_2 \\ \vdots \\ S_{n-1} \\ S_n \end{bmatrix}; \quad S_i = \begin{bmatrix} S_{1,1,i} & S_{1,2,i} & \cdots & S_{1,n_u,i} \\ S_{2,1,i} & S_{2,2,i} & \cdots & S_{2,n_u,i} \\ \vdots & \vdots & \ddots & \vdots \\ S_{n_y,1,i} & S_{n_y,2,i} & \cdots & S_{n_y,n_u,i} \end{bmatrix} i = 1, \cdots, n \tag{A.17}$$

where $S_{\ell,m,i}$ is the $i^{\text{th}}$ step response coefficient relating the $m^{\text{th}}$ input to the $\ell^{\text{th}}$ output. $n_u$ and $n_y$ are the number of inputs and outputs, respectively. Note that, with respect to each output, the $M$ matrix dynamics are completely decoupled. Mixing stable, integrating, and unstable outputs requires only the appropriate selection of the last $n_y$ rows of $M$.

### A.2.5 Summary

Modelling via step response model is feasible only when the sytem has finitely many nonzero impulse response coefficients or, equivalently, when the step response of the system becomes constant after a finite number of sampling units. If the system includes unstable modes (such as integrators), they can be expressed by augmenting the step response model as demonstrated in this section. A step response model is an intuitive, but non-parsimonious description of the system. If a state-space model is desired for various reasons (*e.g.*, more efficient on-line computation, *etc.*), one can start with a step response model and then apply model reduction (*e.g.*, balanced realization) to obtain a lower-order model. This will be discussed in detail in a future paper.

## A.3 Modelling Disturbances and Noise

Disturbances and measurement noise are inherent in every physical system. In this section, we discuss the type of disturbances and measurement noise that we treat in this article. Admittedly, the disturbance/measurement noise descriptions introduced here do not cover every physical system. The reason for restricting our discussion to these particular disturbance/noise structures is that, under these disturbance/noise descriptions, we can generalize MPC *without* introducing further complexity to the technique. In addition, they are the simplest, yet practically meaningful disturbance/noise descriptions for feedback control purposes. As we shall demonstrate

through several examples in Section A.9), many interesting, practically relevant control problems can be treated in the framework.

In this work, disturbances and measurement noise are described by adding white noise to the step response model as follows:

$$\mathcal{Y}(k) = M\mathcal{Y}(k-1) + \mathcal{S}\Delta u(k-1) + Tw(k-1) \tag{A.18}$$

$$y(k) = N\mathcal{Y}(k) \tag{A.19}$$

$$\hat{y}(k) = y(k) + v(k) \tag{A.20}$$

$T$ is a matrix containing the step response coefficients of outputs to changes in disturbances. Naturally, $n$ should be chosen such that after $n$ time steps, the output responses to step changes in disturbances become constant when $M = M^S$ or change with constant slopes when $M = M^I$. $w(k)$ and $v(k)$ are white noise with the following covariance matrices:

$$E\{w(k)w(k)^T\} = W = \begin{bmatrix} W_1 & & \\ & \ddots & \\ & & W_{n_y} \end{bmatrix} \tag{A.21}$$

$$E\{v(k)v(k)^T\} = V = \begin{bmatrix} V_1 & & \\ & \ddots & \\ & & V_{n_y} \end{bmatrix} \tag{A.22}$$

$\mathcal{Y}(k) = [\ y(k)^T \quad y(k+1|k)^T \quad \cdots \quad y(k+n-1|k)^T\ ]^T$ represents the dynamic states of the system. Physically, $y(\ell|k)$ represents the future process output at time $\ell$ assuming $\Delta u(k+j) = 0; w(k+j) = 0 \quad \forall j \geq 0$. $\hat{y}(k)$ represents the noise-corrupt measurement of $y(k)$.

In this article, we will concentrate on a particular choice of $T$, namely $T =$

$\overbrace{[\ 0\ \ 0\ \ \cdots\ \ 0\ \ I_{n_y}\ ]}^{n}{}^T$. For stable systems (*i.e.*, $M = M^S$), the particular choice of $T$ makes the disturbance integrated white noise (*i.e.*, random walk) added to the process outputs ("type 1" disturbance). Note that, with the assumption of $\Delta u(k) = 0\ \ \forall k \geq 0$ and $y(0) = 0$,

$$y(k+n) = \sum_{j=0}^{k} w(j) \tag{A.23}$$

For integrating systems (*i.e.*, $M = M^I$), the disturbance is interpreted as *double*-integrated white noise added to each output ("type 2" disturbance). In this case, with the assumption of $\Delta u(k) = 0\ \ \forall k \geq 0$ and $y(0) = 0$,

$$y(k+n) = \sum_{m=0}^{k} \sum_{j=0}^{m} w(j) \tag{A.24}$$

In some cases, disturbances for *stable* systems are better described by *double*-integrated white-noise (*i.e.*, random ramps) added to each output ("type 2" disturbance). This is true when the disturbances enter the outputs through "slow" dynamics (relative to the sampling time). For such systems, $M$ can be chosen as $M^I$ of dimension $n+1$ instead of $M^S$. Naturally, the matrix $\mathcal{S}$ should contain one additional step response coefficient matrix such that $S_n = S_{n+1}$. Note that, with this change, the augmented model is equivalent to (A.18)-(A.20) with $M = M^S$ except that the disturbances are now interpreted as double-integrated white-noise at the output as described by (A.24). In all cases, the disturbances at each output are assumed uncorrelated (by requiring that $W$ be a diagonal matrix). The measurement noise at each output is white noise and is also assumed to be uncorrelated.

## A.4 State Estimation

In this section, we develop the optimal state estimation technique for the step response model (A.18)-(A.20); in other words, we will show how to estimate in an optimal

fashion the dynamic states of the system $\mathcal{Y}(k)$ on the basis of the measurements.

### A.4.1 Optimal Estimator Form

For the system (A.18)-(A.20), the two-step optimal estimator (*i.e.*, Kalman filter) based on the measurements at time k is most conveniently expressed in the following two-step form:

**Model Prediction:**

$$\bar{\mathcal{Y}}(k|k-1) = M\bar{\mathcal{Y}}(k-1|k-1) + \mathcal{S}\Delta u(k-1) \tag{A.25}$$

**Correction Based on Measurements:**

$$\bar{\mathcal{Y}}(k|k) = \bar{\mathcal{Y}}(k|k-1) + K\{\hat{y}(k) - \bar{y}(k|k-1)\} \tag{A.26}$$

where

$$\bar{\mathcal{Y}}(k|k-1) = \left[\begin{array}{cccc} \bar{y}(k|k-1)^T & \bar{y}(k+1|k-1)^T & \cdots & \bar{y}(k+n-1|k-1)^T \end{array}\right]^T \tag{A.27}$$

$\bar{y}(\ell|m)$ represents the estimate of $y(\ell)$ based on the measurements up to time $m$. The notation $(\bar{\cdot})$ is used to emphasize the fact that it is the estimated variable. $K$ is the optimal filter gain that can be calculated from

$$K = \Sigma N^T(N\Sigma N^T + V)^{-1} \tag{A.28}$$

where the $n \cdot n_y \times n \cdot n_y$ matrix $\Sigma$ is the positive-definite solution of the following Riccati equation:

$$\Sigma - M\Sigma M^T + M\Sigma N^T(N\Sigma N^T + V)^{-1}N\Sigma M^T - TWT^T = 0 \tag{A.29}$$

One noteworthy point is that, because of the specific model and disturbance/noise assumptions we adopted, the Riccati equation decouples completely with respect to each output. Hence, the optimal filter gain can be computed separately for each output by solving $n_y$ reduced-order Riccati equations.

### A.4.2 Stable Systems with "Step" Output Disturbances

It can be shown that, for a stable SISO system described through (A.18)-(A.20) (where disturbances are integrated white noise at each output), the optimal filter gain (A.28) computed from the Riccati equation (A.29) can be parametrized as follows:

$$K = K^S \equiv [\overbrace{\ f \quad f \quad \cdots \quad f\ }^{n}]^T; \quad 0 < f \leq 1 \tag{A.30}$$

Hence, the optimal filter gain is parametrized by a single real scalar f whose value lies in $(0, 1]$ and is determined by the disturbance-to-noise ratio $(W/V)$. Indeed, for the limiting cases

$$f \to 0 \quad \text{for} \quad W/V \to 0 \tag{A.31}$$

$$f \to 1 \quad \text{for} \quad W/V \to \infty \tag{A.32}$$

This parametrization is independent of model complexity (*e.g.*, system order). Hence, in practice, there is *no* need to solve the Riccati equation; instead, $f$ can be used as an on-line tuning parameter. Such simple parametrization of the optimal filter gain is made possible by the fact that each state of the step response model has a specific physical meaning: it is the future output assuming that all current and future inputs to the process remain constant.

The observer error dynamics (see Section A.7) is determined by the matrix

$$M - KNM = \begin{bmatrix} 0 & 1-f & 0 & 0 & \cdots & 0 & 0 \\ 0 & -f & 1 & 0 & \cdots & 0 & 0 \\ 0 & -f & 0 & 1 & \cdots & 0 & 0 \\ \vdots & \vdots & \vdots & \ddots & \ddots & \ddots & \vdots \\ 0 & -f & 0 & 0 & \cdots & 0 & 1 \\ 0 & -f & 0 & 0 & \cdots & 0 & 1 \end{bmatrix} \tag{A.33}$$

The eigenvalues of $M - KNM$ follow from the characteristic equation

$$\lambda^{n-1}(\lambda - 1 + f) = 0 \Rightarrow \lambda_1 = \cdots = \lambda_{n-1} = 0; \lambda_n = 1 - f \tag{A.34}$$

Note that, in the case of no measurement noise ($W/V \to \infty$), a dead-beat observer results ($f = 1$).

Extension to MIMO systems is trivial since the Riccati equation for the optimal estimation problem is completely decoupled with respect to each output. Hence,

$$K = K^S \equiv \mathcal{I} \cdot \text{diag}\{f_1, f_2, \cdots, f_{n_y}\} \tag{A.35}$$

where $\mathcal{I} = [\overbrace{\ I_{n_y} \quad I_{n_y} \quad \cdots \quad I_{n_y}\ }^{n}]^T$ and $f_i$ depends on the disturbance-to-noise ratio of the $i^{\text{th}}$ output measurement.

### A.4.3 Integrating Systems with "Ramp" Output Disturbances

It can be shown that for an integrating SISO system described through (A.18)-(A.20), the optimal filter gain (A.28) computed from the Riccati equation (A.29) can be

parametrized by two real scalars whose values lie in $(0, 1]$:

$$K = K^I \equiv f_a \begin{bmatrix} 1 \\ 1 \\ 1 \\ \vdots \\ 1 \end{bmatrix} + f_b \begin{bmatrix} 0 \\ 1 \\ 2 \\ \vdots \\ n-1 \end{bmatrix} \quad 0 < f_a, f_b \leq 1 \tag{A.36}$$

Again, for the limiting cases

$$f_a, f_b \to 0 \quad \text{for} \quad W/V \to 0 \tag{A.37}$$

$$f_a, f_b \to 1 \quad \text{for} \quad W/V \to \infty \tag{A.38}$$

We emphasize that the above parametrization is again independent of model complexity. Hence, regardless of the step response model, $f_a$ and $f_b$ are completely determined by the disturbance-to-noise ratio $(W/V)$ alone. This implies that $f_a$ and $f_b$ can be computed *off-line* by solving an appropriate $2 \times 2$ Riccati equation. In principle, $f_a$ and $f_b$ can also be tuned *on-line* together for best performance, but this may present some difficulty since it requires a two-dimensional search. Hence, we will look for a way to combine two parameters into one. Note that the observer error dynamics is determined by the matrix

$$M - KNM = \begin{bmatrix} 0 & 1-f_a & 0 & 0 & \cdots & 0 & 0 \\ 0 & (-f_a - f_b) & 1 & 0 & \cdots & 0 & 0 \\ 0 & (-f_a - 2f_b) & 0 & 1 & \cdots & 0 & 0 \\ \vdots & \vdots & \vdots & \ddots & \ddots & \ddots & \vdots \\ 0 & (-f_a - (n-2)f_b) & 0 & 0 & \cdots & 0 & 1 \\ 0 & (-f_a - (n-1)f_b) & 0 & 0 & \cdots & -1 & 2 \end{bmatrix} \tag{A.39}$$

The eigenvalues of $M - KNM$ are calculated from the characteristic equation

$$\lambda^{n-2}(\lambda^2 - \lambda(2 - f_a - f_b) + (1 - f_a)) = 0 \Rightarrow$$
$$\lambda_1 = \cdots = \lambda_{n-2} = 0; \quad \lambda_{n-1,n} = \frac{2 - f_a - f_b}{2} \pm \sqrt{\frac{(2 - f_a - f_b)^2}{4} - 1 + f_a} \tag{A.40}$$

Note that, in the case of no measurement noise (*i.e.*, $W/V \rightarrow \infty$), a dead-beat observer results ($\lambda_{n-1}, \lambda_n \rightarrow 0$). In general, $0 < f_a, f_b < 1$ yields a complex pair eigenvalues. We postulate to parametrize the observer gain through one adjustable parameter by requiring that the observer poles $\lambda_{n-1}$ and $\lambda_n$ be real and equal. This rule leads to the following relationship between $f_a$ and $f_b$:

*Rule for Single Parameter Tuning of the Estimator*

$$f_b = 2 - f_a - 2\sqrt{1 - f_a} \tag{A.41}$$

Hence, $f_a$ is the only adjustable parameter taking a value between 0 and 1. Our numerical experience suggests that this $f_b/f_a$ relation and the resulting observer performance are very similar to those of the optimal observer. An alternative to this approach is to correlate $f_a$ and $f_b$ empirically by solving $2 \times 2$ Riccati equations for various disturbance-to-noise ratios. Such calculation has to be carried out only once since the parameters are completely determined by the disturbance-to-noise ratio alone and are independent of model.

Again, owing to the decoupling property of the Riccati equation, extension to

MIMO systems is trivial. Hence,

$$K = K^I \equiv \mathcal{I}\begin{bmatrix} f_{1a} & & & \\ & f_{2a} & & \\ & & \cdots & \\ & & & f_{n_y a} \end{bmatrix} + \begin{bmatrix} 0 \\ I_{n_y} \\ 2I_{n_y} \\ \vdots \\ (n-1)I_{n_y} \end{bmatrix} \begin{bmatrix} f_{1b} & & & \\ & f_{2b} & & \\ & & \cdots & \\ & & & f_{n_y b} \end{bmatrix} \quad \text{(A.42)}$$

$f_{ib}$ can be determined from $f_{ia}$ using the rule (A.41), eliminating the need for a two-dimensional search or for solving a $2 \times 2$ Riccati equation.

### A.4.4 General Output Disturbance

For cases where $T \neq \begin{bmatrix} 0 & 0 & \cdots & 0 & I_{n_y} \end{bmatrix}^T$, it seems that a simple parametrization of the optimal filter gain does not exist. Hence, it is necessary to find explicitly the positive-definite solution to the Riccati equation (A.29). One exception is the singular noise case (*i.e.*, $V = 0$). In this case, the optimal filter gain may be written as

$$K = \begin{bmatrix} I & T_2(T_1)_\ell^{-1} & \cdots & T_{n-1}(T_1)_\ell^{-1} & T_n(T_1)_\ell^{-1} \end{bmatrix}^T \quad \text{(A.43)}$$

assuming that all eigenvalues of $M - KNM$ lie inside the unit disk. Violation of this assumption means that the filter gain computed by (A.43) leads to an unstable state estimator. In order to calculate $K$ through (A.43), it is also required that the first step response coefficient matrix has a left inverse $(T_1)_\ell^{-1}$. This is always satisfied for cases where $T_i$ is a diagonal matrix (for $1 \leq i \leq n$), since in these cases one can always redefine the disturbances such that $T_1$ is nonsingular.

## A.5 Prediction

The dynamic states of the optimal estimators developed in the previous section represent the current and future outputs assuming all current and future inputs are zero (*i.e.*, $\Delta u(k+j) = 0$ for $j \geq 0$). The predictive controller computes the best current and future control moves based on the prediction of future outputs. Then future outputs can be expressed in terms of current and $(m-1)$ future inputs through the following equation:

$$\bar{\mathcal{Y}}_p^m(k+1|k) = M_p \bar{\mathcal{Y}}(k|k) + \mathcal{S}_p^m \Delta\mathcal{U}(k) \tag{A.44}$$

where

$$M_p = \begin{bmatrix} I_{p\cdot n_y \times p\cdot n_y} & 0 \end{bmatrix} M \tag{A.45}$$

$$\mathcal{S}_p^m = \begin{bmatrix} S_1 & 0 & \cdots & \cdots & 0 \\ S_2 & S_1 & 0 & \cdots & 0 \\ \vdots & \vdots & \ddots & \ddots & \vdots \\ S_m & S_{m-1} & \cdots & \cdots & S_1 \\ \vdots & \ddots & \ddots & \ddots & \vdots \\ S_p & S_{p-1} & \cdots & \cdots & S_{p-m+1} \end{bmatrix}; \quad \Delta\mathcal{U}(k) = \begin{bmatrix} \Delta u(k) \\ \Delta u(k+1) \\ \vdots \\ \vdots \\ \Delta u(k+m-1) \end{bmatrix} \tag{A.46}$$

The notation $\bar{\mathcal{Y}}_p^m(k+1|k)$ denotes the predicted future outputs up to time $k+p$ for constant inputs starting at time $k+m$, based on the measurements up to time $k$. Hence, we allow the flexibility of setting the number of future input moves $m$ ($1 \leq m \leq p$) differently from the output prediction horizon $p$. The equation (A.44) provides the "optimal" prediction of the future outputs based on the current measurements since $\bar{\mathcal{Y}}(k|k)$ is the optimal estimate of the states representing the current and future process outputs assuming $\Delta u(k+j) = v(k+j+1) = w(k,j) = 0 \ \ \forall j \geq 0$ [3]. Note

that it is optimal to develop the prediction with $w(k+j) = v(k+j+1) = 0 \ \ \forall j \geq 0$ since they are white noises.

## A.6 Feedback Control

We adopt the following quadratic optimzation objective (used in QDMC [25]):

$$\min_{\Delta\mathcal{U}(k)} ||\Gamma[\bar{\mathcal{Y}}_p^m(k+1|k) - \mathcal{R}(k+1)]||^2 + ||\Lambda\Delta\mathcal{U}(k)||^2 \tag{A.47}$$

$\mathcal{R}(k+1) = [r(k+1), \cdots, r(k+p)]^T$ is the future output reference vector. $\Gamma$ and $\Lambda$ are weighting matrices that are chosen to be diagonal for most cases. This optimization problem can be cast into the following least-squares problem:

$$\begin{bmatrix} \Gamma\mathcal{S}_p^m \\ \Lambda \end{bmatrix} \Delta\mathcal{U}(k) = \begin{bmatrix} \Gamma & 0 \\ 0 & I_{m\cdot n_u} \end{bmatrix} \begin{bmatrix} \mathcal{R}(k+1) - M_p\bar{\mathcal{Y}}(k|k) \\ 0 \end{bmatrix} \tag{A.48}$$

$$\equiv \begin{bmatrix} \Gamma\mathcal{E}(k+1|k) \\ 0 \end{bmatrix} \tag{A.49}$$

The least-squares solution is

$$\Delta\mathcal{U}(k) = \{(\mathcal{S}_p^m)^T\Gamma^T\Gamma\mathcal{S}_p^m + \Lambda^T\Lambda\}^{-1}(\mathcal{S}_p^m)^T\Gamma^T\Gamma\mathcal{E}(k+1|k) \tag{A.50}$$

The curent control move is implemented:

$$\Delta u(k) = [\ I_{n_u} \ \ 0 \ \ \cdots \ \ 0\ ]\Delta\mathcal{U}(k) \tag{A.51}$$

The controller can be interpreted as a state-observer-based compensator (see Figure A.1) since

$$\Delta u(k) = K_{MPC}(\mathcal{R}(k+1) - M_p\bar{\mathcal{Y}}(k|k)) \tag{A.52}$$

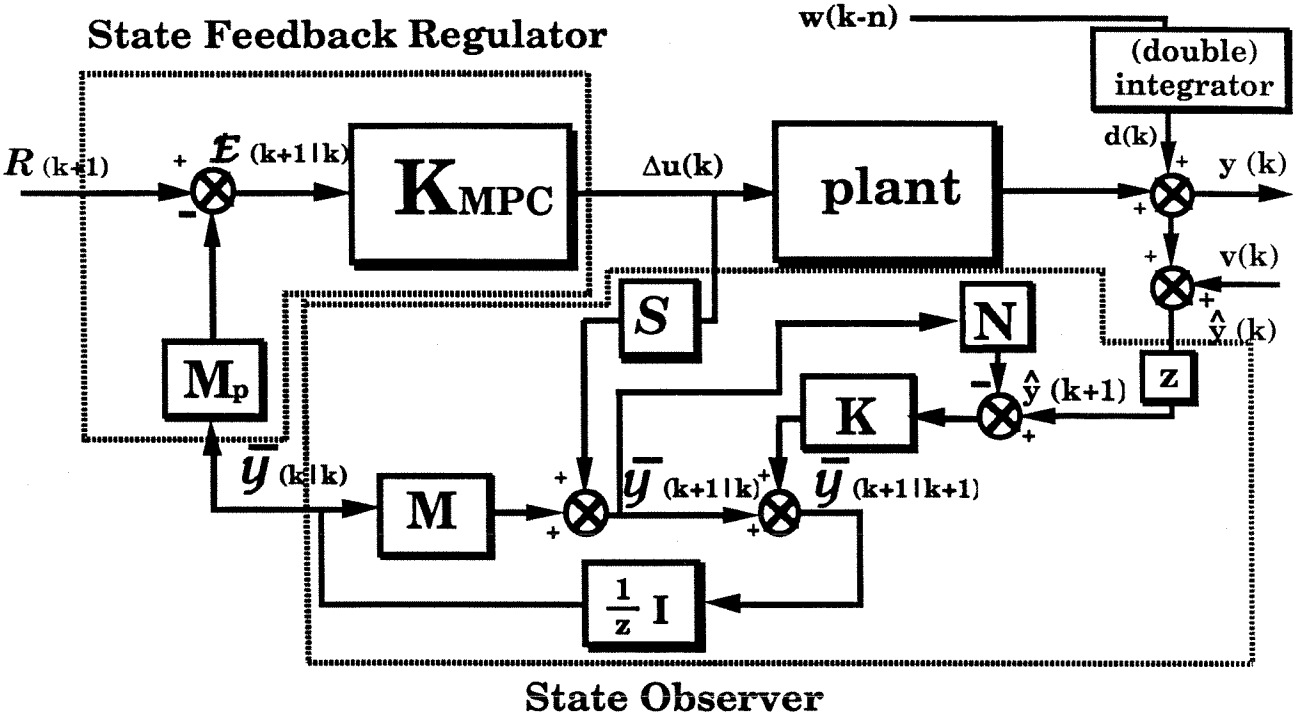


Figure A.1. Interpretation of the MPC Controller as a State-Observer-Based Compensator

where

$$K_{MPC} = [\ I_{n_u}\ \ 0\ \ \cdots\ \ 0\ ]\{(\mathcal{S}_p^m)^T\Gamma^T\Gamma\mathcal{S}_p^m + \Lambda^T\Lambda\}^{-1}(\mathcal{S}_p^m)^T\Gamma^T\Gamma \tag{A.53}$$

## A.7 Closed-Loop Relationships

We can derive the closed-loop relationships between the actual process output $y(k)$ and the system inputs $w(k)$, $v(k)$ and $\mathcal{R}(k)$ using the following relationships:

$$\mathcal{Y}(k) = M\mathcal{Y}(k-1) + \mathcal{S}\Delta u(k-1) + Tw(k-1) \tag{A.54}$$

$$\bar{\mathcal{Y}}(k|k) = (M - KNM)\bar{\mathcal{Y}}(k-1|k-1) + K\hat{y}(k) + (I - KN)\mathcal{S}\Delta u(k-1) \tag{A.55}$$

$$\hat{y}(k) = NM\mathcal{Y}(k-1) + N\mathcal{S}\Delta u(k-1) + NTw(k-1) + v(k) \tag{A.56}$$

$$\Delta u(k-1) = -K_{MPC}M_p\bar{\mathcal{Y}}(k-1|k-1) + K_{MPC}\mathcal{R}(k) \tag{A.57}$$

Simple algebraic manipulations lead to

$$\begin{bmatrix} \mathcal{Y}(k) \\ \bar{\mathcal{Y}}(k|k) \end{bmatrix} = \begin{bmatrix} M & -\mathcal{S}K_{MPC}M_p \\ KNM & M - KNM - \mathcal{S}K_{MPC}M_p \end{bmatrix} \begin{bmatrix} \mathcal{Y}(k-1) \\ \bar{\mathcal{Y}}(k-1|k-1) \end{bmatrix} + \begin{bmatrix} T & 0 & \mathcal{S}K_{MPC} \\ KNT & K & 0 \end{bmatrix} \begin{bmatrix} w(k-1) \\ v(k) \\ \mathcal{R}(k) \end{bmatrix} \tag{A.58}$$

Subtracting the second equation from the first one, we obtain

$$\begin{bmatrix} \mathcal{Y}(k) \\ \mathcal{Y}(k) - \bar{\mathcal{Y}}(k|k) \end{bmatrix} = \begin{bmatrix} M - \mathcal{S}K_{MPC}M_p & \mathcal{S}K_{MPC}M_p \\ 0 & M - KNM \end{bmatrix} \begin{bmatrix} \mathcal{Y}(k-1) \\ \mathcal{Y}(k-1) - \bar{\mathcal{Y}}(k-1|k-1) \end{bmatrix} + \begin{bmatrix} T & 0 & \mathcal{S}K_{MPC} \\ T - KNT & -K & 0 \end{bmatrix} \begin{bmatrix} w(k-1) \\ v(k) \\ \mathcal{R}(k) \end{bmatrix} \tag{A.59}$$

The closed-loop transfer function from $\begin{bmatrix} \check{w}^T(z) & \check{v}^T(z) & \check{\mathcal{R}}^T(z) \end{bmatrix}^T$ to $\check{y}(z)$ can be expressed as follows (the notation $\check{(\cdot)}(z)$ represents the z-transform of the signal):

$$\check{y}(z) = \left[\begin{array}{cc|ccc} M - \mathcal{S}K_{MPC}M_p & \mathcal{S}K_{MPC}M_p & T & 0 & \mathcal{S}K_{MPC} \\ 0 & M - KNM & T & -K & 0 \\ \hline N & 0 & 0 & 0 & 0 \end{array}\right] \begin{bmatrix} \check{w}(z) \\ z\check{v}(z) \\ z\check{\mathcal{R}}(z) \end{bmatrix} \tag{A.60}$$

where

$$\left[\begin{array}{c|c} A & B \\ \hline C & D \end{array}\right] \equiv C(zI - A)^{-1}B + D \tag{A.61}$$

**Remarks:**

1. *Closed-Loop Stability*

   The eigenvalues of the closed-loop matrix are those of $M - KNM$ and $M - SK_{MPC}M_p$. Hence, the closed-loop system is stable if and only if all eigenvalues of $M - KNM$ (*i.e.*, observer poles) and $M - SK_{MPC}M_p$ (*i.e.*, regulator poles) lie strictly inside the unit disk.

   - The observer poles are guaranteed to lie inside the unit disk from the property of the Riccati equation.
   - The regulator poles are functions of the tuning parameters (*e.g.*, $p$, $m$, $\Gamma$, $\Lambda$) and can be made to be stable by proper tuning. Under infinite input/output prediction horizon ($m = p = \infty$), the MPC regulator is equivalent to the LQ optimal regulator (computed from the Riccati equation) and is therefore stable.
   - The system cannot be stabilized by adjusting the filter parameters, when the MPC tuning parameters are selected such that $M - SK_{MPC}M_p$ is unstable.

2. *Tuning for Sensitivity and Robustness*

   The closed-loop expressions provide insights and guidelines for selecting various tuning parameters so that a desirable closed-loop response may be achieved.

   - Note that the observer dynamics affect the closed-loop transfer function from disturbance ($w$) and measurement noise ($v$), but not from the output reference vector ($\mathcal{R}$). On the other hand, the regulator dynamics affect all closed-loop tranfer functions.
   - The closed-loop transfer function from $\check{v}(z)$ to $\check{y}(z)$ is the complementary sensitivity function which has a direct relevance to the closed-loop system's

sensitivity and robustness. Observer poles, which are adjusted through the filter parameters, directly affect the complementary sensitivity function. Hence, the adjustable parameters we introduced for the estimator can be used to adjust the speed of disturbance response and system robustness.

3. *Asymptotic Disturbance Rejection Property*

   The closed-loop system rejects "persistent" disturbances (steps for stable systems and ramps for integrating systems) with no offset as long as the observer/regulator poles are placed in the unit disk. This can be seen from the closed-loop relationship from $w(k)$ to $y(k)$: $y(k)$ is simply expressed as a white-noise passed through stable (closed-loop) dynamics.

## A.8 Connection with Coventional MPC

In this section, we make a connection between the new state-estimation-based MPC and the conventional MPC techniques such as Dynamic Matrix Control [15] and Internal Model Control [24]. It is shown that the state-estimation-based MPC is a direct extension.

### A.8.1 Connection with DMC

In DMC, the prediction of the future process outputs is carried out through the following equations:

**Model Update:**

$$\tilde{\mathcal{Y}}(k) = M\tilde{\mathcal{Y}}(k-1) + \mathcal{S}\Delta u(k) \tag{A.62}$$

**Prediction with Correction Based on Measurements:**

$$\tilde{\mathcal{Y}}_p^m(k+1|k) = M_p\tilde{\mathcal{Y}}(k) + \mathcal{S}_p^m\Delta u(k) + T^p(\hat{y}(k) - \tilde{y}(k)) \tag{A.63}$$

where

$$\mathcal{T}^p = \mathcal{T}_I^p \equiv [\overbrace{\ I_{n_y} \quad I_{n_y} \quad \cdots \quad I_{n_y}\ }^{p}]^T \quad \text{for type 1 disturbances} \tag{A.64}$$

$$\mathcal{T}^p = \mathcal{T}_{II}^p \equiv [\overbrace{\ 2I_{n_y} \quad 3I_{n_y} \quad \cdots \quad (p+1)I_{n_y}\ }^{p}]^T \tag{A.65}$$

$$- [\overbrace{\ I_{n_y} \quad 2I_{n_y} \quad \cdots \quad pI_{n_y}\ }^{p}]^T \cdot \frac{1}{z} \quad \text{for type 2 disturbances}$$

For stable systems, the prediction from (A.62)-(A.63) is entirely equivalent to the prediction from the state-estimation-based prediction equation (A.44) in the *absence* of measurement noise ($f = 1$ for type 1 disturbances and $f_a = 1$ and $f_b = 1$ for type 2 disturbances). Hence, DMC does not perform noise filtering. For integrating systems, the conventional MPC leads to an "internally unstable" closed-loop system (the signal $\hat{y}(k) - \tilde{y}(k)$ can grow unbounded). This internal instability arises from the fact that $\tilde{y}(k)$ is not an estimate of the true output since it does not account for the effect of disturbances. The new approach discussed in this paper does not suffer from the same deficiency.

## A.8.2 Connection with IMC

In the Internal Model Control (IMC) framework shown in Figure A.2, the feedback signal $\hat{y}(k) - \tilde{y}(k)$ is passed through a low-pass filter $F$ for noise reduction and robustness; the filtered signal is then used as the input to the prediction equation (A.63) [50]. For stable systems with type 1 disturbances, the adjustable estimator parameter $f$ can be shown to play the same role as the IMC filter. More specifically, the prediction from the optimal state estimation is equivalent to that from equations (A.62)-(A.63)

when the feedback signal $\hat{y}(k) - \tilde{y}(k)$ is passed through the following IMC filter:

$$F = \begin{bmatrix} \frac{f_1 z}{z-(1-f_1)} & & \\ & \cdots & \\ & & \frac{f_n z}{z-(1-f_n)} \end{bmatrix} \tag{A.66}$$

For stable systems with type 2 disturbances, in order to obtain the prediction equivalent to that from the optimal state estimation, $\mathcal{T}^p$ in the prediction equation (A.63) has to be chosen as follows:

$$\mathcal{T}^p = \mathcal{T}^p_{II_f} \equiv \begin{bmatrix} F_1 \\ F_2 \\ \vdots \\ F_p \end{bmatrix} \tag{A.67}$$

where

$$F_1 = \begin{bmatrix} \frac{(f_{1a}+f_{1b})z^2-f_{1a}z}{z^2-(2-f_{1a}-f_{1b})z+(1-f_{1a})} & & \\ & \cdots & \\ & & \frac{(f_{ny a}+f_{ny b})z^2-f_{ny a}z}{z^2-(2-f_{ny a}-f_{ny b})z+(1-f_{ny a})} \end{bmatrix} \tag{A.68}$$

$$F_2 = \begin{bmatrix} \frac{(f_{1a}+2f_{1b})z^2-(f_{1a}+f_{1b})z}{z^2-(2-f_{1a}-f_{1b})z+(1-f_{1a})} & & \\ & \cdots & \\ & & \frac{(f_{ny a}+2f_{ny b})z^2-(f_{ny a}+f_{ny b})z}{z^2-(2-f_{ny a}-f_{ny b})z+(1-f_{ny a})} \end{bmatrix} \tag{A.69}$$

$$\vdots \qquad \vdots \tag{A.70}$$

$$F_p = \begin{bmatrix} \frac{(f_{1a}+pf_{1b})z^2-(f_{1a}+(p-1)f_{1b})z}{z^2-(2-f_{1a}-f_{1b})z+(1-f_{1a})} & & \\ & \cdots & \\ & & \frac{(f_{ny a}+pf_{ny b})z^2-(f_{ny a}+(p-1)f_{ny b})z}{z^2-(2-f_{ny a}-f_{ny b})z+(1-f_{ny a})} \end{bmatrix} \tag{A.71}$$

In general, there is *no* $F$ such that

$$\mathcal{T}^p_{II_f} = \mathcal{T}^p_{II} \cdot F \tag{A.72}$$

The exceptions are when $p = 1$ and when $f_{ia} = f_{ib}\ \forall i$ (this relation does not hold for the optimal estimator in general). When $p = 1$, the following IMC filter gives the equivalence (*i.e.*, $\mathcal{T}^p_{II_f} = \mathcal{T}^p_{II} \cdot F$):

$$F = \frac{z}{2z-1}\begin{bmatrix} \frac{(f_{1a}+f_{1b})z^2 - f_{1a}z}{z^2-(2-f_{1a}-f_{1b})z+(1-f_{1a})} & \cdots & \frac{(f_{ny_a}+f_{ny_b})z^2 - f_{ny_a}z}{z^2-(2-f_{ny_a}-f_{ny_b})z+(1-f_{ny_a})} \end{bmatrix} \tag{A.73}$$

This result implies that, for systems with type 2 disturbances, the IMC filter that will give the same performance as the linear quadratic optimal output feedback or new state-estimation-based MPC will be generally quite complex. Indeed, in order to establish the equivalence, $F$ must be chosen as

$$F = (Q)_r^{-1} Q_{II_f} \tag{A.74}$$

where $(Q)_r^{-1}$ denotes a right inverse of the IMC controller $Q$ (with R = 0) and $Q_{II_f}$ is a dynamic operator relating the input $w_i$ to the output $w_o$ through following equations:

$$\tilde{\mathcal{Y}}(k) = M^I \tilde{\mathcal{Y}}(k-1) + \mathcal{S}\Delta u(k-1) \tag{A.75}$$

$$\Delta u(k) = Q w_o(k) \tag{A.76}$$

$$w_o(k) = -K_{MPC}(M_p \tilde{\mathcal{Y}}(k) + \mathcal{T}^p_{II_f} w_i(k)) \tag{A.77}$$

Such an $F$ will be extremely complex in general. Exceptions are minimum-phase systems (*i.e.*, systems that have no zero outside the unit disk and are of relative degree 1) for which choosing $p = m = 1$ yields the MPC regulator that is equivalent to the linear quadratic optimal state feedback regulator (assuming zero input weight has been used).

The IMC design philosophy is to make the IMC controller ($Q$ in Figure A.2) to be

close to the inverse of the plant model ($\tilde{P}^{-1}$). This assures that the complementary sensitivity function is approximately $F$. In our framework, we can take a similar approach: Namely, we may abandon the input weighting completely (*i.e.*, $\Lambda = 0$) and use the filter parameters (having a direct connection to $F$) as the only adjustable parameters for robustness. For minimum-phase systems with type 1 disturbances, it can be shown that the closed-loop transfer function from the output disturbance $\check{d}(z)$ to the output $\check{y}(z)$ for $\Lambda = 0$ is as follows:

$$\mathcal{F}_{yd} = I - \begin{bmatrix} \frac{f_1}{z-(1-f_1)} & & \\ & \cdots & \\ & & \frac{f_n}{z-(1-f_n)} \end{bmatrix} \tag{A.78}$$

Hence, for minimum-phase systems, the state-estimation-based MPC with zero input weighting gives a first-order closed-loop response of time constant $-T/\ln(1-f_i)$. For minimum-phase systems with type 2 disturbances, the closed-loop transfer function from the output disturbance $\check{d}(z)$ to the output $\check{y}(z)$ for $\Lambda = 0$ is as follows:

$$\mathcal{F}_{yd} = I - \begin{bmatrix} \frac{(f_{1a}+f_{1b})z-f_{1a}}{z^2-(2-f_{1a}-f_{1b})z+(1-f_{1a})} & & \\ & \cdots & \\ & & \frac{(f_{ny a}+f_{ny b})z-f_{ny a}}{z^2-(2-f_{ny a}-f_{ny b})z+(1-f_{ny a})} \end{bmatrix} \tag{A.79}$$

With the tuning rule (A.41), the state-estimation-based MPC with zero input weighting gives a second-order closed-loop response of time constants $-T/\ln\sqrt{1-f_i}$. This IMC-based tuning approach simplifies controller tuning considerably; however, for "ill-conditioned" MIMO systems such as a high-purity distillation column, the input weighting may serve as a useful tuning parameter since it can prevent the control system from being "directionally sensitive" [37].

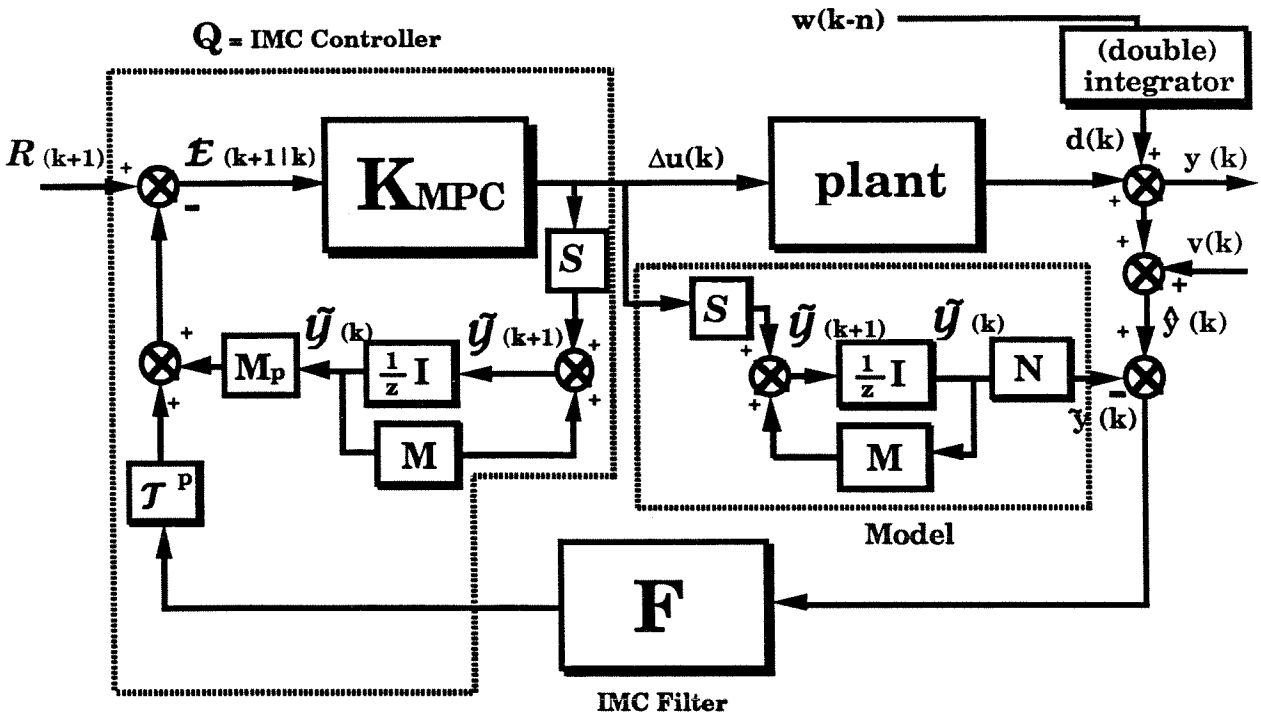


Figure A.2. Block Diagram of Internal Model Control

## A.9 Numerical Example

### A.9.1 Example A: Distillation Column Base Level Control

#### Problem Description

The behavior of the liquid level in the column base of a distillation column can be described as follows:

$$y(s) = Pu(s) + d(s) \tag{A.80}$$

where $u(s)$ represents the steam input (manipulated variable) and $d(s)$ represents the effect of various disturbances on the liquid level. The following model form was found to describe the behavior of many industrial columns adequately [8,50]:

$$P = \frac{1}{s}(1 - 2e^{-\theta s}) \tag{A.81}$$

Hence, it is an integrating system and exhibits inverse response behavior. The objective of the closed-loop control is to maintain a constant liquid level in the face of disturbances $d$. In this example, we treat the following two types of disturbances:

$$d(s) = d_I \equiv \frac{1}{s}P(s) \quad \text{Step Disturbance at the Input} \tag{A.82}$$

$$d(s) = d_O \equiv \frac{1}{s^2} \quad \text{Ramp Disturbance at the Output} \tag{A.83}$$

In practice, the dead-time $\theta$ is often not known exactly. To investigate the robustness of MPC controllers to dead-time uncertainty, we choose the following transfer functions as the model and the real plant:

*Model*

$$\tilde{P} = \frac{1}{s}(1 - 2e^{-s}) \tag{A.84}$$

*Plant*

$$P = P_0 \equiv \frac{1}{s}(1 - 2e^{-s}) \tag{A.85}$$

$$P = P_- \equiv \frac{1}{s}(1 - 2e^{-0.5s}) \tag{A.86}$$

$$P = P_+ \equiv \frac{1}{s}(1 - 2e^{-1.5s}) \tag{A.87}$$

$$\tag{A.88}$$

When the plant is described by $P_0$, the model matches the plant exactly. When the plant is described either by $P_-$ or by $P_+$, the model has a dead-time error of 1/2 minute.

## Results from State-Estimation-Based MPC

Since the system is an integrating system with type 2 disturbances, we used the state-estimation technique described in Section A.4.3. The following MPC parameters were

used:

- Sampling Time: 0.1 minute
- Number of Step-Response Coefficients (n): 50
- Prediction Horizon (p): 50 sampling units
- Number of Calculated Input Moves (m): 10 sampling units
- Input Weighting: 0
- Output Weighting: 1

The filter parameter $f_a$ was varied to examine its effect on the robustness of the resulting closed-loop system and $f_b$ was set according to the single parameter tuning rule (A.41). The closed-loop responses to the disturbances $d_I$ and $d_O$ (starting at t=1) for $P = P_0, P_-$, and $P_+$ are shown in Figures A.3 - A.5 respectively. In order to stabilize the closed-loop system with 1/2 minute delay errors ($P = P_-$ or $P = P_+$), the parameter $f_a$ had to be chosen as low as 0.1 (choosing $f_a = 0.2$ resulted in instability for $P = P_+$). The simulations show that the filter parameter $f_a$ indeed determines the speed of the closed-loop response and can be used to affect the robustness of the closed-loop system.

## A.9.2 Example B: SISO System with "Slow" Disturbances

### Problem Description

Let us consider a single-input/single-output system described by

$$y(s) = \frac{100}{s+1}u(s) + d(s) \tag{A.89}$$

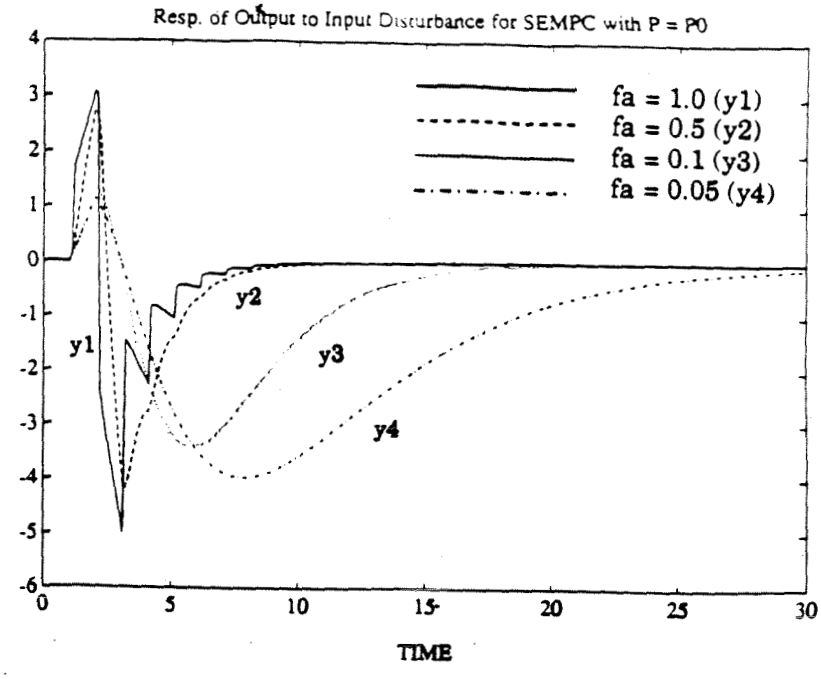


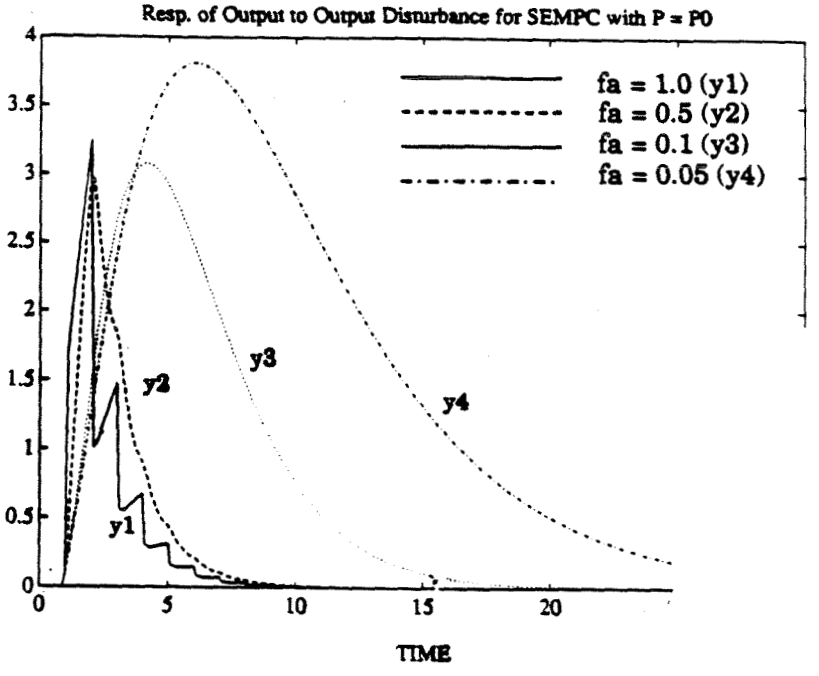


Figure A.3. Responses of the Output to Input/Output Disturbances for $P = P_0$ Under State-Estimation-Based MPC

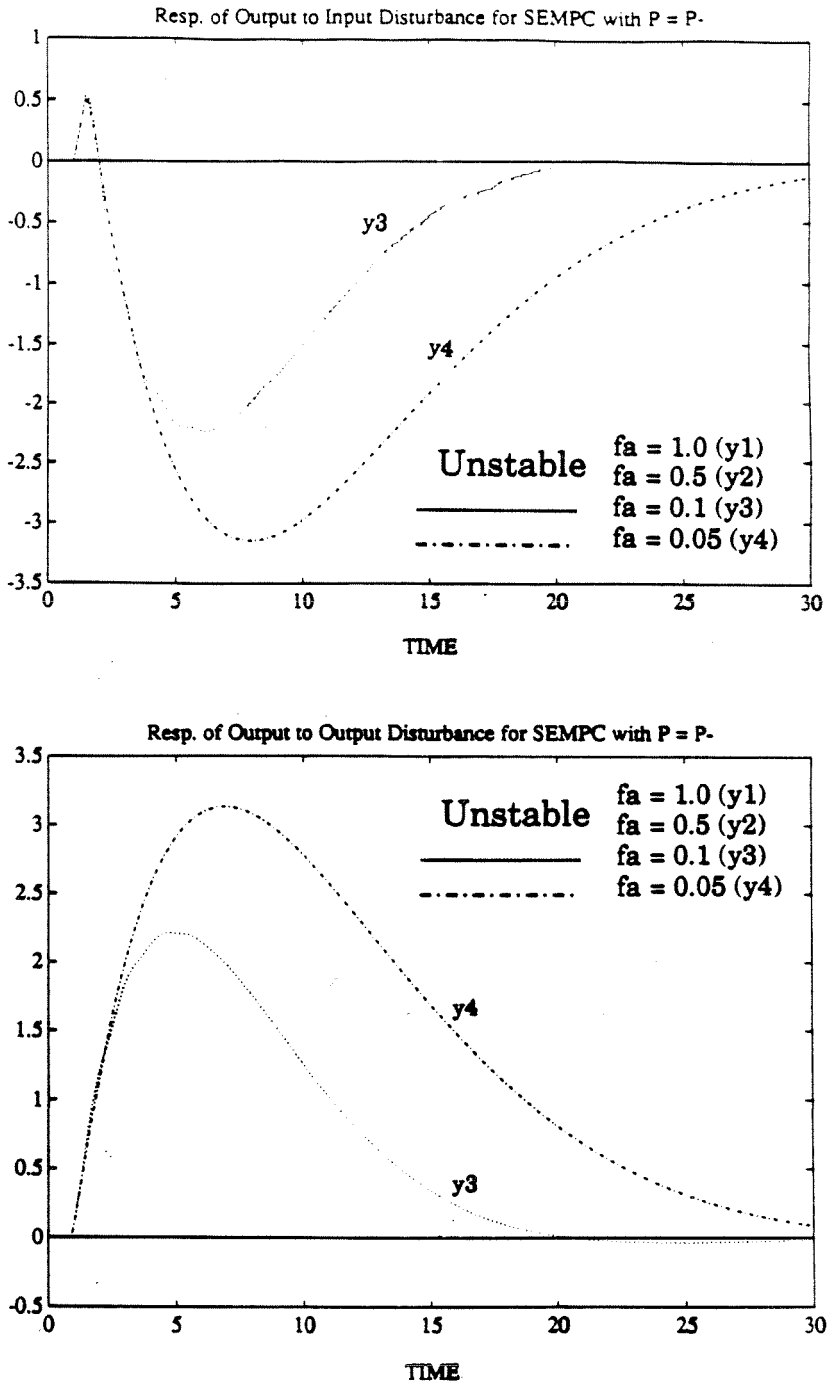


Figure A.4. Responses of the Output to Input/Output Disturbances for $P = P_-$ Under State-Estimation-Based MPC

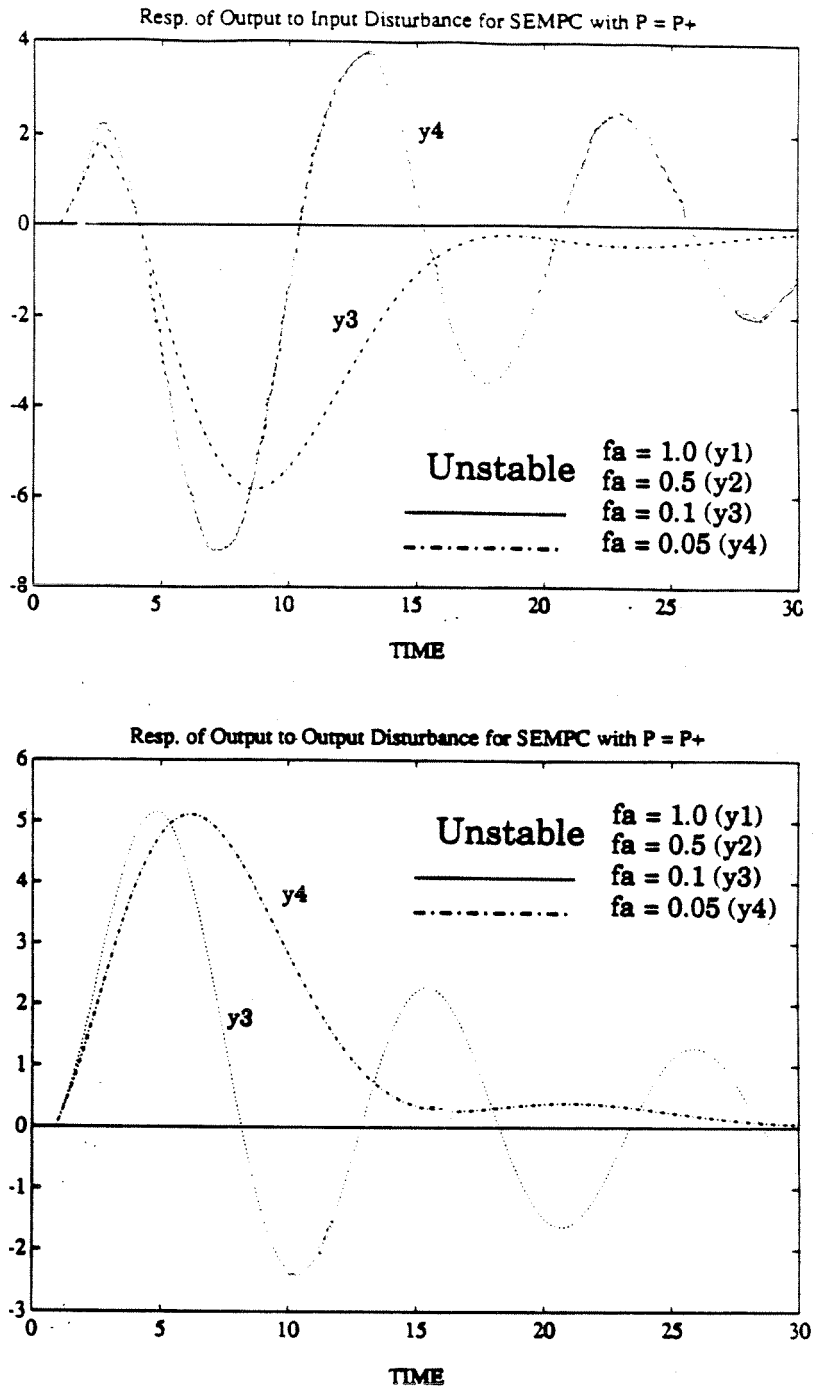


Figure A.5. Responses of the Output to Input/Output Disturbances for $P = P_+$ Under State-Estimation-Based MPC

and subjected to the following disturbances:

$$d(s) = d_A(s) \equiv \left(\frac{100}{100s+1}\right)\frac{1}{s} \quad \text{Disturbance A} \tag{A.90}$$

$$d(s) = d_B(s) \equiv \frac{1}{s} \quad \text{Disturbance B} \tag{A.91}$$

Hence, Disturbance A is a step disturbance added to the output through "slow" dynamics and Disturbance B is simply a step disturbance added to the output directly.

## Results

We use the state-estimation-based MPC to minimize the effect of the disturbances on the output. The sampling time, prediction horizon, number of input moves, and input/output weights are chosen as in Example A. We compare the results obtained from using two different types of state estimators: a Type 1 estimator for which the disturbance is assumed to be integrated white noise ($M = M^S$) and a Type 2 estimator for which the disturbance is assumed to be double-integrated white noise ($M = M^I$). Figure A.6 shows the closed-loop simulations of the output to Disturbances A and B (starting at t=1) under the MPC controller with a Type 1 estimator. Figure A.7 shows the same closed-loop simulations when the Type 1 estimator is replaced by a Type 2 estimator. Although the MPC controller with the Type 1 estimator rejects Disturbance B (a step disturbance at the output) adequately, the responses of the output to Disturbance A (a "slow" disturbance) with the same controller are poor. The settling times for all values of $f$ are unacceptably long. This is because an MPC controller with a Type 1 estimator projects the future outputs assuming the disturbance remains constant in the future; this is clearly not justified for Disturbance A. On the other hand, for the MPC controller with a Type 2 estimator, the responses of the output to Disturbance A are completely adequate. This improvement is due to the fact that an MPC controller with a Type 2 estimator projects the

future outputs assuming that the *slope* of the disturbance remains constant in the future. For disturbance A, this assumption is well justified for the chosen prediction horizon. While the responses of the output to Disturbance B are not as good as those obtained for the Type 1 estimator, they are also quite acceptable.

## A.10 Conclusions

In this article, we presented a state-space formulation of Model Predictive Control. Based on state-estimation techniques, we showed that MPC can be generalized to integrating systems and systems with white measurement noise without introducing additional complexity to MPC. We showed that under simple, but meaningful disturbance/noise assumptions, the special structure of the step response model allows us to parametrize the optimal estimator in terms of a real parameter vector that can be used for on-line tuning. The state-space perspective also led to very simple tuning rules for stability and robustness: namely, the MPC controller can be interpreted as a state-observer-based compensator and its stability, sensitivity and robustness are determined by the observer poles (which can be determined directly by the introduced adjustable parameter) and regulator poles (which are determined by prediction horizon, input weighting, *etc.*). We also made a connection between the new technique and the traditional MPC techniques such as Internal Model Control and Dynamic Matrix Control. Several examples demonstrated that the new state-estimation-based MPC can treat a wider range of problems for which the conventional techniques either would not have been applicable or would have led to poor results regardless of tuning.

**Acknowledgement:** Support from the National Science Foundation and the Petroleum Research Fund administered by the American Chemical Society is gratefully acknowledged.

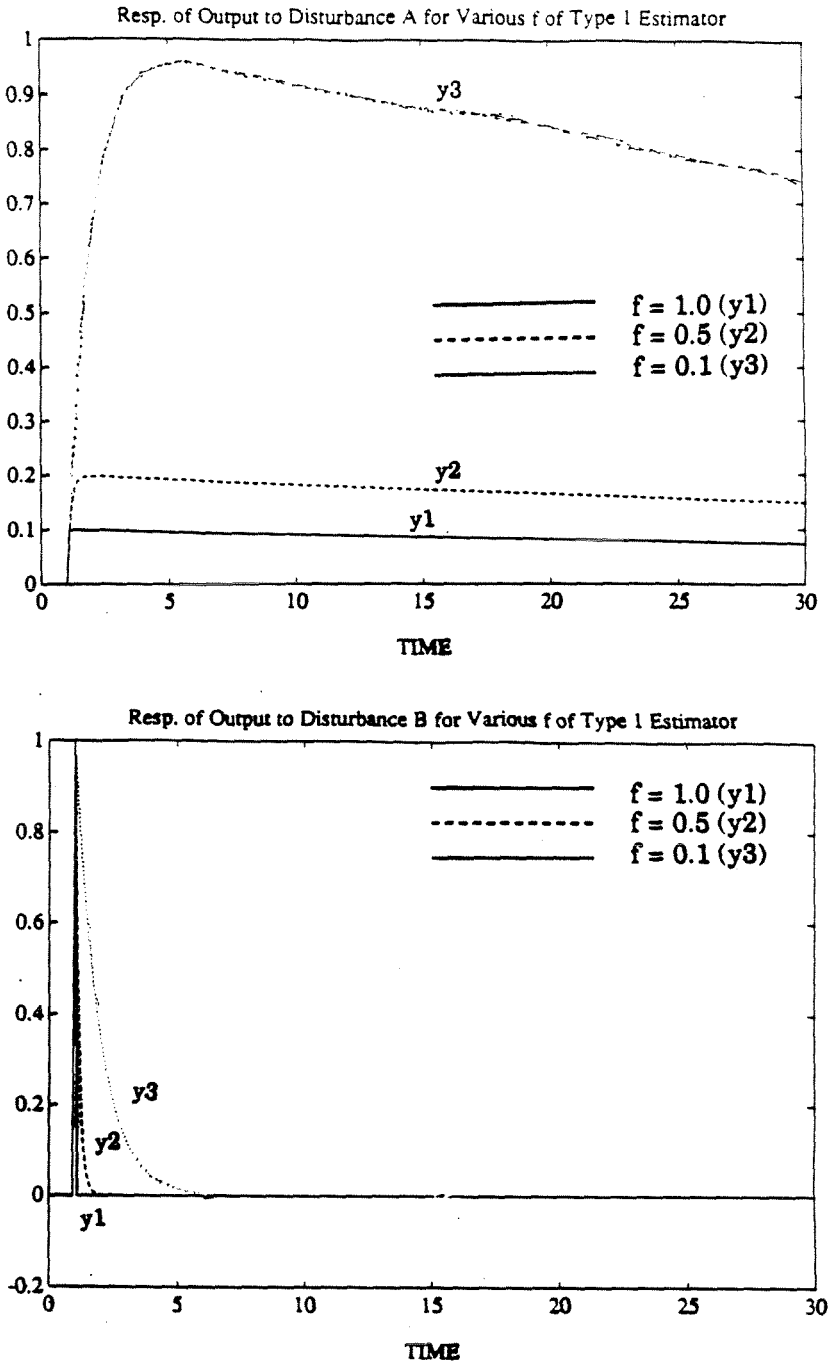


Figure A.6. Responses of the Output to Disturbances A and B Under MPC with a Type 1 Estimator

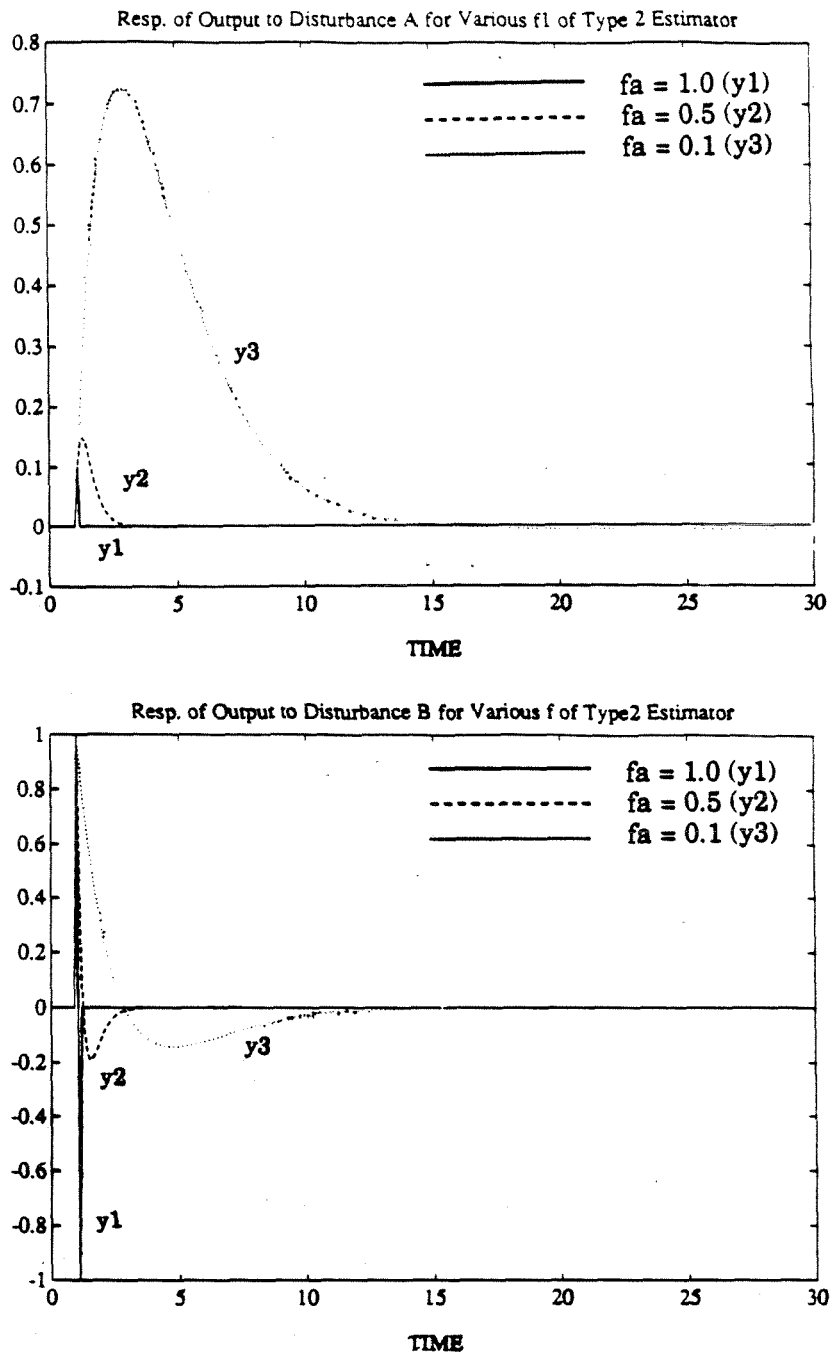


Figure A.7. Responses of the Output to Disturbances A and B Under MPC with a Type 2 Estimator

# Appendix B

# Case Study: A High-Purity Distillation Column

## Abstract

The typical literature problems studied in robust control involve the design of a controller for a system with specific actuators and sensors. However, the success of most process control applications depends on more than just controller design. For example, a correct control structure selection is as important to the successful closed-loop control as the controller design. In addition, various operational aspects, such as constraint handling and sensor/actuator failure tolerance, that are often neglected in the literature, can be critical. In this article, we bring together a number of robust control theories to develop systematic methods for control structure selection and controller design. As case study, we use a high purity distillation column separating an ideal binary mixture. Distillation can benefit immensely from tight, reliable control; however, the control is complicated by many practical issues such as large model uncertainty, distinct high and low gain directions, and long sampling delays and operational unreliability of the composition measurements. Even though the potential benefits of robust control for distillation control are high, its application to industrial distillation columns has been virtually nonexistent. It is demonstrated in this work that the Structured Singular Value Theory provides a convenient framework to develop a pratical, systematic control structure selection method. The control struc-

ture selection method is applied to the sensor selection problem for the high-purity distillation column. In addition, robust control and optimization techniques are combined into a control technique that incorporates practical aspects such as constraint handling and actuator/sensor failure tolerance as well as robustness. Through the application to the high-purity distillation column, the technique is shown to be an effective practical solution to complex process control problems.

## B.1 Introduction

The typical robust control problems studied in the literature are stated as follows: Design a controller for a given system with specific sensors and actuators such that performance specifications are met despite model uncertainty. However, this alone does not fully address the problem of designing a successful robust control system in practice. One of the reasons is that the success of most process control applications depends on more than just controller design. For example, control structure selection which refers to the choice of actuators/sensors and their pairing is as important as control system design. A wrong choice of actuators/sensors may put fundamental limitations on the system's closed-loop performance that cannot be overcome by "smart" controller design. Even the problem of designing a control system for a chosen set of actuators and sensors is not as simple in practice as most control literature states. "Robust performance" (*i.e.*, guaranteeing a certain performance level for all plants within the prescribed uncertainty set) is rather an ill-defined concept in practice, since rigorous, yet nonconservative modelling of system uncertainty is virtually impossible for most complex practical systems. In addition, performance of a control system in practical applications is judged upon many other aspects than mere robustness. The control system's ability to handle hard process constraints and actuator/sensor failures is as important as its robustness to model uncertainty.

Distillation column control serves as a good industrial example to elucidate this

point. Distillation is a unit operation in chemical engineering that can benefit significantly from improved control. Improved product composition control enables distillation columns to be operated at a point closer to the economically optimal operating point leading to significant energy savings and higher product yields. Application of robust control theories can potentially bring significant advances in the state-of-the-art of distillation control. However, even after a decade of numerous theoretical advancements in robust control, control structure selection decisions for industrial distillation control are still carried out in an intuitive, *ad hoc* fashion rather than systematically. In addition, most industrial columns are currently controlled by single-loop PID controllers. The main reason for the lack of application of elegant robust control theories is that the control problem for distillation columns is far too complex for most theories to be applied directly. Firstly, there are at least five actuators and as many temperature measurements as the number of trays available for the product composition control. From these actuators and sensors, an appropriate subset must be selected since three of the actuators must be used for inventory and pressure control and using all temperature measurements results in an unnecessarily complex and expensive control system. Secondly, modelling the uncertainty rigorously and parsimoniously including all nonlinear effects is practically impossible for distillation columns. Without a rigorous uncertainty model, application of complex robust design methods is not justified. Thirdly, the actuators naturally have constraints on their magnitudes and rates of change. In addition, there may be some hard constraints imposed on the outputs for safety reasons. Lastly, measurements of the key controlled variables, the product compositions, have significant delays associated with them and are operationally unreliable. The control system must be able to incorporate multi-rate (MR) sampled measurements, that is "fast-sampled" secondary measurements, the tray temperatures, and "slow-sampled" primary measurement, the composition measurements. In addition, it should maintain performance integrity in the face of

frequent actuator/composition-measurement failures.

In this work, we bring together a number of robust control theories developed during the past decade and tailor them into a unified control structure selection and control system design methodology that is applicable to practical problems. As a secondary objective, we wish to identify some of the shortcomings of available robust control theories in terms of their practical applicability and tools that would help bring these theories closer to practical problems. As case study, we use a high-purity distillation column that has been previously studied by many investigators in the context of robust control [60,57,41]. First, we apply a general, systematic control structure selection methodology based on the Structured Singular Value (SSV) Theory [48,41,39] to the sensor placement problem for the distillation column. We show that, even when the complete knowledge of the system uncertainty is not available, the SSV Theory can be useful in reducing the number of control structure candidates and obtaining insights that are helpful in eventually identifying a proper candidate. Next, we show how robust control and on-line optimization techniques can be combined and tailored into a design method that addresses relevant issues such as model uncertainty, constraints, measurement/actuator failure tolerance, and multi-rate sampling. The control system design method proposed is by no means "the answer" to all practical robust control problems. It should be viewed rather as a current, practical answer to complex practical control problems such as the composition control problem in distillation columns. By presenting what we believe is the best current solution to these control problems, we hope to encourage theoreticians to conduct more research on aspects of robust control that would help narrow the extant gap between theory and practice.

## B.2 General Framework

### B.2.1 Description of Distillation Column and its Control Problem

The distillation column we study in this paper is depicted in Figure B.1(a). The column has 41 stages including the reboiler and the condenser, and separates an ideal binary mixture into two high-purity (99% molar composition) products. For details about the column's operating conditions and modelling assumptions used, readers are referred to Appendix A of Morari & Zafiriou [50]. The main disturbances entering the column are those in the feed since its flowrate ($F$) and composition ($z_F$) can change significantly according to the conditions of other plant units. The objective of distillation control is to maintain the product compositions at a specified operating point despite these disturbances. The available manipulated variables are reflux ($L$), boilup ($V$), distillate flow ($D$), bottom flow ($B$), and overhead vapor flow ($V_T$). Three of these variables must be used for the condensor/reboiler inventory control and column pressure control. In order to simplify the presentation somewhat, we assume in this paper that the variables $D$, $B$, and $V_T$ are used for the condenser/reboiler inventory and pressure control respectively, and the variables $L$ and $V$ are to be used for the composition control. This so called "LV configuration" is the configuration that is most commonly used in industry. For the purpose of feedback control, six temperature measurements are available: the temperatures of the reboiler ($T_1$), of Tray # 7 ($T_7$), of Tray # 17 ($T_{17}$), of Tray # 25 ($T_{25}$), of Tray # 5 ($T_{35}$), and of the condenser ($T_{41}$). These measurements are sampled every minute (which is adquate for the desired closed-loop bandwidth) and are subjected to measurement noise ($v_s$) arising from the column pressure variation and other sources. Among the six temperatures, an appropriate subset is to be selected. In addition to the temperature measurements, measurements of the product compositions are available through composition analyzers. However, the sampling rates and delays for these

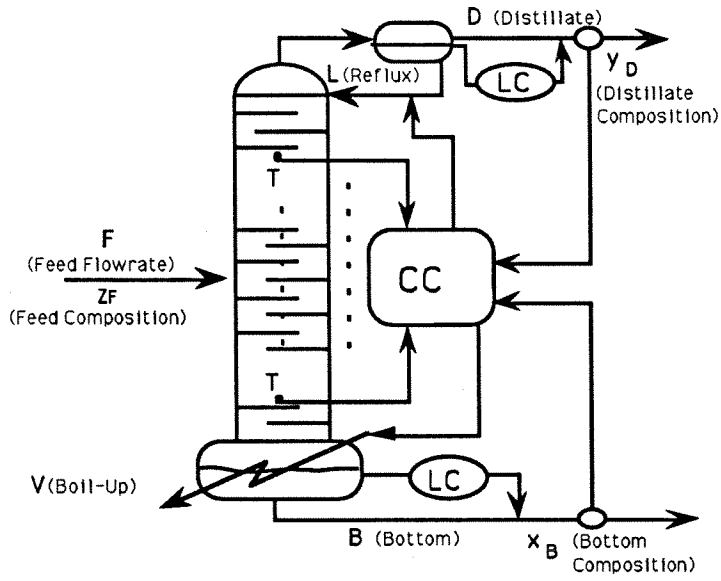


(a) High-Purity Distillation Column

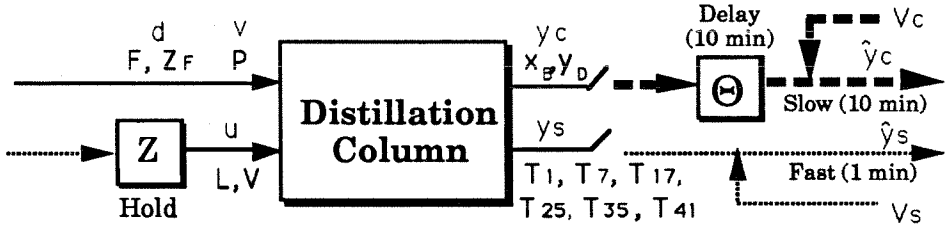


(b) LV Composition Control Problem

Figure B.1. Schematic Representation of High-Purity Distillation Column and its Control Prolblem

measurements are too long (both 10 minutes) and their operational reliability too low to be effective for the desired closed-loop control by themselves. Figure B.1(b) summarizes the control problem in terms of block diagram. For all analyses and design in this paper, we use a 13th order discrete-time linear model derived from the full 41st order continuous-time linearized model through balanced realization and standard discretization techniques [46,3]. The validity of these models were checked carefully through frequency-domain analyses and simulations.

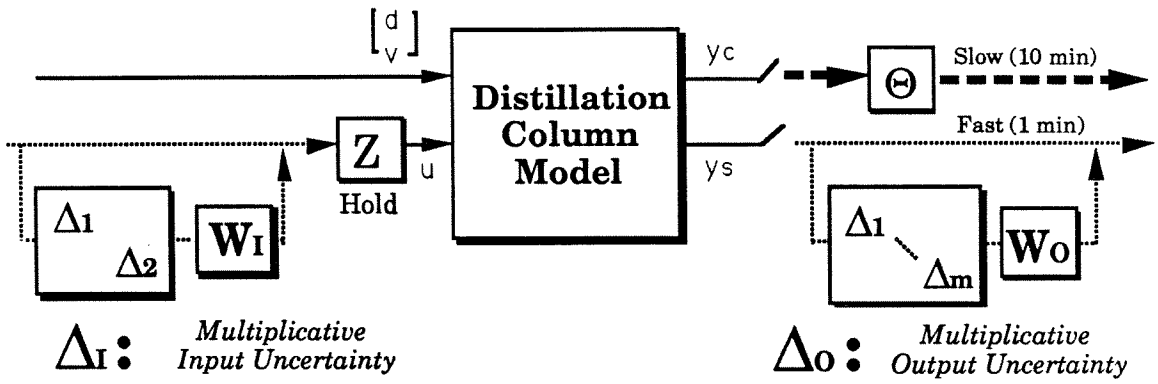


Figure B.2. Parsimonious Uncertainty Modelling for High-Purity Distillation Column: Input and Output Multiplicative Uncertainty

## B.2.2 Uncertainty Modelling

Modelling system uncertainty rigorously and nonconservatively for practical systems is a very difficult task. Currently, there exists no general methodology that enables engineers to carry out this important task. Traditionally, researchers have suggested a conservative approach (overmodelling) to modelling system uncertainty so that "robust performance" indeed guarantees the specifed performance level. However, our experience with complex chemical systems such as distillation columns and packed-bed reactors has convinced us that it is almost impossible to obtain a practically useful uncertainty description that encompasses *all* system/model mismatch including the effects of nonlinearity [9]. Hence, in this work, we take the approach of "parsimonious" uncertainty modelling, that is we model only the uncertainty that we believe exists and is important for closed-loop stability and performance. The uncertainty structure we chose is shown in Figure B.2. $\Delta_I$ represents the structured multiplicative uncertainty on the inputs; it can be interpreted as relative errors on the actuator signals $L$ and $V$. $\Delta_O$ is the structured multiplicative uncertainty on the outputs; it is interpreted as relative errors on the sensor signals. The precise mathematical nature of these uncertainty blocks will be given in the following section. The particular uncertainty

structure was chosen for the following reasons:

- Such types of uncertainty always exist, especially in distillation columns.
- They are important for closed-loop stability and performance since they lie within the feedback path.
- The multiplicative input uncertainty was shown to be the dominating uncertainty for LV high-purity distillation columns because of their ill-conditioning property [60].

For control structure selection, the "parsimonious" uncertainty modelling approach is clearly justified since control strucuture selection involves eliminating undesirable candidates for which a controller achieving "robust performance" cannot be found for the given uncertainty structure and level. An overly conservative uncertainty description will either leave no viable candidate or eliminate some of the desirable candidates. For control system performance analysis, we should take "robust performance" as a minimum necessary robustness requirement. The closed-loop performance of a control system should be ultimately judged through simulation and actual implementation. This is true for almost all complex process control problems, where rigorous modelling of uncertainty is difficult.

### B.2.3 Structured Singular Value Analysis

Since the objective of the paper is not to present a full account of the Structured Singular Value (SSV) Theory, our discussion on the subject will be brief and somewhat incomplete. For a complete and rigorous discussion on the subject, readers are referred to Doyle [17]. We will develop this paper in the discrete-time setting; however, all theories presented in the paper (except for the finite receding horizon control technique) have their continuous-time counterparts. The SSV analysis is not applicable to multi-rate sampled-data systems without introducing approximations

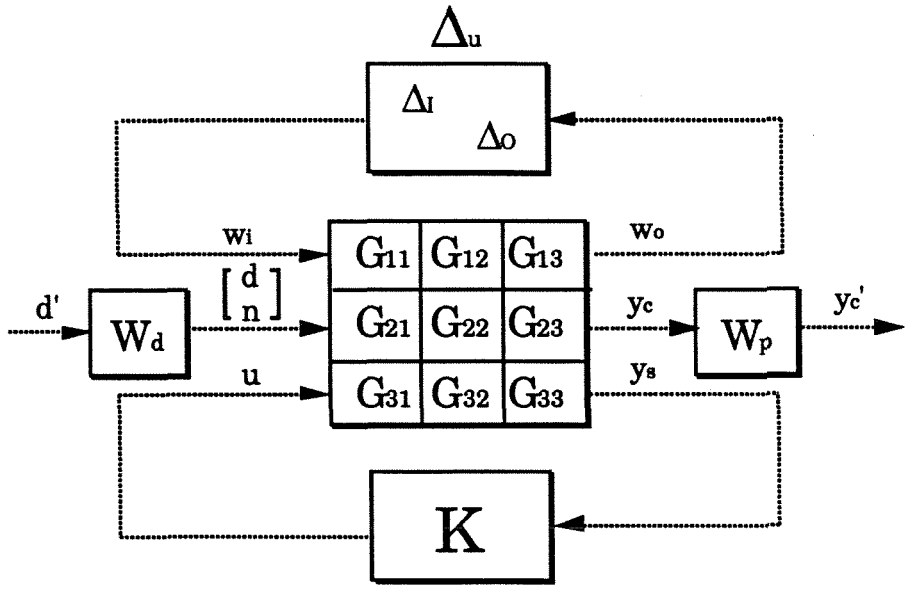


Figure B.3. Putting the High-Purity Distillation Column Control Problem Into SSV Framework

[50] or conservativensss [16]. Hence, we use the SSV analysis to analyze the control systems involving the secondary measurements only. In the discrete-time setting, we can manipulate the block diagram of Figure B.2 and express the closed-loop system as a Linear Fractional Transformation (LFT) of $G$ and $\Delta_u$, as shown in Figure B.3. $G$ is the pulse transfer function model relating the input vectors ($w_i$, $d$, $v_s$ and $u$) to the output vector ($w_o$, $y_c$, and $y_s$). $\Delta_u$ is a structured norm-bounded perturbation to $G$ that belongs to the set $\mathbf{B\Delta_u}$ defined at each frequency as follows:

$$\mathbf{B\Delta_u} = \{\Delta_u \in \mathbf{\Delta_u} : \bar{\sigma}(\Delta_u) \leq 1\} \tag{B.1}$$

$$\mathbf{\Delta_u} = \left\{ \begin{bmatrix} \Delta_1 & & \\ & \cdots & \\ & & \Delta_\ell \end{bmatrix} : \Delta_i \in \mathcal{C},\ 1 \leq i \leq n \right\} \tag{B.2}$$

$\ell$ is the number of actuators (2 for this problem) plus the number of temperature measurements used. $W_d$ and $W_p$ represent user-chosen frequency weighting functions

that are used to normalize the external input and controlled output signals. The standard definition of "robust performance" is that the "worst-case" induced $\ell_2$ norm (*i.e.*, the energy norm) of the closed-loop operator from the weighted external input vector $d'$ to the weighted output error vector $y'_c$ is less than one. Mathematically, robust performance condition is expressed as follows:

$$\max_{\Delta \in \mathbf{B}\boldsymbol{\Delta}_\mathbf{u}} \max_{d' \in \ell_2} \frac{||\mathcal{F}_{y'_c d'}(\Delta_u, K)||_{\ell_2}}{||d'||_{\ell_2}} < 1 \tag{B.3}$$

where $\mathcal{F}_{y'_c d'}(\Delta_u, K)$ is the closed-loop operator from $d'$ to $y'_c$. Doyle [20] showed that, when the closed-loop system is *nominally* stable, robust performance can be tested conveniently through the following frequency-by-frequency condition on a function called $\mu$ (see Doyle [17] for definition of $\mu$):

$$\mu \left[ \begin{array}{cc} \boldsymbol{\Delta}_\mathbf{u} & \\ & \boldsymbol{\Delta}_\mathbf{p} \end{array} \right] \left( N_{11} + N_{12} K (I - N_{22} K)^{-1} N_{21} \Big|_{z = e^{j\omega_n}} \right) < 1 \quad 0 \le \omega \le \omega_n \tag{B.4}$$

where

$$\boldsymbol{\Delta}_\mathbf{p} = \left\{ \Delta : \Delta \in {}^{\dim\{y'_c\} \times \dim\{d'\}} \right\} \tag{B.5}$$

$$N_{11} = \left[ \begin{array}{cc} I & \\ & W_p \end{array} \right] \left[ \begin{array}{cc} G_{11} & G_{12} \\ G_{21} & G_{22} \end{array} \right] \left[ \begin{array}{cc} I & \\ & W_d \end{array} \right] \tag{B.6}$$

$$N_{12} = \left[ \begin{array}{cc} I & \\ & W_p \end{array} \right] \left[ \begin{array}{c} G_{13} \\ G_{23} \end{array} \right] \tag{B.7}$$

$$N_{21} = \left[ \begin{array}{cc} G_{31} & G_{32} \end{array} \right] \left[ \begin{array}{cc} I & \\ & W_d \end{array} \right] \tag{B.8}$$

$$N_{22} = G_{33} \tag{B.9}$$

and $\omega_n$ is the Nyquist frequency corresponding to the sampling time of the secondary measurements (*i.e.*, $\omega_n = \frac{\pi}{T}$). In this work, we use instead the following robust performance condition based on a very "tight" upperbound (exact for $\mathbf{\Delta_u}$ involving less than 3 blocks and close within 98-99% for most problems) of $\mu$:

$$\inf_{D \in \mathcal{D}_{rp}} \bar{\sigma} \left\{ D \left( N_{11} + N_{12} K (I - N_{22} K)^{-1} N_{21} \right) \Big|_{z=e^{j\omega_n}} D^{-1} \right\} < 1 \quad 0 \leq \omega \leq \omega_n \quad \text{(B.10)}$$

where

$$\mathcal{D}_{rp} = \{ \text{diag} \left[ d_1, \cdots, d_n, I_{\dim\{y_c'\}} \right] : d_j \in \mathcal{R}_+ \} \quad \text{(B.11)}$$

## B.3 Control Structure Selection

In this section, we present a control structure selection methodology based on the SSV theory and its application to the high-purity distillation column. First, we propose a general approach to the control structure selection problem and propose screening tools that can be used in efficient elimination of undesirable candidates. Next we introduce a simple robust control system design method called "Inferential Loop-Shaping," and screening tools that can help further reduce the number of candidates in the context of this particular design approach. The results obtained from applying these screening tools and the design method to the high-purity column are presented.

### B.3.1 General Approach to Control Structure Selection

The approach we propose for control structure selection is illustrated in Figure B.4. *Control structure candidates* consist of all possible combinations of the available actuators and sensors. Owing to the combinatorial nature of the problem, the number of candidates is often very large. For the distillation column under consideration, there are 10 different actuator combinations (since 2 actuators must be selected out of 5) and 63 different sensor combinations (since the number of sensors is not fixed).

This leads to 630 control structure candidates. Naturally, a method to reduce the number of candidates before applying detailed analyses will be of significant practical value. Since we formulated "robust performance" as a minimum necessary robustness requirement, the first proposed step is to eliminate those candidates for which a controller achieving the "robust performance" does not exist no matter what controller design method is used. The criteria that can be used to accomplish this screening will be referred to as "*general screening tools.*" This screening process leaves candidates for which a control system with satisfactory performance may potentially exist. However, this alone may not reduce the number of candidates to a low enough level. Also, it is not clear if control design methods available to the engineer can lead to a controller achieving the "robust performance." Hence, an additional screening may be carried out subsequently in the context of a chosen design approach. That is, one may choose to further eliminate those candidates for which the particular design approach under consideration does not yield a controller achieving "robust performance." The criteria that can be used under a particular design approach will be called "*design-dependent screening tools.*" If the screening under a particular design approach does not leave any viable candidate, one has to assume a more complex, involved design approach and repeat the screening process. Once the number of candidates is reduced down to a low enough level, one can apply more detailed analysis methods or evaluate each candidate through the actual control system design and simulation.

### B.3.2 General Screening Tools

Due to the space limitation, our discussion on the theoretical aspects of the proposed screening tools will be rather brief. Readers are referred to Lee *et al.* [39] for details. In order to facilitate the exposition, we limit our discussion to open-loop stable systems. However, all screening tools presented are applicable to open-loop unstable

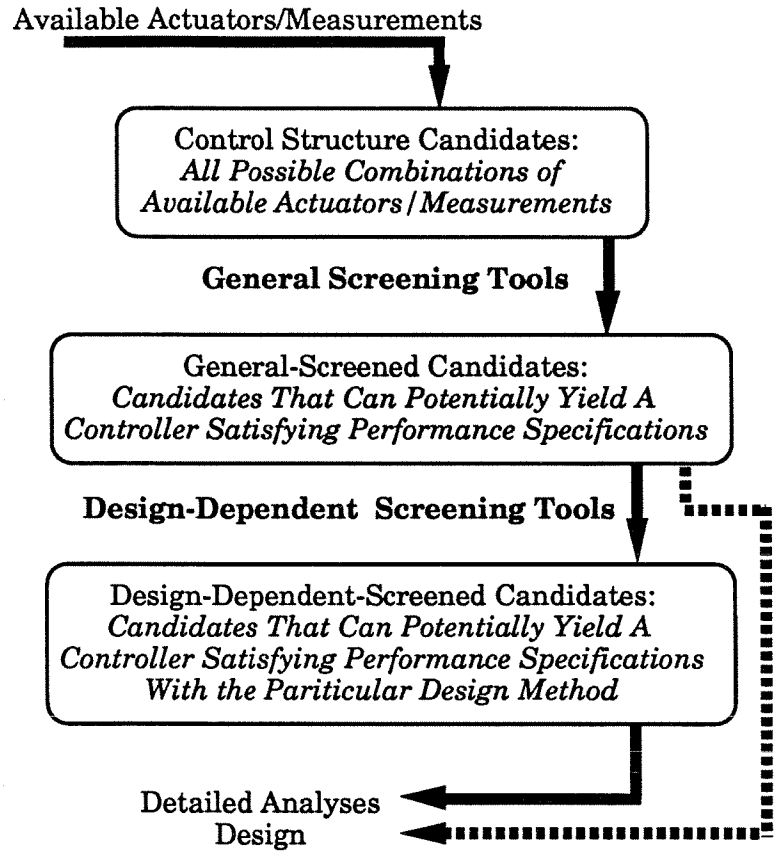


Figure B.4. Schematic Representation of Proposed Control Structure Selection Procedure

systems as well.

Since the objective is to eliminate those candidates for which a controller achieving "robust performance" does not exist, it is natural to use as screening tools necessary and sufficient or necessary conditions for the existence of such a controller. Invoking the Youla parametrization of all stabilizing controllers ($K \in \{\tilde{K} : \tilde{K} = -Q(I + N_{22}Q)^{-1}, Q \in \mathcal{RH}_\infty\}$) and substituting it to the condition (B.10), a necessary and sufficient condition for the existence of a robustly performing controller for a particular control structure can be stated as follows:

$$\inf_{Q \in \mathcal{RH}_\infty} \sup_{0 \le \omega \le \omega_n} \inf_{D(\omega) \in \mathcal{D}_{rp}} \bar{\sigma} \left[ D(\omega) \left( N_{11} + N_{12} Q N_{21} \right)|_{z=e^{j\omega_n}} D^{-1}(\omega) \right] < 1 \qquad \text{(B.12)}$$

The restriction of $Q \in \mathcal{RH}_\infty$ implies that it should be analytic outside the open unit disk. Unfortunately, the coupling of the parameters $Q$ and $D$ makes the condition (B.12) a nonconvex optimization and there is currently no general method of checking it. Hence (B.12) is not a viable screening tool.

At this point, let us consider dropping the *causality* requirement on $Q$, that is we allow the controller parameter $Q$ to be acausal meaning the current/future inputs of $Q$ can affect its past outputs. With relaxation of the causality requirement, the condition (B.12) can be transformed into the following frequency-by-frequency condition:

$$\inf_{Q\in\mathcal{C}^K}\inf_{D\in\mathcal{D}_{rp}} \bar{\sigma}(D(N_{11}+N_{12}QN_{21})|_{z=e^{j\omega_n}}D^{-1}) < 1 \quad 0 \le \omega \le \omega_n \tag{B.13}$$

The superscript $\{\cdot\}^K$ in $\mathcal{C}^K$ implies that it is the set of complex matrices of size $\dim\{u\} \times \dim\{y_m\}$. By reparametrizing $\tilde{Q}$ such that the matrices pre- and post-multiplying $\tilde{Q}$ in (B.13) are both unitary, the condition (B.13) can be written as

$$\inf_{\hat{Q}\in\mathcal{C}^K}\inf_{D\in\mathcal{D}_{rp}} \bar{\sigma}(D(N_{11}+\hat{N}_{12}\hat{Q}\hat{N}_{21})|_{z=e^{j\omega_n}}D^{-1}) < 1 \quad 0 \le \omega \le \omega_n \tag{B.14}$$

where $\hat{N}_{12} = N_{12}(N_{12}^*N_{12})^{-1/2}$ and $\hat{N}_{21} = (N_{21}N_{21}^*)^{-1/2}N_{21}$. $\hat{N}_{12}$ and $\hat{N}_{21}$ are both unitary matrices for all $\omega$. The following theorem shows that the condition (B.14) can be checked through two separate conditions each of which is a convex optimization problem.

**Theorem B.1** *Let $R \in \mathcal{C}^{n\times n}, U \in \mathcal{C}^{n\times r}$ and $V \in \mathcal{C}^{t\times n}$. Suppose $U^*U = I_r, VV^* = I_t$ and $U_\perp \in \mathcal{C}^{n\times(n-r)}$ and $V_\perp \in \mathcal{C}^{(n-t)\times n}$ are chosen such that $\begin{bmatrix} U & U_\perp \end{bmatrix} \in \mathcal{C}^{n\times n}$ and $\begin{bmatrix} V \\ V_\perp \end{bmatrix} \in \mathcal{C}^{n\times n}$ are unitary. Then*

$$\inf_{Q\in\mathcal{C}^{r\times t}}\inf_{D\in\mathcal{D}_{rp}} \bar{\sigma}(D(R+UQV)D^{-1}) < \alpha \tag{B.15}$$

*if and only if* $\exists X \in \mathcal{D}_{rp}$ *such that*

$$\lambda_{max}[V_\perp(R^*XR - \alpha^2 X)V_\perp^*] < 0 \tag{B.16}$$

*and*

$$\lambda_{max}[U_\perp^*(RX^{-1}R^* - \alpha^2 X^{-1})U_\perp] < 0 \tag{B.17}$$

**Proof** See Lee *et al.* [39]. ■

**Comments:**

1. (B.16) and (B.17) are convex with respect to $X$ and $X^{-1}$ respectively. Each of the two conditions is a necessary condition for the existence of a controller achieving robust performance and can be checked through standard algorithms such as cutting plane method.

2. Checking the conditions (B.16)-(B.17) together is more difficult and is not resolved at the moment except for the two block cases where $X$ can be parametrized in terms of a single positive scalar.

Using the results from Theorem B.1, we now propose the following screening tools:

**General Screening Tool #1** *Eliminate the control structures for which*

$$\inf_{X\in\mathcal{D}_{rp}} \lambda_{max}\left[(\hat{N}_{21})_\perp(N_{11}^*XN_{11} - X)(\hat{N}_{21})_\perp^*|_{z=e^{j\omega_n}}\right] \geq 0 \quad \text{for some } \omega \in [0,\omega_n] \tag{B.18}$$

**General Screening Tool #2** *Eliminate the control structures for which*

$$\inf_{X\in\mathcal{D}_{rp}} \lambda_{max}\left[(\hat{N}_{12})_\perp^*(N_{11}XN_{11}^* - X)(\hat{N}_{12})_\perp|_{z=e^{j\omega_n}}\right] \geq 0 \quad \text{for some } \omega \in [0,\omega_n] \tag{B.19}$$

**General Screening Tool #3 (2 Full-Block Cases)** *Eliminate the control structures for which*

$$\mathcal{T}_{FC}(\omega) \bigcap \mathcal{T}_{FI}(\omega) = \emptyset \quad \text{for some } \omega \in [0, \omega_n] \tag{B.20}$$

*where*

$$\mathcal{T}_{FC}(\omega) = \left\{ s \in \mathcal{R}_+ : \lambda_{max} \left[ (\hat{N}_{21})_\perp \left( N_{11}^* \begin{bmatrix} sI & \\ & I \end{bmatrix} N_{11} - \begin{bmatrix} sI & \\ & I \end{bmatrix} \right) (\hat{N}_{21})_\perp^* \Big|_{z=e^{j\omega_n}} \right] < 0 \right\} \tag{B.21}$$

$$\mathcal{T}_{FI}(\omega) = \left\{ t \in \mathcal{R}_+ : \lambda_{max} \left[ (\hat{N}_{12})_\perp^* \left( N_{11} \begin{bmatrix} tI & \\ & I \end{bmatrix} N_{11}^* - \begin{bmatrix} tI & \\ & I \end{bmatrix} \right) (\hat{N}_{12})_\perp \Big|_{z=e^{j\omega_n}} \right] < 0 \right\} \tag{B.22}$$

### B.3.3 Design-Dependent Screening Tools for Inferential Loop-Shaping

#### Inferential Loop-Shapiing

Inferential Loop-Shaping (ILS) is an extension of the multivariable loop-shaping design technique to systems with secondary measurements. We present the technique briefly, and readers are referred to Lee & Morari [41] for details.

In the standard multivariable loop-shaping, frequency-domain bounds on the maximum singular values of the sensitivity and complementary sensitivity functions that guarantee robust performance are derived and used for controller design [20]. Such bounds cannot be used for inferential control problems in general since the sensitivity function does not have the same relevance to closed-loop performance as in the

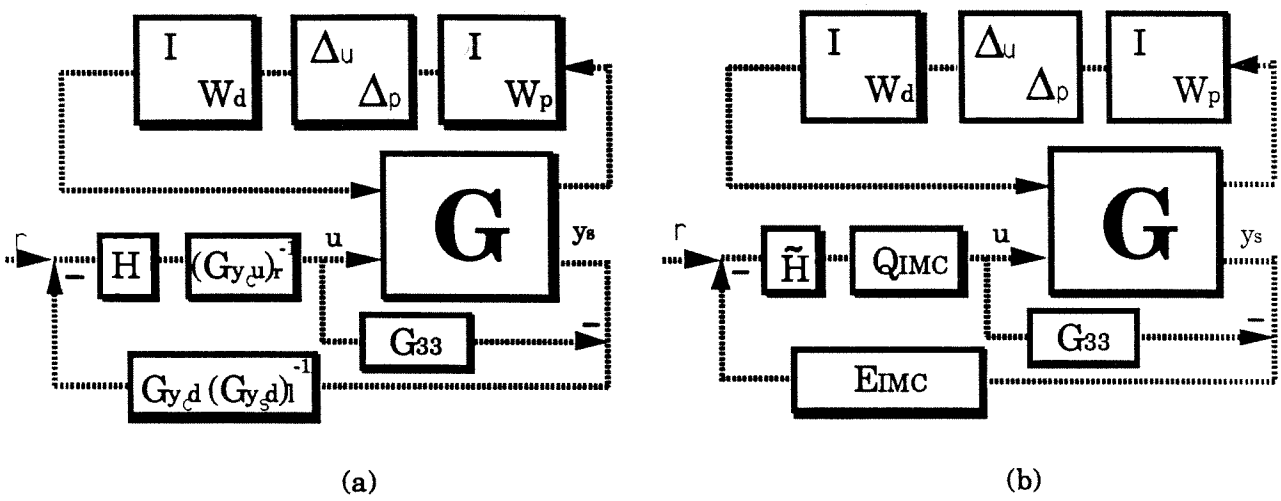


Figure B.5. "Pseudo-Complementary Sensitivty" Function for Inferential Loop-Shaping

standard loop-shaping problems. Hence, a natural extension of the standard loop-shaping technique to systems with secondary measurements is to use the bounds on those functions that play similar roles as the sensitivity and complementary sensitivity functions in the standard loop-shaping problems. Figure B.5(a) shows a parametrization of the controller $K$ in terms of $H$ that has similar implications to closed-loop stability and performance as the complementary sensitivity function does. Note that $H$ is the closed-loop transfer function from the setpoint $r$ to the controlled variable $y_c$ and $S = I - H$ is the closed-loop transfer function from $G_{y_c d}d$ to $y_c$. The following theorem enables the calculation of the "tighest" bounds on the maximum singular values of $S$ and $H$ guaranteeing robust performance.

**Theorem B.2** *Let $M \in \mathcal{C}^{n\times m}$ be written as*

$$M = R_{11} + R_{12}L(I - R_{22}L)^{-1}R_{21} \tag{B.23}$$

*where*

$$R_{11} \in \mathcal{C}^{n\times m}, R_{12} \in \mathcal{C}^{n\times p}, R_{21}, \in \mathcal{C}^{k\times m}, R_{22} \in \mathcal{C}^{k\times p} \text{ and } L \in \mathcal{C}^{p\times k} \tag{B.24}$$

*Define*

$$f(c_L) = \mu \begin{bmatrix} \mathbf{\Delta_{RP}} & \\ & \mathbf{\Delta_L} \end{bmatrix} \begin{bmatrix} R_{11} & R_{12} \\ c_L R_{21} & c_L R_{22} \end{bmatrix} \tag{B.25}$$

*where*

$$\begin{aligned} \mathbf{\Delta_{RP}} &= \left\{ \Delta : \Delta = \begin{bmatrix} \Delta & & \\ & \ddots & \\ & & \Delta_\ell \end{bmatrix} ; \sum_{i=1}^{\ell} m_i = m \quad \sum_{i=1}^{\ell} n_i = n, \quad \Delta_i \in \mathcal{C}^{m_i \times n_i} \right\} \\ \mathbf{\Delta_L} &= \left\{ \Delta : \Delta \in \mathcal{C}^{p \times k} \right\} \\ & c_L \in \Re^+ \end{aligned} \tag{B.26}$$

*Assume*

$$\mu_{\mathbf{\Delta_{RP}}}(R_{11}) < 1 \quad \text{and} \quad \det(I - R_{22}L) \neq 0 \tag{B.27}$$

*then*

$$\mu_{\mathbf{\Delta_{RP}}}(M) < 1 \tag{B.28}$$

*if*

$$\bar{\sigma}(L) < c_L^* \tag{B.29}$$

*where $c_L^*$ is that smallest $c_L$ that solves $f(c_L) = 1$.*

**Proof** See Skogestad & Morari [59]. ■

$c_L^*$ can be easily calculated through a simple search procedure such as bisection method since $f(c_L)$ is a non-decreasing function of $c_L$. The robust performance bounds on $\bar{\sigma}(S)$ and $\bar{\sigma}(H)$ are derived using Theorem B.2 by setting $L = S$ and $L = H$ respectively. The key point is that, since $S$ and $H$ both parametrize $K$, robust performance condition is satisfied if either of the bounds is satisfied at each frequency. In general, the bound on $\bar{\sigma}(S)$ is applicable in the low up to cross-over frequency region and the

bound on $\bar{\sigma}(H)$ is applicable in the cross-over to high frequency region.

One potential problem is that a right inverse of $G_{y_cu}$ and a left inverse of $G_{y_sd}$ may not exist. In addition, the usefulness of the bounds for control system design is somewhat limited when $(G_{y_cu})_r^{-1}$ or $G_{y_cd}(G_{y_sd})_\ell^{-1}$ are non-proper and/or have poles outside the unit disk. In this case, the stability and causality of $H$ does not necessarily imply the internal stability and causality of the controller $K$. Hence, $H$ is limited to those functions that yield stable, proper $(G_{y_cu})_r^{-1}HG_{y_cd}(G_{y_sd})_\ell^{-1}$, making a direct design of $H$ difficult. We can overcome this difficulty by replacing $(G_{y_cu})_r^{-1}$ and $G_{y_cd}(G_{y_sd})_\ell^{-1}$ with $Q_{IMC}$ and $E_{IMC}$ that represent the IMC controller [50] and the IMC estimator [41], as shown in Figure B.5(b). $Q$ is an approximate stable inverse of $G_{y_cu}$ through spectral factorization [50], and $E$ can be obtained using the modified Kalman filter technique with zero noise covariance matrix [49]. Now the loop-shaping bounds on $\bar{\sigma}(\tilde{S})$ and $\bar{\sigma}(\tilde{H})$ can be derived and used for design instead. With this approach, the only restriction on the "peudo-complementary sensitivity" function $\tilde{H}$ is that it should be stable and causal.

## Screening Tools for Inferential Loop-Shaping

At steady state, it is necessary that the robust performance condition is satisfied for $\tilde{S} = 0$ in order for the loop-shaping bounds to be feasible. This can be expressed in terms of the following theorem:

**Theorem B.3** *(Referring to Figure B.5(b))*

$c_{\tilde{S}}^*(0) > 0$ *if and only if*

$$\mu\begin{bmatrix} \Delta_u^* & \\ & \Delta_p \end{bmatrix}(\hat{R}(0)) < 1 \tag{B.30}$$

*where*

$$\hat{R} = \begin{bmatrix} G_{11} - G_{13}Q_{IMC}E_{IMC}G_{33} & (G_{11} - G_{13}Q_{IMC}E_{IMC}G_{32})W_d & G_{13}Q_{IMC} \\ W_p(G_{21} - G_{23}Q_{IMC}E_{IMC}G_{31}) & W_p(G_{22} - G_{23}Q_{IMC}E_{IMC}G_{32})W_d & W_pG_{23}Q_{IMC} \\ -E_{IMC}G_{31} & -E_{IMC}G_{32}W_d & 0 \end{bmatrix} \tag{B.31}$$

**Proof** Trivial from the fact that $f(c_{\tilde{S}})$ is a nondecreasing function of $c_{\tilde{S}}$ and hence $f(0) < 1$ in order for $c^*_{\tilde{S}}$ to be nonzero. ■

The condition (B.30) can be easily tested by letting $E_{IMC}(0) = G_{y_cd}(G_{y_sd})^{-1}_{\ell}$ and $Q_{IMC}(0) = (G_{y_cu})^{-1}_{r}$. When $(G_{y_sd})^{-1}_{\ell}$ and/or $(G_{y_cu})^{-1}_{r}$ do not exist, one can use $E_{IMC}(0) = G^T_{y_sd}(G_{y_sd}G^T_{y_sd})^{-1}$ and $Q_{IMC}(0) = (G^T_{y_cu}G_{y_cu})^{-1}G^T_{y_cu}$, which correpond to the least square solutions. Noting that we cannot expect a feasible bound on $\bar{\sigma}(\tilde{H}(0))$ since $\tilde{H} = 0$ implies open-loop, we can state the condition (B.30) as a screening tool.

**ILS Screening Tool # 1:** *Eliminate the candidates for which*

$$\mu\begin{bmatrix} \mathbf{\Delta} & \\ & \mathbf{\Delta_p} \end{bmatrix}(\hat{R}(0)) \geq 1 \tag{B.32}$$

The frequency-domain robust bounds on $\bar{\sigma}(\tilde{S})$ and $\bar{\sigma}(\tilde{H})$ can be useful for measurement selection purpose as well:

**ILS Screening Tool # 1:** *Eliminate the candidates for which $(c^*_{\tilde{S}}, c^*_{\tilde{H}})$ are infeasible, that is neither of the bounds may be satisfied in a certain frequency region.*

Since the calculation of $c_{\tilde{S}}(\omega)$ and $c_{\tilde{H}}(\omega)$ can possibly require numerically involved tasks such as spectral factorization and solving a Riccati equation, for the purpose of measurement selection, one may ignore the stability/causality requirement and simply use $Q_{IMC} = (G_{y_sd})^{-1}_{\ell}$ and $E_{IMC} = (G_{y_cu})^{-1}_{r}$ or the least square solutions

$E_{IMC} = G_{y_s d}^T (G_{y_s d} G_{y_s d}^T)^{-1}$ and $Q_{IMC} = (G_{y_c u}^T G_{y_c u})^{-1} G_{y_c u}^T$ if the correponding left and/or right inverse do not exist.

### B.3.4 Application to the High-Purity Distillation Column

Due to the space limitation, we do not present the results obtained from applying the general screening tools. Interested readers are referred to Lee *et al.* [39] for the application of these tools to a multi-component distillation column. In this section, we present the results from applying the ILS design-dependent screening tools to the high-purity distillation column. In order to simplify the presentation, we limit our discussion to those candidates consisting of 1 or 2 temperature measurements — the use of more temperature measurements were found to be unnecessary for this problem. Hence, the following candidates are considered:

- **One Temperature Measurement**

$$y_s^1 = T_1; \quad y_s^2 = T_7; \quad y_s^3 = T_{17}; \quad y_s^4 = T_{25}; \quad y_s^5 = T_{35}; \quad y_s^6 = T_{41}$$

- **Two Temperature Measurements**

$$y_s^6 = \begin{pmatrix} T_1 \\ T_7 \end{pmatrix}; \quad y_s^7 = \begin{pmatrix} T_1 \\ T_{17} \end{pmatrix}; \quad y_s^8 = \begin{pmatrix} T_1 \\ T_{25} \end{pmatrix}; \quad y_s^9 = \begin{pmatrix} T_1 \\ T_{35} \end{pmatrix};$$

$$y_s^{10} = \begin{pmatrix} T_1 \\ T_{41} \end{pmatrix}; \quad y_s^{11} = \begin{pmatrix} T_7 \\ T_{17} \end{pmatrix}; \quad y_s^{12} = \begin{pmatrix} T_7 \\ T_{25} \end{pmatrix}; \quad y_s^{13} = \begin{pmatrix} T_7 \\ T_{35} \end{pmatrix};$$

$$y_s^{14} = \begin{pmatrix} T_7 \\ T_{41} \end{pmatrix}; \quad y_s^{15} = \begin{pmatrix} T_{17} \\ T_{25} \end{pmatrix}; \quad y_s^{16} = \begin{pmatrix} T_{17} \\ T_{35} \end{pmatrix}; \quad y_s^{17} = \begin{pmatrix} T_{17} \\ T_{41} \end{pmatrix};$$

$$y_s^{18} = \begin{pmatrix} T_{25} \\ T_{35} \end{pmatrix}; \quad y_s^{19} = \begin{pmatrix} T_{25} \\ T_{41} \end{pmatrix}; \quad y_s^{20} = \begin{pmatrix} T_{35} \\ T_{41} \end{pmatrix}$$

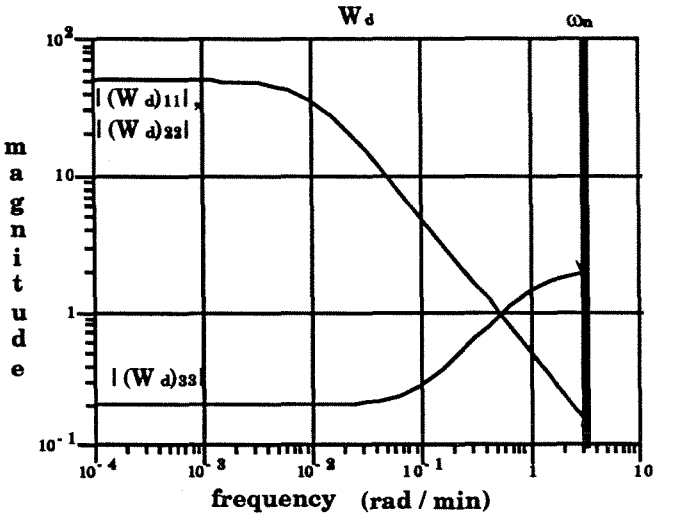


Figure B.6. Frequency Dependence of Disturbance Weight $W_d$

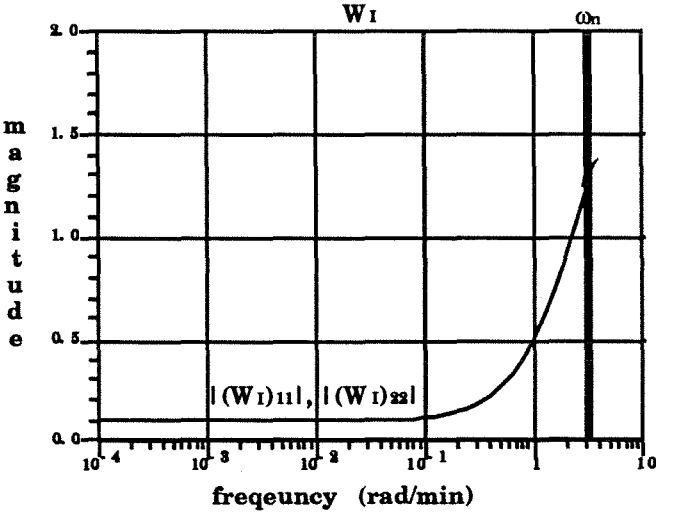


Figure B.7. Frequency Dependence of Input Uncertainty Weight $W_I$

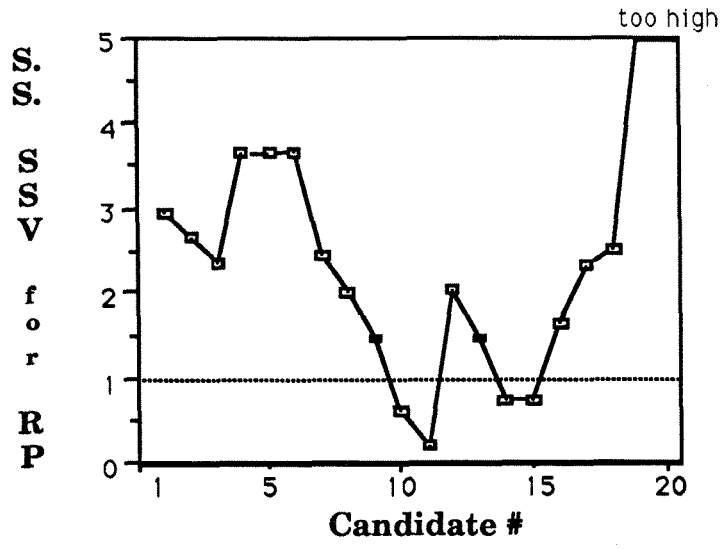


Figure B.8. Results from Applying ILS Screening Tool #1

The disturbance weight ($W_d$) and input uncertainty weights ($W_I$) we used for the measurement selection and controller design are plotted in Figure B.6 and Figure B.7 respectively. The performance weight $W_p$ and the output uncertainty weight $W_O$ were chosen as constant-scalar-times-identity matrices; the constant scalars $W_p$ and $W_O$ were 1 and 0.1 respectively. The chosen disturbance/performance weights specify that the disturbances are attenuated *at least* by the factor of 50 at steady state and the measurement noise is attenuated by the factor of more than 2 in the cross-over to high frequency region. The input uncertainty weight allows up to 10 % errors at steady state and time delay errors of approximately 1 minute on each actuator signal. The output uncertainty weight allows up to 10 % errrors at every frequency on each sensor signal.

The results from applying the ILS Screening Tool #1 to the candidates are shown in Figure B.8. Only 4 of the 20 candidates passed the screening: $y_s^{10}, y_s^{11}, y_s^{14}$, and $y_s^{15}$. For these four candidates, the robust performance bounds on $\bar{\sigma}(\tilde{S})$ and $\bar{\sigma}(\tilde{H})$ are derived (the stability/causality requirement on $Q_{IMC}$ and $E_{IMC}$ were ignored for the moment). The derived bounds are plotted in Figure B.9. Clearly, the candidate $y_s^{14}$

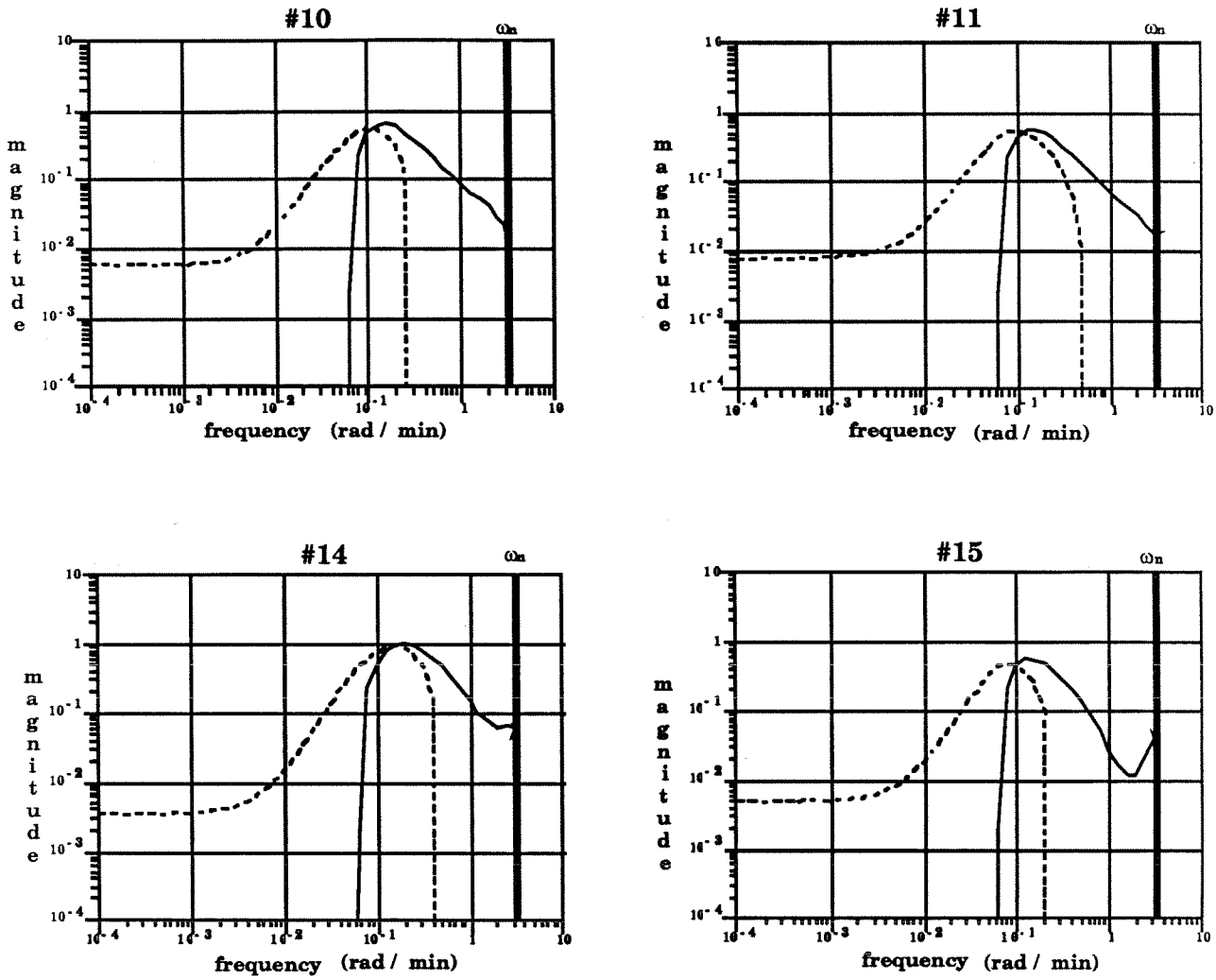


Figure B.9. Results from Applying ILS Screening Tool #2: RP Bounds on $\bar{\sigma}(\tilde{S})$ and $\bar{\sigma}(\tilde{H})$

yielded the most "feasible" bounds, especially around the cross-over frequency region. Hence, we next rederived the bounds for $y_s^{14}$ with the internal stability/causality requirements (Figure B.10). $Q_{IMC}$ was chosen as $\frac{z-1}{z^2}G_{y_cu}^{-1}$ (the optimal choice for ramp disturbances) and $E_{IMC}$ was designed through the Kalman filter technique (with infinite disturbance-to-noise ratio) as $G_{y_sd}$ had zeros outside the unit disk. The following $H$ satisfied at least one of the bounds at every frequency (except for a very narrow frequency band around the cross-over frequency where the conservativeness

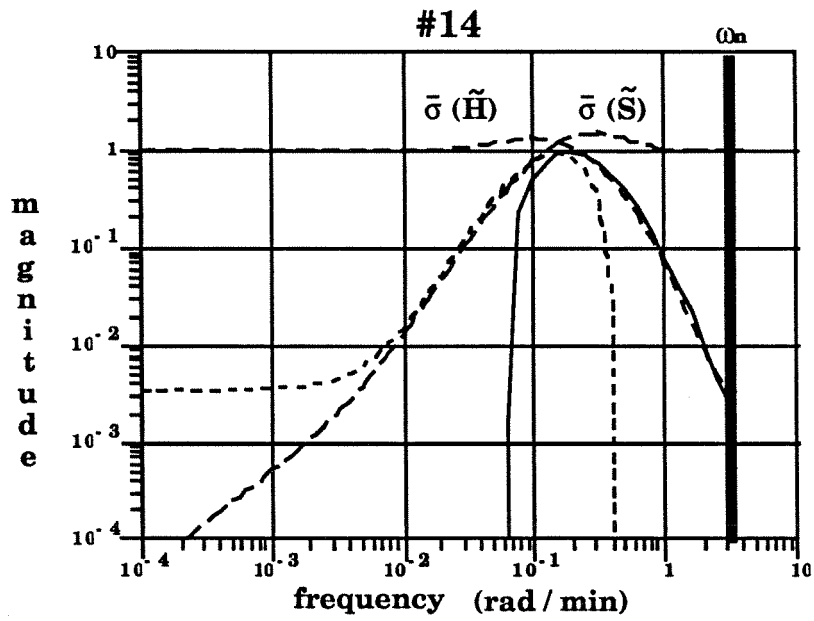


Figure B.10. Satisfying Robust Performance Bounds on $\bar{\sigma}(\tilde{S})$ and $\bar{\sigma}(\tilde{H})$

of the bounds is the greatest) as can be seen from Figure B.10:

$$H = \frac{0.0113z^3 + 0.0227z^2 - 0.0255z - 0.0058}{z^4 - 2.9468z^3 + 3.2225z^2 - 1.5494z + 0.2765} I \tag{B.33}$$

For each of the other three candidates, $H$ was designed such that its respective bounds are satisfied for as wide a frequency range as possible. The SSV for robust performance for all of the four candidates are shown in Figure B.11. As expected, $y_s^{14}$ is the only candidate that achieves "robust performance." Figure B.12 shows for the candidates $y_s^{10}, y_s^{11}, y_s^{14}, y_s^{15}$ and $y_s^{16}$ the simulated responses of the end-product compositions to the step disturbances in $F$ and $z_F$ in the presence of white measurement noise. The magnitudes of the flowrate and composition disturbances were chosen to be 0.2 and 0.1 respectively; they correpond to 20% of the steady-state values. The specific input and output multiplicative uncertainty used for the simulation were both diag$(0.1, -0.1)$. In addition, we appled time delay errors of 1 minute on both actuators. The simulation

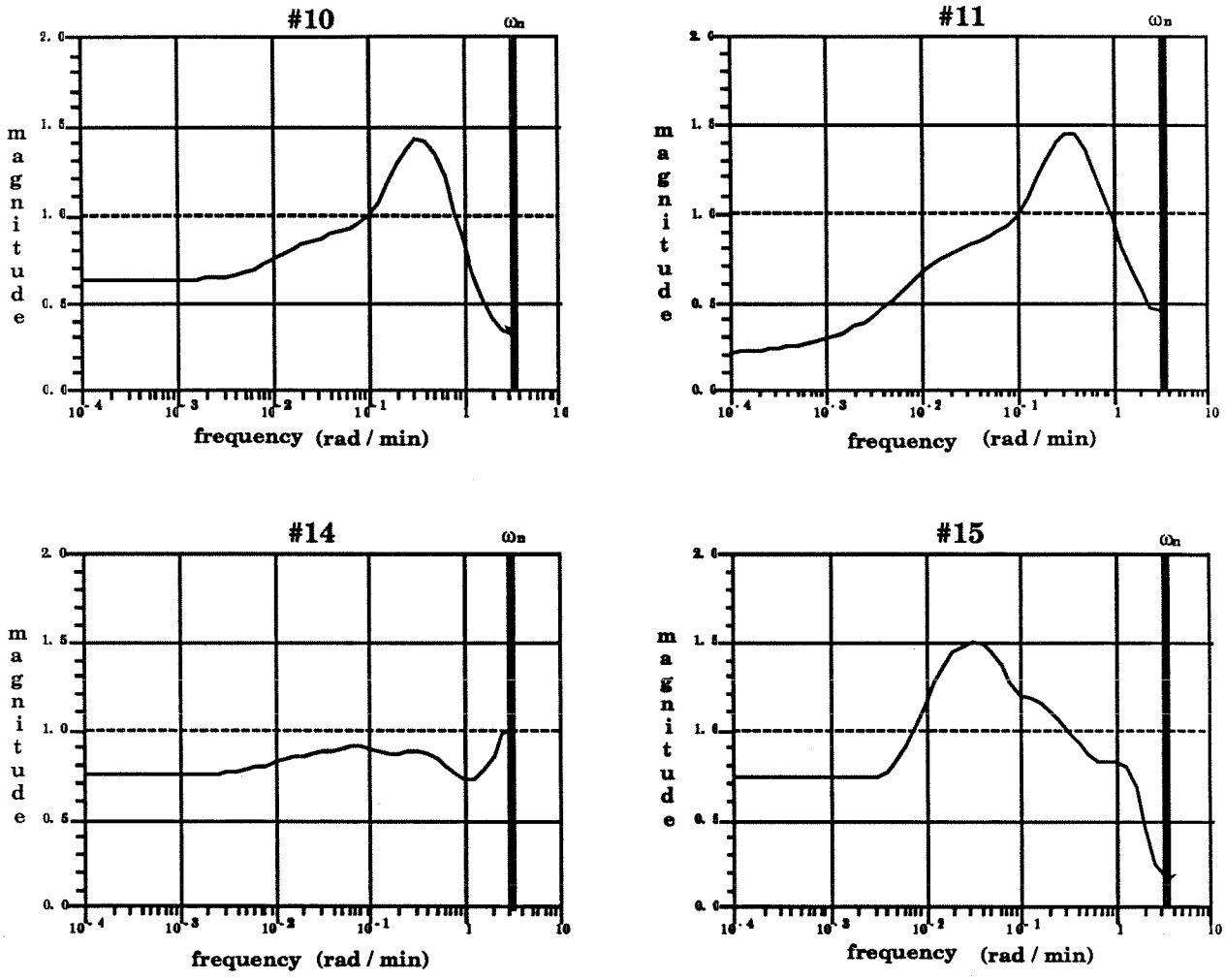


Figure B.11. Structured Singular Value ($\mu$) for Robust Performance

results show that the candidates with sensors placed close to the reboiler and/or the condenser ($y_s^{10}, y_s^{11}, y_s^{15}$) show extreme sensitivity to measurement noise. This is because the signal-to-noise ratios for these sensors are poor. On the other hand, the candidate with sensors placed too far away from the reboiler and/or condenser ($y_s^{16}$) shows minimum sensitivity to measurement noise, but yields large steady-state offsets. This is because the model uncertainty makes the inference of the product compositions from these sensors inaccurate. According to the simulation, $y_s^{14}$ is the best compromise between the two opposing trends; this fits well with the results obtained from our measurement selection method.

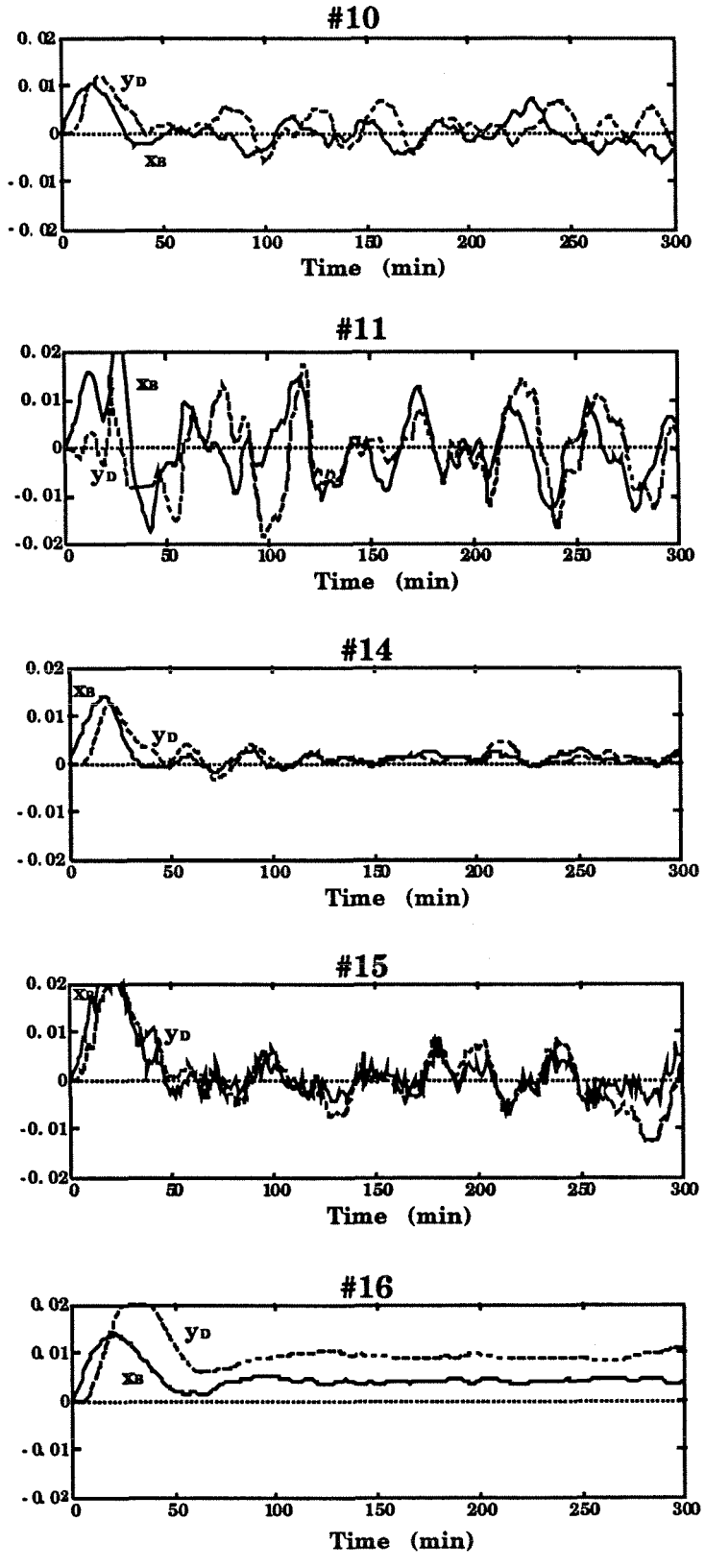


Figure B.12. Simulated Responses of Top/Bottom Product Compositions to Step Disturbances in Feed Flowrate and Composition in the Presence of White Measurement Noise

# B.4 Robust Control System Design for MR Sampled-Data Systems with Hard Constraints

## B.4.1 Overview

During the past decade or so, a number of robust multivariable controller design methods have been developed: LQG/LTR [20], Internal Model Control [24,50], and $\mu$-Synthesis [17] to name a few. However, their practical applications to complex processes such as distillation columns have been few. Some of the shortcomings of these methods as solutions to practical control problems are as follows:

- In order to minimize the SSV explicitly in the design phase (as $\mu$-Synthesis does), a rigorous uncertainty model is required; however, such a model is often unavailable in practice.

- A lack of on-line tuning parameters for most robust control design techniques (with the exception of the IMC technique) make the resulting controllers somewhat inflexible to unforeseen changes in the process.

- Most techniques involve iterative design algorithms of high theoretical/numerical complexity, which makes application by practitioners difficult.

- Because process constraints are not explicitly addressed within the framework of most robust controller design methods, constraint handling must be done through anti-windup schemes and other *ad hoc* means like mode-switching.

- The issuse of actuator/sensor failure tolerance cannot be addressed straightforwardly within the formulation of most techniques.

- Most techniques are not applicable to multi-rate sampled-data systems.

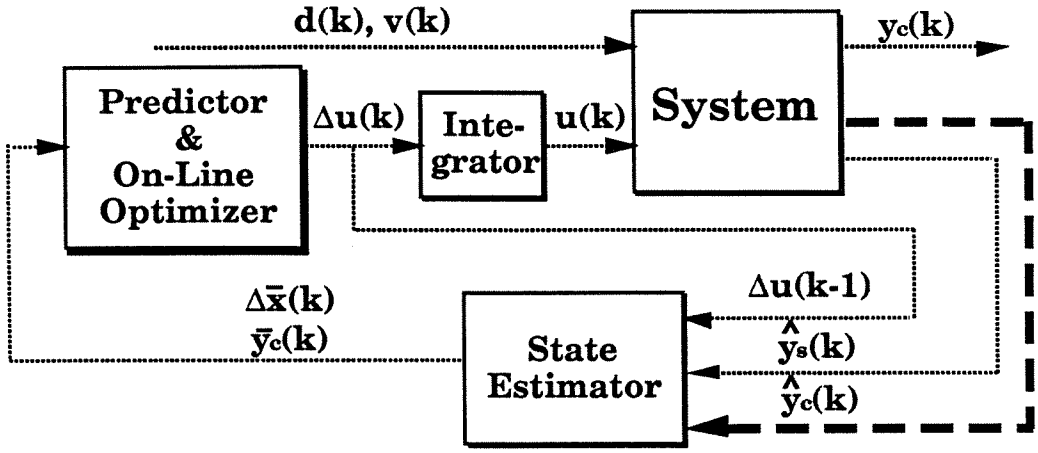


Figure B.13. Schematic Representation of Finite Receding Horizon Control of MR Sampled-Data Systems Through State Estimation and On-Line Optimization

## B.4.2 Finite Receding Horizon Control

Motivated by the apparent lack of a control system design method that addresses *all* of these important practical issues, Lee *et al.* [37] proposed a control technique that combines the state estimation and optimization techniques in the context of finite receding horizon control. Figure B.13 gives a schematic representation of the technique. In this paper, we present only the main ideas of the technique. Readers are referred to Lee *et al.* [37] for details.

### Modified State-Space Model for Control System Design

We start with the following standard state-space model:

$$x(k) = Ax(k-1) + B_u u(k-1) + B_d d(k-1) \tag{B.34}$$

$$\hat{y}_s(k) = C_s x(k) + v_s(k) \tag{B.35}$$

$$\hat{y}_c(\beta k) = C_c x(\beta k - \theta) + v_c(k) \tag{B.36}$$

We formulated the problem such that the primary measurements $\hat{y}_c$ are available at every $\beta$ sampling unit with delay of $\theta$ ($\beta$ and $\theta$ can be vectors for more general

formulation). After some algebraic manipulation, (B.34)-(B.36) can be transformed into the following state-space represention:

$$\begin{bmatrix} \Delta x(k) \\ y_c(k) \\ y_s(k) \end{bmatrix} = \begin{bmatrix} A & 0 & 0 \\ C_c A & I & 0 \\ C_s A & 0 & I \end{bmatrix} \begin{bmatrix} \Delta x(k) \\ y_c(k) \\ y_s(k) \end{bmatrix} + \begin{bmatrix} B_u \\ C_c B_u \\ C_s B_u \end{bmatrix} \Delta u(k) + \begin{bmatrix} B_d \\ C_c B_d \\ C_s B_d \end{bmatrix} \Delta d(k) \tag{B.37}$$

$$\hat{y}_s(k) = y_s(k) + v_s(k) \tag{B.38}$$

$$\hat{y}_c(nk) = y_c(\beta k - \theta) + v_c(k) \tag{B.39}$$

The new state-space representation is useful for two reasons: For state estimation, when $\Delta d$ is modelled as white-noise, the disturbance vector $d$ is modelled as a random step, which is reasonable for most processes. For feedback control, integral action is automatically guaranteed even when a nonzero weight is imposed on the control input vector $\Delta u$.

## State Estimator

The "state estimator" estimates the current dynamic states $\Delta x(k)$, $y_c(k)$, and $y_s(k)$ based on the measurements $\hat{y}_s(k)$ and $\hat{y}_c(k)$ (if available). The optimal estimator under a certain stochastic assumptions on $\Delta d$,$v_s$, and $v_c$ can be obtained through the MR Kalman filter technique; the detailed design procedure can be found in Lee *et al.* [37].

## Predictor and On-Line Optimizer

The "predictor" provides the optimal prediction of $p$ future controlled outputs in terms of $m$ current/future control moves, based on the current state estimates $\Delta\bar{x}$ and $\bar{y}_c$. $p$ and $m$ are user-chosen parameters. Mathematically, the prediction equation

is in the form

$$\bar{\mathcal{Y}}^p(k) = f(\Delta\bar{x}(k), \bar{y}_c(k), \Delta\mathcal{U}^m(k)) \tag{B.40}$$

where $f$ is a linear function (see Lee *et al.* [37] for the exact form) and

$$\bar{\mathcal{Y}}^p(k) = \left[ \bar{y}_c(k+1|k), \quad \cdots \quad \bar{y}_c(k+p|k) \right] \tag{B.41}$$

$$\Delta\mathcal{U}^m(k) = \left[ \Delta u(k), \quad \cdots \quad \Delta u(k+m-1) \right] \tag{B.42}$$

$\bar{y}_c(k+i|k)$ is the prediction of $y_c(k+i)$ based on the measurements at time $k$.

The "on-line optimizer" calculates $\Delta\mathcal{U}^m(k)$ based on the following objective function:

$$\min_{\Delta\mathcal{U}^m(k)} \sum_{i=1}^{p} \bar{y}_c^T(k+i|k)\Lambda\bar{y}_c(k+i|k) + \sum_{\ell=0}^{m-1} \Delta u^T(k+\ell)\Gamma\Delta u(k+\ell) \tag{B.43}$$

under various *constraints* on $\Delta u$, $u$, and $\bar{y}_c$. Quadratic Programming (QP) can be applied directly for the constrainted optimization [25]. In the context of finite receding horizon control, the first control move $\Delta u(k)$ is implemented and the whole optimization is repeated in the next sampling time. In the absence of constraints, the optimal control law relating $\Delta\bar{x}(k)$ and $\bar{y}_c(k)$ to $\Delta u(k)$ is a constant function; hence, the technique in its unconstrained form can be interpreted as a state-observer-based constant feedback controller.

## Actuator / Sensor Failure Handling

The on-line optimizer provides a natural way of handling an actuator failure. One can simply put a zero constraint on the failed actuator move. In the case of unreliable primary measurements, one can replace the MR Kalman filter with a cascaded Kalman filter shown in Figure B.14. The "auxiliary" estimator estimates the errors in the estimates of $y_c$ ($e_c$) on the basis of the difference between the actual measurement $\hat{y}_c$

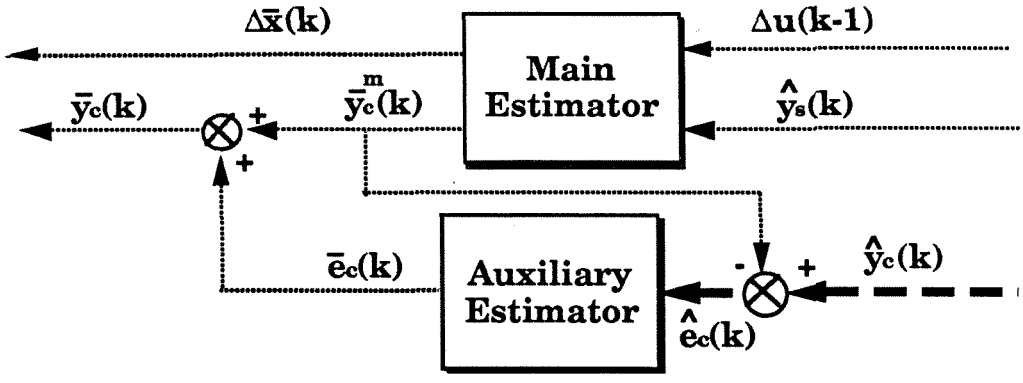


Figure B.14. Cascaded Kalman Filter for Unreliable Primary Measurements

and the estimate of $y_c$ from the main estimator ($\hat{e}^c = \hat{y}_c - \bar{y}_c^m$). The auxiliary estimator can often be designed to be decentralized and a failure of a primary measurement can be dealt straightforwardly by turning off the part of the estimator corresponding to the failed measurement.

## Robustness Tuning

The on-line tuneable parameters for the control technique are as follows: the prediction horizon ($p$), the number of control moves ($m$), and the output and input weights ($\Lambda$ and $\Gamma$). The disturbance/noise covariance matrices used for the Kalman filter design are also user-chosen parameters, but they cannot be viewed as on-line tuning parameters since a Riccati equation has to be resolved when these parameters are changed. The abundance of on-line tuning/design parameters make the control technique flexible, but controller tuning complex. Often, a convenient on-line tuning parameter is the input weight, which has also shown to be an effective means to the directional sensitivity of ill-conditioned systems [37]. For the cascaded Kalman filter, the "optimal" auxiliary estimator can often be conveniently parametrized in terms of a real vector whose dimension is the same as that of $y_c$ [38]. They provide natural on-line tuning parameters with direct implications on the speed of the closed-loop

response.

### B.4.3 Application to High-Purity Distillation Column

We apply the proposed control technique to the high-purity distillation column with temperature sensors in Tray #7 and Tray #35 (Candidate #14). We do not use the composition measurements since the steady-offsets for the ILS controller based on these measurements were shown to be negligible. Readers are referred to Lee *et al.* [37] for the application of the MR version of the technique to the column. The following constraints on the actuators were imposed:

$$-0.6 \leq L \leq 0.6; -0.6 \leq V \leq 0.6; |L|, |V| \leq 0.1 \tag{B.44}$$

The following parameters were used for the control move calculation:

$$p = 30; \quad m = 10; \quad \Lambda = \begin{bmatrix} 1 & 0 \\ 0 & 1 \end{bmatrix}; \quad \Gamma = \begin{bmatrix} 0.1 & 0 \\ 0 & 0.1 \end{bmatrix}; \tag{B.45}$$

The state estimator was designed using the following covariance matrices:

$$E\{\Delta d(k)\Delta d^T(k)\} = \begin{bmatrix} 1 & \\ & 1 \end{bmatrix}; \quad E\{v_s(k)v_s^T(k)\} = \begin{bmatrix} 2 & \\ & 2 \end{bmatrix}; \tag{B.46}$$

The simulated responses of the product compositions when the column is subjected to the same feed disturbances as in Section B.3.4 are plotted in Figure B.15. The model uncertainty and measurement noise were also chosen same as before. Note that the responses in the absence of constraints are better than those obtained using the ILS controller. We emphasize the fact that the tuning parameters were chosen without much effort; no elaborate trial-and-error or search techniques were used. Figure B.16 shows the simulated responses in the face of actuator failures. The control system

maintains performance integrity even with only one working actuator.

## B.5 Conclusion

In this article, our main objective was to bring together a number of robust control theories and to tailor them into practical control structure selection and controller design methods suitable for complex processes like high-purity distillation columns. By doing so, our main intention was to bring forward the aspects of current robust control theories that are useful and those that are problematic for practical control problems. We showed that the Structured Singular Value Theory provides a powerful framework to develop a systematic control structure selection method that is useful even when the complete knowledge of the process uncertainty is unavailable. On the other hand, for control system design, most robust control theories address only a subset of the issues which are of paramount importance to the success of the application. At present, there is no unified, rigorous robust control system design method that is suitable for complex practical control problems. We presented what we believed to be the best current solution to these complex problems. It is our hope that this case study has exposed some of the new challenges for the researchers working in the area of robust control.

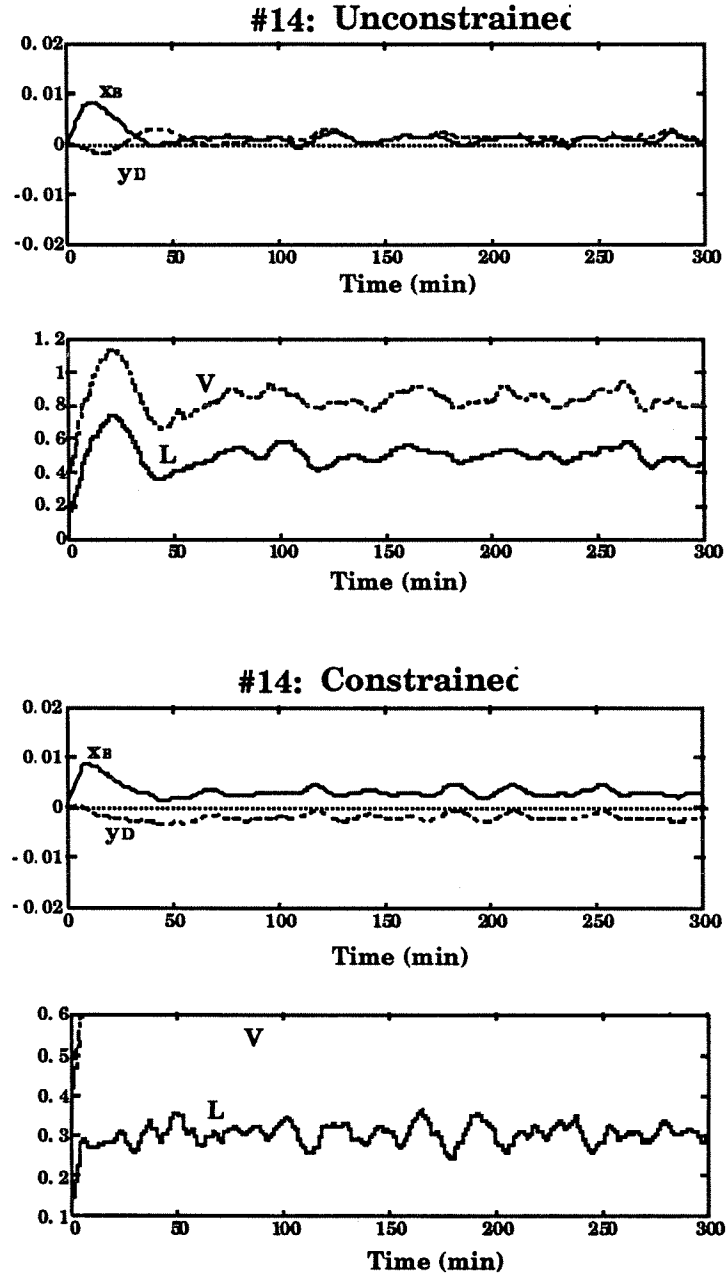


Figure B.15. Simulated Responses of Top/Bottom Product Compositions to Step Disturbances in Feed Flowrate and Composition in the Presence of White Measurement Noise

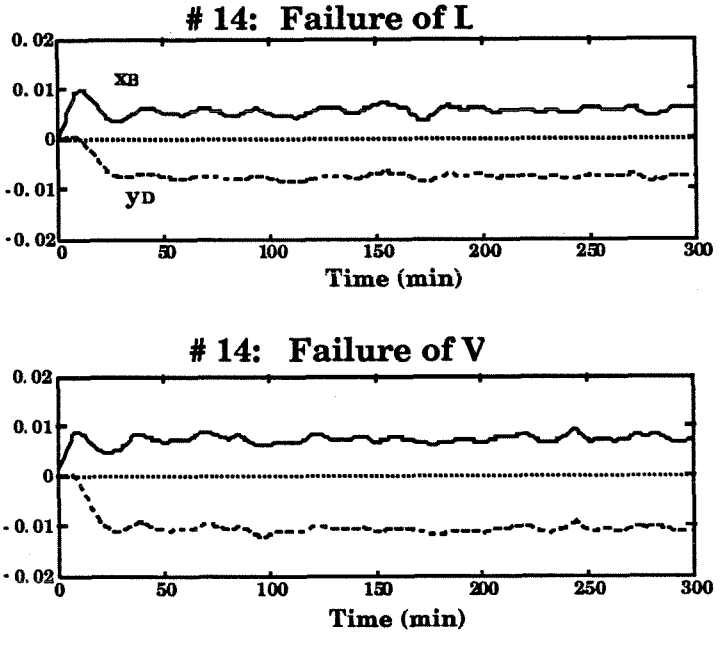


Figure B.16. Simulated Responses of Top/Bottom Product Compositions to Step Disturbances in Feed Flowrate and Composition in the Presence of White Measurement Noise and Actuator Failures

# Bibliography

[1] N. Amit. *Optimal Control of Multirate Digital Control Systems.* PhD thesis, Standford University, Stanford, CA, 1980. Aeronautical Engineering.

[2] Y. Arkun. *Design of Steady-State Optimizing Control Structures for Chemical Processes.* PhD thesis, University of Minnesota, Minneapolis, MN, 1978. Chemical Engineering.

[3] K. J. Åström and B. Wittenmark. *Computer Controlled Systems: Theory and Design.* Prentice-Hall, Englewood Cliffs, NJ, 1984.

[4] K. J. Åström and B. Wittenmark. *Adaptive Control.* Addison Wesley, New York, NY, 1989.

[5] B. W. Bequette and T. F. Edgar. The equivalence of non-interacting control system design methods in distillation. In *Proceedings of American Control Conf.*, pages 31–37, 1986.

[6] S. Boyd and C. H. Baratt. *Linear Controller Design: Limits and Performance.* Prentice Hall, Englewood Cliff, NJ, 1990.

[7] C. Brosilow and M. Tong. The structure and dynamics of inferential control systems. *AIChE Journal*, 24:492–500, 1978.

[8] P. S. Buckely, W. L. Luyben, and J. P. Shunta. *Design of Distillation Control Systems.* Instrument Society of America, Research Triangle Park, NC, 1985.

[9] H. M. Budman, C. Webb, and M. Morari. Robust inferential control for a packed-bed reactor. In *Proceedings of American Control Conf.*, pages 575–580, 1990.

[10] P. J. Campo. *Studies in Robust Control of Systems Subject to Constraints.* PhD thesis, California Institute of Technology, Pasadena, CA, 1989. Chemical Engineering.

[11] T. Chen and B. Francis. $H_\infty$-optimal sampled-data control. In *Proceedings of IEEE Conference on Decision and Control*, 1990.

[12] D. W. Clarke, C. Mohtadi, and P. S. Tuffs. Generalized Predictive Control: Part I. the basic algorithm. *Automatica*, 23:137–148, 1987.

[13] D. W. Clarke, C. Mohtadi, and P. S. Tuffs. Generalized Predictive Control: Part II. extensions and interpretations. *Automatica*, 23:149–160, 1987.

[14] C. R. Cutler and R. B. Hawkins. Application of a large predictive multivariable controller to a hydrocracker second stage reactor. In *Proceedings of American Control Conf.*, pages 284–291, 1988.

[15] C. R. Cutler and B. L. Ramaker. Dynamic Matrix Control: A computer control algorithm. In *Proceedings of American Control Conf.*, pages Paper WP5–B, 1980.

[16] R. L. Dailey. *Conic Sector Analysis for Digital Systems with Structured Uncertainties.* PhD thesis, California Institute of Technology, Pasadena, CA, 1987. Electrical Engineering.

[17] J. C. Doyle. *Lecture Notes in Advances in Multivariable Control.* ONR/Honeywell Workshop, Minneapolis, MN, 1984.

[18] J. C. Doyle, K. Glover, P. Khargonekar, and B. Francis. State-space solutions to standard $H_2$ and $H_\infty$ control problems. *IEEE Trans. Autom. Control*, AC-34(8):831–847, 1989.

[19] J. C. Doyle, R. S. Smith, and D. F. Enns. Control of plants with input saturation nonlinearities. In *Proceedings of American Control Conf.*, pages 2147–2152, 1987.

[20] J. C. Doyle and G. Stein. Multivariable feedback design: Concepts for a classical/modern synthesis. *IEEE Trans. Autom. Control*, AC-26(4):4–16, 1981.

[21] J.C. Doyle. Guaranteed margins for LQG regulators. *IEEE Trans. Autom. Control*, 23(4):756–757, 1978.

[22] J.C. Doyle. Analysis of feedback systems with structured uncertainties. *Inst. Electrical Engineers Proc.*, 129(6):242–247, 1982.

[23] B. A. Francis. *A Course in $H_\infty$ Control Theory.* Springer-Verlag, Heidelberg, 1987.

[24] C. E. Garcia and M. Morari. Internal model control: 1. a unifying review and some new results. *Ind. Engr. Chemical Process Des. and Dev.*, 21:308–323, 1982.

[25] C. E. Garcia and A. M. Morshedi. Quadratic Programming solution of Dynamic Matrix Control (QDMC). In *Proceedings of American Control Conf.*, 1984.

[26] G. C. Goodwin and K. S. Sin. *Adaptive Filtering, Prediction and Control.* Prentice-Hall, Englewood Cliffs, NJ, 1984.

[27] G. Gu, P. P. Khargonekar, and E. B. Lee. Approximation of infinite-dimensional systems. *IEEE Trans. Autom. Control*, AC-34(6):610–618, 1989.

[28] M. T. Guilandoust, A. J. Morris, and M. T. Tham. An adaptive estimation algorithm for inferential control. *Ind. Engr. Chemical Res.*, 27:1658–1664, 1988.

[29] T. J. Harris, J. F. MacGregor, and J. D. Wright. Optimal sensor location with an application to a packed-bed tubular reactor. *AIChE Journal*, 26(6):910–916, 1980.

[30] M. I. J. Hautus. *Prc. Eed. Akad. Wetensch.*, A 72:443, 1969.

[31] B. Joseph and C. B. Brosilow. Inferential control of processes. *AIChE Journal*, 24:485–509, 1978.

[32] B. Joseph, C. B. Brosilow, J. C. Howell, and W. R. D. Kerr. Multi-temps give better control. *Hydrocarbon Processing*, 3:127–131, 1976.

[33] P. Kabamba and S. Hara. On computing the induced norm of sampled-data systems. In *Proceedings of American Control Conf.*, pages 319–320, 1989.

[34] S. Kumar and J. H. Seinfeld. Optimal location of measurements for distributed parameter system. *IEEE Trans. Autom. Control*, AC-23:690–698, 1978.

[35] S. Kumar and J. H. Seinfeld. Optimal location of measurements in tubular reactors. *Chemical Engr. Sci.*, 33:1507–1516, 1978.

[36] H. Kwakernaak and R. Sivan. *Linear Optimal Control Systems.* Wiley-Interscience, New York, NY, 1972.

[37] J. H. Lee, M. S. Gelormino, and M. Morari. Model predictive control of multi-rate sampled-data systems: A state-space approach. *International Journal of Control*, (submitted), 1990.

[38] J. H. Lee, M. Morari, and C. E. Garcia. State-space interpretation of model predictive control. *Automatica*, (submitted), 1990.

[39] J. H. Lee, M. Morari, and A. Packard. Screening tools for robust control structure selection. *Automatica*, (in preparation), 1990.

[40] J.H. Lee and M. Morari. Robust control of nonminimum-phase systems through the use of secondary measurements: Inferential and inferential cascade control. *Automatica*, (submitted), 1990.

[41] J.H. Lee and M. Morari. Robust measurement selection. *Automatica*, (to appear), 1991.

[42] S. Li, K. Y. Lim, and D. G. Fisher. A state space formulation for model predictive control. *AIChE Journal*, 35:241–249, 1982.

[43] L. Ljung. *System Identification: Theory for the User.* Prentice-Hall, Englewood Cliffs, NJ, 1987.

[44] W. L. Luyben. Parallel cascade control. *Ind. Engr. Chemical Fundam.*, 12:463–467, 1973.

[45] T. Mejdell. *Estimators for Product Composition in Distillation Columns.* PhD thesis, Norwegian Institute of Technology, Trondheim, Norway, 1990. Chemical Engineering.

[46] B. C. Moore. Principal component analysis in linear systems: Controllability, observability and model reduction. *IEEE Trans. Autom. Control*, AC-26:17–32, 1981.

[47] C. Moore, J. Hackney, and D. Canter. Selecting sensor location and type for multivariable processes. In *Shell Process Workshop*, pages 291–308. Butterworth Publishers, Boston, MA, 1987.

[48] M. Morari and J. H. Lee. Robust control structure selection. In *Signal Processing Part 2: Control Theory and Applications*, pages 195–219. Springer-Verlag, New York, NY, 1990.

[49] M. Morari and G. Stephanopoulos. Minimizing unobservability in inferential control schemes. *International Journal of Control*, 31:367–377, 1980.

[50] M. Morari and E. Zafiriou. *Robust Process Control.* Prentice Hall, Englewood Cliffs, NJ, 1989.

[51] C.N. Nett and V. Manousiouthakis. Euclidean condition and block relative gain: Connections, conjectures and clarifications. *IEEE Trans. Autom. Control*, 5:405–407, 1987.

[52] A. Packard. *What's New with $\mu$: Structured Uncertainty in Multivariable Control.* PhD thesis, University of California, Berkeley, CA, 1988. Electrical Engineering.

[53] N.G. Patke, P.B. Deshpande, and A.C. Chou. Evaluation of inferential and parallel cascade schemes for distillation control. *Ind. Engr. Chemical Process Des. and Dev.*, 21:266–272, 1982.

[54] D.M. Prett and M. Morari. *Shell Process Control Workshop.* Butterworth, Stoneham, MA, 1987.

[55] J. Richalet, A. Rault, J. L. Testud, and J. Papon. Model predictive heuristic control: Application to industrial processes. *Automatica*, 14:413, 1978.

[56] N. L. Ricker. The use of Quadratic Programming for constrained Internal Model Control. *Ind. Engr. Chemical Process Des. and Dev.*, 24:925–936, 1985.

[57] N. L. Ricker. Model predictive control with state estimation. *Ind. Engr. Chemical Res.*, 29:374–382, 1990.

[58] R. Rouhani and R. K. Mehra. Model Algorithmic Control (MAC): Basic theoretical properties. *Automatica*, 18:401, 1982.

[59] S. Skogestad and M. Morari. Some new properties of the structured singular value. *IEEE Trans. Autom. Control*, AC-33:1151–1154, 1988.

[60] S. Skogestad, M. Morari, and J. Doyle. Robust control of ill-conditioned plants: High-purity distillation. *IEEE Trans. Autom. Control*, AC-33:1092–1105, 1988.

[61] R. Weber and C. Brosilow. Use of secondary measurements to improve control. *AIChE Journal*, 18:614–623, 1972.

[62] W. M. Wonham. *Linear Multivariable Control: A Geometric Approach.* Springer-Verlag, New York, NY, 1979.

[63] D. C. Youla, J. J. Bongiorno, and H. A. Jabr. Modern Wiener-Hopf design of optimal controllers: Part I. the single input-output case. *IEEE Trans. Autom. Control*, AC-21:319–338, 1976.

[64] E Zafiriou. Robust model predictive control of processes with hard constraints. *Computers and Chemical Engr.*, 14:359–371, 1990.

[65] G. Zames. Feedback and optimal sensitivity: Model reference transformations, multiplicative seminorms and approximate inverses. *IEEE Trans. Autom. Control*, AC-26:301–320, 1981.